BUREAU OF RECLAMATION

Directed Outflow Project Technical Report 4

Directed Outflow Project, California

California-Great Basin Region

U.S. Department of the Interior

June 2023

Mission Statements

The Department of the Interior (DOI) conserves and manages the Nation's natural resources and cultural heritage for the benefit and enjoyment of the American people, provides scientific and other information about natural resources and natural hazards to address societal challenges and create opportunities for the American people, and honors the Nation's trust responsibilities or special commitments to American Indians, Alaska Natives, and affiliated island communities to help them prosper.

The mission of the Bureau of Reclamation is to manage, develop, and protect water and related resources in an environmentally and economically sound manner in the interest of the American public.

Directed Outflow Project Technical Report 4

Directed Outflow Project, California
California-Great Basin Region

prepared by

Bureau of Reclamation, Bay-Delta Office
801 I Street, Suite 140, Sacramento, CA 95814

Report Editors and Project Managers
Nick G. Bertrand, Kristin K. Arend, Ph.D., & Brian Mahardja
Science Division, U.S. Bureau of Reclamation, Bay-Delta Office

Administering Office
U.S. Bureau of Reclamation Bay-Delta Office
David Mooney, Ph.D., P.E.; Bay-Delta Office Manager
Mario Manzo, Bay-Delta Deputy Office Manager
Josh Israel, Ph.D., Bay-Delta Science Division Chief

Chapter Lead Authors*
Leticia Maria Cavole, Ph.D.
Tena S. Dhayalan
Rachel A. Fichman
Tien-Chieh Hung, Ph.D.
Calvin Y. Lee
Levi S. Lewis, Ph.D.
*** See individual chapters for full list of coauthors**

Cover Photos: Cover Images: top left: Electron microscope images showing the impact of the preservative ExCell Plus on Delta Smelt otoliths, photos by John Grimsich, University of California, Berkeley, Berkeley CA, 94720. USA.; top right: Fresh Delta Smelt and an ExCell Plus preserved Delta Smelt at week 52, photos by Wilson Xieu, University of California, Davis, Davis, California, 95616, USA.; Middle left: Two Delta Smelt from the temperature and food limitation experiment. Fish were tagged with unique identifiers to allow tracking throughout the experiment. These two individuals are the same age, with one being food limited for 70 days while the other was fed ad libitum, photos by Feng Zhao, University of California, Davis, Davis, California, 95616, USA.; Middle right: images of four different histological tissue samples in four different preservatives: gill, liver, oocytes, and spermatocytes, in Ethanol, Formalin, ExCell Plus, and Liquid Nitrogen, photos by Swee Teh, University of California, Davis, Davis, California, 95616, USA; bottom: Interagency team released cultured delta smelt from the UC Davis Fish Conservation and Culture Lab into an enclosure near Rio Vista. Fish acclimated for 48 hours before release into the Delta. Pictured (left to right): Ryan Cook (USFWS), Taylor Senegal (USFWS), Melinda Baerwald (DWR). Photo by: Leanne Pearl, Fish Conservation Physiology Lab, University of California, Davis, California 95616, USA.

Disclaimer

This document does not represent and should not be construed to represent determination, concurrence, or policy of the U.S. Bureau of Reclamation or the U.S. Government.

Any use of trade, product, or firm names is for descriptive purposes only and does not imply endorsement by Reclamation or the U.S. Government.

1. REPORT DATE	**2. REPORT TYPE**	**3. DATES COVERED** *(From - To)*
June 10, 2023	Research	

4. TITLE AND SUBTITLE Directed Outflow Project: Technical Report 4	**5a. CONTRACT NUMBER** **5b. GRANT NUMBER** **5c. PROGRAM ELEMENT NUMBER**
6. AUTHOR(S) Editors: Nick G. Bertrand, Kristin K. Arend, & Brian Mahardja, Chapter Lead Authors: Leticia Maria Cavole, Tena S. Dhayalan, Rachel A. Fichman, Tien-Chieh Hung, Calvin Y. Lee, Levi S. Lewis	**5d. PROJECT NUMBER** **5e. TASK NUMBER** **5f. WORK UNIT NUMBER**
7. PERFORMING ORGANIZATION NAME(S) AND ADDRESS(ES) Bureau of Reclamation Bay Delta Office 801 I St., Suite 140 Sacramento CA 95814	**8. PERFORMING ORGANIZATION REPORT NUMBER**
9. SPONSORING/MONITORING AGENCY NAME(S) AND ADDRESS(ES) United States Bureau of Reclamation Bay Delta Office 801 I St., Suite 140 Sacramento CA 95814	**10. SPONSOR/MONITOR'S ACRONYM(S)** **11. SPONSOR/MONITOR'S REPORT NUMBER(S)**

12. DISTRIBUTION/AVAILABILITY STATEMENT Available from the National Technical Information Service (NTIS), Operations Division, 5285 Pt. Royal Rd, Springfield VA 22161; and
U.S. Bureau of Reclamation, Bay Delta Office Website: https://www.usbr.gov/mp/bdo/index.html

13. SUPPLEMENTARY NOTE

14. ABSTRACT The U.S. Bureau of Reclamation's Directed Outflow Program (DOP), along with collaborating agencies and non-governmental groups, are continuing efforts to evaluate the hypothesized benefits of outflow/outflow alteration to habitats and species of the Sacramento-San Joaquin Delta and connecting upper estuary (Delta). A particular focus of the DOP is to improve ecological understanding of the critically endangered Delta Smelt (*Hypomesus transpacificus*), a small short-lived osmerid fish endemic to the Delta. The DOP technical report series (https://www.usbr.gov/mp/bdo/directed-outflow.html) aims to periodically showcase ongoing DOP-related research studies. Results from DOP-related studies are anticipated to assist decision-making processes and better inform general management actions to benefit Delta habitat conditions and species such as Delta Smelt.

15. SUBJECT TERMS
Directed Outflow Project, Fall X2, Salinity, Delta Smelt, Zooplankton, Contaminants, Growth, Condition, San Francisco Bay, Delta

16. SECURITY CLASSIFICATION OF:			**17. LIMITATION OF ABSTRACT**	**18. NUMBER OF PAGES**	**19a. NAME OF RESPONSIBLE PERSON**
				349	Joshua Israel, Ph.D.
a. REPORT	**b. ABSTRACT**	**a. THIS PAGE**			**19b. TELEPHONE NUMBER** *(Include area code)* 916-414-2405

This Page Intentionally Left Blank

Table of Contents

LIST OF TABLES

LIST OF FIGURES

Suggested Citation

ENTIRE REPORT

Bertrand, N.G., K.K. Arend, and B. Mahardja. Directed Outflow Project: Technical Report 4. U.S. Bureau of Reclamation, Bay-Delta Office, California-Great Basin Region, Sacramento, CA. June 10, 2023, 349 pp.

CHAPTER WITHIN REPORT

Hung, T.C., B.G. Hammock, M. Sandford, M. Stillway, M. Park, J.C. Lindberg, S.J. Teh, 2023. Temperature and Salinity Preferences of Endangered Delta Smelt (Hypomesus Transpacificus, Actinopterygii, Osmeridae) Pages 9-33 in Bertrand, N.G., K.K. Arend, and B. Mahardja., editors. Directed Outflow Project: Technical Report 4. U.S. Bureau of Reclamation, Bay-Delta Office, California-Great Basin Region, Sacramento, CA. June 10, 2023, 349 pp.

Directed Outflow Project Collaborators

April Smith, ICF

Andrew Kalmbach, ICF

Andrew Schultz, U.S. Fish and Wildlife Service

Brian Mahardja, U.S. Bureau of Reclamation *

Bruce Hammock, U.C. Davis*

Calvin Lee, ICF*

Christian Denney, U.C. Davis

Tena S. Dhayalana, U.C. Davis

Christina Burdi, California Department of Fish and Wildlife*

Colin Brennan, ICF

Darcy Austin, State Water Contractors

Denise (Barnard) Goodman, U.S. Fish and Wildlife Service*

Feng Zhao, U.C. Davis

Franklin D. Trana, U.C. Davis

J. Ryan Cook, U.S. Fish and Wildlife Service

James Hobbs, California Department of Fish and Wildlife & U.C. Davis*

Jason Hassrick, ICF*

Jennifer Pierre, State Water Contractors

John Brandon, ICF

John Grimich, U.C. Davis

Johnathan Huang, U.C. Davis

Kristin Arend, U.S. Bureau of Reclamation*

Leticia Maria Cavole, U.C. Davis

Levi Lewis, U.C. Davis*

Lori Smith, U.S. Fish and Wildlife Service

Luke Ellison, U.C. Davis

Mike Tillotson, ICF

Malte Willmes, Norwegian Institute for Nature Research, Trondheim, Norway

Marie Stillway, U.C. Davis*

Nann Fangue, UC Davis

Nick Bertrand, U.S. Bureau of Reclamation*

Rachel Fichman, U.C. Davis

Ramona Zeno, ICF

Randy Baxter, California Department of Fish and Wildlife

Robert Lusardi, U.C. Davis

Shawn Acuña, Metropolitan Water District of Southern California*

Steve Slater, California Department of Fish and Wildlife*

Swee Teh, U.C. Davis*

Taylor Senegal, U.S. Fish and Wildlife Service*

Teague Corning, ICF

Tena S. Dhayalana, U.C. Davis

Tien-Chieh Hung, U.C. Davis

Tomofumi Kurobe, U.C. Davis

Troy Stevenson, U.C. Davis

Vanessa Mora, California Department of Fish and Wildlife

Wilson Xieu, U.C. Davis

***denotes DOP Investigator Team**

This Page Intentionally Left Blank

Acknowledgments

The Directed Outflow Project is a collaborative research program led by the U.S. Bureau of Reclamation that includes state and federal agencies, academic institutes, and the private sector, including the U.S. Fish and Wildlife Service (USFWS), California Department of Water Resources (DWR), California Department of Fish and Wildlife (CDFW), University of California Davis, Metropolitan Water District of Southern California, and ICF. Permitting for this work was facilitated through CDFW (SC-4086, SC-13523, S-190810003-19127-002 and Memorandum of Understanding issued by CDFW's Delta Habitat Conservation Program and Fisheries Branch) and USWFS (TE-108507, sub-permit FWSLFWO-6.1, 1-1-96-F-1 and 1-1-98-I-1296 and USFWS BO 2022-000128-S7-001 Reclamation DOP). This study was supported by contributions from multiple agency field sampling activities of fish and zooplankton (CDFW, USFWS, DOP [USBR]), as well as informed by DWR DAYFLOW. Funding and contractual support was provided by USBR (special thanks to Megan Bryant, Teresa Brown, Rosana Yousef Goarji, Mouang Phan, Nandini Johnson, Brooke White, Thomas Eckert, John Ridilla, Rob Downing, Delyssa Bloxson and Leanne Henderson), DWR, Metropolitan Water District of Southern California (special thanks to Shawn Acuña), State Water Contractors (SWC; special thanks to Jennifer Pierre, Darcy Austin and SWC staff) and State and Federal Contractors Water Agency (special thanks to Laura Valoppi). We acknowledge the support of many people from the Delta community. Further acknowledgement sections are located within each chapter of this report.

This Page Intentionally Left Blank

Background and Purpose

The U.S. Bureau of Reclamation's (Reclamation) Directed Outflow Program (DOP), along with collaborating agencies and non-governmental groups, are continuing efforts to evaluate the hypothesized benefits of outflow/outflow alteration and improve ecological understanding of the critically endangered Delta Smelt (*Hypomesus transpacificus*), a small short-lived osmerid fish endemic to the Sacramento-San Joaquin Delta and connecting upper estuary (Delta). The DOP technical report series (https://www.usbr.gov/mp/bdo/directed-outflow.html) aims to periodically showcase ongoing DOP-related research studies. Each chapter within this report is intended for eventual submittal to a peer-reviewed scientific journal or may have already been accepted or published, thus formatting may vary among chapters. Comments at the top of the title page of each chapter will alert the reader of those chapters already published or submitted to a peer-reviewed journal. The following provides additional background information.

In 2008, the U.S. Fish and Wildlife Service (USFWS) issued a Biological Opinion (2008 BiOp; USFWS 2008) on Central Valley Project/State Water Project operations that concluded aspects of those operations jeopardize the continued existence of Delta Smelt and adversely modify the species' critical habitat. Action 4 (Fall X2 Action) of the 2008 BiOp required Delta outflow be maintained at an average X2 (average position of the 2 ppt isohaline from Golden Gate) no greater than 74 km for September and October following wet years and 81 km following above normal years (water-year type [wet, above normal, below normal, dry, critical] is based on measured unimpaired runoff; https://cdec.water.ca.gov/reportapp/javareports?name=WSIHIST). In 2011, Reclamation produced a fall outflow adaptive management plan based on the science underlying the Fall X2 Action and outlining how adaptive management might proceed (Reclamation 2012).

In spring 2016, USFWS requested augmentation of summer outflow from the Sacramento River to benefit the habitat and declining population of Delta Smelt, although the action never occurred. Slightly thereafter the Delta Smelt Resiliency Strategy (DSRS) was finalized in July 2016 (CNRA 2016). The DSRS articulated a suite of actions that could be implemented in the next few years to benefit Delta Smelt based on concepts detailed in Baxter et al. (2015). These actions included augmentation of Delta outflow to push the low salinity zone (0.5-6 ppt) seaward and routing of water through Yolo Bypass Toe Drain to promote food production, to benefit Delta Smelt.

In winter of 2016/2017 Reclamation formed the DOP to assist in evaluating outflow-related hypotheses and predictions (Table 1-1) using targeted paired biological and physical monitoring. The over-arching hypothesis is summer and fall habitat conditions are improved for juvenile Delta Smelt when X2 moves seaward (USBR 2012; Brown et al. 2014), especially when X2 overlaps the Suisun Bay-Marsh area of the Delta. Predictions are largely based on conceptual models within Baxter et al. (2015) (figures 48 and 49 in particular) and predictions in Brown et al. (2014).

In August of 2016, Reclamation and California Department of Water Resources (DWR) jointly requested a Reinitiation of Consultation on the Coordinated Long-Term Operation of the Central Valley Project (CVP) and State Water Project (SWP). The USFWS accepted the request shortly after and stated therein: "…new information is demonstrating the increasingly imperiled state of the delta smelt and its designated critical habitat, and that emerging science shows the importance of outflows to all life stages of delta smelt and to maintaining the primary constituent elements of designated critical habitat." The new Biological Opinion on operations was finalized in October of 2019 (2019 BiOp; USFWS 2019). The Delta Smelt Summer-Fall Habitat Action (SFHA) and additional measures in Table 2-1 of the 2019 BiOp outlines multiple outflow-related actions geared toward benefitting Delta Smelt habitat and ultimately its population. Such actions include the following:

> Fall X2: Modify water operations to maintain X2 at 80 km in above normal and wet water years in September and October. Maintain low salinity habitat in Suisun Marsh and Grizzly Bay when water temperatures are suitable. Manage the low salinity zone to overlap with turbid water and available food supplies. Establish contiguous low salinity habitat from Cache Slough Complex to the Suisun Marsh.
>
> Suisun Marsh Salinity Control Gate: The freshening of Montezuma Slough through gate operations could provide additional low salinity habitat for Delta Smelt to forage, spawn and rear.
>
> Suisun Marsh and Roaring River Distribution System Food Subsidies Study: Add fish food to Suisun Marsh through coordinating managed wetland flood and drain operations in Suisun Marsh, Roaring River Distribution System food production, and reoperation of the Suisun Marsh Salinity Control Gates.
>
> North Delta Food Subsidies/Colusa Basin Drain Study: Augment flow in the Yolo Bypass in July and/or September by closing Knights Landing Outfall Gates and routing water from Colusa Basin into Yolo Bypass to promote fish food production.
>
> Sacramento River Deepwater Ship Channel Food Study: Repair or replace the West Sacramento lock system to hydraulically reconnect the ship channel with the mainstem of the Sacramento River in combination with augmented nutrient concentrations. The ship channel has the potential to flush food production into the north Delta for Delta Smelt.

While much has been learned regarding the impacts of environmental conditions on Delta Smelt habitat, some uncertainty remains as to how outflow-related actions, such as those listed above, may affect certain habitat factors and fish and prey species' response. We anticipate results from DOP-related studies will assist structured decision-making processes involving Delta Smelt and better inform general management actions to benefit the wild Delta Smelt population, including augmentation of the population through supplementation using cultured fish.

As Delta Smelt populations declined and wild Delta Smelt catch reached all-time lows in 2021 the ability of DOP studies to focus on wild fish to evaluate these actions became more limited. However, in 2022 Reclamation, DWR, CDFW and USFWS began to release hatchery Delta

Smelt under a short-term program called Experimental Release. The goal of this program was to begin releasing Delta Smelt bred at the Fish Conservation and Culture Laboratory and test methods for release prior to the development of a full supplementation program. Over the program's first three years 200 days post hatch fish would be released between December and February with the intent for them to spawn in the months after February. All fish recaptured from these releases would be processed following DOP protocols. The data collected from these fish would be used to inform the key hypotheses of the DOP and to evaluate the success of Experimental Release when appropriate.

LITERATURE CITED

Baxter, R., Brown, L.R., Castillo, G., Conrad, L., Culberson, S.D., Dekar, M.P., Dekar, M., Feyrer, F., Hunt, T., Jones, K. and Kirsch, J. 2015. An updated conceptual model of Delta Smelt biology: our evolving understanding of an estuarine fish (No. 90). Interagency Ecological Program, California Department of Water Resources.

Brown, L.R., Baxter, R., Castillo, G., Conrad, L., Culberson, S., Erickson, G., Feyrer, F., Fong, S., Gehrts, K., Grimaldo, L. and Herbold, B. 2014. Synthesis of studies in the fall low-salinity zone of the San Francisco Estuary, September–December 2011. US Geological Survey Scientific Investigations Report, 5041, p.136.

California Natural Resources Agency (CNRA). 2016. Delta Smelt resiliency strategy. CNRA, Sacramento, California. Available: http://resources.ca.gov/docs/Delta-Smelt-ResiliencyStrategy-FINAL070816.pdf. (May 2019).

Schultz, A. A., editor. 2019. Directed Outflow Project: Technical Report 1. U.S. Bureau of Reclamation, Bay-Delta Office, Mid-Pacific Region, Sacramento, CA. November 2019, 318 pp.

United States Bureau of Reclamation (USBR). 2012. Adaptive management of fall outflow for delta smelt protection and water supply reliability [Internet]. Revised milestone draft dated 28 June 2012. Sacramento (CA): U.S. Bureau of Reclamation; 99 pp. Available from: https://www.waterboards.ca.gov/waterrights/water_issues/programs/bay_delta/docs/cmnt081712/dfg/cdfgusbr2012.pdf

United States Fish and Wildlife Service (USFWS). 2008. Formal Endangered Species Act consultation on the proposed coordinated operations of the Central Valley Project (CVP) and State Water Project (SWP): U.S. Fish and Wildlife Service, Sacramento, CA.

United States Fish and Wildlife Service (USFWS). 2019. Biological Opinion for the Reinitiation of Consultation on the Coordinated Operations of the Central Valley Project and State Water Project. U.S. Fish and Wildlife Service, Sacramento, CA.

Table 1: Qualitative predictions regarding the effect of X2 (location of 2 ppt salinity isohaline) in or near the Suisun Bay/Marsh area during summer and fall compared to other regions, and within this area during summer and Fall X2 Action periods.

Dynamic Abiotic Habitat Components	**X2 in/near Suisun Region During Summer or Fall Compared to Other Regions and Within Suisun Region During Summer or Fall X2 Action Periods (in parentheses)**	**Chapters within the DOP Technical Report 4 with Related Data**
Low Salinity Habitat Area	Higher (Increases)	1,6
Habitat Complexity	Higher (Increases)	
Hydrodynamic Complexity	Higher (Increases)	
Water Temperature	Lower (Decreases)	1,7
Turbidity	Higher (Increases)	
Contaminants*	Lower (Decreases)	
Dynamic Biotic Habitat Components		
Delta Smelt Prey Density and Biomass	Higher (Increases)	
Phytoplankton Density and Biomass	Higher (Increases)	
Harmful Algal Constituents/Cyanotoxins	Lower (Decreases)	
Impact of Non-Native Competitors	Lower	
Impact of Non-Native Predators	Lower	
Delta Smelt Responses		
Occupancy/Residence	Greater (Increases)	1,4
Health	Greater (Increases)	2,3,6
Growth	Higher (Increases)	2,3,4,5,6,7
Survival	Higher (Increases)	2,3
Prey Quality, Foraging Success	Better (Increases)	
Fecundity	Higher	2,4,6
Population Range/Distribution	Broader, Less Constricted	1,4
Life History Diversity	Greater, More Even Spread	4

Chapter 1: Temperature and Salinity Preferences of Endangered Delta Smelt (*Hypomesus Transpacificus, Actinopterygii, Osmeridae*)

Authors:

Tien-Chieh Hung[1,*], Bruce G. Hammock[2], Marade Sandford[1], Marie Stillway[2], Michael Park[2], Joan C. Lindberg[1], Swee J. Teh[2]

[1]Fish Conservation and Culture Laboratory
Department of Biological and Agricultural Engineering
University of California, Davis
Davis, CA 95616

[2]Aquatic Health Program
Veterinary Medicine: Anatomy, Physiology, and Cell Biology
University of California, Davis
Davis, CA 95616, USA

***Corresponding author:**

Tien-Chieh Hung thung@ucdavis.edu

ORCID: 0000-0001-9618-5887

Key Words:

fish, abiotic factors, sub-adult, choice, behavioral response

ABSTRACT

Temperature and salinity often define the distributions of aquatic organisms. This is at least partially true for Delta Smelt, an imperiled species endemic to the upper San Francisco Estuary. While much is known about the tolerances and distribution of Delta Smelt in relation to these parameters, little is known regarding the temperature and salinity preferences of the species. Therefore, the temperature and salinity preferences of sub-adult Delta Smelt were investigated across a wide range of thermal (8 to 28˚C) and salinity (0 to 23 ppt) conditions. Replicates of ten fish were allowed to swim between two circular chambers with different temperature or salinity, and the distribution of fish between the chambers was recorded. We found that Delta Smelt showed no temperature preference below 15˚C, a modest aversion to the warmer tank from 15-28˚C, and a strong aversion to the warmer tank with elevated mortality at temperatures above 28˚C. Delta Smelt also preferred lower salinities, and this preference became more pronounced as salinity increased toward 23 ppt. These results indicate that Delta Smelt can tolerate high temperatures and salinities for a short time, and that their preferences for lower temperature and salinity strengthens as these variables increase.

INTRODUCTION

Delta Smelt, *Hypomesus transpacificus* McAllister, 1963, is a small, silvery fish endemic to the upper San Francisco Estuary (SFE), where water from the Pacific Ocean mixes with freshwater from the Sacramento and San Joaquin rivers. Delta Smelt were once abundant in the SFE, inhabiting the freshwater Delta and brackish regions such as Suisun Bay[1]. Today, abundance of Delta Smelt in the wild is extremely low[2], and the species is listed as threatened federally[3] and as endangered under the California Endangered Species Act[4]. Several, potentially interacting, factors are thought to have contributed to the decline in Delta Smelt, including a loss of food resources, decreased turbidity, changing hydrodynamics associated with freshwater exports, loss of tidal wetlands, and an extended recent drought[5,6,7,8,9,10]. The recent drought from 2012-2016 was followed by one of the wettest years on record for California (2017), which provided hope that a natural recovery would occur, similar to that observed in 2011. However, numbers of Delta Smelt did not increase substantially despite high outflow[10], perhaps due to relatively high water temperatures in 2017[11]. Recent abundance trends strongly suggest that Delta Smelt are nearly extinct in the wild, and most recent surveys to locate Delta Smelt have failed to detect the species[12,13]. Then, from December 2021 through February 2022, more than fifty thousand hatchery-raised adult Delta Smelt were reintroduced to the SFE to supplement the wild population, a first for the species. Thus, it is currently unclear whether the wild population is largely of hatchery or wild origin.

Increased temperature and salinity are considered two primary mechanisms by which droughts reduce Delta Smelt range and abundance. Low outflow during droughts shifts the salinity field landward, reducing the quantity and quality of habitat for Delta Smelt[8]. Decreased freshwater outflow is also associated with increased water temperature in the Delta[14,15]. Climate change is expected to exacerbate these effects[16], with projected increases in temperature and salinity

exerting direct effects on physiological and fitness parameters of Delta Smelt and increasing extinction risk (i.e., energy allocation, growth, reproduction)[9,10,17]. For example, elevated water temperatures are associated with declines in otolith increment and condition factor of Delta Smelt collected from the wild[18,19].

Considerable research has been conducted on the salinity range of Delta Smelt in the environment and their tolerances in the laboratory. Delta Smelt have been found at salinities up to 18 ppt in the wild[20] and can survive salinities up to 34 ppt in the lab (96-h adult survival 81.5%)[21]. However, Delta Smelt are historically most abundant[22,23,24] and stomach fullness peaks[25] in the freshwater to low salinity zone (LSZ) of the estuary (0.5 to 6 ppt). The LSZ is a salinity range that moves seaward and landward with freshwater and tidal flows and is centered at a salinity of about 2 ppt[23].

Critical thermal methodology is used to quantify a maximum temperature at which fish are unable to escape unfavorable conditions that would eventually result in their mortality (i.e., CT_{max})[26,27]. Plasticity in high temperature tolerance with changes in acclimation temperatures is commonly observed in fishes, including Inland Silverside (*Menidia beryllina* Cope, 1867), Largemouth Bass (*Micropterus salmoides* Lacépède, 1802), and Delta Smelt[28]. For example, several studies have demonstrated that a warm acclimation temperature can increase a species' CT_{max} relative to optimum acclimation temperature[27]. For Delta Smelt, Swanson et al. reported a critical thermal maximum of 25.4°C when acclimated at 17°C[29]. Komoroske et al. acclimated juvenile Delta Smelt at 18.7°C, which resulted in a lethal CT_{max} of 27-28°C[21]. Davis et al. recorded some of the highest acute upper temperature tolerance limits for juvenile Delta Smelt after 20°C acclimation, with a CT_{max} of 29.7°C ± 0.2 (mean ± SE), with 25% of individuals tolerating temperatures of 30.0-30.7°C[28].

Elevated water temperatures increase the metabolic demand of ectotherms like Delta Smelt, or they may directly cause mortality if the CT_{max} is approached[26,28]. Although ectotherms can generally compensate for elevated metabolic demand by increasing foraging, this may be difficult for Delta Smelt given the low availability of prey in the SFE[25,30,31]. Although Delta Smelt have been found in the wild at temperatures from 6-25°C, they are most often found in areas with temperatures <22°C[20,28,32,33,34]. Unfavorably high temperatures are increasingly characteristic of much of the Delta in the summer and are associated with the absence of Delta Smelt from the central and south Delta[2].

While much is known regarding Delta Smelt temperature and salinity tolerances and distribution in the environment, little is known regarding the temperature and salinity preferences of the species. Distribution data of Delta Smelt in the wild is based on a multitude of variables likely to also influence distribution, such as prey availability, turbidity, predators, and competitors, making it difficult to infer preferences from distribution data. For example, high temperatures may cause individuals to emigrate from a habitat due to a preference for lower temperatures, or temperature may interact with other ecological variables such as prey scarcity. However, temperature and salinity are generally considered as major drivers since most California native fish species were identified as highly vulnerable to warming temperatures[35], and Delta Smelt belongs to a family of fish that does not extend too far south of the San Francisco Estuary along

the eastern Pacific Coast[20]. In addition, the majority of Delta Smelt population is semi-anadromous[36] with movement highly associated with turbidity and salinity gradients in water[32,37]. Moreover, most laboratory-based tolerance studies do not offer individuals a choice, whereas wild animals typically can choose their habitat. Preference data can be especially important for understanding why a population might become extirpated during a drought, which could be caused by a behavioral response, acute mortality, or an interaction between abiotic and ecological variables (e.g., prey, predators, competitors, and disease).

Inferring temperature and salinity preferences of aquatic organisms from behavioral experiments is well-established. For example, Hirvonen et al. used a y-maze fluvarium where Arctic Charr (*Salvelinus alpinus* Linnaeus, 1758) could choose between control water or stimulus water with fish odor[38]. A y-maze was also used by Correia et al. to explore the influence of turbidity and prey chemical cues on the foraging behavior of Red Swamp Crayfish (*Procambarus clarkii* Girard, 1852)[39]. Nay et al. used a shuttlebox system to test for an interaction between habitat complexity and temperature in a common coral reef fish[40]. Here, we investigated the preferential behavioral response of sub-adult Delta Smelt to thermal and salinity conditions loosely based on critical thermal methodology (CTM). Preference experiments were conducted across a wide range of temperatures and salinities using a shuttlebox system (Loligo Systems, https://www.loligosystems.com/core-shuttle-box-system). The shuttlebox system consisted of two tanks connected by a narrow passage, allowing individuals to select the tank with the most suitable conditions. Our hypotheses were that 1) Delta Smelt will avoid the environment with higher temperature or salinity after that parameter reaches a certain level, but only below the lethal level at which a choice is no longer possible; 2) temperature and salinity preferences will strengthen as the water becomes increasingly warm or saline, respectively; and 3) differences in acclimation temperature will alter temperature preference, with higher acclimation temperature lessening any preference for cool water.

MATERIALS AND METHODS

Fish collection and care

Cultured Delta Smelt at juvenile to sub-adult stages (38 to 69 mm in fork length; mean ±SD: 55.7 ±6.65 mm) were transported from the UC Davis Fish Conservation and Culture Laboratory (FCCL) in Byron, CA, to the UC Davis Aquatic Health Program in Davis, CA. Fish were held in a recirculating, biofiltered system at 16°C, using reconstituted water prepared according to the United States Environmental Protection Agency guidelines[41]. Water quality was kept within the physiological ranges of the Delta Smelt during pre-experimental culture (total alkalinity of 80 mg/L, hardness of 102.5 mg/L, electrical conductivity of 530 µmhos/cm, salinity of 0.4 ppt, and pH of 7.6). The fish were fed four times a day at 3% body mass per day with a mixture of formulated 4/6 NRD diet (INVE Aquaculture, Salt Lake City, Utah) and 370 Hikari plankton food (By-Rite Pet Supply, Hayward, California)[42]. Uneaten food was removed at the end of each one hour feeding by siphoning the bottom of the tank. A 25% water change was performed every day. Periodic lighting was provided (14-h light: 10-h dark photoperiod) with fluorescent lighting.

Delta Smelt (n=120) were then transferred to and held in three 300-L circular tanks and acclimated for one week prior to the preference trials (one 300-L tank for each acclimation/trial procedure). For the temperature preference trials, fish were held in acclimation tanks at either 14°C ('cold') or 17°C ('warm'), to determine how acclimation temperature affected preference values. For the salinity preference trials, Delta Smelt were slowly acclimated from 16°C (culture temperature at the FCCL) to 20°C over the course of one week in 0.4 ppt reconstituted water in the third 300-L tank. Fish used for the experiment were euthanized using buffered tricaine methanesulfonate (MS-222, 500 mg L^{-1}) at the end of the study.

Testing system configuration

The shuttlebox testing system consisted of two connected circular chambers, two mixing towers, and two water resource tanks. A narrow passageway connected one chamber with the other, allowing fish to swim between the chambers. Water recirculated among the chambers and the mixing towers, as shown in Figure S1-1. The working volume of each circular chamber was 120.5 L (100 cm in diameter and 15 cm in depth), and the total volume of water in the recirculating system was 270 L. Water was aerated with an air stone in each mixing tower to provide adequate dissolved oxygen levels. Due to the sensitivity of Delta Smelt to light[42], only four infrared lights (Infrared basking spot lamp PT2142-R20/75W, Exo Terra's, MA) were used to provide indirect illumination throughout the study (lights directed towards the ground underneath the circular chambers). A digital video camera (Pentax TV Lens 4.2 mm 1:1.6) was mounted overhead while the movement of fish was recorded by the CamStudio Recorder (version 2.7.2, http://camstudio.org/) at a frequency of 2 frames per minute. Images were analyzed using the ShuttleSoft behavior software (version 2.6.3, http://www.loligosystems.com/software).

Flow and temperature simulations and validation

The flow patterns and temperature distribution inside the shuttlebox testing system were numerically simulated to understand the degree of mixing between the two chambers. The configuration of the system and the computational grids were built using Gambit (version 2.0.4, ANSYS Inc.). The grids representing the flow domain were created by partitioning the volume of the system into many small control volumes after the model was created. The numerical solutions to the governing equations for fluid flow in each of the grids were solved with a software package, Fluent (version 6.3.26, http://www.ansys.com/products/fluids/ansys-fluent). Fluent uses a finite volume method to approximate the solution to the governing equations for fluid and particle flows in each of the control volumes. The power law was used to solve the momentum discretization. The calculated results were displayed graphically. The simulations of temperature distribution were validated using HOBO pendant temperature/light probes (Onset, MA), a thermocouple reader with six probes (Tegam Inc., OH) and flow patterns were validated with the addition of food dye.

Experimental design

There is some evidence that Delta Smelt exhibit shoaling behavior[43], so three replicates of ten fish per replicate were used during each preference trial to test their volitional movements in the shuttlebox apparatus. Most similar studies have examined the behavioral responses of a single fish to different levels of an environmental stimulus[44,45,46,47], rather than the multiple fish used here.

Delta Smelt were not fed during the preference trials—which lasted up to six days—to avoid introducing any factors that could elicit a preference for a particular side of the shuttlebox. Hammock et al. found that six days of fasting at 16°C did not influence most biomarkers of nutritional stress in Delta Smelt (with hepatosomatic index as an exception)[48]; therefore, we do not expect that fasting would affect preferences during the experimental trials. Nevertheless, we included 'time since last feeding' as a covariable in our preliminary analyses. We found that it was not a significant predictor for either temperature or salinity preference; therefore, it was not included in the model comparisons presented here.

Temperature preference trials

Temperature preference trials were 6-days in length and included temperatures ranging from 8-28°C at a salinity of 0.4 ppt. Temperature target pairs (i.e., the nominal water temperatures of the two circular tanks of the shuttlebox system) included the following: [8, 10], [10, 12], [12, 14], [14, 16], [16, 18], [18, 20], [20, 22], [22, 24], [24, 26], and [26, 28]°C (±0.5°C). Ten fish were arbitrarily selected from either the 'cold' or 'warm' acclimation tanks and placed into the shuttlebox system for an additional six-hour acclimation period (to recover from handling stress) before beginning each six-day temperature trial. For 14˚C-acclimated fish, we placed fish in the shuttlebox chambers at 12 and 14˚C and acclimated for a 6-hr period; for 17˚C-acclimated fish, the 6-hr acclimation period started at 14 and 16˚C. To begin the experiment, the number of fish in each tank was counted every thirty minutes over a six-hour period using a video monitor at the initial temperatures (12 and 14˚C or 14 and 16˚C). Then, we kept the cooler temperature tank at the same temperature but changed the warmer temperature tank down 4˚C to the next lower assigned pair and, once temperatures had stabilized, the distribution of fish between the tanks was again recorded every 30 min for six hours. We kept lowering temperatures and collecting distribution data until we had collected data at the lowest pair, 8 and 10˚C. Temperatures were then raised, pausing at each temperature pair to collect distribution data as above, until we reached the final temperature pair, 26 and 28˚C. Once data were collected at the highest temperature pair, the fish were removed from the tanks and the process began again with 10 different fish once temperatures had stabilized at 13 and 15˚C or 15 and 17˚C. Each tank alternated being decreased or increased in 4°C increments over the course of each of the eight 6-day trials. Thus, only one tank changed temperature at a time (4ºC increase or decrease), such that each tank alternated serving as the 'warmer' tank (Figure S1-2). This strategy provided an incentive for the fish to swim between the chambers to stay at their preferred temperature and minimized any tank effect (i.e., an innate preference for a particular tank). Ten fish were used for each trial; three trials were performed for the fish acclimated to 14°C and five trials for those acclimated to 17°C. Thus, 80 fish total were used in the temperature preference experiments. The

distributions of individuals for each of the 30-minute periods were averaged, rounded to the nearest integer, and used as the response variable in the analysis.

Salinity preference trials

Salinity preference trials were 20-hrs in length and consisted of a broad range of salinities, ranging from freshwater to 23 ppt. Salinity target pairs included the following: [0, 0.5], [3, 5], [8, 10], [13, 15], [17, 20], and [20, 23] (±0.5 ppt). Salinity trials were tested at a temperature of 20°C, within the range of temperatures Delta Smelt commonly inhabit in the wild[31] during summer saltwater intrusion. Instant Ocean sea salt (Spectrum Brand Inc., USA) was used to adjust salinity. Ten fish were arbitrarily selected from the freshwater acclimation tank and placed into the shuttlebox system for an additional six-hour acclimation period before each trial to recover from handling stress. The system salinity was increased manually every three hours in a series of 3 ppt increments with a target salinity difference of 3 ppt between the two shuttlebox chambers (actual difference was 2.2 ppt, SD = 0.9 ppt). We note that the salinity differences between the tanks were smaller at lower salinities because the differences were harder to maintain. Unlike the temperature trials during which water could be recirculating in the system throughout the trial periods, water for the salinity trials needed to be discharged in order to maintain the salinities in the source tanks for adjusting the salinity in the chambers (Figure S1-1). Therefore, two approaches were used to reduce the amount of reconstituted fresh and saline water needed and to make the trial possible: 1) one random chamber was assigned to be the one with a higher salinity throughout the trial period and 2) we reduced the duration of each salinity pair to three hours from the six hours used in the temperature trials. The total number of fish in each tank was counted every 15 minutes during the last two hours of each salinity trial once the salinity stabilized, using a video monitor after the system salinity reached the assigned level. Ten fish were used for each trial, and three trials were performed; thus, 30 fish total were used in the salinity preference experiments. The distributions of individuals for each of the 15-minute periods were averaged, rounded to the nearest integer, and used as the response variable in the analysis.

Data analysis

The temperature preference data were plotted to check for potential thresholds and nonlinearities and then analyzed using model comparison[49]. A series of five models were fit using R in which the proportion of fish in the cooler tank was the response variable and a binomial distribution of error was used[49,50]. 'Trial' was included as a random effect in all models to account for the repeated measurements from the same group of ten fish[49]. Data from trials with >50% mortality were not used to fit models. We included an intercept model (null; Model 1), a model with temperature in the warmer of the two tanks as a linear effect (Model 2), temperature of the warmer tank binned into <28 and >28°C (Model 3), and temperature in the warmer tank binned into <14, 14-28, and >28°C (Model 4; Table 1-1). Of these models, Model 4 was best, so Model 5 included the three-bin temperature variable plus a parameter for acclimation temperature (14 or 17°C; Table 1-1). We note that the binned temperature variables were assigned post-hoc, based on the plots of the temperature preference results, and were meant to account for the nonlinear

relationship between temperature preference and water temperature apparent from the data. The models were fit in R using the 'glmer' command from the 'lme4' package[51]. The models were compared using Akaike Information Criterion corrected for small sample size (AIC_c)[49]. Statistical significance was determined by examining 95% confidence intervals of parameter estimates.

The salinity preference data were also analyzed by first plotting the data to check for thresholds and nonlinearities, and then comparing a series of binomial models with a random effect for 'trial'. The proportion of individuals in the less saline tank was the response variable. The salinity preference data appeared fairly linear, so three models were fit: an intercept model (null; Model 1), a model with salinity in the more saline tank as the predictor variable (Model 2), and a model with the difference in salinity between the two tanks as the predictor variable (Model 3). The intercept model tested whether there was a salinity preference (if the 95% CI of the model did not overlap 50%), while the model with a salinity parameter tested whether the proportion in the fresher tank changed across the salinity gradient. Model 3 was included to test whether the apparent strengthening of the preference of Delta Smelt for the fresher water (see Results) was due to an increase in the difference between the fresh and more saline tanks at higher salinities (the correlation coefficient between salinity in the higher tank and the difference in salinity between the higher and lower tanks was 0.72). Neither the top-ranked temperature nor the salinity model was over-dispersed based on tests for over-dispersion using the 'dispersion_glmer' command from the R package 'blmeco'[52].

Ethics declarations

All the fish transportation, handling, euthanizing, and the experimental procedures were following protocols approved by UC Davis Institutional Animal Care and Use Committee (protocol #18125). The use of fish was permitted under the Federal Fish and Wildlife Permit (#TE027742-3) and California Endangered Species Act Memorandum of Understanding.

RESULTS

Temperature preference trials

Numerical simulation demonstrated that the flow exchange between the two chambers was negligible (Figure 1-1) and that temperature was uniformly distributed across each chamber. The numerical simulation demonstrates that the testing system was able to maintain a difference between the chambers (the average difference between the cooler and warmer tanks was 1.3°C [SD=0.5°C]). However, ambient air temperature had a significant effect on the water surface, especially when the difference between the air and water temperature was large (Figure S1-3). In addition to the numerical simulation, the flow pattern validation using food dye also showed minimal water exchange between the two chambers.

The proportion of Delta Smelt in the cooler tank was influenced by temperature, as models that included temperature as a predictor received 99.57% of the AIC_c weight (Table 1-1). The top-ranked temperature model included the temperature of the warmer tank as a predictor, divided

into three bins (Table 1-1; Figure 1-2a and 1-2b). This model included a parameter for the low (9.1-13.2°C), medium (14.0-28.0°C), and high temperature (28.1-28.8°C) bins. For the lowest temperature bin (<14°C), a higher percentage of Delta Smelt were in the warmer tank, with a model predicted percentage of fish in the cooler tank of 47.1%. However, this percentage did not differ significantly from 50% (95% CI: 41.5, 52.5%), indicating no statistically significant preference for the warmer water. For the medium temperature bin (14-28°C) there was a slight but statistically significant preference for the cooler tank, with a predicted percentage in the cooler tank of 55.1% (95% CI: 51.9-58.4%). In the highest temperature bin (>28°C), Delta Smelt showed a strong preference for the lower temperature tank, with a predicted percentage in the cooler tank of 82.5% (95% CI: 65.1, 96.7). While the second ranked model, which included acclimation temperature, received some AIC_c weight, the acclimation parameter was not significant (acclimation temperature parameter = -0.03, 95% CI: -0.11, 0.05; Table 1-1). We note that there was a parabolic relationship between the difference in temperature between the two tanks and water temperature (Figure 1-2c and 1-2d). The temperature gradient was more difficult to maintain above and below ~18-20°C, resulting in smaller differences between the tanks. Although a constant difference in temperature between the tanks would have been preferable, the temperature gradient was not a good predictor of Delta Smelt preference based on comparisons between Figure 1-2b and 1-2c.

Although Delta Smelt demonstrated a strong preference for the cooler tank in the highest temperature bin, we observed increased mortality at 28°C, regardless of acclimation temperature (14 or 17°C; Figure 1-2). No difference in behavior was observed up to 27°C (aside from the slight preference for the cooler tank), whereas above 27°C all individuals swam to the water surface and exhibited increased operculum movement and frequent gulping of air. The dissolved oxygen (DO) concentration in both chambers at the highest temperature pair (27.0±0.1°C and 29.4±0.1°C) was 7.45±0.04 mg/L and 7.12±0.03 mg/L, respectively, which represents 95.4% and 95.1% of oxygen saturation and was well within acceptable limits for the Delta Smelt.

Salinity preference trials

In the salinity trials, the mean difference between the tanks was 2.2 ppt (SD = 0.9 ppt). The proportion of Delta Smelt in the fresher tank was influenced by salinity, as the top-ranked model included salinity (Table 2). In addition, Delta Smelt exhibited a statistically significant preference for the fresher tank (i.e., the confidence interval of the model did not include 0.5 across almost the entire salinity range; Figure 1-3a and 1-3b, and the parameter estimate for salinity in the more saline tank was significant [0.03; 95% CI 0.01, 0.04]). This was likely driven by a stronger preference for fresher water by Delta Smelt at higher salinities rather than the larger difference in salinities between the tanks at higher salinities (Figure 1-3c and 1-3d), as the model with salinity as a predictor outperformed the model with the difference in salinities between the tanks (i.e., Model 2 versus 3, respectively; Table 2). Based on model predictions, 59% of the fish preferred the fresher tank at the lower end of the salinity range (0.2 ppt), and 73% preferred the fresher tank at the higher end (22.0 ppt; Figure 1-3).

DISCUSSION

Animals live in complex environments where they modify their behavior to balance short-term survival with longer-term fitness[53,54,55]. The behavioral response depends on how the animal assesses a range of variables and how it reacts to maximize fitness. In the SFE, Delta Smelt catch decreases substantially in apparent response to increased salinities[20,22,23,24] or temperatures[20,28,32,33,34]. It is unclear whether this is a behavioral or acute response, or a response to a covariable (e.g., predator or prey density). Our study evaluated the preferences of sub-adult Delta Smelt to a range of temperatures and salinities. Given the extreme drought conditions that California continues to endure, it is particularly important to consider how abiotic factors such as temperature and salinity play into Delta Smelt distribution, health, and fitness in the wild.

In our experiments, temperature preferences of sub-adult Delta Smelt were barely detectable across the vast majority of temperatures examined, with only a very modest preference for the cooler water across most of the temperature range. While the mean temperature gradient between the tanks was also fairly modest at 1.3°C, teleosts can detect small temperature differences, including as small as 0.03°C[56]. For example, Tuna (*Euthynnus affinis*) modify their behavior to temperature changes of 0.1°C[57]. Thus, the temperature gradient should have been sufficient for a teleost like Delta Smelt to detect and respond to. A slight preference for cooler temperatures likely lowers metabolic demand of Delta Smelt, preserving energy in their food limited habitat[31]. At the highest temperatures, however, clear signs of stress were observed and the preference for the cooler tank was sharply delineated. Showing little to no influence of acclimation temperature was surprising, given the considerable research showing that increases in maximum thermal tolerance can be expected with higher acclimation temperatures[27,28,29,58]. For Delta Smelt, Komoroske et al. acclimated post-larval stages of Delta Smelt at target temperatures of 12°C, 16°C, and 19°C, and found that while Delta Smelt acclimated at the lowest temperature had significantly reduced CT_{max} values compared to the medium- and high-temp acclimation fish, there was no difference in CT_{max} between the medium- and high-temp acclimation fish[21]. Possible explanations for the discrepancies are that our experiments evaluated the preferences rather than CT_{max} and subadult rather than juvenile Delta Smelt.

Swanson et al. reported that the critical thermal maximum for adult Delta Smelt is 25.4°C[29]. However, in our study, and in Komoroske et al., the fish appeared calm at 25°C, and only started to appear agitated when the temperature reached 27°C[21]. Perhaps the most plausible explanation for the differences between Swanson et al.[29] and more recent studies is that the Delta Smelt in our study and others[21,28,59] were obtained from the hatchery where Delta Smelt are cultured (FCCL), whereas Swanson et al. used wild-caught Delta Smelt in their CTM experiments[29]. It is likely that the culture conditions at the FCCL are more optimal than those in the wild, which could account for the higher tolerance of the Delta Smelt we observed[60]. The wild-caught Delta Smelt underwent antibacterial and antifungal treatments during their acclimation period[29], which also may have affected their temperature tolerance. In addition, cultured sub-adult Delta Smelt feeding on natural prey in unfiltered, untreated water pumped from the Delta also survived up to 27°C[59]. Other explanations for the difference in CT_{max} values include a slower temperature adjustment during the preference trial period in the present study (6 hours), a potential social

component (possibly better performance in the presence of companions), or genetic differences in the test populations[61]. In any case, given that the current wild population appears to be at least partially comprised of hatchery raised Delta Smelt (or their offspring), our results are likely to be increasingly applicable to Delta Smelt in the wild.

Delta Smelt at the highest temperatures showed a strong preference for the lower temperature tank, yet we still observed signs of stress such as the increased flaring of operculum and gulping for air when fish were at the top of the water column[62]. As DO concentrations at 27°C were well within the physiological range sufficient for Delta Smelt, a possible reason for them to stay near the water surface is that the water temperature at the surface was cooler than in the shuttlebox tanks (room temperature = 20°C), which may have allowed the fish to regulate their body temperature. Heat conduction through the body surface in fish is a key mechanism in temperature regulation[63,64]. Moreover, fish have a highly specialized ability to differentiate temperature regimes and can behaviorally avoid conditions detrimental to their survival if a more suitable habitat is available[65,66,67]. Heat-induced hyperactivity assists with this escape behavior[27].

In contrast to the temperature preference trials, Delta Smelt did not show signs of agitation or distress at high salinity. However, Delta Smelt showed a clear preference for the fresher water across a wide salinity range, and this preference increased in strength as salinity increased. Thus, our results indicate that Delta Smelt are able to tolerate a wide range of salinity despite their affinity for freshwater, which is consistent with the findings reported by others[21,29]. Consistent with our results, Delta Smelt distribution in the wild indicates a preference for lower salinity waters, especially during the summer where salinities are in the 1-2 ppt range[22,29,68]. Delta Smelt exhibit survival rates above 80% at 34 ppt in laboratory experiments, and show no differences in metabolic demand from freshwater to 12 ppt[25,69]. Thus, although the preference for fresher water provides a mechanism for why Delta Smelt distribution in the wild is restricted to the LSZ, it remains unclear why the species shows a preference for lower salinities. Our results are in-line with the assessment that Delta Smelt may be highly vulnerable to climate change[35] and also indicated the conditions of SFE are becoming less favorable for the species. The findings in this study also provide valuable information in terms of Delta Smelt temperature and salinity preference to water managers and habitat restoration projects in the SFE to conserve the species.

CONCLUSION

It is important to observe fish as they approach an environmental threshold to learn their behavioral response before conditions become acute. Movement away from an adverse condition is the behavioral response we attempted to capture here. Delta Smelt exhibited behavioral responses to both temperature and salinity, but with differing functional responses. The aversion of Delta Smelt to warm water was barely detectable over a wide range of temperatures, but became quite pronounced near the CT_{max} of the species (i.e., a nonlinear response to temperature). Results of the temperature preference study support the finding by Nobriga et al. that Delta Smelt capture probabilities decrease abruptly at temperatures higher than 24°C in the SFE[33] and suggest that the species is actively avoiding high temperatures in the wild. Our findings also suggest Delta Smelt will strongly avoid certain areas with sub-acute temperatures,

such as some parts of Yolo Bypass floodway in summer[70]. We want to emphasize that our findings are most applicable to sub-adult Delta Smelt, as younger or older life-stages may have different preferences, as with temperature tolerances[21]. Like with temperature, the preference of Delta Smelt for fresher water became more pronounced as salinity increased, but strengthened linearly from freshwater to 23 ppt. Results of the salinity preference study align with Delta Smelt distribution in the wild, in that Delta Smelt actively seek out fresher water at the sub-adult stage, despite their ability to tolerate far higher salinities.

REFERENCES

1. Moyle, P. B. Inland fishes of California. Berkeley, CA: University of California Press (2002).
2. Moyle, P. B., Brown, L. R., Durand, J. R., & Hobbs, J. A. Delta Smelt: Life history and decline of a once-abundant species in the San Francisco Estuary. *San Franc. Estuary Watershed Sci.* **14**, 1-28 (2016).
3. U. S. Fish and Wildlife Service. Endangered and threatened wildlife and plants: determination of threatened status of the Delta Smelt. *Federal Register* **58**, 12854-12864 (1993).
4. California Department of Fish and Wildlife. State and federally listed endangered and threatened animals of California. California Department of Fish and Wildlife, The Natural Resources Agency, North Highlands (2017).
5. Moyle, P. B. & Bennett, W. A. The future of the Delta ecosystem and its fish, Technical Appendix D. Comparing Futures for the Sacramento-San Joaquin Delta. San Francisco (CA): Public Policy Institute of California (2008).
6. Lund, J. R. *et al.* Comparing futures for the Sacramento-San Joaquin Delta. University of California Press: Public Policy Institute of California (2010).
7. Moyle, P. B., Bennett, W. A., Fleenor, W. E. & Lund, J. R. Habitat variability and complexity in the upper San Francisco Estuary. *San Franc. Estuary Watershed Sci.* **8**, 1-24 (2010).
8. Feyrer, F., Newman, K., Nobriga, M. & Sommer, T. Modeling the effects of future outflow on the abiotic habitat of an imperiled estuarine fish. *Estuaries Coast.* **34**, 120-128 (2011).
9. Cloern, J. E. & Jassby, A. D. Drivers of change in estuarine-coastal ecosystems: Discoveries from four decades of study in San Francisco Bay. *Rev. Geophys.* **50**, RG4001 (2012).
10. Moyle, P. B., Hobbs, J. A. & Durand, J. R. Delta Smelt and water politics in California. *Fisheries* **43**, 42-60 (2018).
11. Mahardja, B. *et al.* Resistance and resilience of pelagic and littoral fishes to drought in the San Francisco Estuary. *Ecol. Appl.* **31**, e02243 (2021).

12. Börk, K., Moyle, P., Durand, J., Hung, T.-C. & Rypel, A. L. Small populations in jeopardy: delta smelt case study. *Environ. Law Reporter* **50**, 10714-10722 (2020).

13. Moyle, P. B. 2021. Experimental habitats for hatchery Delta Smelt. *California WaterBlog* https://californiawaterblog.com/2021/07/25/experimental-habitats-for-hatchery-delta-smelt/ (2021).

14. Jeffries, K. M. *et al.* Effects of high temperatures on threatened estuarine fishes during periods of extreme drought. *J. Exp. Biol.* **219**, 1705-1716 (2016).

15. Bashevkin, S. M. & Mahardja, B. Seasonally variable relationships between surface water temperature and inflow in the upper San Francisco Estuary. *Limnol. Oceanogr.* **67**, 684-702 (2022).

16. Brown, L. R. *et al.* Coupled downscaled climate models and ecophysiological metrics forecast habitat compression for an endangered estuarine fish. *PLoS One* **11**, e0146724 (2015).

17. Kurobe, T. *et al.* Reproductive strategy of Delta Smelt Hypomesus transpacificus and impacts of drought on reproductive performance. *PLoS One* **17**, e0264731 (2022).

18. Lewis, L. S. *et al.* Otolith-based approaches indicate strong effects of environmental variation on growth of a critically endangered estuarine fish. *Mar. Ecol. Prog.* **676**, 37-56 (2021).

19. Hammock, B. G. *et al.* Patterns and predictors of condition indices in a critically endangered fish. *Hydrobiologia* **849**, 675–695 (2021).

20. Bennett, W. A. Critical assessment of the delta smelt population in the San Francisco Estuary, California. *San Franc. Estuary Watershed Sci.* **3**, article 1 (2005).

21. Komoroske, L. M. *et al.* Ontogeny influences sensitivity to climate change stressors in an endangered fish. *Conserv. Physiol.* **2**, cou008 (2014).

22. Moyle, P. B., Herbold, B., Stevens, D. E. & Miller, L. W. Life history of delta smelt in the Sacramento-San Joaquin Estuary, California. *Trans. Am. Fish. Soc.* **121**, 67-77 (1992).

23. Kimmerer, W. J., MacWilliams, M. L. & Gross, E. S. Variation of fish habitat and extent of the low-salinity zone with freshwater flow in the San Francisco Estuary. *San Franc. Estuary Watershed Sci.* **11** (2013).

24. Sommer, T. & Meija, F. A place to call home: A synthesis of delta smelt habitats in the upper San Francisco Estuary. *San Franc. Estuary Watershed Sci.* **9** (2013).

25. Hammock, B. G. *et al.* Foraging and metabolic consequences of semi-anadromy for an endangered estuarine fish. *PLoS One* **12**, e0173497 (2017).

26. Cox, D. Effects of three heating rates on the critical thermal maximum of Bluegill. In W Gibbons, R Sharitz, eds, *Thermal Ecology.* National Technical Information Service, Springfield, IL, pp 158–163 (1974).

27. Beitinger, T. L., Bennett, W. A. & McCauley, R. W. Temperature tolerances of North American freshwater fishes exposed to dynamic changes in temperature. *Environ. Biol. Fishes* **58**, 237–275 (2000).

28. Davis, B. E. *et al.* Sensitivities of an endemic, endangered California smelt and two non-native fishes to serial increases in temperature and salinity: implications for shifting community structure with climate change. *Conserv. Physiol.* **7**, coy076 (2019).

29. Swanson, C., Reid, T., Young, P. S. & Cech, J. J. Jr. Comparative environmental tolerances of threatened delta smelt (Hypomesus transpacificus) and introduced wakasagi (H. nipponensis) in an altered California estuary. *Oecologia* **123**, 384-390 (2000).

30. Hammock, B. G., Hobbs, J. A., Slater, S. B., Acuña, S. & Teh, S. J. Contaminant and food limitation stress in an endangered estuarine fish. *Sci. Total Environ.* **532**, 316-326 (2015).

31. Hamilton, S. A. & Murphy, D. D. Analysis of limiting factors across the life cycle of delta smelt (Hypomesus transpacificus). *Environ. Manage.* **62**, 365-382 (2018).

32. Feyrer, F., Nobriga, M. L. & Sommer, T. R. Multidecadal trends for three declining fish species: Habitat patterns and mechanisms in the San Francisco Estuary, California, USA. *Can. J. Fish. Aquat. Sci.* **64**, 723-734 (2007).

33. Nobriga, M. L., Sommer, T. R., Feyrer, F. & Fleming, K. Long-term trends in summertime habitat suitability for delta smelt (Hypomesus transpacificus). *San Franc. Estuary Watershed Sci.* **6**, article 1 (2008).

34. Brown, L. R. *et al.* Implications for future survival of delta smelt from four climate change scenarios for the Sacramento–San Joaquin Delta, California. *Estuaries Coast.* **36**, 754-774 (2013).

35. Moyle, P., Kiernan, J. D., Crain, P. K. & Quiñones, R. M. Climate change vulnerability of native and alien freshwater fishes of California: A systematic assessment approach. *PLoS One* **8**, e63883 (2013).

36. Hobbs, J. A., Lewis, L. S., Willmes, M., Denney, C. & Bush, E. Complex life histories discovered in a critically endangered fish. *Sci. Rep.* **9**, 16772 (2019).

37. Bennett, W. A. & Burau, J. R. Riders on the storm: Selective tidal movements facilitate the spawning migration of threatened Delta Smelt in the San Francisco Estuary. *Estuaries Coast.* **38**, 826-835 (2015).

38. Hirvonen, H., Ranta, E., Piironen, J., Laurila, A. & Peuhkuri, N. Behavioral responses of naive Arctic charr to chemical cues from salmonid and non-salmonid fish. *Oikos* **88**, 191-199 (2000).

39. Correia, A. M., Bandeira, N. & Anastacio, P. M. Influence of chemical and visual stimuli in food-search behaviour of Procambarus clarkii under clear conditions. *Mar. Freshw. Behav. Physiol.* **40**, 189-194 (2007).

40. Nay, T. J. *et al.* Habitat complexity influences selection of thermal environment in a common coral reef fish. *Conserv. Physiol.* **8**, coaa070 (2020).

41. Horning, W. B. & Weber, C. I. Short-term methods for estimating the chronic toxicity of effluents and receiving waters to freshwater organisms. EPA/600/4-85/014, pp. 58–75 (1985).

42. Lindberg, J. *et al.* Aquaculture methods for a genetically managed population of endangered delta smelt. *N. Am. J. Aquac.* **75**, 186-196 (2013).

43. Ferrari, M. C. O. *et al.* Effects of turbidity and an invasive waterweed on predation by introduced largemouth bass. *Environ. Biol. Fishes* **97**, 79-90 (2014).

44. Petersen, M. F. & Steffensen, T. F. Preferred temperature of juvenile Atlantic cod Gadus morhua with different haemoglobin genotypes at normoxia and moderate hypoxia. *J. Exp. Biol.* **206**, 359-364 (2003).

45. Meager, J. J. & Utne-Palm, A. C. Effect of turbidity on habitat preference of juvenile Atlantic cod, Gadus morhua. *Environ. Biol. Fishes* **81**, 149-155 (2008).

46. Serrano, X., Grosell, M. & Serafy, J. E. Salinity selection and preference of the grey snapper Lutjanus griseus: field and laboratory observations. *J. Fish Biol.* **76**, 1592-1608 (2010).

47. Stol, J. A., Svendsen, J. C. & Enders, E. C. Determining the thermal preferences of Carmine Shiner (Notropis percobromus) and Lake Sturgeon (Acipenser fulvescens) using an automated shuttlebox. *Can. Tech. Rep. Fish. Aquat. Sci.* 3038 (2013).

48. Hammock, B. G. *et al.* The health and condition responses of Delta Smelt to fasting: A time series experiment. *PLoS One* **15**, e0239358 (2020).

49. McElreath, R. Statistical rethinking: A Bayesian course with examples in R and Stan. CRC Press (2016).

50. R Core Team. R: A language and environment for statistical computing (2021).

51. Bates, D., Maechler, M. & Bolker, B. lme4: Linear mixed-effects models using S4 classes (2012).

52. Korner-Nievergelt, F. *et al.* Bayesian data analysis in ecology using linear models with R, BUGS and Stan. Elsevier (2015).

53. Gilliam, J. F. & Fraser, D. F. Habitat selection under predation hazard: test of a model with foraging minnows. *Ecology* **68**, 1856-1862 (1987).

54. Metcalfe, N. B., Fraser, N. H. & Burns, M. D. Food availability and the nocturnal vs. diurnal foraging trade-off in juvenile salmon. *J. Anim. Ecol.* **68**, 371-381 (1999).

55. Walters, C. J. & Juanes, F. Recruitment limitation as a consequence of natural selection for use of restricted feeding habitats and predation risk taking by juvenile fishes. *Can. J. Fish. Aquat. Sci.* **50**, 2058-2070 (1993).

56. Bull, H. O. Studies on conditioned responses in fishes. Part VII. Temperature perception in teleosts. *J. Mar. Biol. Assoc. U. K.* **21**, 1-27 (1936).

57. Steffel, S., Magnuson, J. J., Dizon, A. E. & Neill, W. H. Temperature discrimination by captive free-swimming tuna, Euthynnus affinis. *Trans. Am. Fish. Soc.* **105**, 588-591 (1976).

58. Dülger, N. *et al.* Thermal tolerance of European Sea Bass (Dicentrarchus labrax) juveniles acclimated to three temperature levels. *J. Therm. Biol.* **37**, 79-82 (2012).

59. Hung, T.-C. *et al.* A pilot study of the performance of captive-reared delta smelt Hypomesus transpacificus in a semi-natural environment. *J. Fish Biol.* **95**, 1517-1522 (2019).

60. Navarro, I. & Gutie´rrez, J. Fasting and starvation. *Biochemistry and molecular biology of fishes*. 4: Elsevier. p. 393-434 (1995).

61. Finger, A. J. *et al.* A conservation hatchery population of Delta Smelt shows evidence of genetic adaptation to captivity after 9 generations. *J. Hered.* **109**, 689-699 (2018).

62. Middaugh, D. P., Davis, W. R. & Yokum, R. L. The response of larval fish, Leiostomus xanthurus, to environmental stress following sublethal cadmium exposure. *Contrib. Mar. Sci.* **19**, 13-19 (1975).

63. Stevens, E. D. & Sutterlin, A. M. Heat transfer between fish and ambient water. *J. Exp. Biol.* **65**, 131-145 (1976).

64. Beitinger, T. L., Thommes, M. M. & Spigarelli, S. A. Relative roles of conduction and convection in the body temperature change of gizzard shad, Dorosoma cepedianum. *Comp. Biochem. Physiol.* **57A**, 275-279 (1977).

65. Neill, W. H. & Magnuson, J. J. Distributional ecology and behavioral thermoregulation of fishes in relation to heated effluents from a power plant at Lake Monona, Wisconsin. *Trans. Am. Fish. Soc.* **103**, 663-710 (1974).

66. Coutant, C. C. Temperature selection by fish–a factor in power plant impact assessments. pp. 575–597. In: *Environmental Effects of Cooling Systems at Nuclear Power Plants*, Internat. Atomic Energy Agency, Vienna (1975).

67. Richards, F. P., Reynolds, W. W. & McCauley, R. W. Temperature preference studies in environmental impact assessment: an overview with procedural recommendations. *J. Fish. Res. Board Can.* **34**, 728-761 (1977).

68. Swanson, C., Mager, R. C., Doroshov, S. I. & Cech, J. J. Jr. Use of salts, anesthetics, and polymers to minimize handling and transport mortality in delta smelt. *Trans. Am. Fish. Soc.* **125**, 326-329 (1996).

69. Komoroske, L. M. *et al.* Sublethal salinity stress contributes to habitat limitation in an endangered estuarine fish. *Evol. Appl.* **9**, 963-981 (2016).

70. Feyrer, F., Sommer, T. & Harrell, W. Importance of flood dynamics versus intrinsic physical habitat in structuring fish communities: evidence from two adjacent engineered floodplains on the Sacramento River, California. *N. Am. J. Aquac.* **26**, 408-417 (2006).

ACKNOWLEDGEMENTS

We would like to acknowledge S. Serrato and G. Wu (Aquatic Health Program, UC Davis, CA) for their dedication to system operation, fish husbandry, and water quality monitoring. We also acknowledge the FCCL for providing fish and Interagency Ecological Program and the US Bureau of Reclamation (R10AC20014) for funding the study.

AUTHOR CONTRIBUTIONS

TCH, JCL, and SJT conceptualized and designed the experiments. TCH and MP conducted the study. TCH and BGH analyzed data. TCH, JCL and SJT oversaw the rearing and care of fish for the study. TCH drafted the original manuscript with detailed edits from BGH, MS, MS, JCL, and SJT. TCH, BGH, JCL and SJT acquired funding.

DATA AVAILABILITY STATEMENT

Data are available upon request to the corresponding author.

COMPETING INTERESTS

The authors declare no competing interests.

FIGURES

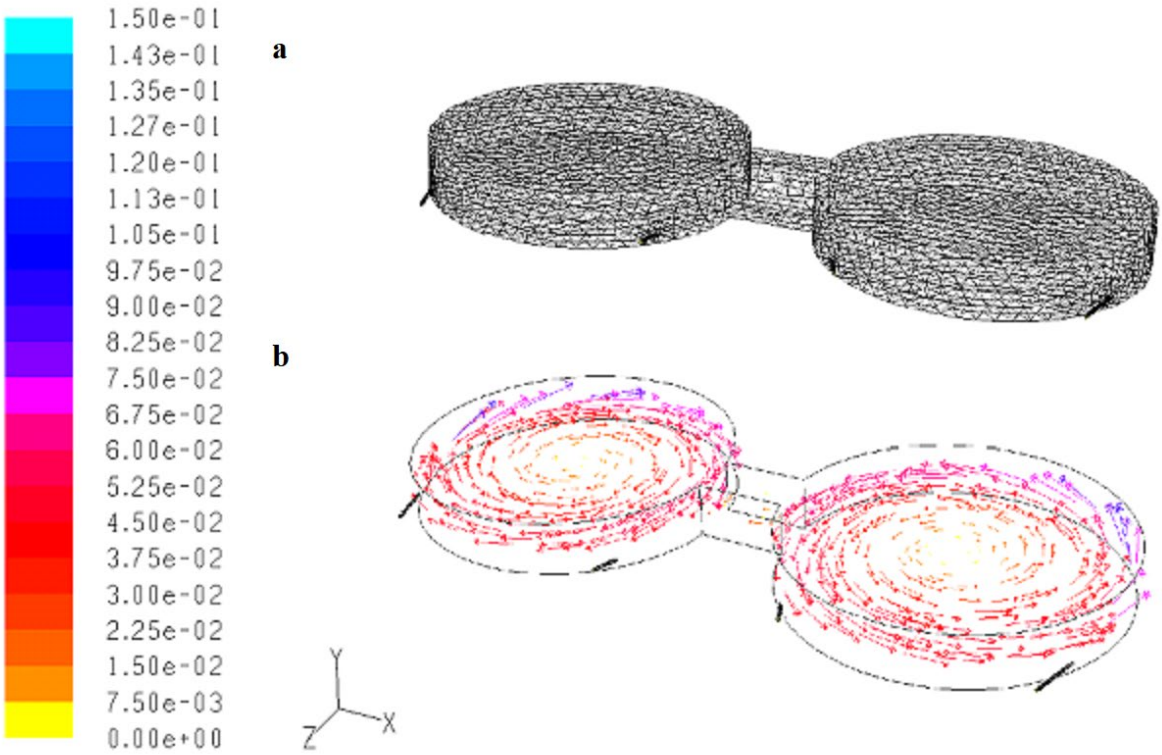

Figure 1-1: Numerical simulation of the flow patterns in the testing system.

(a) The configuration of the model and computational grids used and (b) velocity vectors (m/s) at the middle of cross section of the system.

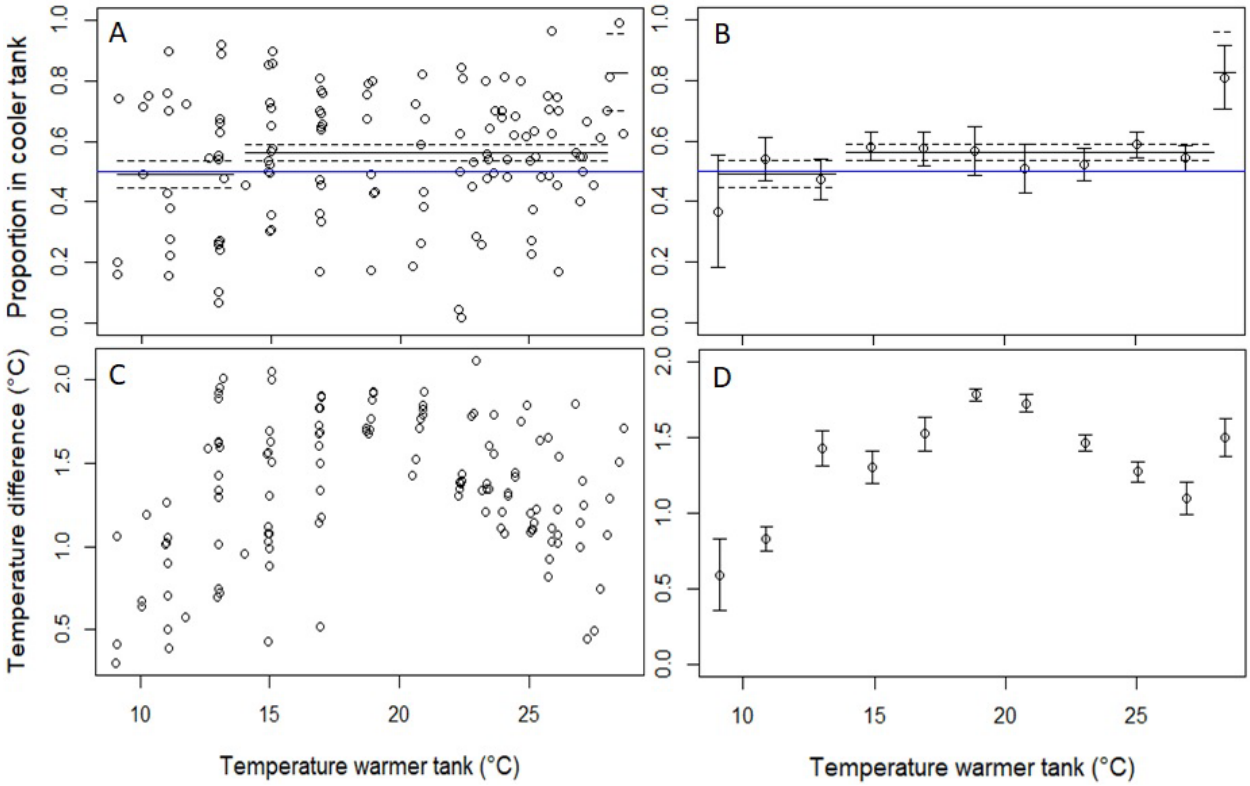

Figure 1-2: Panel (a) shows the proportion of sub-adult Delta Smelt in the cooler tank versus water temperature in the warmer tank.

The solid black line represents the top-ranked model and the dashed lines are the 95% CI. Panel (b) shows the difference in water temperature between the higher and lower temperature tank by temperature in the warmer tank. Panel (c) shows the same as panel (a), but with means ±SE for temperature bins rather than raw data. Panel (d) shows the same as panel (b) but with means calculated for temperature bins. The mean temperature difference between the warmer and cooler tanks was 1.3°C (SD = 0.5°C). Note that the blue, horizontal line indicates no preference (i.e., a y-intercept of 0.5).

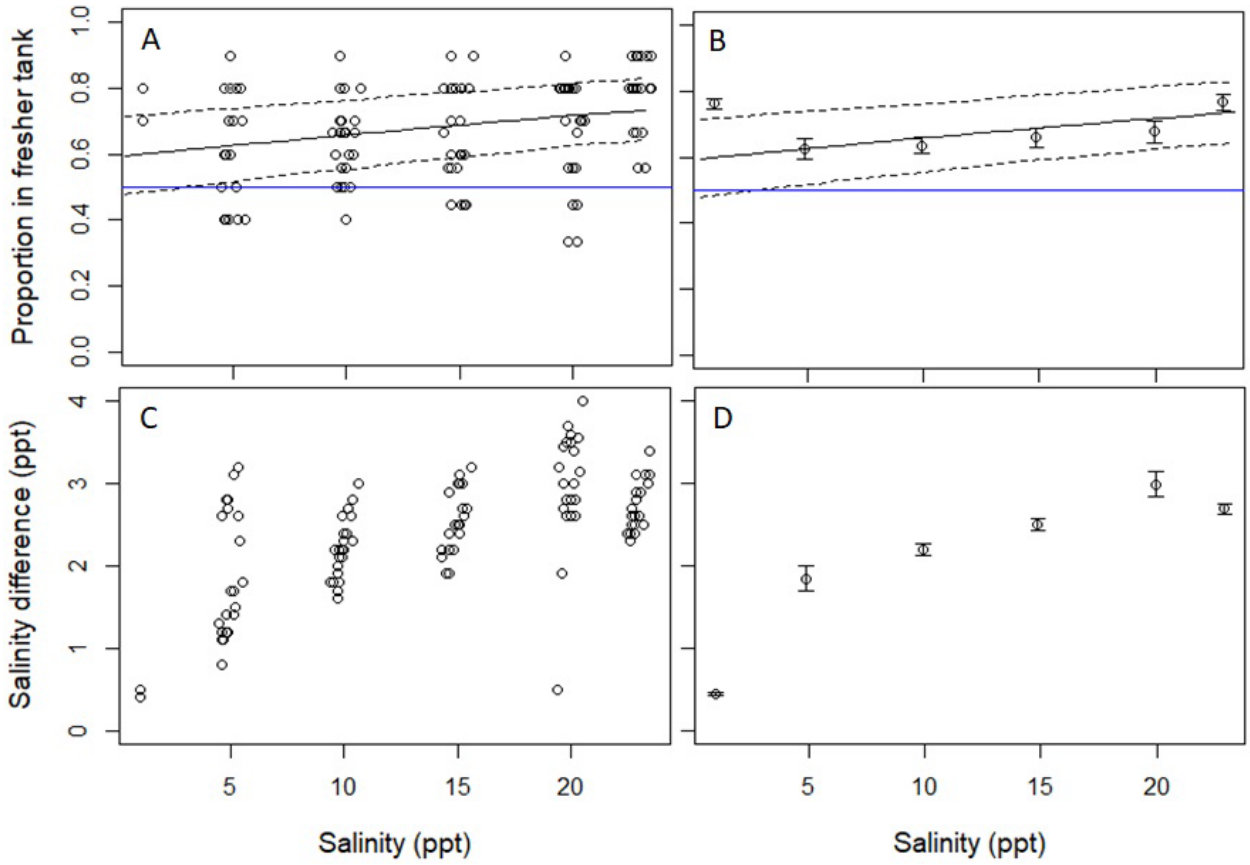

Figure 1-3: Panel (a) shows the proportion of sub-adult Delta Smelt in the fresher tank versus salinity in the higher salinity tank.

The solid line represents the top-ranked (intercept model) and the dashed lines are the 95% CI. Panel (b) shows a scatterplot of the difference in salinity between the two tanks by salinity in the higher salinity tank. Panel (c) shows the same plot as panel (a) but with means calculated for temperature bins. Panel (d) shows the mean difference in salinity between the two tanks by salinity in the higher salinity tank. An average salinity difference of 2.2 ppt was maintained between the two tanks (SD = 0.9 ppt). Note that the blue, horizontal line indicates no preference (i.e., a y-intercept of 0.5).

TABLES

Table 1-1: Model comparison for the temperature preference experiment.

'Temp 3bins' is a variable in which the temperature of the warmer tank was divided into three bins, low (9.1-13.2°C), medium (14.0-28.0°C), and high temperature (28.1-28.8°C). 'Temp 2bins' is a variable in which the temperature of the warmer tank was divided into two bins, <28.0°C and >28.0°C. 'Temp' is the temperature in the warmer tank as a continuous variable. 'Acclimation T' is the temperature at which Delta Smelt were acclimated (14 or 17°C).

Model #	Model	ΔAIC_c	df	AIC_c wt
4	Temp 3bins	0.0	4	0.6022
5	Temp 3bins + Acclimation T	1.5	5	0.2849
3	Temp 2bins	3.9	3	0.0875
2	Temp	6.7	3	0.0212
1	Intercept	9.9	2	0.0043

ΔAIC_c: difference between model of interest and top-ranked model in Akaike Information Criterion Units corrected for small sample size, *df*: degrees of freedom, and *AIC_c wt*: Akaike weight.

Table 1-2: Model comparison for the salinity preference experiment.

'Sal' is the salinity of the more saline tank, 'Sal difference' is the difference in salinity between the two tanks, which was correlated with 'Sal' (i.e, the higher salinities had larger differences in salinity between the two tanks).

Model #	Model	ΔAIC_c	df	AIC_c wt
2	~Sal	0.0	3	0.937
3	~Sal difference	6.2	3	0.041
1	~Intercept	7.5	2	0.022

ΔAIC_c: difference between model of interest and top-ranked model in Akaike Information Criterion Units corrected for small sample size, *df*: degrees of freedom, and *AIC_c wt*: Akaike weight.

SUPPLEMENTAL MATERIAL

Tien-Chieh Hung[1,*], Bruce G. Hammock[2], Marade Sandford[1], Marie Stillway[2], Michael Park[2], Joan C. Lindberg[1], Swee J. Teh[2]

[1]Fish Conservation and Culture Laboratory
Department of Biological and Agricultural Engineering
University of California, Davis
Davis, CA 95616

[2]Aquatic Health Program
Veterinary Medicine: Anatomy, Physiology, and Cell Biology
University of California, Davis
Davis, CA 95616, USA

***Corresponding author:**

thung@ucdavis.edu

Supplemental Figures

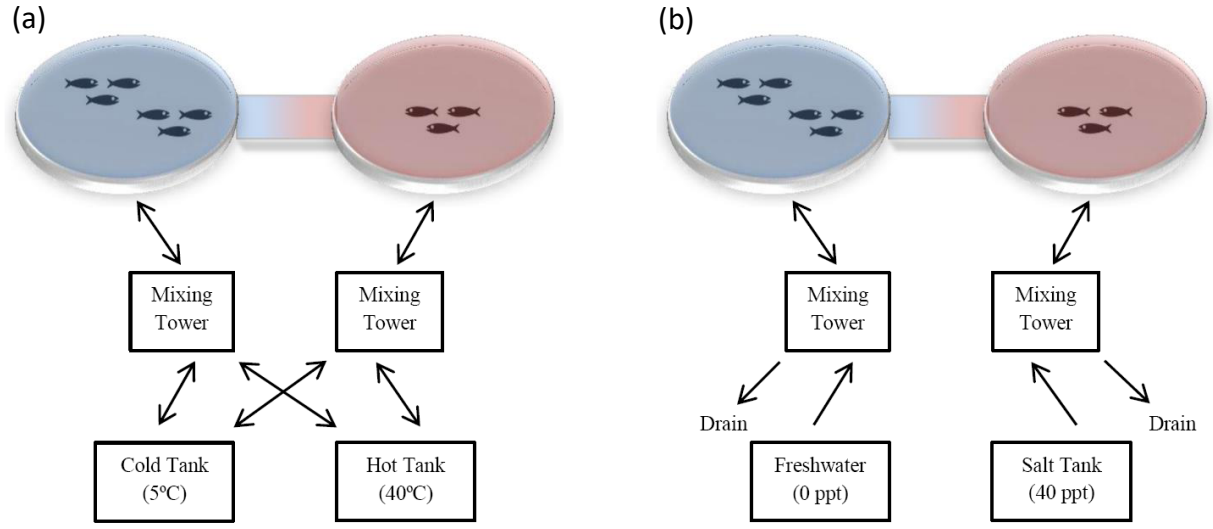

Figure S1-1: Schematic diagrams of the testing system for (a) temperature and (b) salinity trials.

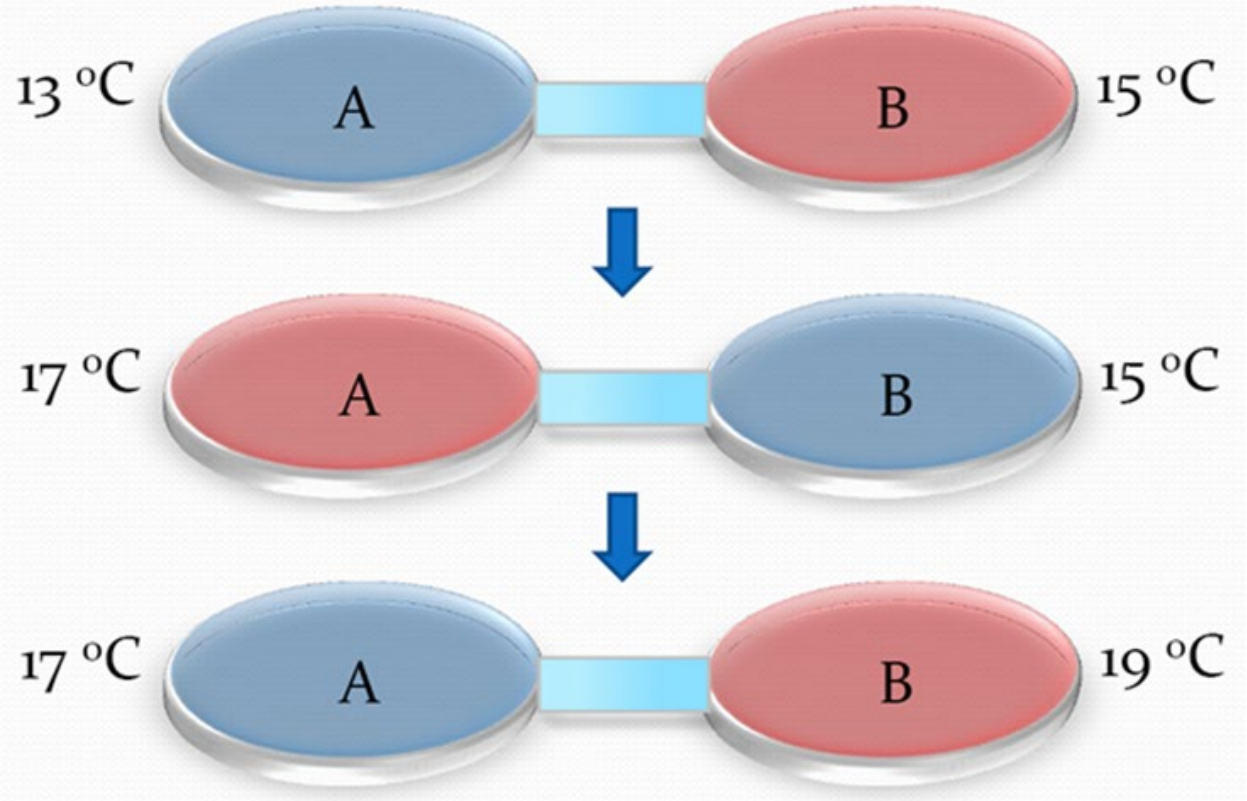

Figure S1-2: Operational strategy of temperature trials.

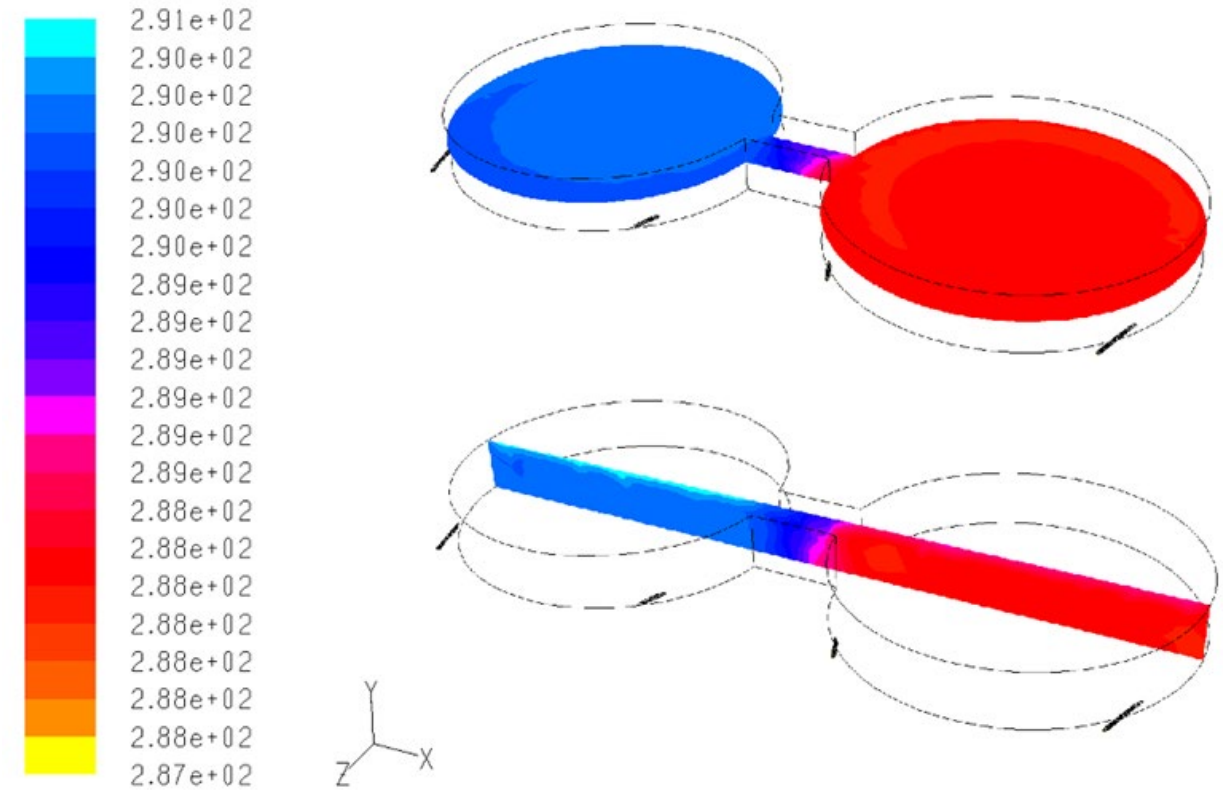

Figure S1-3: Temperature distribution at the middle of cross section of the testing system. The unit is Kelvin (K).

Chapter 2: Liver Glycogen as a Sensitive Indicator of Food Limitation in Delta Smelt

Authors:

Tena S. Dhayalan[a], Franklin D. Tran[a], Tien-Chieh Hung[b], Taylor J. Senegal[c], Vanessa Mora[d], Levi S. Lewis[e], Swee J. Teh[a], Bruce G. Hammock[a,*]

[a]Aquatic Health Program, School of Veterinary Medicine, Department of Anatomy, Physiology, and Cell Biology, University of California, Davis, 1089 Veterinary Medicine Drive, Vet Med 3B, Davis, CA 95616, USA

[b]Fish Conservation and Culture Laboratory, Biological and Agricultural Engineering Department, University of California, Davis, One Shields Avenue, Davis, CA 95616, USA

[c]U.S. Fish and Wildlife Service, 850 S. Guild Ave, Suite 105, Lodi, CA 95240, USA

[d]California Department of Fish and Wildlife, 2109 Arch Airport Road, Suite 100, Stockton, CA, 95206, USA

[e]Otolith Geochemistry and Fish Ecology Laboratory, Department of Wildlife, Fish, and Conservation Biology, University of California, Davis, One Shields Avenue, Davis, CA 95616, USA

*Corresponding author: brucehammock@gmail.com

Keywords:

fish, fasting, biochemistry, energy reserves, biomarker

ABSTRACT

Assessing habitat quality is a major goal of conservationists and restoration practitioners, but to associate habitat quality with biomarkers of vagile animals, the biomarkers must respond rapidly. Here we identified a biomarker capable of rapidly detecting food limitation in the imperiled Delta Smelt (*Hypomesus transpacificus*), a pelagic fish endemic to the San Francisco Estuary (SFE). We conducted an experiment with fed and unfed treatments of hatchery-raised, sub-adult Delta Smelt that were sampled at 12 time points: 0, 1, 2, 3, 4, 5, 6, 7, 9, 11, 14, and 21 days. We then compared four biomarkers using Day 21 fish: RNA/DNA in liver, triglycerides in liver, glycogen in liver, and glycogen in muscle. Of the three liver endpoints, glycogen had the largest, most significant difference between treatments at Day 21, so we compared it to muscle glycogen across all time points. Liver glycogen declined after just one day of fasting and remained depressed in the fasting treatment across all subsequent time points. Muscle glycogen also responded rapidly, taking only two days to decline in the fasting treatment, but the difference was small and inconsistent across subsequent time points. When applied to hatchery-released

Delta Smelt collected from the SFE, we found that liver glycogen concentrations were less than half that of the fed hatchery fish, consistent with the hypothesis of food limitation in the wild, but also several other potential causes. This study highlights the utility of biochemically determining liver glycogen concentrations of wild-caught Delta Smelt to provide insight into local habitat quality.

INTRODUCTION

Many fishes experience periods of food limitation due to declines in food supply, high water temperature, estivation, or migration. In some cases, individuals do not survive these periods, resulting in population declines (Theilacker 1986; Hurst 2007; Le Pape & Bonhommeau 2015; Saulnier et al. 2020). Therefore, considerable interest exists in detecting food limitation in wild fish populations, particularly in commercial or imperiled species. However, due to differences in physiology and life history strategies, fish have evolved species-specific responses to food limitation (e.g., mobilization of preferred energy stores) which can change based on environmental factors, making them difficult to predict even within a species (Valtonen 1974; Coban & Sen 2011; Vornanen et al. 2011; Liew et al. 2012; Jiao et al. 2020). For example, although most fishes utilize carbohydrates as a primary source of energy during initial stages of food limitation, Goldfish prioritize protein metabolism (Storer 1967; Liew et al. 2012), while Mudskippers initially metabolize lipids (Lim & Ip 1989). Variation in the temperature among fasting studies adds further complexity, as biomarkers of food limitation respond more quickly at higher temperatures (Brown et al. 2004; Volkoff & Rønnestad 2020; Pham et al. 2022). Given the large variation among fishes and fasting studies, identifying the initial responses to food limitation and their timings necessitates species and temperature-specific experiments.

There are a variety of indicators used to assess nutritional condition in fish, at scales ranging from molecular to whole-body. RNA/DNA is a proxy for recent growth because RNA concentration increases with increasing protein synthesis, while DNA concentration remains constant. RNA/DNA can respond to changes in feeding and growth within 1-3 days (Bulow 1970; Buckley et al. 1999; Yandi & Altinok 2018) and is widely used to assess recent nutritional condition, and therefore habitat quality (e.g., Tanaka et al. 2008). While RNA/DNA is typically measured in muscle, it can also be measured in the liver. For example, liver RNA/DNA decreased within two weeks of fasting in juvenile Copper Rockfish (12 °C; Hack et al. 2019) and after three weeks of fasting in Zebrafish (28 °C; Fan et al. 2019). More recent methods quantify the expression of genes related to growth or energy metabolism to evaluate nutritional stress. For example, the expression of insulin is reduced after three days of fasting in Yangtze Sturgeon (Zhang et al. 2022), and transcriptional activity of genes controlling lipid metabolism differs between fasted and fed European Sea Bass after 15 days (Rimoldi et al. 2016).

Quantifying energy stores like carbohydrates and lipids can also provide valuable insight into nutritional status. Glycogen, a major form of carbohydrate storage in fishes, can be a sensitive biomarker to food limitation (Navarro & Gutiérrez 1995; Hemre et al. 2002; Furné et al. 2012). The main sites of glycogen storage are the liver and skeletal muscle; the liver maintains blood glucose levels through glycogenolysis and muscle glycogen serves as a form of local energy

(Rossi et al. 2015; Soengas & Aldegunde 2002). Some fishes utilize liver glycogen over muscle glycogen during periods of food limitation (Barcellos et al. 2010; Navarro et al. 1992), while some favor muscle glycogen (Lim & Ip 1989), and others utilize both simultaneously (Black & Love 1986; Mehner & Weiser 1994). Triglycerides are the most readily available lipid reserve, with studies showing increased plasma triglyceride levels following 1-3 days of fasting in European Sea Bass and Rainbow Trout (22-24 °C; Pérez-Jiménez et al. 2007; Bermejo-Poza et al. 2020). Triglycerides and glycogen in liver can both respond quickly to food limitation, with lower concentrations of both energy stores observed in Nile Tilapia after just one day of fasting at 30 °C (Wang et al. 2019).

Condition factor, hepatosomatic index, and stomach fullness are widely used gravimetric indicators of nutritional status. Condition factor reflects the 'plumpness' of a fish and is sensitive to fasting because weight generally responds to fasting more readily than length (Weatherley & Gill 1981; Hvas et al. 2021). The liver is especially sensitive to fasting, responding through glycogen depletion, hepatocyte atrophy, mitochondrial enlargement, and necrosis (Weis 1972; Storch & Juario 1983; Panserat et al. 2019). These responses result in a rapid decrease in liver weight relative to the body, as measured by hepatosomatic index. For example, differences between fed and unfed juvenile Nile Tilapia were detected after two weeks using hepatosomatic index, while condition factor took three weeks to respond (25 °C; Abdel-Tawwab et al. 2006). Stomach fullness quantifies recent foraging success and has been widely used to study feeding habits and diet composition (Gill & Hart 1994; Nemerson & Able 2004; Hung et al. 2019; Carniatto et al. 2020). However, stomach fullness is best paired with other biomarkers because it can overestimate the importance of slowly digested prey or indigestible remains, and it provides an instantaneous snapshot of food consumption that may not represent overall nutritional status of the fish (Hyslop 1980; Amundsen & Sánchez-Hernández 2019).

One fish for which biomarkers sensitive to food limitation have yet to be validated is the Delta Smelt, *Hypomesus transpacificus*— a small, pelagic, imperiled species endemic to the San Francisco Estuary (SFE). The SFE is formed by the confluence of the Sacramento and San Joaquin rivers and the Pacific Ocean in California, USA. Despite high nutrient concentrations in the SFE, phytoplankton, zooplankton, and pelagic fish, including the Delta Smelt, have all exhibited similarly timed, negative exponential declines in abundance beginning in the early 1970s (Hammock et al. 2019a). While there are many explanations for the decline in pelagic fish, the loss of pelagic primary productivity and resultant prey scarcity is perhaps the most widely accepted (e.g., Feyrer et al. 2003; Sommer et al. 2007; Miller et al. 2012).

A recent study by Hammock et al. (2020) compared the sensitivities—defined as the time taken for a biomarker to respond to a stressor at constant water temperature—of many biomarkers of food limitation in Delta Smelt, including condition factor, hepatosomatic index, RNA/DNA in muscle, triglycerides in muscle, and histopathologic responses in the liver. Hepatosomatic index was the most sensitive measure of food limitation examined, declining significantly after four days of fasting at 16 °C, followed by condition factor at seven days. This was the rationale for subsequently modeling hepatosomatic index and condition factor of Delta Smelt as a function of environmental variables such as water temperature, salinity, and zooplankton abundance

(Hammock et al. 2021). However, Delta Smelt could conceivably swim a considerable distance in four days given their estimated swimming speed of 0.72 km/h (Swanson et al. 1998), especially if aided by currents (Bennett and Burau 2015). Thus, even our most sensitive biomarkers give individuals time to move among habitats of varying quality, obscuring the relationship between the level of hepatosomatic index or condition factor and the point of collection. Moreover, the two biochemical biomarkers examined in the muscle by Hammock et al. (2020) were particularly insensitive, with responses to fasting first occurring after 28 days for RNA/DNA and 14 days for triglycerides, and inconsistently thereafter.

The present study is divided into three parts. First, Delta Smelt were fasted in an experiment similar to Hammock et al. (2020). In the experiment, we compared the responses of four biochemical biomarkers to fasting: RNA/DNA in liver, triglycerides in liver, glycogen in liver, and glycogen in dorsal muscle. Given the insensitivity of RNA/DNA and triglycerides in dorsal muscle observed in Hammock et al. (2020), our aim was to identify biomarkers that are highly sensitive to fasting in Delta Smelt. Therefore, we focused on biochemical responses in the liver, the center of many metabolic processes. However, muscle glycogen was of particular interest because Delta Smelt have small livers, which are useful for histopathology (e.g., Teh et al. 2020). Liver histopathology can leave little to no tissue for biochemical assays, especially for younger life stages. Second, we summarized the work to date on biomarkers of food limitation for Delta Smelt in terms of their sensitivities and dynamic (or linear) ranges – defined as the extent to which a biomarker responds linearly to a stressor. Finally, we applied the most sensitive of the four biomarkers to hatchery-raised Delta Smelt that were released into the wild and eventually recaptured (i.e., supplemental Delta Smelt). In the future, applying highly sensitive biomarkers to Delta Smelt collected from the wild will provide insight into habitat suitability, which will assist in restoration and conservation efforts.

MATERIALS AND METHODS

Fasting experiment

The fasting experiment was conducted at the UC Davis Fish Conservation and Culture Laboratory (FCCL) near Byron, CA, USA. Inasmuch as possible, this experiment followed the methods of our previous fasting experiment on Delta Smelt, described in Hammock et al. (2020; i.e., the same building, tanks, feed, life-stage, water temperature, etc.). On Sept 16, 2020, 800 sub-adult Delta Smelt were divided equally among eight, circular black tanks with working volumes of 290 L. The fish were given two weeks to acclimate to their new surroundings. During this period, tanks were fed to satiation following standard FCCL feeding protocol with Bio-vita Crum #1 (Bio-Oregon, Longview, WA). Five-micron particle filters were placed on the water inlets to each tank, and filters were changed weekly during the acclimation period and experiment to eliminate any potential food in the inflow. After the acclimation period ended on Oct 1, we randomly assigned four tanks to the ‘No Feeding’ treatment, and four to the ‘Feeding’ treatment. The ‘No Feeding’ treatment tanks were not provided food for the duration of the experiment. The ‘Feeding’ treatment tanks were fed to satiation as usual. Fish were 149 days post-hatch (dph) when the treatments were imposed (in Hammock et al. 2020, the fish were 157

dph when fasting began). Fish were sampled between ~10:30 am and 12:30 pm on the following time points: Day 0, 1, 2, 3, 4, 5, 6, 7, 9, 11, 14, and 21. We prioritized sampling early time points to focus on indicators of mild food limitation, as our previous study was successful in identifying several indicators of moderate to severe food limitation which were observed at later time points (Hammock et al. 2020). We ended the experiment at 21 days to avoid inflicting starvation-induced mortality, which began after 21 days in Hammock et al. (2020).

Test replicates were observed daily, mortalities were removed when present, and only live fish were sampled and analyzed for biomarkers. Water quality was measured approximately every three days throughout the experiment. Parameters included dissolved oxygen, salinity, pH, total ammonia-nitrogen, nitrite, and nitrate. Water temperature was measured hourly using HOBO temperature loggers placed in the tanks (Onset, MA, USA). Three fish from each tank were sampled on Day 0 of the experiment. Five fish were sampled from each tank for the remainder of the time points, except for Day 21, on which 15 fish were sampled from each tank. Thus, 68 fish were sampled from each tank, and 544 fish were sampled in total. Sampled fish were caught with an aquarium net, euthanized with an overdose of buffered Tricaine methanesulfonate (MS-222), blotted dry on a paper towel, wrapped in aluminum foil, and flash-frozen in liquid nitrogen. The study protocol was approved on May 14, 2020, by the University of California, Davis, Institutional Animal Care and Use Committee (protocol # 21737).

Application to supplemental Delta Smelt

From Dec 2021 through Feb 2022, more than fifty thousand adult Delta Smelt, raised at FCCL, were released into the SFE to evaluate survival, distribution and reproductive success for future supplementation to the wild population (Hung et al. 2022). From Dec 2021 through Mar 2022, 75 of these fish were recaptured during routine agency fish monitoring trawls and confirmed to be of hatchery origin based on adipose fin clips (hereafter ‘supplemental fish’). Of the 75 supplemental fish, 69 were flash-frozen immediately following collection, but the other 6 were kept live in buckets for several hours until they could be flash-frozen. All 75 supplemental fish were transported to UC Davis in liquid nitrogen for analysis.

Sample processing

We dissected 619 Delta Smelt (544 experimental fish and 75 supplemental fish) following a similar protocol to Teh et al. (2016). Briefly, Delta Smelt were removed from liquid nitrogen, photographed, measured for fork length, and weighed on an analytical balance (±0.01 mg). Liver and dorsal muscle were excised as the fish thawed over 5–10 min, weighed on an analytical balance (±0.01 mg), and then again flash frozen in liquid nitrogen for storage. Tissues were stored at -80˚C until processing for biochemistry.

Bioassays for experimental fish

The mean body weight of Delta Smelt from our experiment was small (mean 0.4 g), so we had insufficient tissue to run all four assays for every time point on each individual fish. Therefore, we identified the most promising bioassays by initially comparing each bioassay endpoint using Day 21 fish, making the assumption that the assays showing the most significant results on Day

21 would likely be the most sensitive to fasting. For the 21-day time point, liver and muscle samples from five fish per tank were pooled, resulting in three homogenate samples from each of the eight tanks (i.e., 12 pooled samples of 5 fish each for 60 fish of each treatment). The four assays were run on the homogenates, with liver glycogen having the most significant difference between the two treatments of the three liver assays. We therefore ran glycogen bioassays on liver for the remaining time points. Although the muscle glycogen endpoint was not as promising as liver glycogen based on the Day 21 results, we ran it for all time points as tissue limitation was not an issue.

Liver RNA/DNA

RNA/DNA in liver was measured using the ethidium bromide fluorometric technique reported by Caldarone et al (2001). Samples were evaluated using a microplate reader (Tecan Infinite M200).

Liver triglycerides

We measured liver triglyceride concentration using an adipogenesis assay kit (Catalog #K610-100, Biovision, CA, USA), as per the manufacturer's instructions and standardized to protein concentration that we determined following Lowry et al. (1951). Samples were evaluated using a microplate reader (Tecan Infinite M200). Triglyceride concentration is reported in nmol of triglyceride per mg of protein.

Liver and muscle glycogen

Muscle glycogen was measured for all experimental Delta Smelt, while liver glycogen was measured for all experimental and supplemental Delta Smelt. Muscle and liver tissue were homogenized in ice-cold Tris-EDTA buffer (5 mM Tris-HCl, 0.5 mM EDTA, pH 7.5) to reach a homogenate concentration of 1 mg tissue/20 µl Tris-EDTA buffer. Homogenates were then boiled at 100˚C for 10 min to denature enzymes that could alter glycogen concentrations. Homogenates were centrifuged, the supernatant collected, and was stored at -80˚C until glycogen measurement. Glycogen concentration was measured following the colorimetric method reported by Roehrig & Allred (1974) with modification. Briefly, 10 µl of homogenate was incubated with 7 units amyloglucosidase in 0.05M sodium acetate buffer pH 4.5 (Sigma-Aldrich #10115) at 60˚C for 30 min. Samples were then incubated in 1 unit glucose oxidase (Sigma-Aldrich #G7141), 2.5 purpurogallin units peroxidase (Sigma-Aldrich #P6782), and 0.125 mg o-dianisidine (Spectrum # TCI-D3864) in 0.1M sodium phosphate buffer pH 6 at 37˚C for 30 min and read on a spectrophotometer at 500 nm (Tecan Infinite M200). We used aliquots of 0-7 µg of bovine liver glycogen (Sigma-Aldrich # G0885) and D-(+)-Glucose (Sigma-Aldrich # G8270) to develop a standard curve. Samples were run in duplicate when sufficient homogenate was available. Glycogen is reported in µg of glycogen per mg of tissue.

Statistical analyses

Day 21: Liver RNA/DNA, liver triglycerides, liver glycogen, and muscle glycogen

The measurements from Day 21 fish were analyzed with four ANOVAs, one for each of the four bioassays. Each ANOVA included two predictors: *treatment* (Feeding and No Feeding) and *tank* (tanks 1 through 8). *Tank* was included as a random effect to account for the multiple measurements from the same tank. The liver and muscle glycogen variables were $\log_{10}$-transformed to address heterogeneity of variance (i.e., far greater variance in the Feeding than the No Feeding treatment).

Day 1 - 21: Liver and muscle glycogen

Separate factorial ANOVAs were performed on the liver and muscle glycogen results following Hammock et al. (2020). For both ANOVAs, predictors included *day*, *treatment*, a *day* by *treatment* interaction, *body weight*, a *body weight* by *treatment* interaction, and *tank* as a random effect. The *day* by *treatment* interaction was to account for any changing influence of treatment during the experiment. That is, we expected the influence of fasting to increase as the experiment progressed, from no treatment effect at Day 0 to a strong treatment effect by Day 21. The body weight of individuals was included as a predictor to test whether larger, more dominant fish had more glycogen-rich tissue (During preliminary analyses, we compared condition factor, fork length, and body weight as predictors. Body weight performed the best, so it was included in the analysis presented here). The *body weight* by *treatment* interaction tested the possibility that fish size had less influence on glycogen concentration in the No Feeding treatment (i.e., pervasive glycogen depletion, regardless of fish size). Interactions between *day* and *treatment* were deconstructed using planned linear contrasts (i.e., 'test slices' in JMP at each time point). Both liver and muscle glycogen were $\log_{10}$-transformed to account for the heterogeneity of variance apparent in plots of the residuals (higher variance in the Feeding treatment).

Application to supplemental Delta Smelt

We were interested in comparing the supplemental Delta Smelt to the fed and fasted experimental Delta Smelt to assess if the supplemental fish appeared to be receiving sufficient nutrition in the wild. Therefore, the liver glycogen concentrations of fish from the Feeding and No Feeding treatments and supplemental Delta Smelt were compared with an ANOVA. Because liver glycogen was stable from Day 1 – 14 and then appeared to decline from Day 14 – 21, the No Feeding treatment was divided into Day 1 – 14 and Day 21. Day 0 fish, from before the treatments were imposed, were excluded from the analysis. To account for the potential loss of liver glycogen while the supplemental fish were held in buckets for several hours, we analyzed these "bucket" fish separately from the other supplemental Delta Smelt. Thus, there were five treatments: Feeding (Day 1 – 21), No Feeding (Day 1 – 14), No Feeding (Day 21), Supplemental, and Bucket. The predictors included *group* (the four treatments) and *body weight*. Liver glycogen was $\log_{10}$-transformed to account for the heterogeneity of variance between groups, as above. In our preliminary analysis, we found no clear patterns in liver glycogen across characteristics such as sex, sexual maturity, and age, indicating that comparing the supplemental

fish, which were released as adults, to the sub-adults from our experiment, is reasonable. However, given larger sample size or age range this could change, as is seen in other species (Chang & Idler 1960, Valtonen 1974, Ng et al. 1986, Coban & Sen 2011). All analyses were performed in JMP Pro 16 at alpha = 0.05.

RESULTS

Water quality

Water quality was maintained at optimal levels for Delta Smelt throughout the study. Dissolved oxygen was 99.3 % (SD = 1.5), salinity was 0.31 (SD = 0.06), pH was 8.13 (SD = 0.07), total ammonia-nitrogen was 0.02 mg/L (SD = 0.02), nitrite was 0.012 mg/L (SD = 0.017), and nitrate was 0.92 mg/L (SD = 0.32), averaged over the acclimation and experimental periods. Water temperature averaged 15.9 °C (SD = 0.20), with a range of 15.5 to 16.3°C.

Mortality

In the present study, mortality rates were 18% and 11% for the Feeding and No Feeding treatments at termination on Day 21 (excluding the acclimation period). In Hammock et al. (2020), mortality rates were ~20% for both the Feeding and No Feeding treatments on Day 21, at which point mortality began increasing in the No Feeding treatment above control rates. Thus, mortality rates were somewhat lower than our previous experiment, and we avoided inducing mortality due to starvation.

Day 21: Liver RNA/DNA, liver triglycerides, liver glycogen, and muscle glycogen

On Day 21, the sample means of all four biomarkers were lower in the No Feeding treatment (Figure 2-1). Specifically, liver RNA/DNA was higher in the Feeding treatment by 2.1-fold (ANOVA, $F_{1,6} = 30.57$, P = 0.0015, Figure 2-1A). Liver triglycerides (nmol/mg protein) was higher in the Feeding treatment by 2.2-fold (ANOVA, $F_{1,6} = 19.95$, P = 0.0043, Figure 2-1B). Liver glycogen (µg glycogen/mg tissue) was 4.9-fold higher in the Feeding treatment (ANOVA, $F_{1,6} = 60.52$, P = 0.0002, Figure 2-1C). Finally, muscle glycogen (µg glycogen/mg tissue) was 1.4-fold higher in the Feeding treatment, although not significantly so (ANOVA, $F_{1,6} = 4.2498$, P = 0.0865, Figure 2-1D). Thus, liver glycogen showed the most significant difference at the final time point, and was therefore the most promising of the liver endpoints as a sensitive biomarker of fasting.

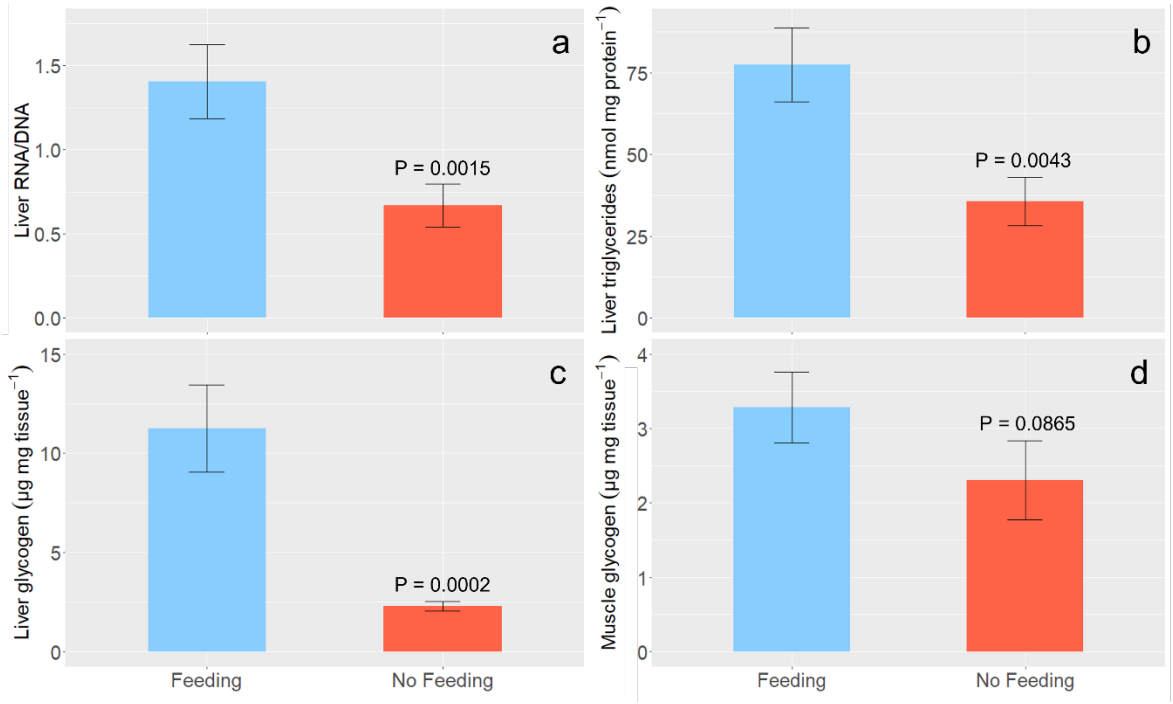

Figure 2-1: Mean liver RNA/DNA (panel a), liver triglycerides (panel b), liver glycogen (panel c), and muscle glycogen (panel d) for Delta Smelt from the Feeding and No Feeding treatments on Day 21. Error bars are ±SE

Day 0 – 21: Liver and muscle glycogen

For liver glycogen, there was an interaction between *day* and *treatment* (ANOVA, $F_{11, 379.3} = 2.45$, $P < 0.0057$), as the influence of the No Feeding treatment increased as the experiment progressed (Figure 2-2A). In the No Feeding treatment, liver glycogen declined rapidly from Day 0 to Day 1, was fairly stable from Day 1 through Day 14, and then declined again on Day 21 (Figure 2-2A). In contrast, liver glycogen remained fairly constant in the Feeding treatment, albeit with high variance. Based on the series of linear contrasts, *treatment* (Feeding and No Feeding) became significant on Day 1 (linear contrast, $P = 0.0002$) and stayed significant for the remainder of the experiment (Figure 2-2A). The sample means from the No Feeding treatment on days 1-14 ranged between 4.7-7.6 µg glycogen/mg tissue, indicating that liver glycogen concentrations below ~8 µg glycogen/mg tissue signifies moderate food limitation, at least in sub-adult, hatchery-raised Delta Smelt. A concentration below 2.5 µg glycogen/mg tissue indicates more severe starvation, as seen on Day 21. There was also a significant interaction between *body weight* and *treatment* (ANOVA, $F_{1,380.6} = 14.01$, $P = 0.0002$). Liver glycogen increased strongly with body weight in the Feeding treatment, but body weight had little to no influence on liver glycogen in the No Feeding treatment (Figure 2-3).

Muscle glycogen was lower overall in the No Feeding than in the Feeding treatment (ANOVA, $F_{1, 6.7} = 19.27$, $P = 0.0035$), but there was not a significant interaction between *day* and *treatment* (Feeding vs No Feeding; ANOVA, $F_{11, 397.5} = 1.27$, $P = 0.24$). Nevertheless, we ran linear

contrasts for each time point, as we did for liver. The contrasts showed that the treatment differences were inconsistent through time, with a significant influence of treatment on Days 2, 3, 5, 7, and 14, but nonsignificant differences on Days 0, 1, 4, 6, 9, 11, and 21 (Figure 2-2). In contrast to liver glycogen, there was no interaction between body weight and treatment (ANOVA, $F_{1, 401.4} = 0.38$, $P = 0.54$).

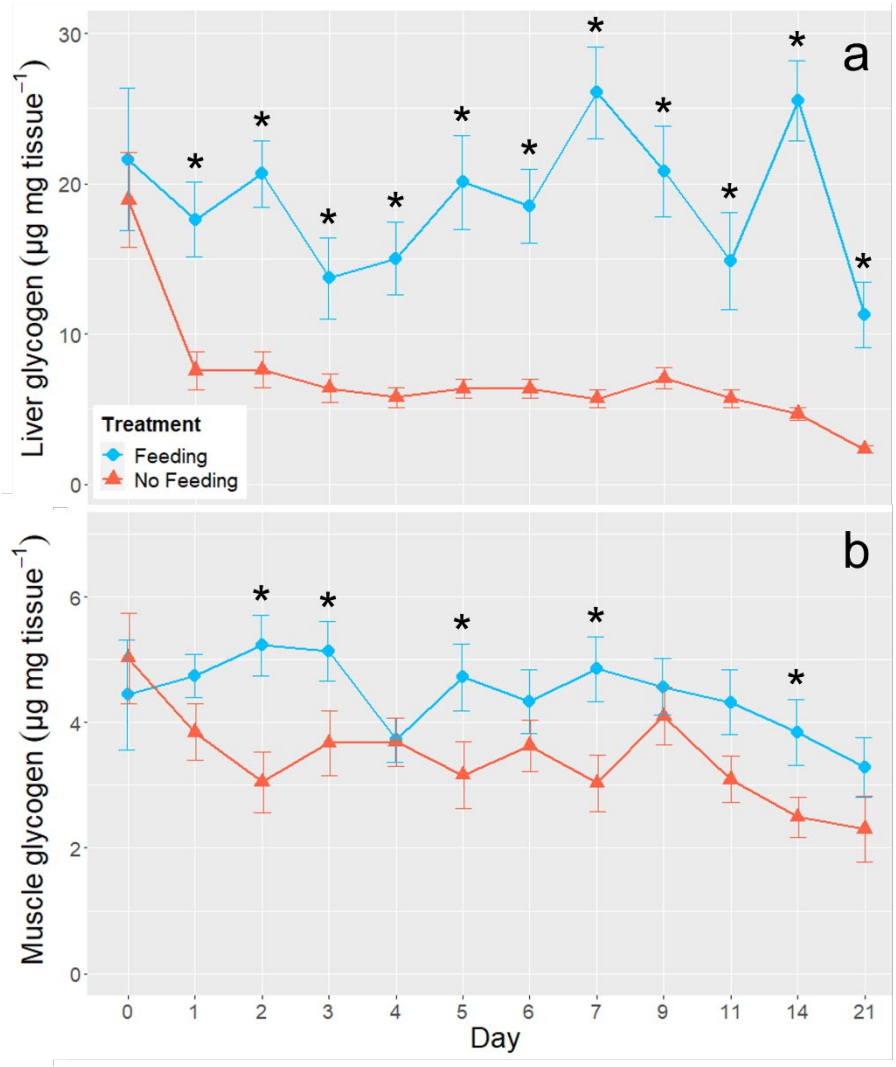

Figure 2-2: Mean liver (panel a) and muscle (panel b) glycogen concentration ±SE in the Feeding and No Feeding treatments across time.

The Feeding treatment is shown in blue circles, while the No Feeding treatment is shown in red triangles. Significant differences, based on linear contrasts, are indicated by asterisks. The x-axis is not to scale

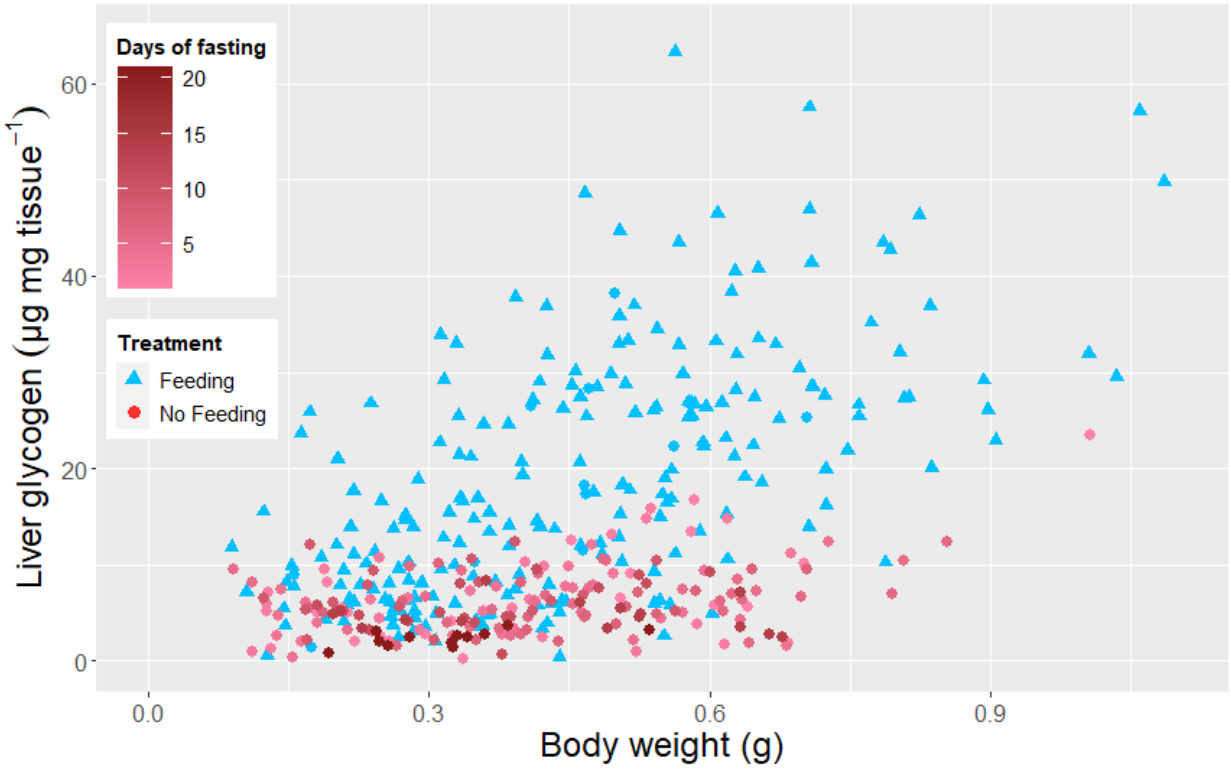

Figure 2-3: Interaction between body weight and treatment (Feeding and No Feeding) on liver glycogen concentration.

The Feeding treatment is shown as blue triangles and the No Feeding treatment is shown as red circles. Fish sampled on Day 0 from the No Feeding tanks are shown as blue circles because they were recently fed when sampled (i.e., treatments had not yet been imposed). Days of fasting are represented by the shade of red, with the shade darkening as the length of fast increases

Comparing biomarkers of food limitation

Figure 4 compares the sensitivities and dynamic ranges of biomarkers of nutritional stress examined in response to fasting in the current study, Hammock et al. (2020), and Lewis et al. (in progress) at 16 °C in sub-adult Delta Smelt. As demonstrated in the current study, biochemically measured liver glycogen is a highly sensitive biomarker of food limitation, but it has a relatively narrow dynamic range. That is, it responded rapidly to fasting, but it stayed fairly constant from days 1 through 14, making it of little use distinguishing among populations under mild to moderate food limitation (Figures 2-2 and 2-4). However, Hammock et al. (2020) and Lewis et al. (in progress) have identified biomarkers with wider dynamic ranges. For instance, otolith increment combines high sensitivity with a wide dynamic range, although it is used retrospectively, meaning that fish were sampled 56 days into the fasting experiment and a decline in otolith increment was detected three days after fasting began (Lewis et al. in progress). Thus, it is more useful for reconstructing growth history than inferring habitat quality from which a vagile fish is collected. Condition factor combined the second widest dynamic range—Day 7 through 56—with the third best sensitivity (7 days; Figure 2-4). Hepatosomatic index also

provided a valuable combination of sensitivity (4 days) and dynamic range (days 4-21). The histological biomarkers in liver (i.e., hepatocyte area, single cell necrosis, autophagosomes, and glycogen depletion) were most effective for detecting moderate to severe starvation.

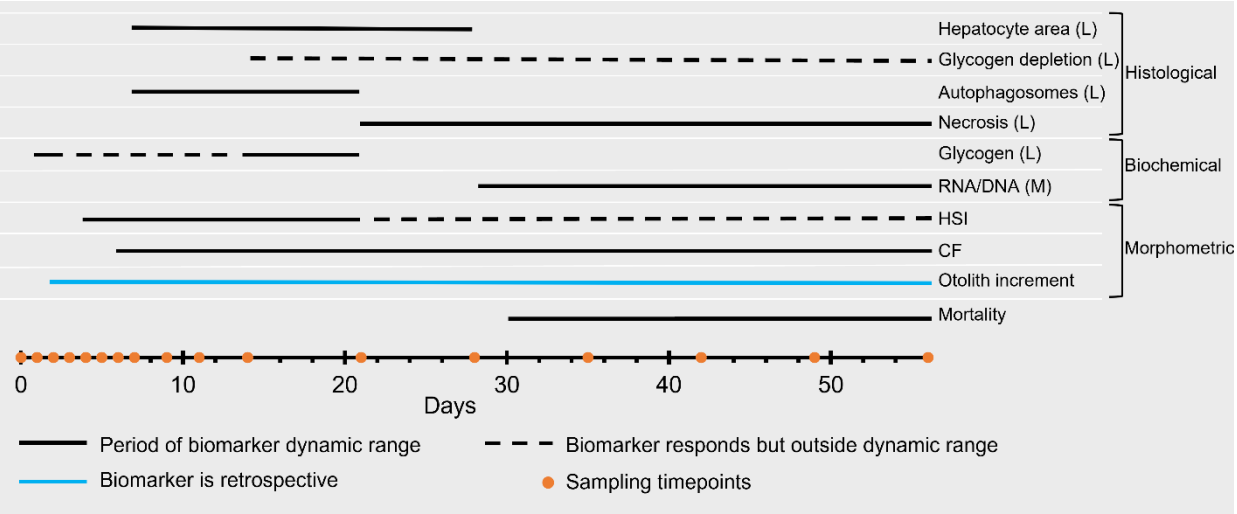

Figure 2-4: Comparison of biomarkers for detecting food limitation in sub-adult Delta Smelt, including results from the present study, Hammock et al. (2020), and Lewis et al. (in progress).

Fasting increases in duration from left (0 days) to right (56 days). Dynamic range refers to the period over which the biomarker changes in response to increasingly severe food limitation. Sensitivity is the time taken for the biomarker to respond significantly to fasting at constant water temperature (16 °C). 'L' is liver tissue and 'M' is muscle tissue. Orange dots represent days on which fish were sampled, but not every biomarker was measured at every time point. Muscle glycogen and muscle triglycerides were excluded from this figure due to their insensitivity and inconsistent response to fasting, while liver RNA/DNA and liver triglycerides were excluded because data was only available for one day of sampling (Day 21).

Application to supplemental Delta Smelt

Liver glycogen concentrations of the supplemental fish were significantly lower than the Feeding treatment fish (ANOVA, $F_{4, 135.5} = 70.5$, $P < 0.0001$, Figure 2-5), with an average liver glycogen concentration of less than half of that of the Feeding fish. The Supplemental fish were also statistically indistinguishable from the No Feeding fish (Figure 2-5). The mean liver glycogen concentration of the Bucket fish was roughly half that of the Supplemental fish, although the difference was not significant (Figure 2-5).

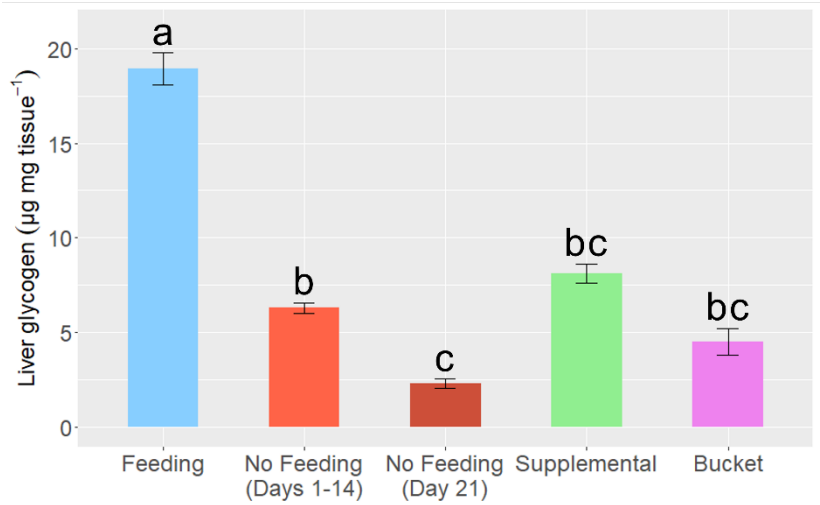

Figure 2-5: Mean liver glycogen concentrations for Feeding, No Feeding (Days 1-14, or mild to moderate food limitation), No Feeding (Day 21, or severe food limitation), Supplemental, and 'Bucket' Delta Smelt, ±SE.

Supplemental Delta Smelt were collected from the San Francisco Estuary and flash frozen on boats, and Bucket fish are supplemental Delta Smelt that were kept live in a bucket for several hours before flash-freezing, potentially depressing their glycogen stores. Treatments with different letters are significantly different based on a Tukey's HSD test.

DISCUSSION

Given the relative insensitivity of biomarkers currently used to detect food limitation in Delta Smelt, our goal was to identify more sensitive biomarkers that could be used to better assess local habitat quality. We found that liver glycogen showed the most significant difference between fed and fasted fish using Day 21 Delta Smelt, so we compared liver glycogen to muscle glycogen for all time points (Day 0-21). In fishes, there exist three common metabolic strategies during periods of food limitation: rapid glycogen depletion, partial protection of glycogen reserves, and complete protection of glycogen reserves (Sheridan & Mommsen 1991; Soengas et al. 1996; Pérez-Jiménez et al. 2007). In Delta Smelt, liver glycogen was rapidly depleted initially with the concentration dropping 60% from Day 0 to Day 1 in the No Feeding treatment. This is consistent with other studies that report liver glycogen depletion in various fishes in as little as one day (Mehner & Wieser 1993; Soengas et al. 1996; Rossi et al. 2015; Wang et al. 2019). However, from Day 1 through 14, sub-adult Delta Smelt partially protected remaining liver glycogen, until it was nearly depleted by Day 21. With little difference between fish fasted one day to two weeks, liver glycogen appears ineffective for differentiating between mild and moderate food limitation in Delta Smelt. Similar partial protection of liver glycogen has been observed in Black Carp, where glycogen was depleted in the first three days of fasting and then remained constant for a week or more (Dai et al. 2022). Liver glycogen could be useful in differentiating between moderate and severe food limitation; however, since it declined from

Day 14 to 21. In contrast to liver glycogen, muscle glycogen was almost fully protected throughout the 21 days of fasting. Muscle glycogen is similarly conserved during the first 21 days of fasting in Rainbow Trout (Harmon et al. 2011), Brown Trout (Navarro et al. 1992), and Jundiá (Barcellos et al. 2010). Thus, our study demonstrates that biochemically measuring liver glycogen concentration is highly sensitive to detecting food limitation, albeit with a narrow dynamic range until moderate levels of starvation are reached (~Day 14). Muscle glycogen responded to fasting but was too protected to have utility as a biomarker of food limitation in Delta Smelt.

Variance was considerably higher among individuals in the Feeding treatment than the No Feeding treatment in terms of liver glycogen. This difference can be largely explained by the interaction between body weight and treatment (Feeding and No Feeding), in which liver glycogen increased with fish weight in the Feeding treatment but not in the No Feeding treatment (Figure 2-3). However, the cause of this interaction is uncertain. Larger fish may have outcompeted smaller fish for food in the Feeding treatment, leading to higher glycogen concentrations in the livers of larger fish. Competition for food is common in aquaculture, resulting in size grading and separation to encourage growth of smaller fish and reduce size variability (Magnuson 1962; Saoud et al 2005; Torrans & Ott 2018). In the No Feeding treatment, a competitive advantage for food was presumably impossible, possibly resulting in little to no influence of body weight on liver glycogen. However, food competition cannot entirely account for the treatment by body weight interaction, because there were average sized fish in the Feeding treatment with low liver glycogen values. Another possibility is that this variation in liver glycogen is due to phenotypic variation among individuals. Whatever the cause, future studies will need sufficiently large sample sizes to offset the variance apparent in a well-fed population.

A shortcoming of glycogen concentration as a biomarker of nutritional stress is its limited specificity. In addition to food limitation, glycogen can deplete due to handling or toxic stress (Haux et al. 1985; Vijayan & Moon 1992; Hemre & Krogdahl 1996). For example, muscle glycogen declines after five minutes of chase and capture in European Sea Bass (Samaras et al. 2016). Rapid depletion of muscle glycogen during sampling may therefore have hindered our ability to detect differences between treatments, along with the maintenance of minimum levels of muscle glycogen throughout our 21-day experiment. However, Delta Smelt may not exhibit this depletion since muscle glycogen remains constant after one hour of handling stress in Atlantic Salmon (Hemre & Krogdahl 1996). Handling stress can also deplete liver glycogen, as seen in the supplemental fish held in buckets for several hours, though the decline was not statistically significant (Figure 2-5).

Both the lack of specificity and narrow dynamic range of liver glycogen can be addressed by using the biomarker in combination with other endpoints. For example, condition factor declined throughout our previous 56-day experiment, allowing for the differentiation among mild, moderate, and severe starvation (Hammock et al. 2020). In addition, autophagosomes are indicators of moderate food limitation stress, and necrosis in liver indicates severe starvation. Stomach fullness may help with interpretation as well, given its specificity and sensitivity to

food limitation (Hobbs et al. 2006; Hammock et al. 2019b). However, even stomach fullness can be difficult to use as a sole indication of nutritional status because it is influenced by variables besides foraging success, such as water temperature and prey digestibility, and only represents recent foraging success of the fish (Robinson et al. 2010; Fall & Fiksen 2020). Identifying stressors is always difficult when interpreting biomarkers of wild fish due, for example, to the variability of habitat quality, migration patterns, and life history strategies (Hook et al. 2014), but using a combination of well-characterized biomarkers with differing sensitivities and dynamic ranges can aid interpretation.

Progression of starvation in Delta Smelt

The results from this study, Hammock et al. (2020), and Lewis et al. (In progress) yield a more comprehensive understanding of the progression of starvation in sub-adult Delta Smelt and how it compares to other teleosts. Here, we demonstrate that liver glycogen drops substantially on the first day of fasting, stabilizes for two weeks, and then declines again from days 15-21. In Hammock et al. (2020), hepatosomatic index declined after four days, likely due to a combination of glycogen loss, water loss, and autophagosomal degradation. Hepatosomatic index seems especially sensitive to fasting in Delta Smelt, since it typically responds to fasting after two weeks in other fishes, even at higher temperatures than our study (22-29 °C; Uchida et al. 2003; Abdel-Tawwab et al. 2006; Barcellos et al. 2010; Xu et al. 2019; Bermejo-Poza et al. 2020). Condition factor was also fairly responsive in Delta Smelt, declining at seven days in Hammock et al. (2020), consistent with declines seen after one week in Rainbow Trout at 23 °C (Bermejo-Poza et al. 2020), and two weeks in Atlantic Salmon and Mozambique Tilapia at 28 °C and 12 °C, respectively (Uchida et al. 2003; Hvas et al. 2021). Moving forward, applying the liver glycogen biomarker—which is far more sensitive than hepatosomatic index and condition factor—to wild caught Delta Smelt could inform management actions. For example, measuring the liver glycogen of wild Delta Smelt before and after opening the Suisun Marsh Salinity Control Gate could validate whether the action improves Delta Smelt food intake (Sommer et al. 2020). Nevertheless, biomarkers like condition factor with wide dynamic ranges will remain useful, even if they lack the sensitivity of liver glycogen.

Due to their role in metabolism, hepatocytes shrink in response to fasting, with the timing usually associated with the mobilization of hepatic energy stores (Power et al. 2000; Séité et al. 2019). Our results are consistent with this timeline as hepatocyte area declined after seven days of fasting in Hammock et al. (2020) following the rapid depletion of liver glycogen described in the present study. The timing of the decline in hepatocyte size is identical to that of Milkfish, albeit at much higher temperatures (26-30 °C; Storch & Juario 1983). Autophagosomes were apparent in the liver after seven days of fasting in Delta Smelt (Supplemental material), likely to digest hepatocyte organelles that became superfluous without food. This is slower than the appearance of autophagosomes in Zebrafish liver after two days of fasting combined with cold stress at 11 °C, and faster than Rainbow Trout muscle after two weeks of fasting at 18 °C (Seilez et al. 2010; Lu et al. 2019). The near-complete depletion of liver glycogen observed in the present study from days 15-21 corresponds with moderate to severe glycogen depletion scores observed histologically beginning at 14 days in Hammock et al. (2020).

In the present study, the timing of the near-complete depletion in liver glycogen on Day 21 in the No Feeding treatment coincided with initial signs of severe starvation in our previous work. In Hammock et al. (2020), hepatosomatic index in the No Feeding treatment stopped decreasing after Day 21, and mortality began increasing. The plateau in hepatosomatic index correlated with the disappearance of hepatic autophagosomes and the onset of necrosis in liver, both on Day 21 (Supplemental material). This indicates that organelles available for digestion were exhausted and autophagy could no longer extend hepatocyte survival (Hammock et al. 2020). Liver necrosis occurred considerably sooner in Delta Smelt than in Rainbow Trout, in which it took 70 days of fasting to become apparent, though this experiment was run at 8-10 °C (Karatas et al. 2021). Thus, despite its relative insensitivity, histopathology remains especially useful, because lesions like single cell necrosis in liver indicates severe stress (Figure 2-4). Triglycerides in liver also decreased by Day 21 in the current study but may have declined earlier in the fasting period. There is evidence of rapid triglyceride depletion in other fishes, though at higher temperatures (e.g., one day in Nile Tilapia at 30 °C, Wang et al. 2019; one week in Rainbow Trout at 23 °C, Bermejo-Poza et al. 2020). Declines in RNA/DNA in liver were also observed on Day 21 in the present study, which is similar to reductions occurring after 2-3 weeks of fasting in other fishes at 12-28 °C (e.g., Hack et al. 2019; Fan et al. 2019). This suggests, in Delta Smelt, RNA/DNA in liver is more sensitive to food limitation than in dorsal muscle which only became detectable at 28 days, just before mortality became statistically elevated around 30 days in the fasting treatment (Hammock et al. 2020).

Application to supplemental Delta Smelt

The fish from the Feeding treatment had liver glycogen levels roughly two-times higher than the supplemental fish. In fact, the supplemental fish had liver glycogen levels that were statistically indistinguishable from the No Feeding fish. Given that the supplemental fish were more mature than the fish in the Feeding treatment, and that liver glycogen increases with size, these results suggest that the supplemental fish experienced food limitation in the SFE. However, this assumption is based on the liver glycogen levels of fed hatchery fish which may not be representative of healthy Delta Smelt in the wild. This apparent food limitation could have also been caused by the stress of the supplementation process or difficulty adjusting to the prey field in the wild. Because Delta Smelt were released repeatedly over several months, the time-at-liberty for these released fish is unknown, so we are unable to identify how long a fish has been in the SFE. Moreover, decreases in glycogen could have been caused by the stress of collection, which could last up to 10 minutes, in comparison to our faster termination of hatchery fish. Nonetheless, the low glycogen levels of the supplemental fish are also consistent with the well-established hypothesis that pelagic fish are prey limited in the SFE (e.g., Feyrer et al. 2003; Miller et al. 2012; Slater & Baxter 2014).

CONCLUSION

Our goal here was to identify sensitive biomarkers for use in comparing habitats from which Delta Smelt are collected, and then apply the most sensitive assay to supplemental Delta Smelt recaptured from the wild. The results of our 21-day fasting study demonstrate that liver glycogen

is highly sensitive to food limitation, with only one day of fasting at 16 °C resulting in a significant decline in liver glycogen. However, liver glycogen has limited specificity and a narrow dynamic range, so the use of a suite of biomarkers would help assess the severity of nutritional stress when applied to fish caught from the wild. For example, biochemically measured liver glycogen and stomach fullness can detect mild food limitation, while autophagosomes in liver, muscle RNA/DNA and liver necrosis indicate moderate to severe starvation. Supplemental Delta Smelt collected from the wild exhibited half the liver glycogen concentrations as fed hatchery fish but also other potential causes. This study demonstrates the potential of liver glycogen to assess habitat suitability, and thereby inform decisions regarding conservation and restoration.

ACKNOWLEDGMENTS

We are grateful to Luke Ellison, Troy Stevenson, and other FCCL staff for raising the experimental Delta Smelt and for help maintaining and monitoring the experiment. We also thank the AHP staff for help dissecting the fish, and USFWS and CDFW field crews for collecting the supplemental fish. The study was funded by the United States Bureau of Reclamation grants R17AC00129 and R22AC00392. The United States Bureau of Reclamation grant R20AC00027 funded the culturing of the Delta Smelt used in the study.

REFERENCES

Abdel-Tawwab, M., Khattab, Y. A. E., Ahmad, M. H., & Shalaby, A. M. E. (2006). Compensatory Growth, Feed Utilization, Whole-Body Composition, and Hematological Changes in Starved Juvenile Nile Tilapia, *Oreochromis niloticus* (L.). *Journal of Applied Aquaculture*, *18*(3), 17–36. https://doi.org/10.1300/J028v18n03_02

Amundsen, P.-A., & Sánchez-Hernández, J. (2019). Feeding studies take guts – critical review and recommendations of methods for stomach contents analysis in fish. *Journal of Fish Biology*, *95*(6), 1364–1373. https://doi.org/10.1111/jfb.14151

Barcellos, L. J. G., Marqueze, A., Trapp, M., Quevedo, R. M., & Ferreira, D. (2010). The effects of fasting on cortisol, blood glucose and liver and muscle glycogen in adult jundiá Rhamdia quelen. *Aquaculture*, *300*(1), 231–236. https://doi.org/10.1016/j.aquaculture.2010.01.013

Bennett, W. A., & Burau, J. R. (2015). Riders on the Storm: Selective Tidal Movements Facilitate the Spawning Migration of Threatened Delta Smelt in the San Francisco Estuary. *Estuaries and Coasts*, *38*(3), 826–835. https://doi.org/10.1007/s12237-014-9877-3

Bermejo-Poza, R., Villarroel, M., Pérez, C., González de Chavarri, E., Díaz, M. T., Torrent, F., & De la Fuente, J. (2020). Fasting combined with long catch duration modifies the physio-metabolic response and flesh quality of rainbow trout. *Aquaculture Research*, *51*(3), 1244–1255. https://doi.org/10.1111/are.14475

Black, D., & Love, R. M. (1986). The sequential mobilisation and restoration of energy reserves in tissues of Atlantic cod during starvation and refeeding. *Journal of Comparative Physiology B*, *156*(4), 469–479. https://doi.org/10.1007/BF00691032

Brown, J. H., Gillooly, J. F., Allen, A. P., Savage, V. M., & West, G. B. (2004). Toward a Metabolic Theory of Ecology. *Ecology*, *85*(7), 1771–1789. https://doi.org/10.1890/03-9000

Buckley, L., Caldarone, E., & Ong, T.-L. (1999). RNA–DNA ratio and other nucleic acid-based indicators for growth and condition of marine fishes. *Hydrobiologia*, *401*(0), 265–277. https://doi.org/10.1023/A:1003798613241

Bulow, F. J. (1970). RNA–DNA Ratios as Indicators of Recent Growth Rates of a Fish. *Journal of the Fisheries Research Board of Canada*, *27*(12), 2343–2349. https://doi.org/10.1139/f70-262

Caldarone, E. M., Wagner M., St. Onge-Burns J., Buckley L. J. (2001) Protocol and Guide for Estimating Nucleic Acids in Larval Fish Using a Fluorescence Microplate Reader. Ref Doc 01-11:1-22, National Marine Fisheries Service, Woods Hole, MA. http://www.nefsc.noaa.gov/nefsc/publications/ crd/crd0111/crd0111.pdf

Carniatto, N., Cunha, E. R., Thomaz, S. M., Quirino, B. A., & Fugi, R. (2020). Feeding of fish inhabiting native and non-native macrophyte stands in a Neotropical reservoir. *Hydrobiologia*, *847*(6), 1553–1563. https://doi.org/10.1007/s10750-020-04212-2

Chang, V. M., & Idler, D. R. (1960). *Biochemical studies on Sockeye Salmon during spawning migration XII. Liver Glycogen*. *38*, 553–558.

Coban, M. Z., & Sen, D. (2011). Examination of liver and muscle glycogen and blood glucose levels of Capoeta umbla (Heckel, 1843) living in Hazar Lake and Keban Dam Lake (Elazig, Turkey). *African Journal Biotechnology*, *10*. https://doi.org/10.5897/AJB11.807

Dai, Y., Shen, Y., Guo, J., Yang, H., Chen, F., Zhang, W., Wu, W., Xu, X., & Li, J. (2022). Glycolysis and gluconeogenesis are involved of glucose metabolism adaptation during fasting and re-feeding in black carp (Mylopharyngodon piceus). *Aquaculture and Fisheries*. https://doi.org/10.1016/j.aaf.2022.04.003

Fall, J., & Fiksen, Ø. (2020). No room for dessert: A mechanistic model of prey selection in gut-limited predatory fish. *Fish and Fisheries*, *21*(1), 63–79. https://doi.org/10.1111/faf.12415

Fan, X., Hou, T., Sun, T., Zhu, L., Zhang, S., Tang, K., & Wang, Z. (2019). Starvation stress affects the maternal development and larval fitness in zebrafish (Danio rerio). *Science of The Total Environment*, *695*, 133897. https://doi.org/10.1016/j.scitotenv.2019.133897

Feyrer, F., Herbold, B., Matern, S. A., & Moyle, P. B. (2003). Dietary shifts in a stressed fish assemblage: Consequences of a bivalve invasion in the San Francisco Estuary. *Environmental Biology of Fishes*, *67*(3), 277–288. https://doi.org/10.1023/A:1025839132274

Furné, M., Morales, A. E., Trenzado, C. E., García-Gallego, M., Carmen Hidalgo, M., Domezain, A., & Sanz Rus, A. (2012). The metabolic effects of prolonged starvation and

refeeding in sturgeon and rainbow trout. *Journal of Comparative Physiology B*, *182*(1), 63–76. https://doi.org/10.1007/s00360-011-0596-9

Gill, A. B., & Hart, P. J. B. (1994). Feeding behaviour and prey choice of the threespine stickleback: The interacting effects of prey size, fish size and stomach fullness. *Animal Behaviour*, *47*(4), 921–932. https://doi.org/10.1006/anbe.1994.1124

Hack, N. L., Cordova, K. L., Glaser, F. L., Journey, M. L., Resner, E. J., Hardy, K. M., Beckman, B. R., & Lema, S. C. (2019). Interactions of long-term food ration variation and short-term fasting on insulin-like growth factor-1 (IGF-1) pathways in copper rockfish (Sebastes caurinus). *General and Comparative Endocrinology*, *280*, 168–184. https://doi.org/10.1016/j.ygcen.2019.04.025

Hammock, B. G., Moose, S. P., Solis, S. S., Goharian, E., & Teh, S. J. (2019a). Hydrodynamic Modeling Coupled with Long-term Field Data Provide Evidence for Suppression of Phytoplankton by Invasive Clams and Freshwater Exports in the San Francisco Estuary. *Environmental Management*, *63*(6), 703–717. https://doi.org/10.1007/s00267-019-01159-6

Hammock, B. G., Hartman, R., Slater, S. B., Hennessy, A., & Teh, S. J. (2019b). Tidal Wetlands Associated with Foraging Success of Delta Smelt. *Estuaries and Coasts*, *42*(3), 857–867. https://doi.org/10.1007/s12237-019-00521-5

Hammock, B. G., Ramírez-Duarte, W. F., Garcia, P. A. T., Schultz, A. A., Avendano, L. I., Hung, T.-C., White, J. R., Bong, Y.-T., & Teh, S. J. (2020). The health and condition responses of Delta Smelt to fasting: A time series experiment. *PLOS ONE*, *15*(9), e0239358. https://doi.org/10.1371/journal.pone.0239358

Hammock, B., Hartman, R., Dahlgren, R., Johnston, C., Kurobe, T., Lehman, P., Lewis, L., Nieuwenhuyse, E., Ramírez-Duarte, W., Schultz, A., & Teh, S. (2021). Patterns and predictors of condition indices in a critically endangered fish. *Hydrobiologia*, *849*, 1–21. https://doi.org/10.1007/s10750-021-04738-z

Harmon, K. J., Bolinger, M. T., & Rodnick, K. J. (2011). Carbohydrate energy reserves and effects of food deprivation in male and female rainbow trout. *Comparative Biochemistry and Physiology Part A: Molecular & Integrative Physiology*, *158*(4), 423–431. https://doi.org/10.1016/j.cbpa.2010.11.017

Haux, C., Maj-Lis, S., & Åke, L. (1985). Physiological stress responses in a wild fish population of perch (Perca fluviatilis) after capture and during subsequent recovery. *Marine Environmental Research*, *15*(2), 77–95. https://doi.org/10.1016/0141-1136(85)90131-X

Hemre, G.-I., & Krogdahl, Å. (1996). Effect of handling and fish size on secondary changes in carbohydrate metabolism in Atlantic salmon, Salmo salar L. *Aquaculture Nutrition*, *2*(4), 249–252. https://doi.org/10.1111/j.1365-2095.1996.tb00067.x

Hemre, G.-I., Mommsen, T. p., & Krogdahl, Å. (2002). Carbohydrates in fish nutrition: Effects on growth, glucose metabolism and hepatic enzymes. *Aquaculture Nutrition*, *8*(3), 175–194. https://doi.org/10.1046/j.1365-2095.2002.00200.x

Hobbs, J. A., Bennett, W. A., & Burton, J. E. (2006). Assessing nursery habitat quality for native smelts (Osmeridae) in the low-salinity zone of the San Francisco estuary. *Journal of Fish Biology*, *69*(3), 907–922. https://doi.org/10.1111/j.1095-8649.2006.01176.x

Hook, S. E., Gallagher, E. P., & Batley, G. E. (2014). The role of biomarkers in the assessment of aquatic ecosystem health. *Integrated Environmental Assessment and Management*, *10*(3), 327–341. https://doi.org/10.1002/ieam.1530

Hung, T.-C., Rosales, M., Kurobe, T., Stevenson, T., Ellison, L., Tigan, G., Sandford, M., Lam, C., Schultz, A., & Teh, S. (2019). A pilot study of the performance of captive-reared delta smelt Hypomesus transpacificus in a semi-natural environment. *Journal of Fish Biology*, *95*(6), 1517–1522. https://doi.org/10.1111/jfb.14162

Hung, T.-C., Hammock, B. G., Sandford, M., Stillway, M., Park, M., Lindberg, J. C., & Teh, S. J. (2022). Temperature and salinity preferences of endangered Delta Smelt (Hypomesus transpacificus, Actinopterygii, Osmeridae). *Scientific Reports*, *12*(1), Article 1. https://doi.org/10.1038/s41598-022-20934-w

Hurst, T. P. (2007). Causes and consequences of winter mortality in fishes. *Journal of Fish Biology*, *71*(2), 315–345. https://doi.org/10.1111/j.1095-8649.2007.01596.x

Hvas, M., Stien, L. H., & Oppedal, F. (2021). The effect of fasting period on swimming performance, blood parameters and stress recovery in Atlantic salmon post smolts. *Comparative Biochemistry and Physiology Part A: Molecular & Integrative Physiology*, *255*. https://doi.org/10.1016/j.cbpa.2021.110913

Hyslop, E. J. (1980). Stomach contents analysis—A review of methods and their application. *Journal of Fish Biology*, *17*(4), 411–429. https://doi.org/10.1111/j.1095-8649.1980.tb02775.x

Jiao, S., Nie, M., Song, H., Xu, D., & You, F. (2020). Physiological responses to cold and starvation stresses in the liver of yellow drum (Nibea albiflora) revealed by LC-MS metabolomics. *Science of The Total Environment*, *715*, 136940. https://doi.org/10.1016/j.scitotenv.2020.136940

Karatas, T., Onalan, S., & Yildirim, S. (2021). Effects of prolonged fasting on levels of metabolites, oxidative stress, immune-related gene expression, histopathology, and DNA damage in the liver and muscle tissues of rainbow trout (Oncorhynchus mykiss). *Fish Physiology and Biochemistry*, *47*(4), 1119–1132. https://doi.org/10.1007/s10695-021-00949-2

Le Pape, O., & Bonhommeau, S. (2015). The food limitation hypothesis for juvenile marine fish. *Fish and Fisheries*, *16*(3), 373–398. https://doi.org/10.1111/faf.12063

Liew, H. J., Sinha, A. K., Mauro, N., Diricx, M., Blust, R., & De Boeck, G. (2012). Fasting goldfish, Carassius auratus, and common carp, Cyprinus carpio, use different metabolic strategies when swimming. *Comparative Biochemistry and Physiology Part A: Molecular & Integrative Physiology*, *163*(3–4), 327–335. https://doi.org/10.1016/j.cbpa.2012.07.012

Lim, A. l. l., & Ip, Y. k. (1989). Effect of fasting on glycogen metabolism and activities of glycolytic and gluconeogenic enzymes in the mudskipper Boleophthalmus boddaerti. *Journal of Fish Biology*, *34*(3), 349–367. https://doi.org/10.1111/j.1095-8649.1989.tb03318.x

Lowry, O. H., Rosebrough, N. J., Farr, A. L., & Randall, R. J. (1951). Protein measurement with the Folin phenol reagent. *The Journal of Biological Chemistry*, *193*(1), 265–275.

Lu, D.-L., Ma, Q., Wang, J., Li, L.-Y., Han, S.-L., Limbu, S. M., Li, D.-L., Chen, L.-Q., Zhang, M.-L., & Du, Z.-Y. (2019). Fasting enhances cold resistance in fish through stimulating lipid catabolism and autophagy. *The Journal of Physiology*, *597*(6), 1585–1603. https://doi.org/10.1113/JP277091

Magnuson, J. J. (1962). An analysis of aggressive behavior, growth, and competition for food and space in medaka (oryzias latipes (pisces, cyprinodontidae)). *Canadian Journal of Zoology*, *40*(2), 313–363. https://doi.org/10.1139/z62-029

Mehner, T., & Wieser, W. (1994). Energetics and metabolic correlates of starvation in juvenile perch (Perca fluviatilis). *Journal of Fish Biology*, *45*(2), 325–333. https://doi.org/10.1111/j.1095-8649.1994.tb01311.x

Miller, W. J., Manly, B. F. J., Murphy, D. D., Fullerton, D., & Ramey, R. R. (2012). An Investigation of Factors Affecting the Decline of Delta Smelt (Hypomesus transpacificus) in the Sacramento-San Joaquin Estuary. *Reviews in Fisheries Science*, *20*(1), 1–19. https://doi.org/10.1080/10641262.2011.634930

Navarro, I., Gutiérrez, J., & Planas, J. (1992). Changes in plasma glucagon, insulin and tissue metabolites associated with prolonged fasting in brown trout (Salmo trutta fario) during two different seasons of the year. *Comparative Biochemistry and Physiology Part A: Physiology*, *102*(2), 401–407. https://doi.org/10.1016/0300-9629(92)90154-I

Navarro, I., & Gutiérrez, J. (1995). Chapter 17 Fasting and starvation. In P. W. Hochachka & T. P. Mommsen (Eds.), *Biochemistry and Molecular Biology of Fishes* (Vol. 4, pp. 393–434). Elsevier. https://doi.org/10.1016/S1873-0140(06)80020-2

Nemerson, D. M., & Able, K. W. (2004). Spatial patterns in diet and distribution of juveniles of four fish species in Delaware Bay marsh creeks: Factors influencing fish abundance. *Marine Ecology Progress Series*, *276*, 249–262. https://doi.org/10.3354/meps276249

Ng, T. B., Tam, P. P. L., & Woo, N. Y. S. (1986). Sexual maturation in the black seabream Mylio macrocephalus Teleostei, Sparidae: Changes in pituitary gonadotropes, hepatocytes and related biochemical constituents in liver and serum. *Cell and Tissue Research*, *245*(1). https://doi.org/10.1007/BF00218102

Panserat, S., Marandel, L., Seiliez, I., & Skiba-Cassy, S. (2019). New Insights on Intermediary Metabolism for a Better Understanding of Nutrition in Teleosts. *Annual Review of Animal Biosciences*, *7*(1), 195–220. https://doi.org/10.1146/annurev-animal-020518-115250

Pérez-Jiménez, A., Guedes, M. J., Morales, A. E., & Oliva-Teles, A. (2007). Metabolic responses to short starvation and refeeding in Dicentrarchus labrax. Effect of dietary composition. *Aquaculture*, *265*(1), 325–335. https://doi.org/10.1016/j.aquaculture.2007.01.021

Pham, L. P., Nguyen, M. V., Jordal, A.-E. O., & Rønnestad, I. (2022). Metabolic rates, feed intake, appetite control, and gut transit of clownfish Amphiprion ocellaris exposed to increased temperature and limited feed availability. *Comparative Biochemistry and Physiology Part A: Molecular & Integrative Physiology*, *274*, 111318. https://doi.org/10.1016/j.cbpa.2022.111318

Power, D. M., Melo, J., & Santos, C. R. A. (2000). The effect of food deprivation and refeeding on the liver, thyroid hormones and transthyretin in sea bream. *Journal of Fish Biology*, *56*(2), 374–387. https://doi.org/10.1111/j.1095-8649.2000.tb02112.x

Rimoldi, S., Benedito-Palos, L., Terova, G., & Pérez-Sánchez, J. (2016). Wide-targeted gene expression infers tissue-specific molecular signatures of lipid metabolism in fed and fasted fish. *Reviews in Fish Biology and Fisheries*, *26*(1), 93–108. https://doi.org/10.1007/s11160-015-9408-8

Robinson, J. M., Josephson, D. C., Weidel, B. C., & Kraft, C. E. (2010). Influence of Variable Interannual Summer Water Temperatures on Brook Trout Growth, Consumption, Reproduction, and Mortality in an Unstratified Adirondack Lake. *Transactions of the American Fisheries Society*, *139*(3), 685–699. https://doi.org/10.1577/T08-185.1

Roehrig, K. L., & Allred, J. B. (1974). Direct enzymatic procedure for the determination of liver glycogen. *Analytical Biochemistry*, *58*(2), 414–421. https://doi.org/10.1016/0003-2697(74)90210-3

Rossi, A., Cazenave, J., Bacchetta, C., Campana, M., & Parma, M. J. (2015). Physiological and metabolic adjustments of Hoplosternum littorale (Teleostei, Callichthyidae) during starvation. *Ecological Indicators*, *56*, 161–170. https://doi.org/10.1016/j.ecolind.2015.04.001

Samaras, A., Papandroulakis, N., Costari, M., & Pavlidis, M. (2016). Stress and metabolic indicators in a relatively high (European sea bass, Dicentrarchus labrax) and a low (meagre, Argyrosomus regius) cortisol responsive species, in different water temperatures. *Aquaculture Research*, *47*(11), 3501–3515. https://doi.org/10.1111/are.12800

Saoud, I. P., Davis, D. A., Roy, L. A., & Phelps, R. P. (2005). Evaluating the Benefits of Size-Sorting Tilapia Fry Before Stocking. *Journal of Applied Aquaculture*, *17*(4), 73–85. https://doi.org/10.1300/J028v17n04_05

Saulnier, E., Le Bris, H., Tableau, A., Dauvin, J. C., & Brind'Amour, A. (2020). Food limitation of juvenile marine fish in a coastal and estuarine nursery. *Estuarine, Coastal and Shelf Science*, *241*, 106670. https://doi.org/10.1016/j.ecss.2020.106670

Seiliez, I., Gutierrez, J., Salmerón, C., Skiba-Cassy, S., Chauvin, C., Dias, K., Kaushik, S., Tesseraud, S., & Panserat, S. (2010). An in vivo and in vitro assessment of autophagy-related

gene expression in muscle of rainbow trout (Oncorhynchus mykiss). *Comparative Biochemistry and Physiology. Part B, Biochemistry & Molecular Biology*, *157*(3), 258–266. https://doi.org/10.1016/j.cbpb.2010.06.011

Séité, S., Pioche, T., Ory, N., Plagnes-Juan, E., Panserat, S., & Seiliez, I. (2019). The Autophagic Flux Inhibitor Bafilomycine A1 Affects the Expression of Intermediary Metabolism-Related Genes in Trout Hepatocytes. *Frontiers in Physiology*, *10*. https://www.frontiersin.org/articles/10.3389/fphys.2019.00263

Sheridan, M. A., & Mommsen, T. P. (1991). Effects of nutritional state on in vivo lipid and carbohydrate metabolism of coho salmon, Oncorhynchus kisutch. *General and Comparative Endocrinology*, *81*(3), 473–483. https://doi.org/10.1016/0016-6480(91)90175-6

Slater, S. B., & Baxter, R. D. (2014). Diet, Prey Selection, and Body Condition of Age-0 Delta Smelt, Hypomesus transpacificus, in the Upper San Francisco Estuary. *San Francisco Estuary and Watershed Science*, *12*(3). https://doi.org/10.15447/sfews.2014v12iss3art1

Soengas, J. L., Strong, E. F., Fuentes, J., Veira, J. A. R., & Andrés, M. D. (1996). Food deprivation and refeeding in Atlantic salmon,Salmo salar: Effects on brain and liver carbohydrate and ketone bodies metabolism. *Fish Physiology and Biochemistry*, *15*(6), 491–511. https://doi.org/10.1007/BF01874923

Soengas, J. L., & Aldegunde, M. (2002). Energy metabolism of fish brain. *Comparative Biochemistry and Physiology Part B: Biochemistry and Molecular Biology*, *131*(3), 271–296. https://doi.org/10.1016/S1096-4959(02)00022-2

Sommer, T., Armor, C., Baxter, R., Breuer, R., Brown, L., Chotkowski, M., Culberson, S., Feyrer, F., Gingras, M., Herbold, B., Kimmerer, W., Mueller-Solger, A., Nobriga, M., & Souza, K. (2007). The Collapse of Pelagic Fishes in the Upper San Francisco Estuary: El Colapso de los Peces Pelagicos en La Cabecera Del Estuario San Francisco. *Fisheries*, *32*(6), 270–277. https://doi.org/10.1577/1548-8446(2007)32[270:TCOPFI]2.0.CO;2

Sommer, T., Hartman, R., Koller, M., Koohafkan, M., Conrad, J. L., MacWilliams, M., Bever, A., Burdi, C., Hennessy, A., & Beakes, M. (2020). Evaluation of a large-scale flow manipulation to the upper San Francisco Estuary: Response of habitat conditions for an endangered native fish. *PLOS ONE*, *15*(10), e0234673. https://doi.org/10.1371/journal.pone.0234673

Storch, V., & Juario, J. V. (1983). The effect of starvation and subsequent feeding on the hepatocytes of Chanos chanos (Forsskal) fingerlings and fry. *Journal of Fish Biology*, *23*(1), 95–103. https://doi.org/10.1111/j.1095-8649.1983.tb02884.x

Storer, J. H. (1967). Starvation and the effects of cortisol in the goldfish (Carassius auratus L.). *Comparative Biochemistry and Physiology*, *20*(3), 939–948. https://doi.org/10.1016/0010-406X(67)90065-5

Swanson, C., Young, P. S., & Cech, J. J., Jr. (1998). Swimming performance of delta smelt: Maximum performance, and behavioral and kinematic limitations on swimming at

submaximal velocities. *Journal of Experimental Biology*, *201*(3), 333–345. https://doi.org/10.1242/jeb.201.3.333

Tanaka, Y., Satoh, K., Yamada, H., Takebe, T., Nikaido, H., & Shiozawa, S. (2008). Assessment of the nutritional status of field-caught larval Pacific bluefin tuna by RNA/DNA ratio based on a starvation experiment of hatchery-reared fish. *Journal of Experimental Marine Biology and Ecology*, *354*(1), 56–64. https://doi.org/10.1016/j.jembe.2007.10.007

Teh, S. J., Baxa, D. V., Hammock, B. G., Gandhi, S. A., & Kurobe, T. (2016). A novel and versatile flash-freezing approach for evaluating the health of Delta Smelt. *Aquatic Toxicology*, *170*, 152–161. https://doi.org/10.1016/j.aquatox.2015.11.009

Theilacker, G. (1986). Starvation-induced mortality of young sea-caught jack mackerel, *Trachurus symmetricus,* determined with histological and morphological methods. *Fishery Bulletin, 84(1)*.

Torrans, L., & Ott, B. (2018). Effect of Grading Fingerling Hybrid Catfish (♀ Channel Catfish × ♂ Blue Catfish) on Growth, Production, Feed Conversion, and Food Fish Size Distribution. *North American Journal of Aquaculture*, *80*(2), 187–192. https://doi.org/10.1002/naaq.10024

Uchida, K., Kajimura, S., Riley, L. G., Hirano, T., Aida, K., & Grau, E. G. (2003). Effects of fasting on growth hormone/insulin-like growth factor I axis in the tilapia, Oreochromis mossambicus. *Comparative Biochemistry and Physiology Part A: Molecular & Integrative Physiology*, *134*(2), 429–439. https://doi.org/10.1016/S1095-6433(02)00318-5

Valtonen, T. (1974). Seasonal and sex-bound variation in the carbohydrate metabolism of the liver of the whitefish. *Comparative Biochemistry and Physiology Part A: Physiology*, *47*(2), 713–727. https://doi.org/10.1016/0300-9629(74)90032-2

Vijayan, M. M., & Moon, T. W. (1992). Acute Handling Stress Alters Hepatic Glycogen Metabolism in Food-Deprived Rainbow Trout (*Oncorhynchus mykiss*). *Canadian Journal of Fisheries and Aquatic Sciences*, *49*(11), 2260–2266. https://doi.org/10.1139/f92-247

Volkoff, H., & Rønnestad, I. (2020). Effects of temperature on feeding and digestive processes in fish. *Temperature*, *7*(4), 307–320. https://doi.org/10.1080/23328940.2020.1765950

Vornanen, M., Asikainen, J., & Haverinen, J. (2011). Body mass dependence of glycogen stores in the anoxia-tolerant crucian carp (Carassius carassius L.). *Naturwissenschaften*, *98*(3), 225–232. https://doi.org/10.1007/s00114-011-0764-5

Wang, J., Du, J.-J., Jiang, B., He, R.-Z., & Li, A.-X. (2019). Effects of short-term fasting on the resistance of Nile tilapia (Oreochromis niloticus) to Streptococcus agalactiae infection. *Fish & Shellfish Immunology*, *94*, 889–895. https://doi.org/10.1016/j.fsi.2019.09.055

Weatherley, A. H., & Gill, H. S. (1981). Recovery growth following periods of restricted rations and starvation in rainbow trout Salmo gairdneri Richardson. *Journal of Fish Biology*, *18*(2), 195–208. https://doi.org/10.1111/j.1095-8649.1981.tb02814.x

Weis, P. (1972). Hepatic ultrastructure in two species of normal, fasted and gravid teleost fishes. *American Journal of Anatomy*, *133*(3), 317–331. https://doi.org/10.1002/aja.1001330306

Xu, Y., Tan, Q., Kong, F., Yu, H., Zhu, Y., Yao, J., & Abouel Azm, F. R. (2019). Fish growth in response to different feeding regimes and the related molecular mechanism on the changes in skeletal muscle growth in grass carp (Ctenopharyngodon idellus). *Aquaculture*, *512*, 734295. https://doi.org/10.1016/j.aquaculture.2019.734295

Yandi, I., & Altinok, I. (2018). Irreversible starvation using RNA/DNA on lab-grown larval anchovy, Engraulis encrasicolus, and evaluating starvation in the field-caught larval cohort. *Fisheries Research*, *201*, 32–37. https://doi.org/10.1016/j.fishres.2018.01.005

Zhang, X., Chen, H., Li, Y., Tang, N., Chen, D., & Li, Z. (2022). The insulin gene as an energy homeostasis biomarker in Yangtze sturgeon (Acipenser dabryanus). *Fish Physiology and Biochemistry*, *48*(3), 693–705. https://doi.org/10.1007/s10695-022-01079-z

SUPPLEMENTAL MATERIAL

Liver ultrastructural

Materials and methods

Livers from two Delta Smelt sampled on Day 21 from the No Feeding treatment from Hammock et al. (2020) was fixed in half-strength Karnosvky fixative and were submitted to electron microscopy services (University of California, Davis) for ultrastructural analysis to confirm the nature of eosinophilic intracytoplasmic vacuoles (lysosome or autophagolysosome).

Results

Figs. A and B show several double-membraned autophagosomes (red arrows) and enlarged mitochondria (white arrows) in a glycogen depleted Delta Smelt liver on Day 21 of fasting (Hammock et al. 2020).

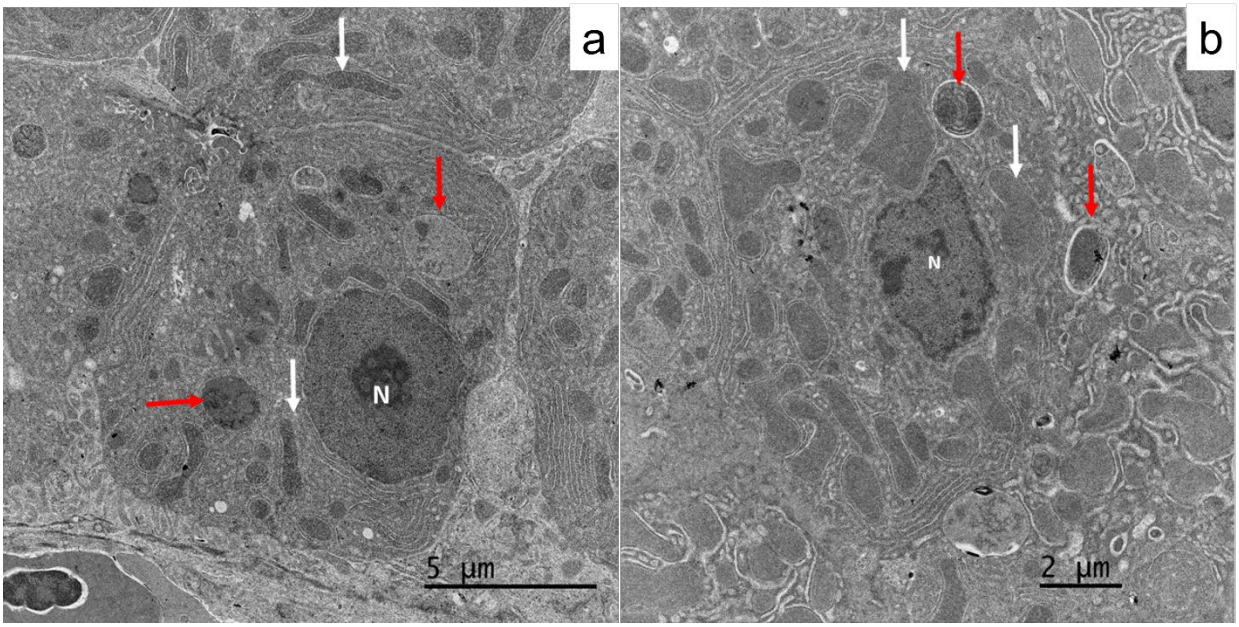

Figure S2-1: Electron microscopy of liver sections from one Delta Smelt fasted until Day 21 from Hammock et al. (2020).

White arrows represent enlarged mitochondria, red arrows represent autophagosomes, and N represents the nucleus

Chapter 3: Experimental Contrasts among Schlerochronologic (Otolith), Morphologic, Histologic, and Molecular Indicators of Health for a Critically Endangered Estuarine Fish

Authors:

Levi S. Lewis[1*], Rachel A. Fichman[1], Christian Denney[1], Wilson Xieu[1], James A. Hobbs[1], Robert Lusardi[1], Malte Willmes[2], Tien-Chieh Hung[3], Luke Ellison[3], Troy Stevenson[3], Andrew A. Schultz[4,5], Swee Teh[6], Bruce G. Hammock[6]

[1] Department of Wildlife, Fish and Conservation Biology, University of California-Davis, Davis, CA, USA

[2] Norwegian Institute for Nature Research, Trondheim, Norway

[3] Fish Conservation and Culture Laboratory, Department of Biological and Agricultural Engineering, University of California Davis, Byron, CA, USA

[4] United States Bureau of Reclamation, Bay-Delta Office, Science Division, Sacramento, CA, United States

[5] U.S. Geological Survey, Southwest Biological Science Center, Grand Canyon Monitoring and Research Center, Flagstaff, AZ, United States [6] Department of Anatomy, Physiology, and Cell Biology, University of California-Davis, Davis, CA, USA

*** Corresponding Author:**

lewis.sci@gmail.com

ABSTRACT

Quantification of fish health and condition is key to understanding habitat suitability and the dynamics of wild populations. Several bioindicators, including gravimetric (mass), histologic (tissues), molecular (genetic), and schlerochronologic (e.g., otolith-based) approaches have been used to study the condition of wild fish populations, but the relative strengths of each approach remain poorly defined. Here, we experimentally manipulated food availability to alter the growth and condition of a critically endangered fish, the Delta Smelt (*Hypomesus transpacificus*). We then contrasted the timing and magnitude of changes in otolith-based growth estimates ($G_{otolith}$) with differences in somatic growth and variation in several other indicators of fish condition including Fulton's condition factor (K), hepatosomatic index (HSI), and RNA:DNA ratios in muscle. Body condition (K) changed within 7 days and exhibited an effect size of 40% between

fed and unfed treatments toward the end of the experiment. HSI exhibited both the largest effect size (143%) and the highest temporal sensitivity (4 days) to food limitation. $G_{otolith}$ responded similarly in time (11 days) and scale (41%) as K, whereas RNA:DNA ratios exhibited a similar effect size (53%) as K but at a lag of nearly 1 month (28 d). Although HSI provided the most sensitive indicator of food limitation, $G_{otolith}$ was directly proportional to changes in K and provided a time-resolved record of overall growth and condition, but not changes in length *per se*, in adult Delta Smelt. Such comparative experimental approaches greatly enhance the interpretation of biomarkers of fish health and condition, and can help identify which indicators are likely to yield the most robust assessments for wild fish populations.

Keywords:

growth, San Francisco Estuary, Delta Smelt, histology, condition, otolith**,** Hypomesus, osmeridae, RNA, DNA,

INTRODUCTION

Fish health and condition

Understanding patterns and drivers in the growth and condition of fishes is key to understanding population dynamics, habitat needs, movements, human impacts, and effective management of fish populations (Shulman & Love 1999, Marshall et al. 1999, Lloret et al. 2012, Peck et al. 2015). The survival of early (i.e., larval and juvenile) life stages, in particular, is strongly influenced by direct mortality due to predation, with mortality rates rapidly decreasing with fish body size, resulting in a positive relationship between growth rate and survival (Houde 1987, Anderson 1988, Bergenius et al. 2002). Since growth is positively associated with feeding success (Houde 1975, 1978), this can result in a positive feedback loop, with higher feeding success further increasing growth rates, thus leading to even greater feeding success and survival (China & Holzman 2014). In contrast, food limitation can result in reduced condition and growth, resulting in increased mortality and reduced fitness (Molony 1993, Rätz & Lloret 2003, Lloret et al. 2012). Furthermore, the reproductive output (i.e., fecundity) of mature female fish increases disproportionately with body size, also resulting in a strong correlation between growth rate and lifetime fitness (Berkeley et al. 2004b a, Damon et al. 2016).

Spatiotemporal variation in the growth, size, and condition of fishes can be affected by food availability, fishing pressure, and environmental factors (Lambert & Dutil 2000, Lloret & Planes 2003, Giacalone et al. 2010). Given that food availability is critical to overall fitness (Oliva-Teles 2012, Hammock et al. 2020), trophic disruption due to pollution, invasive species, hydrologic alterations, and climate change may result in significant declines in fish health and subsequent population dynamics. However, variation in growth and condition in wild fish populations can be challenging to quantify. The development of fish biomarkers, quantitative indicators that can be used to estimate the health or condition of individual fish, can greatly aid in the assessment and management of wild fish populations.

Estimating growth and condition in fishes

Several biological indices have been used to describe the health and condition of fishes. Simple morphometric indices assume that among fish of equal length, heavier fish will contain more energy reserves and are, therefore, healthier than lighter fish (Lloret et al. 2012). Fulton's condition factor (K) relates mass to length as a proxy to provide a size-independent metric for whole-body mass that correlates positively with relative muscle mass, energy reserves, and general health (Hoque et al. 1998, Blackwell et al. 2000, Lloret et al. 2012). Similarly, the hepatosomatic index (HSI) is a gravimetric health proxy that relates liver mass to fish mass, with higher HSI values indicating higher energy (e.g., glycogen) reserves that reflect reduced environmental stressors and higher prey availability and foraging success (Hoque et al. 1998, Peragón et al. 1999, De Pedro et al. 2003, Zeng et al. 2012). Given the sensitivity of livers to food availability, the HSI is a valuable metric for assessing food limitation (Hammock et al. 2020). Similarly, molecular indices, such as the ratio of RNA:DNA in muscle, can also provide an indicator of recent feeding and growth history, with RNA concentrations varying in relation to protein synthesis while DNA concentrations remain static (Buckley 1984, Buckley et al. 1999).

Otoliths as proxies of growth and condition

Otolith-based approaches can provide another valuable tool for assessing growth and condition in wild populations of fishes. Otoliths ('ear stones') are paired calcium carbonate structures found in the inner ears of bony fishes (Pannella 1971, Campana & Neilson 1985). Otoliths accrete daily or annual rings throughout the life of a fish and can preserve a permanent record of its age, hatch date, and growth rate (Campana 1999, Campana & Thorrold 2001, Starrs et al. 2016, Lewis et al. 2021, Xieu et al. 2021). Through the analyses of otolith increment widths, we can reconstruct a time series of growth history, where thinner increments reflect poorer growth and wider increments reflect improved growth conditions (Molony & Sheaves 1998). To assess confidence in otolith-based reconstructions, validation studies examining aging accuracy and precision, as well as otolith-somatic proportionality, are needed. Although otolith-based approaches have been validated for many species (Miller & Storck 1982, Campana 2001, Campana & Thorrold 2001, Roberts et al. 2004, Sakaris et al. 2014), experimental tests of the temporal resolution and relative sensitivity of otolith-based estimates of fish responses to environmental variation (e.g., food limitation) are largely lacking.

Delta Smelt

The Delta Smelt (*Hypomesus transpacificus*) is an endangered annual estuarine fish that is endemic to the upper San Francisco Estuary (SFE), California. Since the 1980s the population has steeply declined, likely due to multiple factors including trophic disruption, invasive species, pollution, habitat loss, hydrologic alterations (e.g., dams, channelization, and water exports), and climate change (Feyrer et al. 2007, Sommer et al. 2007, Moyle et al. 2016, 2018, Hobbs et al. 2017). In particular, the coinciding declines in Delta Smelt and its primary prey (e.g., copepods and mysids) reflect a major collapse in the pelagic food web of the upper SFE that has greatly reduced its carrying capacity and suitability for pelagic fishes (Feyrer et al. 2003, Sommer et al. 2007, Hobbs et al. 2017, Hammock et al. 2019b). With Delta Smelt on the brink of extinction,

and continuing agricultural and municipal demands for the freshwater resources that the species rely on for reproduction and spawning, studies that can disentangle the responses of wild Delta Smelt to natural and anthropogenic factors are critically needed (Hobbs et al. 2017, Moyle et al. 2018). Such studies have utilized a variety of analytical approaches including morphological, gravimetric, histological, genetic, and otolith-based analyses of wild-caught fish (Hammock et al. 2019a, 2021, Teh et al. 2020, Lewis et al. 2021).

Objectives

Although otolith-based tools have been validated for Delta Smelt (Hobbs et al. 2007, Xieu et al. 2021), as for many fish species, experiments examining the sensitivity of otolith-based tools for estimating growth and condition, relative to other biomarkers, would greatly enhance the interpretation of growth and condition estimates for wild-caught individuals. Here, we experimentally manipulated the growth and condition of Delta Smelt by varying food availability. We then contrasted the sensitivities of multiple proxies of Delta Smelt growth and condition in response to food limitation. Specifically, we measured the timing and magnitude of changes in otolith-based growth rates ($G_{otolith}$) and contrasted these with variation in somatic growth (i.e., changes in length and weight), body condition (K), RNA:DNA ratios, HSI, and several histological indicators of liver condition. By experimentally testing and contrasting the temporal resolution and magnitude of the otolith-based metrics with other indicators of fish condition, researchers can improve the application and interpretation of these techniques for wild fish populations.

METHODS

Fish Culture & Experimental Design

Delta Smelt were cultured and reared at the University of California, Davis Fish Conservation and Culture Laboratory in 2018 using standard culture methods (Lindberg et al. 2013, Tsai et al. 2022). Fish were reared in freshwater from the Sacramento-San Joaquin Delta that was bead-filtered, UV-treated, and recirculated in all experimental systems at 16 °C. Fish were fed an age-appropriate *ad libitum* diet (e.g. rotifers and *Artemia* nauplii) until 120 days post-hatch (DPH), after which fish were weaned onto dry feed (Bio-vita Crum #1) (Hung et al. 2022). On September 24, 2018 (at 143 DPH), 800 Delta Smelt with a mean (s.d.) fork length of 45.7 (± 6.4) mm and mean mass of 0.54 (± 0.27) g were transferred from holding tanks into eight experimental tanks at a density of 100 fish per tank. Experimental tanks were 60 cm in depth × 100 cm in diameter, with a wetted depth of 47cm resulting in a water volume of 290 L. Following transfers, all fish were fed (Bio-vita Crum #1) *ad libitum* throughout a 2-wk acclimation period with a food-to-feces ratio of 0.25 at the bottom of the tanks. Feedings occurred five times daily, with tanks siphoned three times weekly. To prevent the ingress of food particles outside of feedings, 5-µm filters were affixed to the inflow of each tank. A few mortalities occurred during the acclimation period; these were replaced with fish from the same cohort so that the initial density in each tank was 100 fish per tank at the start of the experiment.

On October 8, 2018 (Day 0, 157 DPH) two treatments, "unfed" and "fed", were imposed with 4 tanks randomly assigned to each treatment. The unfed treatment received no further feeding for the duration of the eight-week experiment, whereas the fed treatment continued receiving the original feeding regime. Water temperature was measured hourly throughout the experiment (HOBO Water Temp Pro v2, Onset). Every 3-4 days Hach testing kits (Loveland, CO) were used to measure ammonia, nitrite, and nitrate levels while dissolved oxygen, pH, and salinity were measured using a handheld YSI-85 m (YSI Incorporated, Yellow Springs, OH, USA). Each day, all tanks were examined for mortalities, which were recorded, removed, and excluded from analyses. Four fish per tank (n = 32 fish per time point) were sampled on multiple time points from day 0 to the conclusion of the experiment on day 56 (213 DPH, Table 3-1). At the final time point, however, one unfed tank had only 2 fish remaining, resulting in only 30 fish for the final time point. Sampled fish were removed from tanks with an aquarium net, gently dried, wrapped in aluminum foil, and flash-frozen in liquid nitrogen (Teh et al. 2016, 2020, Hammock et al. 2020). Sampling different fish from each tank simulated sampling fish from the wild population, in which obtaining repeated measurements from the same fish is impossible and biomarkers must be able to account for individual variation to have utility (Hammock et al. 2020)

Fish dissections and processing

Flash-frozen Delta Smelt samples were dissected at the UC Davis Aquatic Health Laboratory following a modified version of the methods of Teh et al. (2016). Each fish was removed from liquid nitrogen, photographed, weighed (M, in g), and measured for fork length (FL, in mm). Dorsal muscle tissue was excised, weighed, frozen in liquid nitrogen, and then stored at -80˚C until processing for RNA:DNA. Livers were removed from each fish, weighed, pooled in a 1.5-mL tube (4 livers per tube), placed in liquid nitrogen, and stored at -80˚C for oxidative stress analyses. Masses of tissues were measured on an analytical balance (+/- 0.01 mg). Otoliths were dissected from fish collected on Day 56 and preserved in 95% ethanol following established protocols (Xieu et al. 2021).

Measures of Fish Condition

Several measures of fish condition were previously quantified and contrasted by Hammock et al. (2020) including Fulton's condition factor (K), hepatosomatic index (HSI), and relative RNA abundance (RNA:DNA). K was calculated as $K = (M_B / FL^3) \times 100$ where M_B is body mass (g) and FL is the fork length (mm). HSI was calculated as $HSI = (M_L / M_B) \times 100$, where M_L is the liver mass (g) and M_B is the body mass (g). RNA:DNA was calculated as the ratio of each nucleic acid in skeletal muscle (in µg/mg tissue) based on the ethidium bromide fluorometric technique (Caldarone et al. 2001). Four histological markers in the liver were also assessed including liver lesion score, glycogen depletion, hepatocyte area, and hepatocyte nucleus area (Teh et al. 1997, 2020, Hammock et al. 2020). Liver lesions were scored on a scale from 0 to 3, with three being the most severely damaged. Glycogen depletion was also scored on a 0 to 3 scale, with three being highly depleted (De Pedro et al. 2003). Hepatocyte area and hepatocyte nucleus area were measured and calculated from photos using ImageJ for up to 10 hepatocytes or

nuclei per section of liver tissue, with smaller cells and nuclei areas resulting in lower scores indicating poorer liver condition (Schneider et al. 2012, Hammock et al. 2020). Since changes in HSI reflect the integrated effects of changes in glycogen, cell size, and lesions in the liver, we focused on this metric as an overall indicator of liver condition (Hammock et al. 2020), where higher HSI values represents better liver condition.

Otolith dissection and preparation

Sagittal otoliths from the final (Day 56) time point were analyzed following established protocols (Hobbs et al. 2007, Lewis et al. 2021, Xieu et al. 2021) in order to reconstruct the prior growth history of each fish (Figure 3-1A). Although the design called for 4 fish to be collected per tank per time point (n = 32 per time point), one unfed tank only had 2 fish remaining, resulting in a total of 30 fish (16 fed and 14 unfed) available for otolith analyses. Of those 30 fish, three were removed due to otolith damage that occurred during processing, and one was removed due to deformity, resulting in a final sample size of 26 otoliths (14 fed and 12 unfed) for increment analysis. Otoliths were extracted from fish during dissections using size 10 scalpel blades and ultra-fine tip forceps. Otoliths were mounted onto glass microscope slides using Crystalbond™ (Ted Pella, Redding, CA) thermoplastic glue and stored in plastic microscope slide boxes at the Otolith, Geochemistry, and Fish Ecology Laboratory (Davis, CA).

Mounted otoliths were wet-sanded with 600-1200 grit Buehler MicroCut silicon carbide paper and polished with 0.3-µm Buehler MicroPolish alumina on a Buehler Microcloth (Buehler, Lake Bluff, Illinois, USA) on the sulcus side, then flipped and sanded to expose daily increments. Multiple images were taken of each sanded otolith at 400X magnification using an Amscope MU1000 10MP camera attached to an Olympus CH30 compound microscope. Digital images were stitched together into a single high-resolution composite image using Adobe Photoshop 2020 (v. 21.1.1). The quality of each otolith composite image was ranked on a scale of 0 to 3 (low to high, respectively) based on the clarity of the core and edge increments, with only quality 2 and 3 otoliths used in analyses. Left otoliths were initially sanded, however, right otoliths were prepared in their place if an otolith was broken, lost, or of poor quality (Xieu et al. 2021).

Otolith increment profiles were constructed from each image using ImageJ (v. 1.53) following established protocols (Hobbs et al. 2007, Xieu et al. 2021). All increments were sequentially annotated, enumerated, and measured from the hatch check to the dorsal edge, thus encompassing the full life history of each fish (Figure 3-1). Increment widths were converted from pixels to µm using a conversion ratio calculated from a digital image of a stage micrometer using the same imaging equipment and parameters as used for otoliths. Otolith ring widths were converted to otolith-based estimates of somatic growth ($G_{otolith}$, in mm d^{-1}) using the biological intercept method following (Hobbs et al. 2007, Lewis et al. 2021). The final 56 increments were used to assess the effects of experimental treatments on otolith-based growth rates during the 56-day experiment.

Statistical Analyses

For each condition metric ($G_{otolith}$, K, HSI, and RNA:DNA), linear mixed effects models were constructed to examine patterns among treatments and time points, with tank as a random effect to account for tank effects. Models of otolith accretion included all 56 daily growth estimates for each fish from the final time point, with Fish ID as a random variable to account for individual variation. For each condition metric, planned linear contrasts were used to test for pairwise day*treatment effects using Tukey's range test in the R package "emmeans" (R Core Team 2022). Interpretation of these linear contrasts matched the "test slices" method of (Hammock et al. 2020) with results considered significant for p-values ≤ 0.05. Assuming monotonic responses of each metric to fasting, the temporal sensitivity of each metric was evaluated based on the lag in response to the initiation of treatment, with the lag defined as the time (in days) until the first day that a significant difference between treatments was observed or a given metric (Hammock et al. 2020). Thus, shorter lags indicated higher temporal sensitivity. Magnitudes of effects for each condition metric were assessed by examining the percent difference in mean values between fed and unfed treatments over the last 2 weeks of the experiment. Simple linear models were used to examine relationships between tank-specific means in otolith accretion and variation in somatic growth rates, including fork length (G_{length}) and total mass (G_{mass}), as well as changes in condition (ΔK). A linear model (ANCOVA) was also constructed examining linear relationships between mass and length, with treatment as a fixed effect. All models were constructed and compared using maximum likelihood estimation while assuming a Gaussian distribution. Model assumptions were examined using Q-Q and residual plots, and when necessary, data were transformed to meet model assumptions. All modeling and plotting were conducted using R v. 3.4.2 (R Core Team 2022).

RESULTS

Schlerochronologic (otolith) analysis

Aging accuracy based on full otolith increment profiles was approximately 95% for both fed and unfed treatments (Figure S3-1). Thus aging accuracy was within acceptable limits and matched previous otolith-based studies of Delta Smelt (Xieu et al. 2021). No differences in $G_{otolith}$ values were observed between treatments prior to the beginning of the experiment (Figure 3-2), and both treatments exhibited decreasing $G_{otolith}$ values, as is expected with maturing Delta Smelt whose growth rates decline naturally with age (Xieu et al. 2021) (Figure 3-3a). At 11 days after the beginning of the experiment, fed and unfed treatments diverged significantly, with fed treatments exhibiting significantly higher (larger daily rings) than unfed treatments (Figure 3-3a). Differences were maintained for the remainder of the 56-day experiment, with fed treatments exhibiting a 41% higher mean $G_{otolith}$ value than unfed treatments during the last 2 weeks of the study (Figure 3-2b).

Morphologic, molecular, and histologic analyses

Patterns among treatments in morphologic, molecular, and histologic analyses were previously described in detail by Hammock et al. (2020). Here, the results of this study were adapted and summarized for direct comparison with otolith-based metrics. A significant difference in K between fed and unfed treatments was detected on Day 7, with fed fish exhibiting 39.5% higher K values than unfed fish during the last 2 weeks of the study (Table 3-2, Figure 3-3b). HSI differed significantly between treatments on Day 4, with a 143.4% higher HSI in the fed versus unfed treatment upon completion of the study (Table 3-2, Figure 3-3c). A treatment effect in RNA:DNA was first detected on Day 28, with values being 53.8% higher in fed versus unfed treatments (Table 3-2, Figure 3-3d). Changes in HSI corresponded with several changes in liver histology, including reduced hepatic cell and nucleus areas (HCA and HNA) on Days 17 and 14, respectively, and increased depletion of glycogen (HGD) and liver lesions (HLS) on Day 14 for both metrics (Table 3-2).

Tank-specific variation in somatic growth, condition, and otolith accretion

Delta Smelt from fed treatments exhibited fork lengths that were 2.6 mm (6%) longer than those from unfed treatments during the last 2 weeks of the experiment. In contrast, mass differed between treatments on average by 0.28 g (62%) toward the completion of the experiment. Mean tank-specific otolith accretion rates did not vary significantly with tank-specific changes in length (Table 3-3, Figure 3-4a); however, otolith growth did vary significantly with changes in mass (Table 3-3, Figure 3-4b). Changes in mass varied linearly with changes in length; however, treatments exhibited significantly different y-intercepts, indicative of significant differences between treatments in fish body condition (K) (Table 3-3, Figure 3-4c). Furthermore, a significant linear relationship was observed between otolith accretion rate and overall changes in body condition (Table 3-3, Figure 3-4d).

DISCUSSION

Summary of key findings

An understanding of natural and anthropogenic factors that affect the health and condition of wild fish populations is key to effective management and conservation. To facilitate this, comparative experiments are needed to better understand the relative sensitivities of various bioindicators of fish condition to better inform studies of wild fish populations (Peck et al. 2015). Here, we build upon previous work by Hammock et al. (2020) to experimentally contrast the sensitivity of otolith-based growth histories and several other bioindicators of fish condition to variation in food availability. Results indicated that HSI, K, and $G_{otolith}$ were the most temporally sensitive to changes in food availability, with significant changes detected on Days 4, 7, and 11, respectively (Figures 3-5 and 3-6). In contrast, RNA:DNA values took nearly a month to respond to severe food limitation. HSI exhibited the largest response, varying by over 140% between treatments, whereas condition factor, $G_{otolith}$, and RNA:DNA values all varied by approximately 40-50% between treatments.

Together, these results highlight the patterns observed by Hammock et al. (2020), emphasizing that HSI is highly sensitive to food limitation, likely due to rapid glycogen depletion and reductions in hepatocyte size, as was observed in histological preparations. Furthermore, by contrasting these patterns with daily otolith-based growth estimates, we show that $G_{otolith}$ is relatively sensitive in both time and magnitude and reflects proportional changes in body condition (versus length) for subadult Delta Smelt. Importantly, the otolith-based approach is the only method that can reconstruct full daily chronologies of fish condition from relatively few samples, thus maximizing the scope and value of data from each specimen. Nevertheless, given their relative strengths and ease of collection, a combination of metrics (e.g., K, HSI, and $G_{otolith}$) is likely to provide the most robust assessments of growth and condition in wild fish populations.

Responses of other bioindicators to food limitation

As described by Hammock et al. (2020), Fulton's condition factor in subadult Delta Smelt decreased in relation to food limitation within 7 days and by approximately 40% during the final 2 weeks of the experiment. Similar results have been observed in previous studies of food limitation and condition in fishes (Molony & Sheaves 1998). This result reflects the overall change in body mass (including muscle, lipid, and other energy reserves) relative to changes in length. Given that there were minimal differences (< 5%) in length between treatments, changes in K arose almost entirely due to changes in body mass (> 60% between treatments). Although variation in K can provide meaningful information regarding fish health, changes can be relatively slow and variable in response to food limitation, suggesting that K may not always suffice as a sole indicator of growth and health in fishes (Peck et al. 2015). Nevertheless, in the present study, changes in K were significant within 1 week of food limitation and appeared to provide a relatively sensitive indicator of nutritional stress.

In contrast to K, HSI appeared much more sensitive to food limitation both in the timing (4 days) and magnitude (143%) of the response. Although changes in liver mass also affect K, this result indicates that the liver lost mass much more rapidly than non-hepatic tissues. This rapid change in HSI reflects the numerous pathways in which livers store energy and nutrients for survival when food is limited (Echevarría et al. 1997, Cho 2005). These pathways were reflected in the histological metrics that were also measured (hepatocyte area, hepatocyte nucleus area, glycogen depletion, and liver lesions) and reflected significant changes in response to food limitation. Although the liver histological data may point more directly to specific mechanisms of change, the HSI itself proved to be highly sensitive to treatments, with the added advantage of being quick and easy to measure using simple gravimetric techniques. In contrast to K and HSI, the RNA:DNA ratio took much longer, nearly 1 month, to exhibit significant differences between fed and unfed treatments. It is possible that RNA:DNA is a better measure of growth for earlier life stages of fishes, where rapid responses (e.g., < 3 days) to food limitation have been observed (Buckley et al. 1999).

Accuracy and Precision of Otolith-based Age and Growth Estimates

In this study, we examined the temporal sensitivity and magnitude of otolith-based growth rates and age estimates for fishes that experienced extreme differences in foraging conditions (fed or

unfed) that resulted in a gradient of nutritional stress, with increasing stress through time. In both fed and unfed treatments, we observed relatively low and similar aging errors that corresponded with relatively high aging accuracy, in agreement with previous otolith validation studies (Figure S3-1). For example, cultured Delta Smelt in well-fed conditions have been found to exhibit consistent daily increments up to 270 DPH, well beyond the experimental period ending at 213 DPH (Xieu et al. 2021). Thus, aging accuracy appeared to be unaffected by variation in growth, despite a change in mean increment widths, suggesting that otolith-based ages and estimates of total growth rate (size/age) can be reliably produced, even under food-limited conditions. However, Xieu et al. (2021) also noted that the smallest increments can easily be missed, especially when imaged at lower (e.g., 200X) magnifications. This suggests that extreme reductions in somatic growth and otolith accretion could lead to small, compacted increments that are no longer quantifiable with image analysis. Such a phenomenon would result in missed rings and over-estimates of daily growth rates for individuals experiencing the most extreme reductions in growth due to environmental stress. Thus, otolith-based indices of growth may be most sensitive at mid to high growth rates and less sensitive at the lowest somatic growth rates experienced by fishes. Nevertheless, in the present study, nearly 70% of the variation among tanks in mean changes in fish mass could be explained by corresponding changes in otolith accretion.

Otolith-somatic growth relationship

Otolith-based approaches can provide a valuable toolkit for studying wild fish populations (Campana 1990). This is particularly useful for populations of rare and endangered species, like Delta Smelt, where obtaining large sample sizes of specimens is difficult, and every individual is highly valuable. Here, we found that food limitation resulted in reduced growth and condition that corresponded with a significant 41% difference in $G_{otolith}$ values which was detectible within 11 days of the initiation of food limitation. Similar responses in otolith-based growth indicators have been observed in similar studies that have manipulated fish growth and condition using food limitation (Tzeng & Yu 1992, Molony & Sheaves 1998, Peck et al. 2015). However, some studies have indicated more rapid (e.g., 1-3 day) responses of otolith-based growth estimates to food limitation. The time lag of otolith responses can be dependent on the magnitude of feeding change and fish size or life stage, with otoliths from larvae appearing to respond quicker to food deprivation compared to post-larvae and juveniles (Peck et al. 2015). In contrast, the11-day lagged response in the present study suggests that the more robust energy reserves in older fish may buffer the effects of food limitation on otolith accretion, with somatic responses to food limitation occurring earlier and being more severe than those indicated by changes in otolith increment widths (Molony & Sheaves 1998). Although otoliths may provide conservative estimates of variation in nutritional stress, variation in otolith-based growth rates in this study were similar to changes in K, both in timing and magnitude, suggesting that otolith accretion rates in subadult Delta Smelt likely reflect changes in fish body condition fairly well.

Despite the significant response of $G_{otolith}$ to experimental treatments, variation in increment widths did not correlate significantly with changes in fish length at the tank level, indicative of decoupling between otolith accretion and elongation in subadult Delta Smelt (e.g., greater than

200 DPH). This is likely due the relatively small difference between fed and unfed treatments in fish length, indicating that elongation (G_{length}) per se is insensitive to food limitation in subadult Delta Smelt relative to changes in mass and condition (G_{mass} and ΔK, respectively). Thus back-calculated length-based growth rates (e.g., using the biological intercept method) can provide useful indices for comparing general patterns in fish growth and condition, but are not valid for estimating elongation rates per se for maturing subadult Delta Smelt (e.g., > 200 dph). The decoupling of otolith accretion rates with elongation rates has been observed for other species (Barber & Jenkins 2001, Song et al. 2009), though some have found it to be a short-term effect that is resolved over longer time periods (Baumann et al. 2005). Otolith accretion rates can be influenced by many biological (e.g., ontogenetic stage, reproduction, foraging success) and environmental (e.g., salinity, water temperature, photoperiod) factors that could have different net effects on somatic growth and otolith accretion rates (Campana 1984, Gutiérrez & Morales-Nin 1986, May & Jenkins 1991, Ferron & Leggett 1994, Suthers 1998). Furthermore, such effects could be further differentiated under extreme conditions (Campana 1990, Barber & Jenkins 2001, Baumann et al. 2005). Although tank-specific variation includes significant sources of unmeasured error, it was not practical in this study to individually tag Delta Smelt and statistically evaluate paired somatic growth and otolith accretion rates for each fish. Such a study in the future would likely yield higher statistical power to evaluate the true correlation, or lack thereof, between otolith growth and somatic growth at the individual level.

Nevertheless, nearly 70% of the tank-specific variation in G_{mass} could be explained by corresponding changes in otolith accretion rates (Figure 3-4b). Similarly, variation in fish body condition was significantly correlated with variation in otolith accretion (Figure 3-4d). Thus, for subadult Delta Smelt, otolith accretion rates provided a meaning indicator of relative changes in overall growth and condition. These results suggest that otoliths can be used to evaluate variation in overall growth and condition for wild fish, providing results that are similar to other condition metrics such as K, even under extreme levels of food limitation.

Conclusions

Comparative experimental studies are valuable for contrasting the relative strengths of different indicators of fish health and condition. While several of the biomarkers examined in this study exhibited useful responses to nutritional stress, only the otolith-based approach can provide a life-long chronology of past conditions for each fish. In contrast, K, HSI, and RNA:DNA provided point estimates with varying response and integration times. Thus otolith-based approaches are particularly useful in the study of endangered fishes such as Delta Smelt, where wild specimens have become increasingly scarce, and every specimen is of high value. However, in wild populations, multiple interacting stressors are likely to result in different patterns for various indicators and over different time scales. Thus, combining otolith-based chronologies and other single-point estimates of health and condition (e.g., HSI, K) is likely to provide more robust condition assessments for wild fish populations.

ACKNOWLEDGEMENTS

We thank the many staff at the UC Davis Fish Conservation and Culture Laboratory for their expertise and efforts in culturing and rearing Delta Smelt. Furthermore, we acknowledge the many staff and student researchers at the UC Davis Department of Wildlife, Fish, and Conservation Biology; School of Veterinary Medicine; and Center for Aquatic Biology and Aquaculture for laboratory and logistical support in conducting the study and processing samples. This study was funded by the U.S. Bureau of Reclamation Directed Outflow Project (Grant Nos. R17AC00129 and R22AC00392) to Bruce G. Hammock, L. Lewis, J. Hobbs, and S. Teh. The views expressed herein are those of the authors and do not represent the official opinion of any employer, institution, or government agency.

REFERENCES

Anderson JT (1988) A Review of Size Dependent Survival During Pre-Recruit Stages of Fishes in Relation to Recruitment. J Northw Atl Fish Sci 8:55–66.

Barber MC, Jenkins GP (2001) Differential effects of food and temperature lead to decoupling of short-term otolith and somatic growth rates in juvenile King George whiting. Journal of Fish Biology 58:1320–1330.

Baumann H, Peck MA, Herrmann J-P, Baumann H, Peck MA, Herrmann J-P (2005) Short-term decoupling of otolith and somatic growth induced by food level changes in postlarval Baltic sprat, Sprattus sprattus. Mar Freshwater Res 56:539–547.

Bergenius MA, Meekan MG, Robertson RD, McCormick MI (2002) Larval growth predicts the recruitment success of a coral reef fish. Oecologia 131:521–525.

Berkeley SA, Chapman C, Sogard SM (2004a) Maternal age as a determinant of larval growth and survival in a marine fish, *Sebastes melanops*. Ecology 85:1258–1264.

Berkeley SA, Hixon MA, Larson RJ, Love MS (2004b) Fisheries Sustainability via Protection of Age Structure and Spatial Distribution of Fish Populations. Fisheries 29:23–32.

Blackwell BG, Brown ML, Willis DW (2000) Relative Weight (Wr) Status and Current Use in Fisheries Assessment and Management. Reviews in Fisheries Science 8:1–44.

Buckley L, Caldarone E, Ong T-L (1999) RNA–DNA ratio and other nucleic acid-based indicators for growth and condition of marine fishes. Hydrobiologia 401:265–277.

Buckley LJ (1984) RNA-DNA ratio: an index of larval fish growth in the sea. Mar Biol 80:291–298.

Caldarone E, Wagner M, St. Onge-Burns J, Buckley LJ (2001) Protocol and guide for estimating nucleic acids in larval fish using a fluorescence microplate reader.

Campana SE (2001) Accuracy, precision and quality control in age determination, including a review of the use and abuse of age validation methods. Journal of Fish Biology 59:197–242.

Campana SE (1999) Chemistry and composition of fish otoliths: pathways, mechanisms and applications. Marine Ecological Progress Series 188:263–297.

Campana SE (1990) How Reliable are Growth Back-Calculations Based on Otoliths? Can J Fish Aquat Sci 47:2219–2227.

Campana SE (1984) Lunar cycles of otolith growth in the juvenile starry flounder Platichthys stellatus. Mar Biol 80:239–246.

Campana SE, Neilson JD (1985) Microstructure of Fish Otoliths. Canadian Journal of Fisheries and Aquatic Sciences 42:1014–1032.

Campana SE, Thorrold SR (2001) Otoliths, increments, and elements: keys to a comprehensive understanding of fish populations? Canadian Journal of Fisheries and Aquatic Sciences 58.

China V, Holzman R (2014) Hydrodynamic starvation in first-feeding larval fishes. Proceedings of the National Academy of Sciences 111:8083–8088.

Cho SH (2005) Compensatory Growth of Juvenile Flounder Paralichthys olivaceus L. and Changes in Biochemical Composition and Body Condition Indices during Starvation and after Refeeding in Winter Season. Journal of the World Aquaculture Society 36:508–514.

Damon LJ, Slater SB, Baxter RD, Fujimura RW (2016) Fecundity and reproductive potential of wild female Delta smelt in the upper San Francisco Estuary, California. California Fish and Game 102:188–210.

De Pedro N, Delgado MJ, Gancedo B, Alonso-Bedate M (2003) Changes in glucose, glycogen, thyroid activity and hypothalamic catecholamines in tench by starvation and refeeding. J Comp Physiol B 173:475–481.

Echevarría G, Martínez-Bebiá M, Zamora S (1997) Evolution of Biometric Indices and Plasma Metabolites During Prolonged Starvation in European Sea Bass (Dicentrarchus labrax, L.). Comparative Biochemistry and Physiology Part A: Physiology 118:111–123.

Ferron A, Leggett WC (1994) An Appraisal of Condition Measures for Marine Fish Larvae. In: *Advances in Marine Biology*. Elsevier, p 217–303

Feyrer F, Herbold B, Matern S, Moyle P (2003) Dietary shifts in a stressed fish assemblage: Consequences of a bivalve invasion in the San Francisco Estuary. ENVIRONMENTAL BIOLOGY OF FISHES 67:277–288.

Feyrer F, Nobriga ML, Sommer TR (2007) Multidecadal trends for three declining fish species: Habitat patterns and mechanisms in the San Francisco Estuary, California, USA. Canadian Journal of Fisheries and Aquatic Sciences 64:723–734.

Giacalone VM, D'Anna G, Badalamenti F, Pipitone C (2010) Weight-length relationships and condition factor trends for thirty-eight fish species in trawled and untrawled areas off the coast of northern Sicily (central Mediterranean Sea): WLR, condition factor and trawl-ban. Journal of Applied Ichthyology 26:954–957.

Gutiérrez E, Morales-Nin B (1986) Time series analysis of daily growth in Dicentrarchuslabrax L. otoliths. Journal of Experimental Marine Biology and Ecology 103:163–179.

Hammock BG, Hartman R, Dahlgren RA, Johnston C, Kurobe T, Lehman PW, Lewis LS, Van Nieuwenhuyse E, Ramírez-Duarte WF, Schultz AA, Teh SJ (2021) Patterns and predictors of condition indices in a critically endangered fish. Hydrobiologia.

Hammock BG, Hartman R, Slater SB, Hennessy A, Teh SJ (2019a) Tidal Wetlands Associated with Foraging Success of Delta Smelt. Estuaries and Coasts 42:857–867.

Hammock BG, Moose SP, Solis SS, Goharian E, Teh SJ (2019b) Hydrodynamic Modeling Coupled with Long-term Field Data Provide Evidence for Suppression of Phytoplankton by Invasive Clams and Freshwater Exports in the San Francisco Estuary. Environmental Management 63:703–717.

Hammock BG, Ramírez-Duarte WF, Triana Garcia PA, Schultz AA, Avendano LI, Hung T-C, White JR, Bong Y-T, Teh SJ (2020) The health and condition responses of Delta Smelt to fasting: A time series experiment. PLoS ONE 15:e0239358.

Hobbs JA, Bennett WA, Burton JE, Baskerville-Bridges B (2007) Modification of the biological intercept model to account for ontogenetic effects in laboratory-reared delta smelt (Hypomesus transpacificus). Fishery Bulletin 105:30–38.

Hobbs JA, Moyle PB, Fangue N, Connon RE (2017) Is Extinction Inevitable for Delta Smelt and Longfin Smelt? An Opinion and Recommendations for Recovery. San Francisco Estuary and Watershed Science 15:1–19.

Hoque MT, Yusoff FM, Law T, Syed MA (1998) Effect of hydrogen sulphide on liver somatic index and Fulton's condition factor in Mystus nemurus. Journal of Fish Biology 52:23–30.

Houde ED (1978) Critical food concentrations for larvae of three species of subtropical marine fishes. Bulletin of Marine science 28:395–411.

Houde ED (1975) Effects of stocking density and food density on survival, growth and yield of laboratory-reared larvae of sea bream Archosargus rhomboidalis (L.)(Sparidae). Journal of Fish Biology 7:115–127.

Houde ED (1987) Fish early life dynamics and recruitment variability. In: *Am. Fish. Soc. Symp.* p 17–29

Hung T-C, Ellison L, Stevenson T, Sandford M, Schultz AA, Eads AR (2022) Early Weaning in Endangered Delta Smelt: Effect of Weaning Time on Growth and Survival. North American Journal of Aquaculture 84:249–260.

Lambert Y, Dutil J-D (2000) Energetic consequences of reproduction in Atlantic cod (*Gadus morhua*) in relation to spawning level of somatic energy reserves. Can J Fish Aquat Sci 57:815–825.

Lewis L, Denney C, Willmes M, Xieu W, Fichman R, Zhao F, Hammock B, Schultz A, Fangue N, Hobbs J (2021) Otolith-based approaches indicate strong effects of environmental variation on growth of a Critically Endangered estuarine fish. Mar Ecol Prog Ser 676:37–56.

Lindberg JC, Tigan G, Ellison L, Rettinghouse T, Nagel MM, Fisch KM (2013) Aquaculture Methods for a Genetically Managed Population of Endangered Delta Smelt. North American Journal of Aquaculture 75:186–196.

Lloret J, Faliex E, Shulman GE, Raga J-A, Sasal P, Muñoz M, Casadevall M, Ahuir-Baraja AE, Montero FE, Repullés-Albelda A, Cardinale M, Rätz H-J, Vila S, Ferrer D (2012) Fish Health and Fisheries, Implications for Stock Assessment and Management: The Mediterranean Example. Reviews in Fisheries Science 20:165–180.

Lloret J, Planes S (2003) Condition, feeding and reproductive potential of white seabream Diplodus sargus as indicators of habitat quality and the effect of reserve protection in the northwestern Mediterranean. Mar Ecol Prog Ser 248:197–208.

Marshall CT, Yaragina NA, Lambert Y, Kjesbu OS (1999) Total lipid energy as a proxy for total egg production by fish stocks. Nature 402:288–290.

May H, Jenkins G (1991) Patterns of settlement and growth of juvenile flounder Rhombosolea tapirina determined from otolith microstructure. Mar Ecol Prog Ser 79:203–214.

Miller SJ, Storck T (1982) Daily Growth Rings in Otoliths of Young-of-the-Year Largemouth Bass. Transactions of the American Fisheries Society 111:527–530.

Molony BW (1993) Effects of feeding history on mobilisation and deposition of body constituents and on growth in juvenile Ambassis vachelli (Pisces: Chandidae). Marine Biology 116:389–397.

Molony BW, Choat JH (1990) Otolith increment widths and somatic growth rate: the presence of a time-lag. Journal of Fish Biology 37:541–551.

Molony BW, Sheaves MJ (1998) Otolith increment widths and lipid contents during starvation and recovery feeding in adult Ambassis vachelli (Richardson). Journal of Experimental Marine Biology and Ecology 221:257–276.

Moyle PB, Brown LR, Durand JR, Hobbs JA (2016) Delta smelt: Life history and decline of a once abundant species in the San Francisco Estuary. San Francisco Estuary and Watershed Science 14:1–30.

Moyle PB, Hobbs JA, Durand JR (2018) Delta Smelt and Water Politics in California. Fisheries.

Oliva-Teles A (2012) Nutrition and health of aquaculture fish: Nutrition and health of aquaculture fish. Journal of Fish Diseases 35:83–108.

Pannella G (1971) Fish Otoliths: Daily Growth Layers and Periodical Patterns. Science 173:1124.

Peck MA, Baumann H, Clemmesen C, Herrmann J-P, Moyano M, Temming A (2015) Calibrating and comparing somatic-, nucleic acid-, and otolith-based indicators of growth and condition in young juvenile European sprat (Sprattus sprattus). Journal of Experimental Marine Biology and Ecology 471:217–225.

Peragón J, Barroso JB, García-Salguero L, de la Higuera M, Lupiáñez JA (1999) Carbohydrates affect protein-turnover rates, growth, and nucleic acid content in the white muscle of rainbow trout (Oncorhynchus mykiss)1Publication no. 194 from `Drugs, Environmental Toxics and Cell Metabolism Research Group', Department of Biochemistry and Molecular Biology, Centre of Biological Sciences, University of Granada, Granada, Spain.1. Aquaculture 179:425–437.

R Core Team (2022) R: A language and environment for statistical computing.

Rätz H-J, Lloret J (2003) Variation in fish condition between Atlantic cod (Gadus morhua) stocks, the effect on their productivity and management implications. Fisheries Research 60:369–380.

Roberts ME, Wetzel JE, Brooks RC, Garvey JE (2004) Daily Increment Formation in Otoliths of the Redspotted Sunfish. North American Journal of Fisheries Management 24:270–274.

Sakaris PC, Buckmeier DL, Smith NG (2014) Validation of Daily Ring Deposition in the Otoliths of Age-0 Alligator Gar. North American Journal of Fisheries Management 34:1140–1144.

Schneider CA, Rasband WS, Eliceiri KW (2012) NIH Image to ImageJ: 25 years of image analysis. Nat Methods 9:671–675.

Shulman GE, Love RM (1999) Advances in Marine Biology, 36: the Biochemical Ecology of Marine Fishes. Elsevier, Burlington.

Sommer T, Armor C, Baxter R, Breuer R, Brown L, Chotkowski M, Culberson S, Feyrer F, Gingras M, Herbold B, Kimmerer W, Mueller-Solger A, Nobriga M, Souza K (2007) The collapse of pelagic fishes in the Upper San Francisco Estuary. Fisheries 32:270–277.

Song Z, Fu Z, He C, Shen D, Yue B (2009) Effects of temperature, starvation and photoperiod on otolith increments in larval Chinese sucker, Myxocyprinus asiaticus. Environ Biol Fish 84:159–171.

Starrs D, Ebner BC, Fulton CJ (2016) All in the ears: Unlocking the early life history biology and spatial ecology of fishes. Biological Reviews 91:86–105.

Suthers IM (1998) Bigger? Fatter? Or is faster growth better? Considerations on condition in larval and juvenile coral-reef fish. Austral Ecol 23:265–273.

Teh SJ, Adams SM, Hinton DE (1997) Histopathologic biomarkers in feral freshwater fish populations exposed to different types of contaminant stress. Aquatic Toxicology 37:51–70.

Teh SJ, Baxa DV, Hammock BG, Gandhi SA, Kurobe T (2016) A novel and versatile flash-freezing approach for evaluating the health of Delta Smelt. Aquatic Toxicology 170:152–161.

Teh SJ, Schultz AA, Duarte WR, Acuña S, Barnard DM, Baxter RD, Garcia PAT, Hammock BG (2020) Histopathological assessment of seven year-classes of Delta Smelt. Science of the Total Environment 726.

Tsai Y-JJ, Ellison L, Stevenson T, Mulvaney WJ, Carson EW, Hung T-C (2022) Evaluating the Performance of a Small-Scale Culture System for Delta Smelt. North American Journal of Aquaculture 84:370–380.

Tzeng W-N, Yu S-Y (1992) Effects of starvation on the formation of daily growth increments in the otoliths of milkfish, Chanos chanos (Forsskal), larvae. J Fish Biology 40:39–48.

Xieu W, Lewis LS, Zhao F, Fichman RA, Willmes M, Hung T-C, Ellison L, Stevenson T, Tigan G, Schultz AA, Hobbs JA (2021) Experimental validation of otolith-based age and growth reconstructions across multiple life stages of a critically endangered estuarine fish. PeerJ 9:e12280.

Zeng L-Q, Li F-J, Li X-M, Cao Z-D, Fu S-J, Zhang Y-G (2012) The effects of starvation on digestive tract function and structure in juvenile southern catfish (Silurus meridionalis Chen). Comparative Biochemistry and Physiology Part A: Molecular & Integrative Physiology 162:200–211.

TABLES

Table 3-1: Experimental design. Each metric and its code are listed along with the tissue type, preservation method, sampling time points (T_{sample}, day of the experiment), and the total sample sizes of fish collected per time point (N_t).

Otoliths of fish from the final time point (Day 56) were analyzed, with increment profiles used to reconstruct the daily growth history of each fish, including each day of the experiment (Days 0-56). Table adapted from Hammock et al. (2020).

Category	Metric	Code	Tissue	Preservative	T_{sample}	N_t
Morphologic	Fulton's Condition Factor	K	Fish	Liquid nitrogen	0,1,2,4,7,14,21, 28,35,42,49,56	32
	Hepato-somatic Index	HSI	Liver/Fish	Liquid nitrogen	0,1,2,4,7,14,21, 28,35,42,49,56	32
Histologic	Hepatic Lesion Score	HLS	Liver	Formalin	0,4,7,14,21,28, 35,42,49,56	8
	Hepatic Glycogen Depletion	HGD	Liver	Formalin	0,4,7,14,21,28, 35,42,49,56	8
	Hepatocyte Area	HCA	Liver	Formalin	0,4,7,14,21,28*	8
	Hepatocyte Nucleus Area	HNA	Liver	Formalin	0,4,7,14,21,28, 35,42,49,56	8
Molecular	RNA:DNA	RNA	Muscle	Liquid nitrogen	0,1,2,4,7,14,21, 28,35,42,49,56	32
Schlero-chronologic	Otolith-based Growth Rate	$G_{otolith}$	Otolith	DI water	56	32†

*HCA could not be distinguished from HNA in unfed treatments after 28 DPH.
†Planned sample size was 32, but 26 were included in the final analysis (see methods).

Table 3-2: Summary of final experimental results by metric and treatment.

Final conditions were defined as the period encompassing the last three time points (2 weeks) used by Hammock et al. (2020) (Days 42, 49, and 56), including daily otolith increments from Days 42-56. Mean (s.d.) values are provided separately for each treatment (Fed and Unfed). Differences (Δ) and percent differences between treatments are provided for each metric. Temporal lags (T_{lag}, in days) are provided based on the first time point in which treatment differences were detected by each metric. Morphologic, histologic, and molecular values calculated from Hammock et al. (2020). M – mass (in g), FL – fork length (in mm); other metrics are as in Table 3-1.

Category	**Metric**	**Fed**	**Unfed**	**Δ**	**Δ (%)**	**T_{lag} (d)**
Morphologic	M	0.73 (0.26)	0.45 (0.2)	0.28 (0.45)	61.5	n/a
	FL	50.46 (4.63)	47.83 (5.08)	2.63 (9.71)	5.5	n/a
	K	0.55 (0.08)	0.39 (0.07)	0.15 (0.15)	39.5	7
	HSI	1.67 (0.69)	0.69 (0.18)	0.98 (0.87)	143.4	4
Histologic	HLA†	0.25 (0.62)	2.92 (1.93)	-2.67 (2.55)	-91.4	14
	HGD†	0.5 (0.9)	2.33 (0.78)	-1.83 (1.68)	-78.6	14
	HCA	185.68 (37.66)	101.08 (34.21)	84.6 (71.87)	83.7	14
	HNA	25.68 (5.4)	16.82 (2.96)	8.86 (8.36)	52.6	7
Molecular	RNA	1.85 (0.55)	1.21 (0.43)	0.65 (0.97)	53.8	14
Schlerochronologic	$G_{otolith}$	0.11 (0.01)	0.08 (0.01)	0.03 (0.01)	41.0	11

†Measures for which smaller values indicate higher sensitivity.

*HCA values reflect the final measured timepoints (Days 14, 21, 28; see methods).

Table 3-3: Results of simple linear models comparing mean tank-specific changes in fork length (G_{length}), mass (G_{mass}), condition (ΔK), otolith accretion rate (Accretion), and treatment effects (Treat) during the 56 day experiment (see Figure 3-4).

Significant p-values are in bold (P < 0.05).

Model	Factor	DF	SS	MS	F	P	R2
G_{length} ~ Accretion	Accretion	1	0.007	0.007	2.647	0.155	0.310
	Residuals	6	0.017	0.003			
G_{mass} ~ Accretion	Accretion	1	77.476	77.476	11.988	0.013	0.670
	Residuals	6	38.776	6.463			
G_{mass} ~ G_{length} + Treat	Glength	1	83.695	83.695	361.82	< 0.001	0.986
	Treat	1	31.4	31.4	135.74	< 0.001	
	Residuals	5	1.157	0.231			
ΔK ~ Accretion	Accretion	1	0.033	0.033	8.3908	0.027	0.580
	Residuals	6	0.023	0.004			

Table 3-4: Statistical table for the mixed effects model.

Model describes the model structure, Factor describes the terms of the model, DF is the degrees of freedom, SS is the sum of squared err, MS is the mean squared error, F is the F value, P1 is the p value of the term with significance <0.05 denoted by bolding, P2 is the model significance relative to a null model, and R^2_{GLMM} is the model conditional R_2 as calculated by the r.squaredGLMM() function from the MuMIN package.

Model	**Factor**	**DF**	**SS**	**MS**	**F**	**P1**	**P2**	**R^2_{GLMM}**
HSI ~ treatment + day + (1|tank) + treatment:day	treatment	1	34.945	34.945	133.1105	<0.001	<0.001	0.37
	day	11	6.785	0.617	2.3494	0.009		
	treatment:day	11	15.704	1.428	5.438	<0.001		
K ~ treatment + day + (1|tank) + treatment:day	treatment	1	0.58111	0.58111	110.9594	<0.001	<0.001	0.45
	day	11	0.51474	0.04679	8.9352	<0.001		
	treatment:day	11	0.50994	0.04636	8.8519	<0.001		
RNA ~ treatment + day + (1|tank) + treatment:day	treatment	1	5.46	5.46	20.3598	0.002	<0.001	0.3
	day	11	26.655	2.4232	9.0358	<0.001		
	treatment:day	11	7.998	0.7271	2.7112	0.002		
$G_{otolith}$ ~ treatment * day + (1|tank/fishid)	treatment	1	0.32	0.3244	2.6403	0.002	<0.001	0.84
	day	61	807.06	13.2305	107.6804	<0.001		
	treatment:day	61	62.81	1.0297	8.3804	0.002		

FIGURES

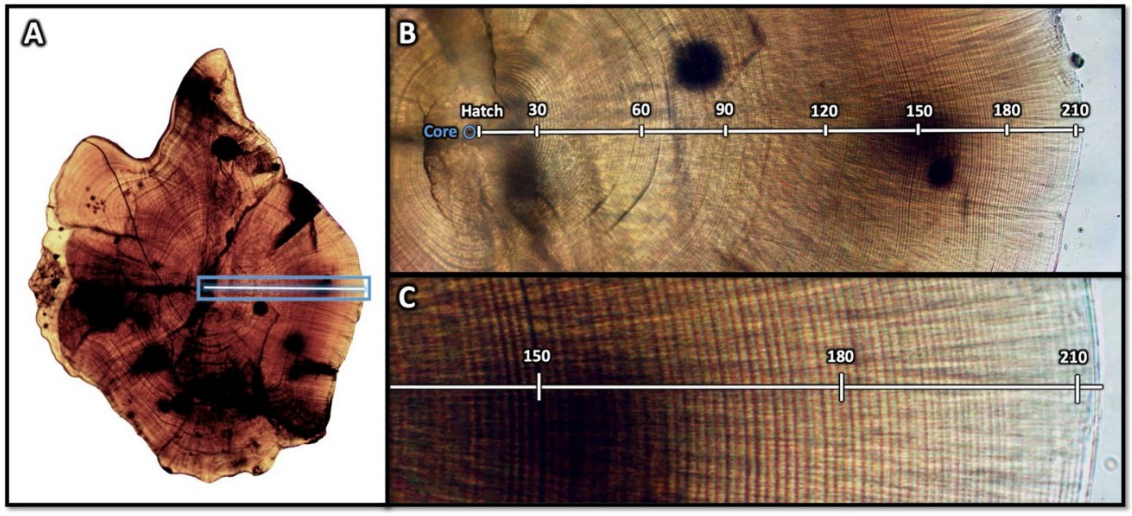

Figure 3-1: Otolith increment analysis in Delta Smelt.

Whole sagittal otoliths (A) are sanded in the sagittal plane, imaged, and daily increments enumerated and measured from the core to the dorsal edge (B). The last 56 dorsal edge increments represent the experimental period (C). Increment widths correspond with the daily otolith accretion rate (μm d^{-1}).

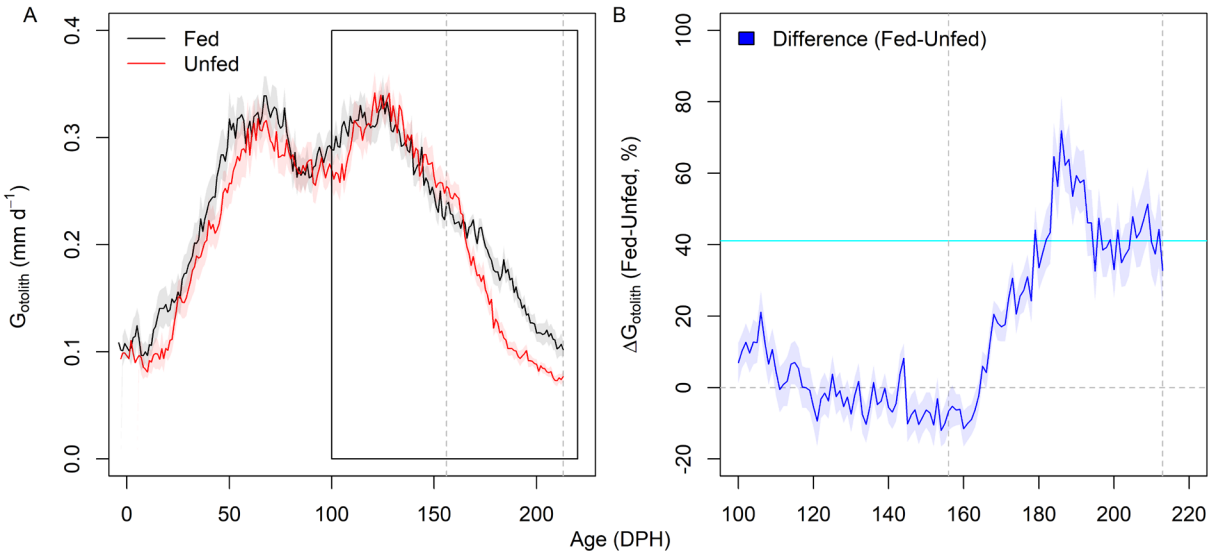

Figure 3-2: Comparison of the otolith-based growth histories of Delta Smelt in fed and unfed treatments.

(A) Full mean (± s.d.) daily growth profiles of fish in each treatment. (B) Percent difference (± se) between fed and unfed treatments (100*(Fed-Unfed)/Fed). The inset box in (A) reflects the period over which differences are shown in (B). The solid blue horizontal line in (B) reflects the mean difference between fed and unfed treatments during the final 2 weeks of the experiment (Days 42-56). The two vertical dashed lines in both (A) and (B) indicate when the experiment began (Day 0, 157 DPH) and ended (Day 56, 213 DPH).

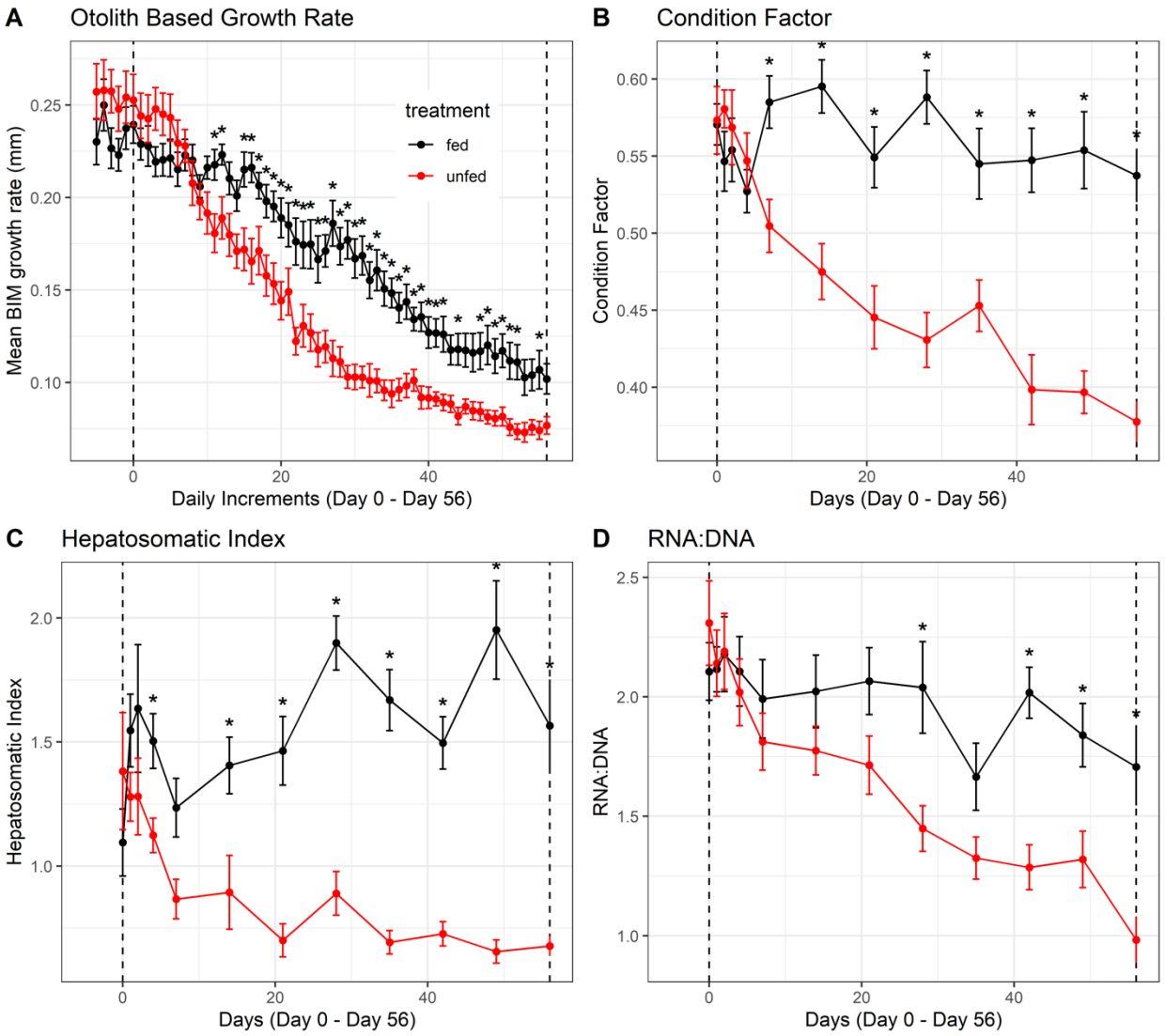

Figure 3-3: Differences between fed and unfed treatments for each experimental time point from Day 0 to Day 56.

(A) BIM-calculated somatic growth rate ($G_{otolith}$, based on accretion rate), (B) Fulton's condition factor (K), C) hepatosomatic index (HSI), and (D) ratio of RNA:DNA. Asterisks (*) represent time points that exhibited significant differences between treatments. Data in (B-D) reconstructed from Hammock et al. (2020).

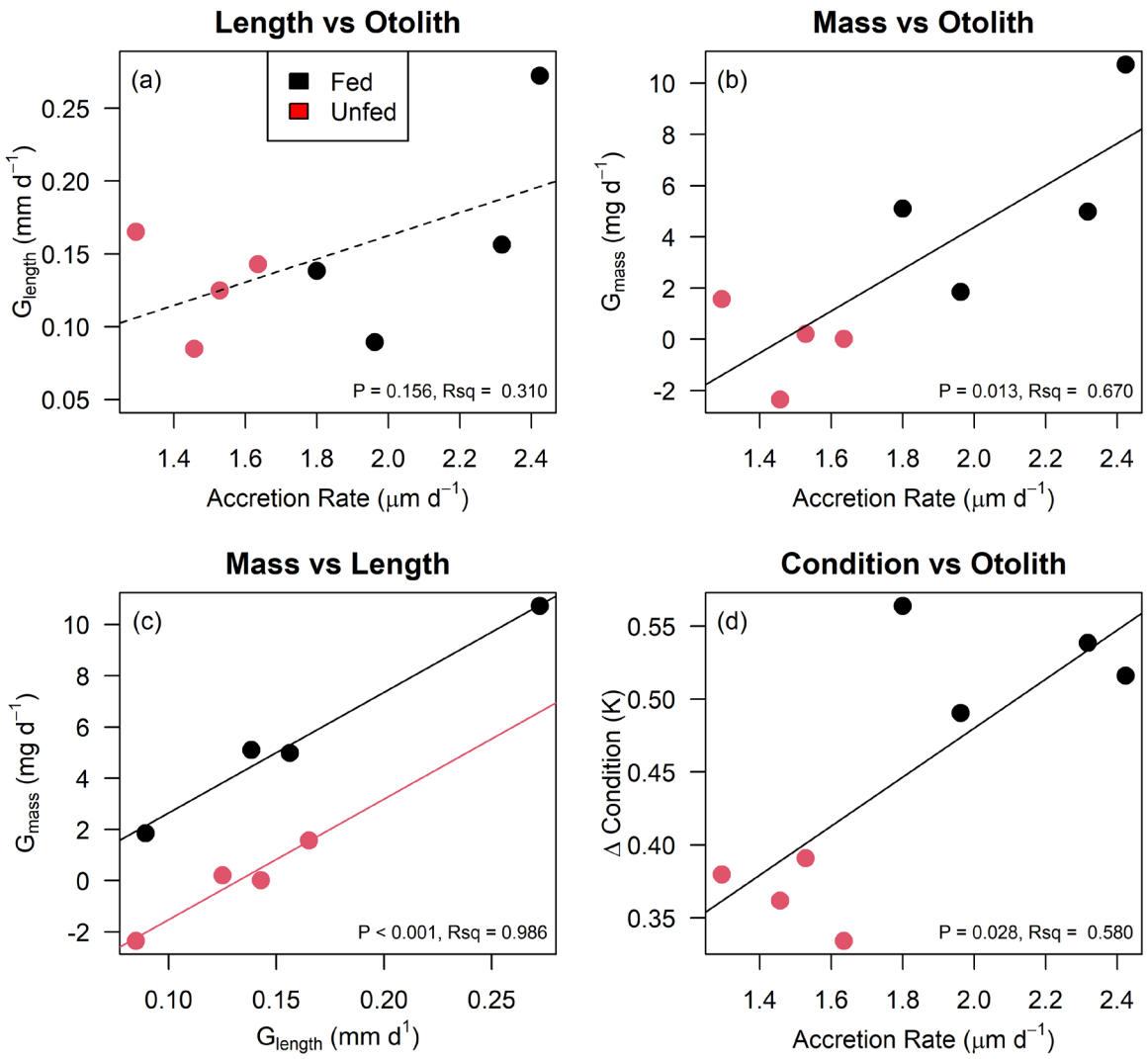

Figure 3-4: Comparison of mean tank-specific growth and condition metrics including length, mass, Fulton's condition factor, and otolith accretion rate.

Solid lines indicate significant ($p < 0.05$) linear relationships; the dashed line is non-significant. Statistical results are in Table 3-3.

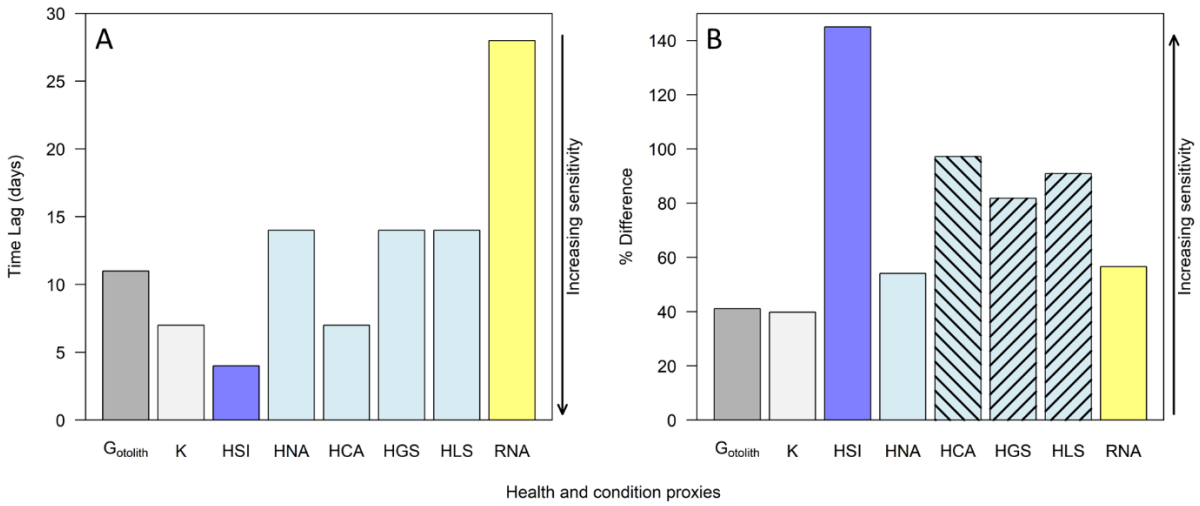

Figure 3-5: Comparative sensitivity of each condition metric to food limitation in Delta Smelt.

(A) Temporal sensitivity as reflected by the timing of the first statistically significant difference between treatments. (B) Dynamic range as estimated by the average percent difference between treatments during the last 2 weeks of the experiment (Days 42-56). Smaller values in (A) reflect higher temporal sensitivity (faster response time) to the onset of food limitation, whereas larger values in (B) reflect a higher dynamic range (a larger proportional response). Shaded bars in (B) indicate caveats: HCA reflects differences in the final 3 time points that could be measured (Days 14, 21, 28); HGD and HLS represent mean differences between qualitative scores (0-3). Metrics as in Table 3-1. Values other than $G_{otolith}$ were calculated from results in Hammock et al. (2020).

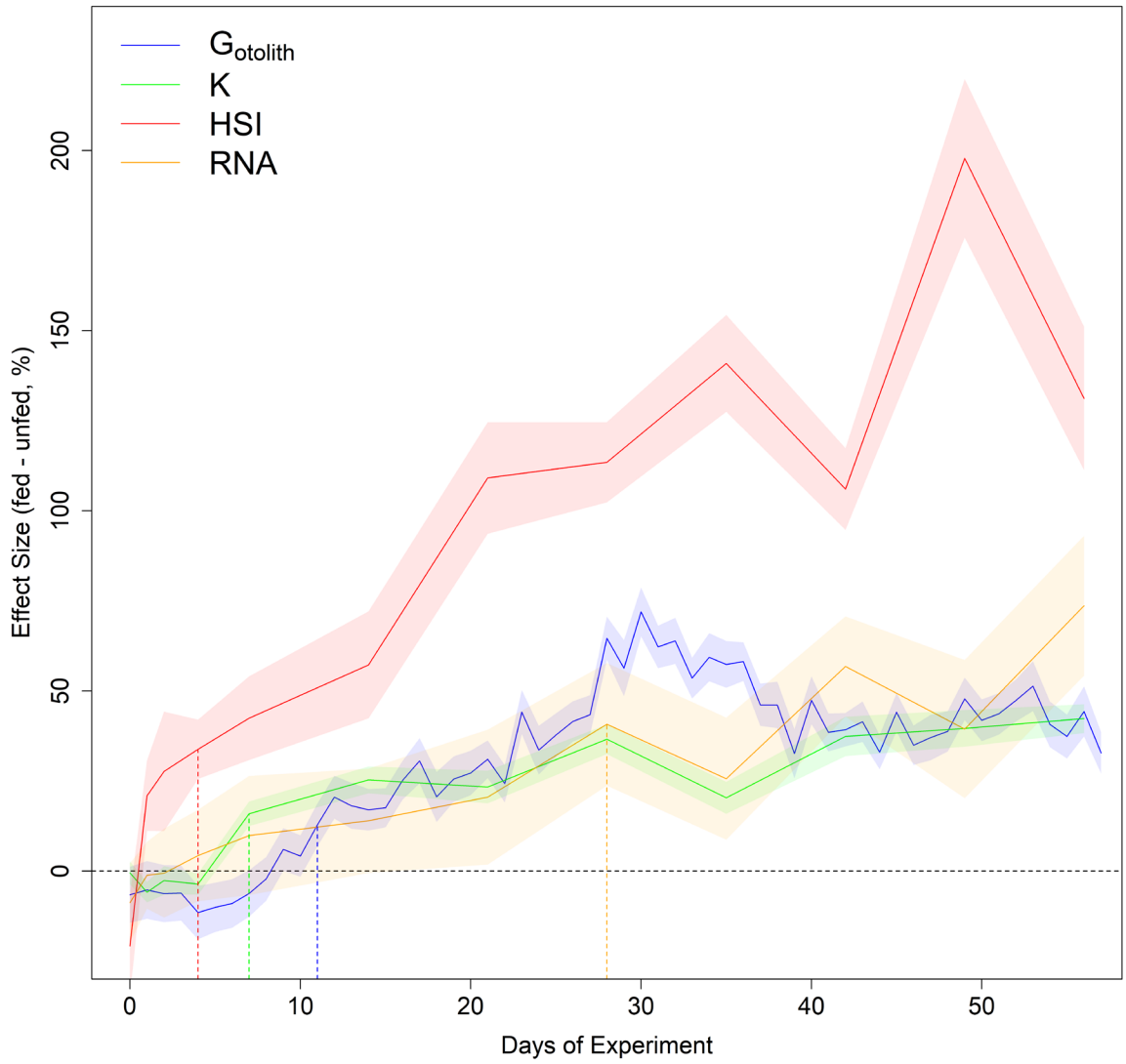

Figure 3-6: Magnitude and timing of the responses of each condition metric to food limitation in Delta Smelt.

Solid lines reflect the mean difference between fed and unfed treatments, with shading reflecting 1 s.e. Vertical lines correspond to the first day of the experiment at which a significant effect was detected. Results for K, HSI, and RNA were calculated from Hammock et al. (2020).

SUPPLEMENT

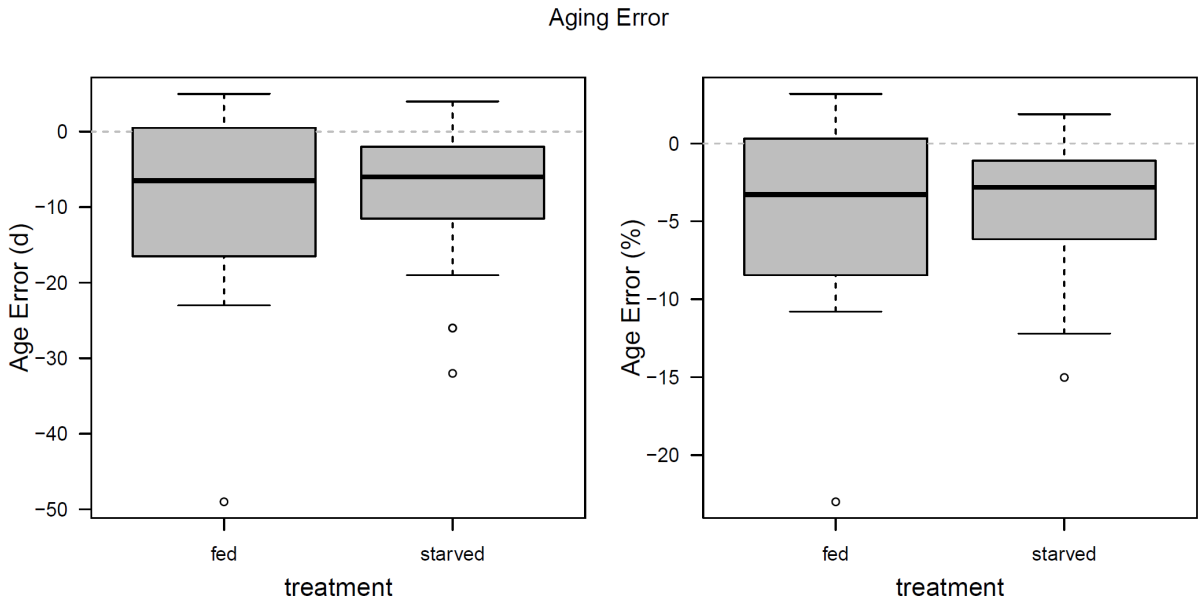

Figure S3-1: Aging error in days (left), and in percent of total age (right).

Box and whisker plots with median line and quartiles shown. Fed treatment on the left, unfed treatment on the right.

This Page Intentionally Left Blank

Chapter 4: Fitness tradeoffs for migratory and resident Delta Smelt

Authors:

Leticia Maria Cavole[1,*], Bruce G Hammock[2], Tomofumi Kurobe[2], Swee J. Teh[2], Malte Willmes[3], Christian Denney[1], James Hobbs[1], Brian Mahardja[4], Andrew Schultz[4,5], Levi S. Lewis[1]

[1] Department of Wildlife, Fish and Conservation Biology, University of California-Davis, Davis, CA, United States

[2] Department of Anatomy, Physiology, and Cell Biology, University of California-Davis, Davis, United States

[3] Norwegian Institute for Nature Research, Trondheim, Norway

[4] United States Bureau of Reclamation, Bay-Delta Office, Science Division, Sacramento, CA, United States

[5] U.S. Geological Survey, Southwest Biological Science Center, Grand Canyon Monitoring and Research Center, Flagstaff, AZ, United States

***Corresponding Author:**

Leticia Cavole
One Shields Ave., Davis, CA, 95616, United States
lmcavole@ucdavis.edu

ABSTRACT

Fishes have evolved diverse migratory life history strategies to persist within dynamic environments. Understanding how life history variation influences growth and reproductive fitness can be key to the effective conservation of imperiled species. The Delta Smelt (*Hypomesus transpacificus*) is an imperiled forage fish that is endemic to the San Francisco Estuary (SFE). This semi-anadromous fish exhibits a complex life history, with migrant and resident phenotypes that can be identified using otolith strontium isotope analysis. Here, we used generalized additive models (GAMs) to examine how overall and size-adjusted differences in body size (e.g., length and weight) and reproductive metrics (e.g., gonad weight, clutch size, and oocyte size) vary among the major Delta Smelt life history phenotypes. Overall, migratory (MIG) and brackish-water resident (BWR) fish exhibited greater body length, total weight, gonad weight, and clutch size relative to freshwater residents (FWR). Size-adjusted models, analogous to body condition, gonadosomatic index, and mass-specific clutch size, were also

greater for fish with the MIG and BWR phenotype. Thus, fish with MIG and BWR life-history phenotypes appeared larger, healthier, and more fecund than FWR fish. Similar patterns have been observed in partially anadromous salmonids, where more diverse life history portfolios are believed to enhance population resilience and stability in dynamic and unpredictable environments. Given that the contemporary Delta Smelt population is dominated (~80%) by the MIG phenotype, it appears that the fitness benefits of migration currently outweigh those of either brackish or freshwater residency in the highly modified San Francisco Estuary.

Keywords:

fitness, reproduction, life-history phenotypes, migration, Delta Smelt, otolith chemistry

INTRODUCTION

Diverse life histories enhance population stability

Many fishes have evolved diverse life history strategies to persist within dynamic and unpredictable environments. For example, variation in body size, age at maturity, longevity, reproductive potential, and migratory behaviors confer population stability and persistence in ecosystems that experience wide-ranging environmental variation (Hutchings & Myers, 1994; Berkeley et al., 2004; Beechie et al., 2006). This is particularly the case in estuaries, where variation in terrestrial and oceanic environmental conditions interact to produce relatively extreme fluctuations in aquatic environments across multiple spatiotemporal scales (Fichman et al., 2021; Moyle et al., 2010; Potter et al., 2013; Teichert et al., 2017). In response, many estuarine species have evolved diverse life history strategies that enhance population stability and resilience (Schindler et al., 2010; J. W. Moore et al., 2014; Brennan et al., 2019; Hobbs et al., 2019; Sturrock et al., 2020).

Costs and benefits of migration and residency

One such life history strategy is partial migration, where a fish population has both resident and migratory contingents. There are trade-offs associated with residency and anadromy in partially migratory fishes, and these benefits and costs vary within and among species, habitats, and life stages. Typically, in sub-tropical and temperate ecosystems, juvenile anadromous fish migrate to the ocean to feed in a highly productive environment at the cost of increased predation risk, while resident fish remain in freshwater habitats with lower food availability and lower predation risk (Chapman et al., 2012; Alò et al., 2021). Nonetheless, given the asymmetrical anthropogenic impacts between marine and inland habitats, resident fish today may also face more pollution and habitat modification than those residing in coastal areas. Therefore, migratory contingents might enhance body and reproductive fitness in comparison with resident contingents.

Reproductive benefits of migration

Migratory phenotypes often grow faster and larger than non-migratory contingents, suggesting a fitness benefit to migrant lineages (Burns & Bloom, 2020; Roff, 1988). For example, the “bigger

is better" hypothesis suggests that larger migratory fish would encounter lower predation risks (benefit). However, migrating across distinct ecosystems (e.g., ocean and river) and long routes often impose physiological and metabolic (e.g., osmoregulatory) challenges, leading to stress-related responses. Accordingly, there are some instances where migratory individuals might reduce body size and increase susceptibility to either higher predation risk or parasite exposure (costs) (Alerstam et al., 2003; Chapman et al., 2012). Overall, migratory fish tend to be larger, and this is relevant because fecundity increases hyper-allometrically with body weight (Barneche et al., 2018); thus, large females contribute disproportionately more offspring than smaller females. This is well-known in large, commercially important species, such as Atlantic cod *Gadus morhua* and Atlantic salmon *Salmo salar*, where large females termed "big old fat fecund female fish" (Hixon et al., 2014) are considered essential to population maintenance and fisheries management. Thus, rapid growth expressed by migratory phenotypes is considered a key fitness benefit, generally increasing the condition and reproductive output of migratory individuals.

While partial migration is relatively well studied in salmonids (Jonsson & Berg, 2003), much less is known about the costs and benefits of partial migration in small pelagic fishes and how responses to environmental variation might differ among life history groups (Saraux et al., 2019; Peck et al., 2021). In anchovies, herrings, and shads, migratory species tend to be larger than non-migratory species, suggesting an adaptation to mitigate energy expenditure during relatively long distance migration routes (Bloom et al., 2018). For example, larger-bodied migrants benefit from improved feeding, respiration, growth, predator-prey interactions, resistance to starvation, and reproductive output (Peters & Peters, 1986). Whether and how fitness metrics vary intra-specifically among individuals exhibiting distinct life histories (hereafter, "phenotypes") remains largely unexplored for small pelagic forage fishes, especially endangered species such as Delta Smelt (*Hypomesus transpacificus*).

Reproductive biology of Delta Smelt

The Delta Smelt is an endangered, pelagic, forage fish that is endemic to the upper San Francisco Estuary (SFE), California, USA. Although an annual species, the Delta Smelt is an iteroparous serial spawner, capable of spawning up to 3-4 clutches during a single spawning season (Mager, 1996; Damon et al., 2016; LaCava et al., 2015; Damon et al., 2016). Fecundity is low relative to other pelagic forage fishes, with a single large female Delta Smelt capable of generating up to ~ 10,000 eggs per clutch. As for many species, fecundity exhibits a classical hyperallometric relationship with body weight (Barneche et al., 2018); therefore, the clutch fecundity of a single large (e.g., 120 mm FL) female Delta Smelt is equivalent to that of ten smaller (e.g., 60 mm FL) individuals (Bennett, 2005; Lindberg et al., 2013; Damon et al., 2016; Kurobe et al., 2016). Furthermore, the largest females are typically the most likely to spawn early and produce multiple clutches during their protracted spawning season (Damon et al., 2016); thus, size and growth appear to be highly correlated with reproductive fitness in Delta Smelt.

The complex life history of Delta Smelt

The Delta Smelt exhibits a complex suite of life histories consisting of three major phenotypes (Hobbs et al., 2019). These include freshwater residents (FWR) that hatch and remain in

freshwater habitats (< 0.5 salinity), brackish-water residents (BWR) which hatch and remain in low-salinity brackish-water habitats (> 0.5 to ~ 6 salinity), and semi-anadromous migrants (MIG) that hatch and rear as larvae in freshwater habitats, but migrate downstream as juveniles to rear in low-salinity brackish-water habitats to adulthood. Regional variation in maturation suggests a linkage between life histories and reproductive biology, with a higher fraction of males exhibiting mature gonads in upstream vs downstream habitats (Hobbs et al., 2019). Furthermore, although reproductive contingents appear to all come from the same population, distinct genetic markers are strongly associated with different Delta Smelt migratory phenotypes, indicating that migratory behaviors are genetically linked and partially inheritable (Campbell et al., 2022). Although much is known about the reproductive biology and condition of Delta Smelt, no studies have examined whether fitness varies among individuals exhibiting these different life history phenotypes.

Study Objectives

Here, we conducted an interdisciplinary study using an extensive archive of Delta Smelt specimens to examine how several measures of fitness vary as a function of an individual's life history strategy. Specifically, we examined whether body size (i.e., total weight and fork length), ovary size, clutch fecundity, and oocyte area vary significantly among resident and migratory Delta Smelt phenotypes. We also examined whether size-adjusted relationships vary among phenotypes, analogous to condition factor, gonadosomatic index, and mass-specific fecundity. Comparisons of fitness and reproductive trait variation between migratory and resident Delta Smelt can provide key insights into the evolution of life history diversity in this species (Campbell et al., 2022), tradeoffs between migration and reproductive investment, and effects of climate change on the performance of each phenotype and the overall population.

MATERIALS AND METHODS

Study site

The San Francisco Estuary (SFE) is the largest estuary on the west coast of the United States. The upper estuary is formed by the confluence of the Sacramento River (north) and the San Joaquin River (south) at the Sacramento – San Joaquin Delta (hereafter "Delta") (Table 4-1), forming a complex of tidal fresh- and brackish- water habitats that are key nursery and spawning sites for hundreds of invertebrates, fish, and waterfowl species. The SFE serves as a case study for understanding life history diversity patterns and tradeoffs due to the ecosystem's highly dynamic nature, anthropogenic changes, and the presence of several fish species of interest to the region's water management. California has a Mediterranean climate, characterized by hot, dry summers and cold, wet winters, with high interannual variation in precipitation (Hanak, 2011; Hanak et al., 2019), including periods of severe droughts and floods that appear to be intensifying with climate change (Dettinger et al., 2016; Wang et al., 2017).

The SFE is also a highly modified and complex socio-ecological system, serving as the hub of California's water conveyance system (Nichols et al., 1986; Scoville, 2019). Much of the fresh

water entering the estuary is captured and diverted for agriculture, with only a small fraction (down to an average of ~ 40% in the 2010s), flowing west through Suisun Bay, San Francisco Bay, and eventually the Pacific Ocean (Reis et al., 2019). In addition to reduced outflows, the system is impacted by numerous dams, levees, loss of wetlands, non-native species, wastewater, fertilizers, and pesticides. Together, these changes have likely led to trophic collapse and the decline of numerous species in recent decades (Sommer et al., 2007; Mac Nally et al., 2010; Hammock, Moose, et al., 2019; Cloern & Jassby, 2012), including the Delta Smelt (Hobbs et al., 2017; Moyle et al., 2018).

Sample collection

A total of 842 Delta Smelt were used in the present study, with samples selected to maximize spatiotemporal dispersion and to provide overlap between otolith and available reproductive fitness metrics (Tables 4-1 to 4-2). Delta Smelt specimens were collected by the California Department of Fish and Wildlife Spring Kodiak Trawl (SKT) Survey. This survey estimates the relative abundance, distribution, and spawning condition of adult Delta Smelt throughout its historic range in the upper SFE. Each of the 39 SKT stations is sampled monthly from January through May, thus sampling across the full geographic range of Delta Smelt as they spawn in the spring (Table 4-1). The survey involves a 10-minute surface tow with a trawl net mouth of 13.8 m^2. At each station, Delta Smelt are collected, individually coded, measured (FL, mm) and sexed. Environmental parameters, including water temperature (°C), specific conductance (µS cm^{-1}), Secchi depth (m), dissolved oxygen (mg L^{-1}), and turbidity (Nephelometric Turbidity Units; NTU), are also collected at the start of each tow. Delta Smelt specimens were flash-frozen in liquid nitrogen on the boat, and kept in liquid nitrogen until dissection (Teh et al., 2016).

Reproductive condition

In the laboratory, several morphometric (e.g., fork length in mm), gravimetric (total weight, liver weight, and gonad weight in g), and histological parameters (e.g., liver and ovary condition) were quantified. Histological examination of the ovary was used to assess sexual maturity (i.e., maturity substage), clutch size (number of oocytes), and oocyte size (area) (Kurobe et al., 2016). To examine the reproductive performance of females, we focused on fish containing enlarged oocytes with cortical alveoli (stage 3), hereafter referred to as “near mature”, and on fish containing oocytes with vitellogenin (stage 4), hereafter referred to as “mature”. These stages were further divided into three maturity substages: early (3.1), middle (3.2), and late (3.3) cortical alveoli; and early (4.1), middle (4.2), and late (4.3) egg yolk bodies. To estimate clutch fecundity size (i.e., number of oocytes released in one spawning event), oocytes in a subsample from the left ovary were counted and scaled up to the total ovary weight. We used a 1× phosphate-buffered saline solution to disperse oocytes and facilitate count estimates using a dissecting microscope. Clutch size (C) was estimated following (Kurobe et al., 2022):

$$C = O_{portion}\, x\, \left(\frac{W_{intact}}{W_{portion}}\right)$$

where C is clutch size, $O_{portion}$ is the number of oocytes in the subsampled portion of the ovary, W_{intact} is the weight of the entire ovary before dissection, and $W_{portion}$ is the weight of the portion of the ovary used to estimate the number of oocytes.

Otolith geochemistry and life-history assignments

Sagittal otoliths from a total of 842 Delta Smelt were dissected, polished, and chemically analyzed following Hobbs et al. (2019) (Tables 4-1 to 4-2). Otoliths were cleaned in ethanol, mounted in the sagittal plane on a microscopic slide, and polished progressively with 800 to 1200 grit wet-dry sandpaper and 0.3-micron alumina polish. Polished otoliths were sonicated in Milli-Q water for 5 minutes and mounted on petrographic slides for strontium isotope ratio ($^{87}Sr/^{86}Sr$) analysis. Otolith $^{87}Sr/^{86}Sr$ ratios were quantified using a laser-ablation multi-collector inductively coupled plasma mass spectrometer (LA-MC-ICP-MS; Nu Plasma HR spectrometer interfaced with a Nd:YAG 213 nm laser) at the UC Davis Interdisciplinary Center for Plasma Mass Spectrometry (UCD/ICPMS). Otolith sections were ablated from the core towards the dorsal edge, reflecting the salinity history for each specimen, from hatch to capture. Analytical parameters for the laser were 40 µm spot diameter, 10µm s^{-1} scan speed, 10 Hz frequency and 5-10 J cm^{-2}. To evaluate machine performance, we used an otolith from a White Seabass, *Atractoscion nobilis* as an external reference material with a known $^{87}Sr/^{86}Sr$ ratio of modern seawater (0.70918) (McArthur et al., 2001).

An established mixing curve using $^{87}Sr/^{86}Sr$ ratios and salinity of freshwater inflow into the Delta (0.7071, 0.4 salinity) and oceanic waters (0.7091, 32.0 salinity) as endmembers was used to convert individual $^{87}Sr/^{86}Sr$ profiles to ambient salinity (Hobbs et al., 2019; Sellheim et al., 2022). Individual $^{87}Sr/^{86}Sr$ otolith profiles were classified into freshwater residents (FWR), brackish-water residents (BWR), and semi-anadromous migrants (MIG) following a supervised procedure, where FWR strontium isotope ratio profiles remained primarily below 0.7075 (salinities < 0.5), BWR profiles remained mostly above 0.7075 (salinities > 0.5), and MIG profiles began below 0.7075 (salinities < 0.5 in the first 30 days-post-hatch, dph) and transitioned to higher salinity values (30-150 dph) of 0.7075-0.7092 (0.5 to > 6 salinity), commonly observed in the low salinity zone (LSZ) of the SFE (Hobbs et al., 2019).

Statistical Analysis

We used hierarchical generalized additive models (GAMs) (Pedersen et al., 2019) to examine whether overall and size-adjusted differences in body and reproductive fitness metrics vary among Delta Smelt phenotypes (MIG, FWR, and BWR). The *overall models* examined how the total weight (TW, g), fork length (FL, mm), gonad weight (GW, g), clutch size (number of oocytes), and oocyte area (in mm^2) of adult specimens vary among the three main life-history phenotypes (FWR, BWR, and MIG) while accounting for other biological (e.g., sex, maturity substage (MS)) and temporal (e.g., year and month) predictors. The *overall models* considered the fixed parametric effect of phenotype, sex, and maturity substage, the smooth nonparametric effect of month with a basis function k =4 using *s(month, k= 4)*, and survey year as a random effect term using *s(year, bs= "re")* (Supplements, **Table S4-1**), and were specified as the following:

$$\text{Model\_TW} <- \log_{10}(\text{TW}) \sim \text{phenotype} + \text{sex} + \text{year} + \text{month}$$
$$\text{Model\_FL} <- \text{FL} \sim \text{phenotype} + \text{sex} + \text{year} + \text{month}$$
$$\text{Model\_GW} <- \log_{10}(\text{GW}) \sim \text{phenotype} + \text{MS} + \text{year} + \text{month}$$
$$\text{Model\_FEC} <- \text{clutch size} \sim \text{phenotype} + \text{MS} + \text{year} + \text{month}$$
$$\text{Model\_EGG} <- \text{oocyte area} \sim \text{phenotype} + \text{MS} + \text{year} + \text{month}$$

The *size-adjusted models* were analogous to body condition, gonadosomatic index, mass-specific clutch size, and (gonad) mass-specific oocyte area by including an interaction term between biological covariates (FL, TW, and GW) and the phenotype classification. For the *size-adjusted* models, a factor smooth was used for modeling biological covariates (e.g., TW, GW, clutch size, and oocyte size) and life history phenotypes (e.g., FWR, BWR, and MIG), allowing for separate smooths for each phenotype with overall similar shape (global smooth model, GS); this is analogous to Generalized Linear Models with varying slopes (Pedersen et al., 2019). The *size-adjusted* models considered the smooth nonparametric effect of phenotype and biological metrics by using *s(biological metric, phenotype, bs= "fs")*, month using *s(month, k= 4)*, survey year using a random term *s(..., bs= "re")*, and the fixed parametric effects of sex and maturity substage (Supplements, **Table S4-2**), and were specified as the following:

$$\text{Model\_TW\_adj} <- \log_{10}(\text{TW}) \sim \text{FL} * \text{phenotype} + \text{sex} + \text{year} + \text{month}$$
$$\text{Model\_GW\_adj} <- \log_{10}(\text{GW}) \sim \text{TW} * \text{phenotype} + \text{MS} + \text{year} + \text{month}$$
$$\text{Model\_FEC\_adj} <- \text{clutch size} \sim \text{TW} * \text{phenotype} + \text{MS} + \text{year} + \text{month}$$
$$\text{Model\_EGG\_adj} <- \text{oocyte area} \sim \text{GW} * \text{phenotype} + \text{MS} + \text{year} + \text{month}$$

Models were fit using the *mgcv* package (Wood, 2012) in R version 4.0.2 (2020-06-22), with assumptions evaluated using the *gam.check( )* function. Several candidate models were examined with the selected model being that with an ecological and biological meaningful structure, and a balance of relatively low Akaike's information criterion (AIC) and high deviance explained (DEV) values (Wood, 2012; Pedersen et al., 2019), (Supplements, Table S4-1-S4-2).

The total weight and gonad weight were $\log_{10}$-transformed to fit model assumptions (Supplements, Figure S4-1 to S4-2). A gaussian family distribution was fit for all models, except for the oocyte area *overall* and *size-adjusted models*, where a gamma family distribution was used to account for the unbalanced and right-skew oocyte area data. For the total weight and fork length models (models 1, 2 and 6), all individuals were examined (Tables 4-1 to 4-2); whereas for the gonad weight (GW), clutch fecundity (FEC), and oocyte area (EGG) models (models 3, 4, 5, 7, 8, and 9), we only used between 339-377 females at maturity substages 3.1, 3.2, 3.3, 4.1, 4.2, and 4.3, corresponding to near mature and mature individuals (Kurobe et al., 2016) (Tables 4-3 to 4-4). The survey year was included as a conventional random effect in all models to account for year-to-year variation in conditions.

Predictions were generated for the total weight, gonad weight, and clutch size (fecundity) for each life history phenotype using the *predict* function (*mgcv* package in R). Standard errors were based on the posterior distribution of each model coefficient and were used to generate confidence intervals. A new data frame containing a fixed set of covariate values was chosen for both the *overall models* and *size-adjusted models.* The fixed set of covariates included the: survey year of 2014, maturity substage of 3.3, month of April, and the female sex, and were used

to generate the predictions. These covariate values (i.e., year, maturity substage, month, and sex) were chosen based on the average environmental conditions frequently experienced by Delta Smelt in their natural environment and the availability of sufficient data to generate representative and reliable predictions. Given that oocyte size is directly correlated with determination of developmental stage, oocyte area should be examined with caution, and no predictions were generated for this parameter.

RESULTS

Delta Smelt sample description

In total, 842 Delta Smelt were examined for body condition (length-weight relationship) (Tables 4-1 to 4-2). Fish were collected primarily from January to March and ranged in size from 48 to 88 mm FL, with mean FL of 67 ± 6.03 mm and mean weight of 2.27 ± 0.65 g. This sample of fish included 54.6% females, 43% males, and 2.4% of undetermined sex (immature). No differences among years were observed in the mean fork length (ANOVA; F=0.032; *P*=0.86) or total weight (ANOVA; F=0.032; *p*=0.86); however, differences between male and female fork lengths (*t*-test=6.11; df=817.56; $p<0.001$) and total weights (*t*-test=7.05; df=813.8; $p<0.001$) were observed, with females being both longer and heavier, on average, than males (Supplements, Table S4-3-S5). Reproductive metrics of mature female Delta Smelt were examined separately (i.e., stages 3.1 through 4.3). Mature females ranged from 51 to 83 mm FL (average = 67.76 ± 6.15 mm), with 377 females included in the subsequent gonad weight *overall* and *size-adjusted* models (Table 4-3), and between 337 and 339 females for the subsequent clutch size and oocyte size *overall* and *size-adjusted* models (Table 4-4).

Differences in body size and reproductive metrics – Overall GAM models

The *overall models* for total weight, fork length and clutch size explained ~ 42-44% of the data variance, while the *overall models* for gonad weight and oocyte explained ~ 86% of the data variance (Table 4-5 and 6). In general, migratory (MIG) and brackish-water resident (BWR) Delta Smelt exhibited greater body length, total weight, gonad weight, and clutch size relative to freshwater residents (FWR) (Table 4-2A,E,I,M), as observed for the significant parametric terms for FWR ($p \leq 0.001$) in comparison to the BWR reference level, while MIG fish were not significantly different from BWR (Table 4-5). Male fish were also significantly lighter and smaller than female fish ($p \leq 0.001$) (Table 4-2B,F). Maturity substage increased with the log of gonad weight and oocyte area but did not alter with clutch fecundity (Table 4-2J,N,R), suggesting that the number of eggs a female will spawn in a year is a fixed and unchanged feature over the progression of the spawning season. Adding the month predictor for the total weight and fork length *overall models* increased approximately two-fold the deviance explained by these models (Supplements, Table S4-1), suggesting that each month is essential for individuals putting on more length and weight in this short-lived, annual forage species. For the oocyte area *overall model*, only the intercept term (BWR) was significant ($p < 0.001$) (Table 4-6), indicating that BWR oocyte area was significantly different from zero and potentially smaller than the oocyte area for FWR and MIG (Table 4-2Q), although sample sizes for this phenotype

are small due to the rarity of this life history strategy (n=30, Table 4-4). The effective degree of freedom for year was the smallest for the oocyte model (EDF=2.4, Table 4-6), potentially due to the low number of years where this parameter was measured (Table 4-2T).

Differences in body condition, gonadosomatic index, mass-specific clutch size, and gonad mass-specific egg area – Size-adjusted GAM models

The final *size-adjusted model* for body condition explained 85.5% of the variance in the total weight data per fork length of all individuals (Table 4-7). The allometric relationship between the $\log_{10}$ total weight (g) vs. fork length (mm) differed significantly among life history phenotypes (EDF=6.84; F=339.728; $p < 0.001$), sexes (male; p=0.007), month (EDF=2.86; F=18.83; $p < 0.001$), and survey years (EDF=5.07; F=4.075; $p < 0.001$), (Table 4-7, Table 4-3A-D). Brackish-water residents (BWR) were slightly larger and heavier than migrants (MIG) and freshwater residents (FWR) (Table 4-3A), and males were significantly lighter (p=0.007) than females (Table 4-7, Table 4-3B).

The final *size-adjusted model* for gonadosomatic index explained 90.3% of the response variance in the gonad weight per body mass of mature females (Table 4-7). The $\log_{10}$-transformed gonad weight (g) vs. total weight (g) relationships differed among life history phenotypes (EDF=8.80; F=33.70; $p < 0.001$), month (EDF=2.53; F=7.75; $p < 0.001$), year (EDF=5.41; F=7.15; $p < 0.001$), and for the latest three maturity substages ($p < 0.001$), (Table 4-7, Table 4-3E-H). Gonadosomatic index increased linearly with body weight for MIG and BWR, but not for FWR, which exhibited larger gonads per total weight at intermediate body weights (~ 2 to 3.2 g), decreasing slightly afterwards (Table 4-3E). Therefore, the heaviest FWR had significantly lighter gonads per body mass than the MIG and BWR fish. Gonads per body mass were also the largest at approximately the middle of the spawning season, between February and April (Table 4-3G).

The final *size-adjusted model* for mass-specific clutch size explained 61.3% of the variance in fecundity (Table 4-7). Clutch size (number of oocytes) vs. total weight (g) followed a similar functional relationship of that of the gonad weight (g) vs. total weight (g). Whereas mass-specific clutch size increased linearly, with total weight for MIG and BWR, we observed a "hockey stick" pattern for FWR, with a change in fecundity at around ~2.5 g TW (Table 4-3I). Whereas maturity substage increased successively through the spawning season for GW and oocyte area, this trend was not observed for the clutch size-adjusted metric (Table 4-3J), i.e., the number of eggs per body mass a female contains doesn't change with the progression of the spawning season. Generally, the size-adjusted reproductive metrics for Delta Smelt (Table 4-3E,I,M) were more responsive to phenotypic variation than fish condition factor (Table 4-3A).

For the gonad mass-specific oocyte area (mm^2), instead of using fish's total weight as a predictor variable, we included gonad weight as the main covariate. The final model explained 89.9% of the variance in this size-adjusted metric (Table 4-7). The oocyte area (mm^2) vs. gonad weight (g) relationship differed significantly among phenotypes, with FWR and MIG having larger eggs per gonad mass (EDF=10.02; F=3.77; p<0.001) on average than BWR (Table 4-3M). The approximate significance of maturity substage (parametric term) was significant for most egg

stages ($p < 0.001$), similar to the gonad weight size-adjusted model (Table 4-3N,F). The effect of year was almost linear (EDF~0.9) for this parameter, suggesting more data would be necessary to infer interannual differences for the oocyte size-adjusted metric.

Model Predictions

We observed that Delta Smelt MIG and BWR individuals were approximately 0.5 g heavier than FWR, representing a difference of ~ 22% of their average body mass (Table 4-4A). MIG and BWR also had heavier gonads (GW~0.037g) and substantially more eggs (clutch size ~1000 oocytes) compared to FWR fish (GW~ 0.027g, clutch size ~ 700 oocytes) (Table 4-4B-C).

Body condition was marginally higher for BWR (Table 4-4D), and both BWR and MIG fish displayed greater gonadosomatic index and size-adjusted clutch sizes than FWR fish (Table 4-4E-F). The largest freshwater residents were substantially less fecund (~1,000 oocytes per clutch) than the largest migrants and brackish-water residents at sexual maturity (~2,000 oocytes per clutch) (Table 4-4F).

DISCUSSION

Summary of findings

In this study, we found that migrant (MIG) and brackish water (BWR) Delta Smelt were larger and more fecund than fresh-water resident (FWR) groups. Specifically, adult MIG and BWR specimens were 22% heavier and females had approximately 300 more eggs than FWR fish, indicating that individuals that moved into downstream habitats comprising the low salinity zone of the San Francisco Estuary (SFE) probably benefitted from greater prey availability (e.g., mysids) and environmental conditions characteristic of these regions (e.g., higher salinity and lower temperature conditions). Interestingly, BWR appear to have smaller eggs than FWR and MIG, suggesting tradeoffs might exist within this species, and that freshwater habitats offer important prey items and energetic sources for investing in egg yolk formation. Nonetheless, sample sizes were small for the rare BWR phenotype, and few years contained data for the oocyte size metric, suggesting future studies should measure this parameter in both field-caught specimens and culture-reared specimens with varying rearing conditions.

Fish body size in migratory and non-migratory groups

Most studies on migratory fish aim to understand the causes of migration (i.e., photoperiod, water temperature, “first-flush” storms) (Northcote, 1984; Grimaldo et al., 2009; Fernandes et al., 2022), the connectivity patterns among populations (Hall et al., 2011; Flitcroft et al., 2019), and the role of habitat dynamics in each life stage (Flitcroft et al., 2016; Brennan & Schindler, 2017). More recently, the biological and economic importance of diverse life history strategies, termed the “portfolio effect” (Brennan et al., 2019), has also been quantified. Less is known about the life history consequences (i.e., growth and reproduction tradeoffs) for exhibiting a migratory *versus* non-migratory strategy, particularly for non-commercial species. Migratory fishes tend to have larger body sizes than non-migratory fish across several clades (Roff, 1988),

and this trend appear to be a deterministic adaptation (i.e., several fish lineages are subjected to related selective forces leading to similar physical traits, such as large body size and high reproductive output) (Burns & Bloom, 2020).

In salmonids, there is high intraspecific diversity in life history strategies. Migratory salmonid populations tend to be larger than non-migratory and land-locked populations, as in steelhead and rainbow trout *Oncorhynchus mykiss* (Kendall et al., 2015). However, there are many instances when long-distance migrants are more fusiform (streamlined), slimmer and smaller than short-distance migrants, suggesting migration requires considerable energy demands (Linley, 1993; K. Moore, 1996; Crossin et al., 2004; Jonsson & Jonsson, 2006). In Clupeiformes, there is high interspecific diversity in life history strategies, and diadromous species tend to be larger than non-diadromous species due to long migration routes (100s-1000s km) (Bloom et al., 2018). Semi-anadromous fish species do not fully transit between marine and freshwater habitats, but nevertheless still experience large environmental variability in salinity, temperature, and productivity conditions between relatively small spatial units. For Delta Smelt, juveniles' rearing habitats are mainly located within the low salinity zone (LSZ, 0.5-6 ppt) of the SFE (Dege & Brown, 2004), where both BWR and MIG co-habit during specific times of the year. In winter and early spring, a portion of the population (semi-anadromous migrants) move upstream from the LSZ to mature and spawn in the lower portions of the Sacramento River. Our finding that MIG fish were larger and more fecund than FWR populations is consistent with the hypothesis that migration is at least partially driven by enhanced growth, possibly related to higher prey availability and foraging success or more suitable environmental conditions for growth (e.g., lower temperatures) (Hammock et al., 2017; Lewis, Denney, et al., 2021). For example, otolith-based growth reconstructions indicate that somatic growth rates of wild Delta Smelt are highest in habitats with cooler temperatures, higher salinity, and higher turbidity (Lewis, Denney, et al., 2021), with all three environmental conditions being more favorable for growth in downstream brackish habitats. Although stomach fullness is highest for young Delta Smelt in freshwater habitats during the summer, for older fish, stomach fullness is higher in brackish regions of the estuary throughout the rest of the year (Hammock et al., 2017).

Otolith strontium isotope analysis suggests that migrant Delta Smelt can move from the San Pablo Bay (salinity 1-20 psu) and Suisun Bay (salinity 1-10 psu) upstream to the Sacramento River (Salinity 0-0.5 psu), potentially migrating ~ 60-80 km (Sommer et al., 2011), usually after the "first flush" winter rainstorm event (Grimaldo et al., 2009). For a fish that is typically less than 10 cm in length at maturity, this can require considerable energy reserves as they might move 800,000 times their body length during their reproductive (upstream) migration. To put it in perspective, this would be equivalent to an average human 1.7 m tall migrating ~ 1,360 km, the same distance as the California coastline. Therefore, we expected to detect larger intraspecific variation in body size for this species, and our results corroborate this assumption. Migrant Delta Smelt were significantly heavier and larger than freshwater residents (Table 4-2A, E), in agreement with migratory contingents of other Osmerids, such as the European Smelt (*Osmerus eperlanus*) and Wakasagi (*Hypomesus nipponensis*), (Maitland & Lyle, 1996; Katayama, 2001).

Nonetheless, Delta Smelt condition factors (*size -adjusted models*) were only marginally distinct among phenotype groups (Table 4-3A). This might be explained by the fact that Delta Smelt are considered poor swimmers, believed to position themselves between the shoal-channel interface and shoreline to take advantage of flood and ebb tidal pulses while moving up and downstream, respectively (Swanson et al., 1998; Bennett & Burau, 2015). Thus, it is not surprising that their body conditions were only slightly different among phenotypes, as the species does not seem to rely on increased body sizes and fat reserves to move, but instead, can take advantage of the dynamic hydrology of the SFE.

Reproductive metrics in migratory and non-migratory groups

Overall, FWR Delta Smelt exhibited lighter gonads and lower gonadosomatic index compared to BWR and MIG (Table 4-2I, 3E). The clutch fecundity (number of oocytes) vs. fork length (mm) relationship yielded a similar relationship to that observed by Damon et al. (2016), (Table 4-3I). The length-fecundity relationship for Delta Smelt is known to be nonlinear (Bennet 2005, Lindberg et al 2013), which can be partially explained by the high complexity of the smoothed phenotype and clutch fecundity interaction term in our size-adjusted models (EDF~9, Table 4-7). Freshwater-residents were mainly captured in Suisun Marsh, Cache Slough, and the Sacramento River Deep Water Ship Channel, where feed conditions, pollutants, water residence times (~2 months), and water temperatures are often outside the species' optimum and might impose serious physiological challenges (Werner et al., 2000; Kuivila & Moon, 2003; Hammock et al., 2015; Hammock, Moose, et al., 2019; Teh et al., 2020; Lenoch et al., 2021; Mahardja et al., 2022), potentially reducing their energy intake and subsequent gonadal and yolk egg investment.

MIG and BWR phenotypes were heavier and more fecund than FWR, and therefore, are expected to arrive earlier at spawning sites and potentially spawn more frequently during the spawning season (Damon et al., 2016). This arrival time is important as these phenotypes would be able to release eggs during the colder periods of their spawning window, in water temperatures of approximately 10-13 °C, known to benefit juvenile and adult health and fitness (Hammock et al., 2022).

Droughts, floods, and growth-reproduction tradeoffs

Although freshwater outflow is not well correlated with the abundance of Delta Smelt (Dege & Brown, 2004; Kimmerer, 2002), our data suggests it is a key factor affecting body condition and reproductive metrics, as recently observed by (Kurobe et al., 2022). Years of critical drought and low outflow, especially in 2015, seem to decrease the body condition and clutch fecundity size for all phenotypes analyzed (Supplements, Table S4-4). This is expected because, during drought years, salinity intrusion into the estuary can push Delta Smelt LSZ habitats landward, shrinking habitat volume and limiting access to relatively productive tidal wetland habitat (Feyrer et al., 2011; Hammock, Hartman, et al., 2019).

Previous work has demonstrated that the proportion of life history phenotypes in Delta Smelt vary with interannual environmental conditions, and that freshwater residents appear to be favored during low outflow and cold conditions, while migrants benefit during high outflow and

warm conditions (Lewis, Willmes, et al., 2021). Here, we extended this analysis, observing that MIG were heavier and displayed higher clutch fecundity size across most years analyzed, irrespective of hydrological conditions (Supplements, Table S4-4). Freshwater residents showed heavier gonads in critically dry (2014-15) and below normal (2016) years (Supplements, Table S4-4B), but overall lower clutch sizes (Table 4-4F), likely because oocytes appeared to be marginally larger for this group (Table 4-3M). Larger oocyte sizes for freshwater residents might occur due to egg hydration or because this contingent has more food available to convert into yolk formation. This trend was also observed for the freshwater contingents of Wakasagi in Japan, although their mean oocyte diameter did not differ significantly between large anadromous fish and small residents (Katayama, 2001). In places where density-dependence factors can increase juvenile mortality rates, trade-offs between egg numbers and egg size can occur, and fecundity can be foregone to egg size (Wootton, 2012). This may have been the case when Delta Smelt was one of the most abundant fishes in the SFE. Also, migration is known to favor egg numbers over egg size (Kinnison et al., 2001), in agreement with patterns suggested here for migrant Delta Smelt.

Several lines of evidence suggest larger body size phenotypes confer increased reproductive fitness in salmonids (Hendry, 2004), a statement that seems to hold true even for relatively short migrants in the Osmeridae family. For example, Chigbu & Sibley (1994) observed that fecundity and egg size trade-offs with body size might occur due to variable environmental conditions, such that in years of adverse conditions, Longfin Smelt (*Spirinchus thaleichthys*) invested less in reproduction. Here, Delta Smelt migrants exhibited higher fecundity than freshwater residents of similar body sizes. Therefore, Delta Smelt foraging behavior in productive habitats downstream (i.e., large mysids) can lead to higher reproductive output and might be a necessary life history strategy and behavior to ensure high reproductive success for this life-history.

Management Implications

Given that MIG constitutes the majority of the Delta Smelt population (Hobbs et al., 2019) and appear to have better body and reproductive fitness, the MIG phenotype is likely better adapted to current environmental conditions in the upper SFE than the FWR and the scarce BWR phenotypes. Therefore, efforts to promote a more natural hydrology that facilitates dispersal and migration and maximizes production in brackish habitats is likely key to the conservation and management of the Delta Smelt population. Furthermore, as the current conservation culture program aims to maximize reproduction outputs and minimize domestication and selection, it may also be valuable to focus on ensuring that life history diversity is represented and remains a conservation priority. Given that cultured Delta Smelt are reared entirely in freshwater, the maintenance and production of fish exhibiting the best-adapted and most fecund MIG phenotype in captivity may be a valuable consideration to enhance the success of supplementation efforts and the conservation of Delta Smelt overall.

ACKNOWLEDGEMENTS

We are grateful to the California Department of Fish and Wildlife for collecting fish, and to Justin Glessner for assisting with geochemical analyses at the UC Davis Interdisciplinary Center for Plasma Mass Spectrometry. Furthermore, we acknowledge the many staff and student researchers at the UC Davis Department of Wildlife, Fish, and Conservation Biology; School of Veterinary Medicine; and Center for Aquatic Biology and Aquaculture for laboratory and logistical support in conducting the study and processing samples. This study was funded by the U.S. Bureau of Reclamation Directed Outflow Project (Grant Nos. R17AC00129 and R22AC00392) to Bruce G. Hammock, L. Lewis, J. Hobbs, and S. Teh. The views expressed herein are those of the authors and do not represent the official opinion of any employer, institution, or government agency.

REFERENCES

Alerstam, T., Hedenström, A., & Åkesson, S. (2003). Long-distance migration: Evolution and determinants. Oikos, 103(2), 247–260.

Alò, D., Lacy, S. N., Castillo, A., Samaniego, H. A., & Marquet, P. A. (2021). The macroecology of fish migration. Global Ecology and Biogeography, 30(1), 99–116. https://doi.org/10.1111/geb.13199

Barneche, D. R., Robertson, D. R., White, C. R., & Marshall, D. J. (2018). Fish reproductive-energy output increases disproportionately with body size. Science, 360(6389), 642–645. https://doi.org/10.1126/science.aao6868

Beechie, T., Buhle, E., Ruckelshaus, M., Fullerton, A., & Holsinger, L. (2006). Hydrologic regime and the conservation of salmon life history diversity. Biological Conservation, 130(4), 560–572. https://doi.org/10.1016/j.biocon.2006.01.019

Bennett, W. A. (2005). Critical Assessment of the Delta Smelt Population in the San Francisco Estuary, California. San Francisco Estuary and Watershed Science, 3(2). https://doi.org/10.15447/sfews.2005v3iss2art1

Bennett, W. A., & Burau, J. R. (2015). Riders on the Storm: Selective Tidal Movements Facilitate the Spawning Migration of Threatened Delta Smelt in the San Francisco Estuary. Estuaries and Coasts, 38(3), 826–835. https://doi.org/10.1007/s12237-014-9877-3

Berkeley, S. A., Hixon, M. A., Larson, R. J., & Love, M. S. (2004). Fisheries Sustainability via Protection of Age Structure and Spatial Distribution of Fish Populations. Fisheries, 29(8), 23–32. https://doi.org/10.1577/1548-8446(2004)29[23:FSVPOA]2.0.CO;2

Bloom, D. D., Burns, M. D., & Schriever, T. A. (2018). Evolution of body size and trophic position in migratory fishes: A phylogenetic comparative analysis of Clupeiformes (anchovies, herring, shad and allies). Biological Journal of the Linnean Society, 125(2), 302–314. https://doi.org/10.1093/biolinnean/bly106

Brennan, S. R., & Schindler, D. E. (2017). Linking otolith microchemistry and dendritic isoscapes to map heterogeneous production of fish across river basins. Ecological Applications, 27(2), 363–377. https://doi.org/10.1002/eap.1474

Brennan, S. R., Schindler, D. E., Cline, T. J., Walsworth, T. E., Buck, G., & Fernandez, D. P. (2019). Shifting habitat mosaics and fish production across river basins. Science, 364(6442), 783–786. https://doi.org/10.1126/science.aav4313

Burns, M. D., & Bloom, D. D. (2020). Migratory lineages rapidly evolve larger body sizes than non-migratory relatives in ray-finned fishes. Proceedings of the Royal Society B: Biological Sciences, 287(1918), 20192615. https://doi.org/10.1098/rspb.2019.2615

Campbell, M. A., Joslin, S. E. K., Goodbla, A. M., Willmes, M., Hobbs, J. A., Lewis, L. S., & Finger, A. J. (2022). Polygenic discrimination of migratory phenotypes in an estuarine forage fish. G3 Genes|Genomes|Genetics, 12(8), jkac133. https://doi.org/10.1093/g3journal/jkac133

Chapman, B. B., Hulthén, K., Brodersen, J., Nilsson, P. A., Skov, C., Hansson, L.-A., & Brönmark, C. (2012). Partial migration in fishes: Causes and consequences. Journal of Fish Biology, 81(2), 456–478.

Chigbu, P., & Sibley, T. H. (1994). Relationship between abundance, growth, egg size and fecundity in a landlocked population of longfin smelt, Spirinchus thaleichthys. Journal of Fish Biology, 45(1), 1–15. https://doi.org/10.1111/j.1095-8649.1994.tb01282.x

Cloern, J. E., & Jassby, A. D. (2012). Drivers of change in estuarine-coastal ecosystems: Discoveries from four decades of study in San Francisco Bay. REVIEWS OF GEOPHYSICS, 50. https://doi.org/10.1029/2012RG000397

Crossin, G. T., Hinch, S. G., Farrell, A. P., Higgs, D. A., Lotto, A. G., Oakes, J. D., & Healey, M. C. (2004). Energetics and morphology of sockeye salmon: Effects of upriver migratory distance and elevation. Journal of Fish Biology, 65(3), 788–810.

Damon, L. J., Slater, S. B., & Baxter, R. D. (2016). Fecundity and reproductive potential of wild female Delta Smelt in the upper San Francisco Estuary, California. California Fish and Game, 102(4), 188–210.

Dege, M., & Brown, L. R. (2004). Effect of Outflow on Spring and Summertime Distribution and Abundance of Larval and Juvenile Fishes in the Upper San Francisco Estuary. American Fisheries Society Symposium, 39:, 49–65.

Dettinger, M., Anderson, J., Anderson, M., Brown, L. R., Cayan, D., & Maurer, E. (2016). Climate Change and the Delta. 14(3), 27.

Fernandes, T. J., Shuter, B. J., Ihssen, P. E., & McMeans, B. C. (2022). The timing of spring warming shapes reproductive effort in a warm-water fish: The role of mismatches between hepatic and gonadal processes. Canadian Journal of Fisheries and Aquatic Sciences, 79(6), 893–911. https://doi.org/10.1139/cjfas-2020-0412

Feyrer, F., Newman, K., Nobriga, M., & Sommer, T. (2011). Modeling the Effects of Future Outflow on the Abiotic Habitat of an Imperiled Estuarine Fish. Estuaries and Coasts, 34(1), 120–128. https://doi.org/10.1007/s12237-010-9343-9

Fichman, R. A., Khen, A., Willmes, M., Kuntz, J., Scott, A. R., Hobbs, J. A., & Lewis, L. S. (2021). The Clever Strategies That Fishes Use to Survive in San Francisco's Dynamic Estuary. Frontiers for Young Minds, 9, 608881. https://doi.org/10.3389/frym.2021.608881

Flitcroft, R. L., Arismendi, I., & Santelmann, M. V. (2019). A review of habitat connectivity research for Pacific salmon in marine, estuary, and freshwater environments. JAWRA Journal of the American Water Resources Association, 55(2), 430–441.

Flitcroft, R. L., Lewis, S. L., Arismendi, I., LovellFord, R., Santelmann, M. V., Safeeq, M., & Grant, G. (2016). Linking Hydroclimate to Fish Phenology and Habitat Use with Ichthyographs. PLOS ONE, 11(12), e0168831. https://doi.org/10.1371/journal.pone.0168831

Grimaldo, L. F., Sommer, T., Van Ark, N., Jones, G., Holland, E., Moyle, P. B., Herbold, B., & Smith, P. (2009). Factors affecting fish entrainment into massive water diversions in a tidal freshwater estuary: Can fish losses be managed? North American Journal of Fisheries Management, 29(5), 1253–1270.

Hall, C. J., Jordaan, A., & Frisk, M. G. (2011). The historic influence of dams on diadromous fish habitat with a focus on river herring and hydrologic longitudinal connectivity. Landscape Ecology, 26(1), 95–107. https://doi.org/10.1007/s10980-010-9539-1

Hammock, B. G., Hartman, R., Dahlgren, R. A., Johnston, C., Kurobe, T., Lehman, P. W., Lewis, L. S., Van Nieuwenhuyse, E., Ramírez-Duarte, W. F., Schultz, A. A., & Teh, S. J. (2022). Patterns and predictors of condition indices in a critically endangered fish. Hydrobiologia, 849(3), 675–695. https://doi.org/10.1007/s10750-021-04738-z

Hammock, B. G., Hartman, R., Slater, S. B., Hennessy, A., & Teh, S. J. (2019). Tidal Wetlands Associated with Foraging Success of Delta Smelt. Estuaries and Coasts, 42(3), 857–867. https://doi.org/10.1007/s12237-019-00521-5

Hammock, B. G., Hobbs, J. A., Slater, S. B., Acuña, S., & Teh, S. J. (2015). Contaminant and food limitation stress in an endangered estuarine fish. Science of the Total Environment, 532, 316–326.

Hammock, B. G., Moose, S. P., Solis, S. S., Goharian, E., & Teh, S. J. (2019). Hydrodynamic Modeling Coupled with Long-term Field Data Provide Evidence for Suppression of Phytoplankton by Invasive Clams and Freshwater Exports in the San Francisco Estuary. Environmental Management, 63(6), 703–717. https://doi.org/10.1007/s00267-019-01159-6

Hammock, B. G., Slater, S. B., Baxter, R. D., Fangue, N. A., Cocherell, D., Hennessy, A., Kurobe, T., Tai, C. Y., & Teh, S. J. (2017). Foraging and metabolic consequences of semi-anadromy for an endangered estuarine fish. PLOS ONE, 12(3), e0173497. https://doi.org/10.1371/journal.pone.0173497

Hanak, E. (2011). Managing California's water: From conflict to reconciliation. Public Policy Instit. of CA.

Hanak, E., Escriva-Bou, A., Gray, B., Green, S., Harter, T., Jezdimirovic, J., Lund, J., Azuara, J., Moyle, P., & Seavy, N. (2019). Water and the Future of the San Joaquin Valley. https://doi.org/10.13140/RG.2.2.24360.83208

Hendry, A. (2004). To sea or not to sea? Anadromy versus non-anadromy in salmonids. Evolution Illuminated : Salmon and Their Relatives. https://ci.nii.ac.jp/naid/10018320834/

Hixon, M. A., Johnson, D. W., & Sogard, S. M. (2014). BOFFFFs: On the importance of conserving old-growth age structure in fishery populations. ICES Journal of Marine Science, 71(8), 2171–2185.

Hobbs, J. A., Lewis, L. S., Willmes, M., Denney, C., & Bush, E. (2019). Complex life histories discovered in a critically endangered fish. Scientific Reports, 9(1), 16772. https://doi.org/10.1038/s41598-019-52273-8

Hobbs, J. A., Moyle, P. B., Fangue, N., & Connon, R. E. (2017). Is Extinction Inevitable for Delta Smelt and Longfin Smelt? An Opinion and Recommendations for Recovery. San Francisco Estuary and Watershed Science, 15(2), 1–19. https://doi.org/10.15447/sfews.2017v15iss2art2

Hutchings, J. A., & Myers, R. A. (1994). The evolution of alternative mating strategies in variable environments. Evolutionary Ecology, 8(3), 256–268. https://doi.org/10.1007/BF01238277

Jonsson, B., & Berg, O. K. (2003). To Sea or Not to Sea? Anadromy Versus Non-Anadromy in Salmonids. Evolution Illuminated: Salmon and Their Relatives, 92.

Jonsson, B., & Jonsson, N. (2006). Life-history effects of migratory costs in anadromous brown trout. Journal of Fish Biology, 69(3), 860–869. https://doi.org/10.1111/j.1095-8649.2006.01160.x

Katayama, S. (2001). Spawning grounds and reproductive traits of anadromous and resident pond smelt, Hypomesus nipponensis, in Lake Ogawara, Japan. Fisheries Science, 67(3), 401–407. https://doi.org/10.1046/j.1444-2906.2001.00275.x

Kendall, N. W., McMillan, J. R., Sloat, M. R., Buehrens, T. W., Quinn, T. P., Pess, G. R., Kuzishchin, K. V., McClure, M. M., & Zabel, R. W. (2015). Anadromy and residency in steelhead and rainbow trout (Oncorhynchus mykiss): A review of the processes and patterns. Canadian Journal of Fisheries and Aquatic Sciences, 72(3), 319–342. https://doi.org/10.1139/cjfas-2014-0192

Kimmerer, W. (2002). Effects of freshwater flow on abundance of estuarine organisms: Physical effects or trophic linkages? Marine Ecology Progress Series, 243, 39–55. https://doi.org/10.3354/meps243039

Kinnison, M. T., Unwin, M. J., Hendry, A. P., & Quinn, T. P. (2001). Migratory Costs and the Evolution of Egg Size and Number in Introduced and Indigenous Salmon Populations. Evolution, 55(8), 1656–1667. https://doi.org/10.1111/j.0014-3820.2001.tb00685.x

Kuivila, K. M., & Moon, G. E. (2003). Potential exposure of larval and juvenile delta smelt to dissolved pesticides in the Sacramento-San Joaquin Delta, California. American Fisheries Society Symposium, 229–242.

Kurobe, T., Hammock, B. G., Damon, L. J., Hung, T.-C., Acuña, S., Schultz, A. A., & Teh, S. J. (2022). Reproductive strategy of Delta Smelt Hypomesus transpacificus and impacts of drought on reproductive performance. PLOS ONE, 17(3), e0264731. https://doi.org/10.1371/journal.pone.0264731

Kurobe, T., Park, M. O., Javidmehr, A., Teh, F.-C., Acuña, S. C., Corbin, C. J., Conley, A. J., Bennett, W. A., & Teh, S. J. (2016). Assessing oocyte development and maturation in the threatened Delta Smelt, Hypomesus transpacificus. Environmental Biology of Fishes, 99(4), 423–432. https://doi.org/10.1007/s10641-016-0483-z

LaCava, M., Fisch, K., Nagel, M., Lindberg, J. C., May, B., & Finger, A. J. (2015). Spawning Behavior of Cultured Delta Smelt in a Conservation Hatchery. North American Journal of Aquaculture, 77(3), 255–266. https://doi.org/10.1080/15222055.2015.1007192

Lenoch, L. K., Stumpner, P. R., Burau, J. R., Loken, L. C., & Sadro, S. (2021). Dispersion and stratification dynamics in the Upper Sacramento River Deep Water Ship Channel. San Francisco Estuary and Watershed Science, 19(4).

Lewis, L. S., Denney, C., Willmes, M., Xieu, W., Fichman, R. A., Zhao, F., Hammock, B. G., Schultz, A. A., Fangue, N., & Hobbs, J. A. (2021). Otolith-based approaches indicate strong effects of environmental variation on growth of a Critically Endangered estuarine fish. Marine Ecology Progress Series, 676, 37–56.

Lewis, L. S., Willmes, M., Cavole, L., Xieu, W., Fichman, R., Hung, T. C., Ellison, T., Stevenson, A., Shultz, A., Hammock, B. G., Teh, S. J., & Hobbs, J. A. (2021). Experimental Assessment of Otolith based Geochemical Reconstructions of Migratory Life History for an Imperiled Estuarine Fish. (in Bertrand, N.G., K.K. Arend, and B. Mahardja., editors. Directed Outflow Project: Technical Report 3. June 10, 2022, 284 pp; pp. 11–27). U.S. Bureau of Reclamation, Bay-Delta Office, California-Great Basin Region. https://www.usbr.gov/mp/bdo/docs/directed-outflow-project-tech-report3.pdf

Lindberg, J. C., Tigan, G., Ellison, L., Rettinghouse, T., Nagel, M. M., & Fisch, K. M. (2013). Aquaculture Methods for a Genetically Managed Population of Endangered Delta Smelt. North American Journal of Aquaculture, 75(2), 186–196. https://doi.org/10.1080/15222055.2012.751942

Linley, T. J. (1993). Patterns of life history variation among sockeye salmon (Oncorhynchus nerka) in the Fraser River, British Columbia. University of Washington.

Mac Nally, R., Thomson, J. R., Kimmerer, W. J., Feyrer, F., Newman, K. B., Sih, A., Bennett, W. A., Brown, L., Fleishman, E., Culberson, S. D., & Castillo, G. (2010). Analysis of pelagic species decline in the upper San Francisco Estuary using multivariate autoregressive modeling (MAR). Ecological Applications, 20(5), 1417–1430. https://doi.org/10.1890/09-1724.1

Mager, R. C. (1996). Gametogenesis, reproduction and artificial propagation of delta smelt, Hypomesus transpacificus. University of California, Davis.

Mahardja, B., Bashevkin, S. M., Pien, C., Nelson, M., Davis, B. E., & Hartman, R. (2022). Escape from the heat: Thermal stratification in a well-mixed estuary and implications for fish species facing a changing climate. Hydrobiologia, 849(13), 2895–2918.

Maitland, P., & Lyle, A. (1996). The smelt Osmerus eperlanus in Scotland.

McArthur, J. M., Howarth, R. J., & Bailey, T. R. (2001). Strontium Isotope Stratigraphy: LOWESS Version 3: Best Fit to the Marine Sr-Isotope Curve for 0–509 Ma and Accompanying Look-up Table for Deriving Numerical Age. The Journal of Geology, 109(2), 155–170. https://doi.org/10.1086/319243

Moore, J. W., Yeakel, J. D., Peard, D., Lough, J., & Beere, M. (2014). Life-history diversity and its importance to population stability and persistence of a migratory fish: Steelhead in two large North American watersheds. Journal of Animal Ecology, 83(5), 1035–1046. https://doi.org/10.1111/1365-2656.12212

Moore, K. (1996). The adaptive significance of body size and shape in sexually mature sockeye salmon (Oncorhynchus nerka). MSc Thesis, University of Washington, Seattle.

Moyle, P. B., Bennett, W. A., Fleenor, W. E., & Lund, J. R. (2010). Habitat Variability and Complexity in the Upper San Francisco Estuary. San Francisco Estuary and Watershed Science, 8(3). https://doi.org/10.15447/sfews.2010v8iss3art1

Moyle, P. B., Hobbs, J. A., & Durand, J. R. (2018). Delta Smelt and Water Politics in California. Fisheries, 43(1), 42–50. https://doi.org/10.1002/fsh.10014

Nichols, F. H., Cloern, J. E., Luoma, S. N., & Peterson, D. H. (1986). The Modification of an Estuary. Science, 231(4738), 567–573. https://doi.org/10.1126/science.231.4738.567

Northcote, T. G. (1984). Mechanisms of fish migration in rivers. In Mechanisms of migration in fishes (pp. 317–355). Springer.

Peck, M. A., Alheit, J., Bertrand, A., Catalán, I. A., Garrido, S., Moyano, M., Rykaczewski, R. R., Takasuka, A., & van der Lingen, C. D. (2021). Small pelagic fish in the new millennium: A bottom-up view of global research effort. Progress in Oceanography, 191, 102494. https://doi.org/10.1016/j.pocean.2020.102494

Pedersen, E. J., Miller, D. L., Simpson, G. L., & Ross, N. (2019). Hierarchical generalized additive models in ecology: An introduction with mgcv. PeerJ, 7, e6876. https://doi.org/10.7717/peerj.6876

Peters, R. H., & Peters, R. H. (1986). The Ecological Implications of Body Size. Cambridge University Press.

Potter, I. C., Tweedley, J. R., Elliott, M., & Whitfield, A. K. (2013). The ways in which fish use estuaries: A refinement and expansion of the guild approach. Fish and Fisheries, 16(2), 230–239. https://doi.org/10.1111/faf.12050

Reis, G., Howard, J., & Rosenfield, J. (2019). Clarifying Effects of Environmental Protections on Freshwater Flows to—And Water Exports from—The San Francisco Bay Estuary. San Francisco Estuary and Watershed Science, 17, 1–22. https://doi.org/10.15447/sfews.2019v17iss1art1

Roff, D. A. (1988). The evolution of migration and some life history parameters in marine fishes. Environmental Biology of Fishes, 22(2), 133–146. https://doi.org/10.1007/BF00001543

Saraux, C., Van Beveren, E., Brosset, P., Queiros, Q., Bourdeix, J.-H., Dutto, G., Gasset, E., Jac, C., Bonhommeau, S., & Fromentin, J.-M. (2019). Small pelagic fish dynamics: A review of mechanisms in the Gulf of Lions. Deep Sea Research Part II: Topical Studies in Oceanography, 159, 52–61. https://doi.org/10.1016/j.dsr2.2018.02.010

Schindler, D. E., Hilborn, R., Chasco, B., Boatright, C. P., Quinn, T. P., Rogers, L. A., & Webster, M. S. (2010). Population diversity and the portfolio effect in an exploited species. Nature, 465(7298), 609–612. https://doi.org/10.1038/nature09060

Scoville, C. (2019). Hydraulic society and a “stupid little fish”: Toward a historical ontology of endangerment. Theory and Society, 48(1), 1–37. https://doi.org/10.1007/s11186-019-09339-3

Sellheim, K., Willmes, M., Lewis, L. S., Sweeney, J., Merz, J., & Hobbs, J. A. (2022). Diversity in Habitat Use by White Sturgeon Revealed Using Fin Ray Geochemistry. Frontiers in Marine Science, 9, 859038. https://doi.org/10.3389/fmars.2022.859038

Sommer, T., Armor, C., Baxter, R., Breuer, R., Brown, L., Chotkowski, M., Culberson, S., Feyrer, F., Gingras, M., Herbold, B., Kimmerer, W., Mueller-Solger, A., Nobriga, M., & Souza, K. (2007). The Collapse of Pelagic Fishes in the Upper San Francisco Estuary: El Colapso de los Peces Pelagicos en La Cabecera Del Estuario San Francisco. Fisheries, 32(6), 270–277. https://doi.org/10.1577/1548-8446(2007)32[270:TCOPFI]2.0.CO;2

Sommer, T., Mejia, F., Nobriga, M., Feyrer, F., & Grimaldo, L. (2011). The Spawning Migration of Delta Smelt in the Upper San Francisco Estuary. San Francisco Estuary and Watershed Science, 9(2). https://doi.org/10.15447/sfews.2014v9iss2art2

Sturrock, A. M., Carlson, S. M., Wikert, J. D., Heyne, T., Nusslé, S., Merz, J. E., Sturrock, H. J. W., & Johnson, R. C. (2020). Unnatural selection of salmon life histories in a modified riverscape. Global Change Biology, 26(3), 1235–1247. https://doi.org/10.1111/gcb.14896

Swanson, C., Young, P. S., & Cech, J. J. (1998). Swimming performance of delta smelt: Maximum performance, and behavioral and kinematic limitations on swimming at

submaximal velocities. Journal of Experimental Biology, 201(3), 333–345. https://doi.org/10.1242/jeb.201.3.333

Teh, S. J., Baxa, D. V., Hammock, B. G., Gandhi, S. A., & Kurobe, T. (2016). A novel and versatile flash-freezing approach for evaluating the health of Delta Smelt. Aquatic Toxicology, 170, 152–161.

Teh, S. J., Schultz, A. A., Duarte, W. R., Acuña, S., Barnard, D. M., Baxter, R. D., Garcia, P. A. T., & Hammock, B. G. (2020). Histopathological assessment of seven year-classes of Delta Smelt. Science of The Total Environment, 726, 138333. https://doi.org/10.1016/j.scitotenv.2020.138333

Teichert, N., Pasquaud, S., Borja, A., Chust, G., Uriarte, A., & Lepage, M. (2017). Living under stressful conditions: Fish life history strategies across environmental gradients in estuaries. Estuarine, Coastal and Shelf Science, 188, 18–26.

Wang, S.-Y. S., Yoon, J.-H., Becker, E., & Gillies, R. (2017). California from drought to deluge. Nature Climate Change, 7(7), 465–468. https://doi.org/10.1038/nclimate3330

Werner, I., Deanovic, L. A., Connor, V., de Vlaming, V., Bailey, H. C., & Hinton, D. E. (2000). Insecticide-caused toxicity to Ceriodaphnia dubia (CLADOCERA) in the Sacramento–San Joaquin River delta, California, USA. Environmental Toxicology and Chemistry: An International Journal, 19(1), 215–227.

Wood, S. (2012). mgcv: Mixed GAM Computation Vehicle with GCV/AIC/REML smoothness estimation.

Wootton, R. J. (2012). Ecology of teleost fishes (Vol. 1). Springer Science & Business Media.

TABLES

Table 4-1: Delta Smelt sample sizes by year and life history phenotype.

Life history phenotypes include BWR: brackish-water residents; FWR: freshwater-residents; MIG: semi-anadromous migrants.

Survey Year	BWR	FWR	MIG	Total
2012	17	41	141	199
2013	18	86	111	215
2014	16	36	185	237
2015	4	9	84	97
2016	NA	9	25	34
2017	NA	5	29	34
2018	1	1	17	19
2019	NA	NA	7	7
Total	**56**	**187**	**599**	**842**

Table 4-2: Delta Smelt sample sizes by month and survey year that were used in models examining variation in body condition.

December samples (month 12) of the previous calendar year were grouped with months of the subsequent "survey year". January (month 1); February (month 2); March (month 3); April (month 4); and May (month 5).

Month	2012	2013	2014	2015	2016	2017	2018	2019	Total
12	NA	NA	NA	23	2	NA	5	5	35
1	84	79	82	15	7	15	9	1	292
2	31	56	48	49	5	7	4	1	201
3	33	56	60	5	7	8	1	NA	170
4	35	15	28	1	13	4	NA	NA	96
5	16	9	19	4	NA	NA	NA	NA	48
Total	**199**	**215**	**237**	**97**	**34**	**34**	**19**	**7**	**842**

Table 4-3: Delta Smelt sample sizes by survey year and life history phenotype that were used for gonadal analysis, including near mature (stage 3) and mature (stage 4) females (Kurobe et al. 2016).

Life history phenotypes as in Table 4-1.

Survey Year	BWR	FWR	MIG	Total
2012	9	17	54	80
2013	13	31	49	93
2014	8	16	92	116
2015	2	7	42	51
2016	NA	7	8	15
2017	NA	1	14	15
2018	NA	NA	7	7
Total	**32**	**79**	**266**	**377**

Table 4-4: Delta Smelt sample size used for clutch size and egg area analysis, including near mature (stage 3) and mature (stage 4) females (Kurobe et al 2016).

Life history phenotypes as in Table 4-1.

Survey Year	BWR	FWR	MIG	Total
2012	9	16	53	78
2013	12	29	45	86
2014	7	14	82	103
2015	2	6	28	36
2016	NA	6	8	14
2017	NA	1	14	15
2018	NA	NA	7	7
Total	**30**	**72**	**237**	**339**

Table 4-5: Results of the 'overall' generalized additive models (GAM) for Delta Smelt body metrics.

Estimated coefficients (*Coeff*), standard error (SE), *t*-statistic (*t*), and *p*-values (*p*) are displayed for parametric terms, and estimated degrees of freedom (*EDF*), reference degrees of freedom (*RDF*), *F*-ratio (*F*), and *p*-values (*p*) are provided for the smooth terms. The overall R^2, deviance explained (*DEV*), and sample sizes (*n*) are provided for each model. Significant *p*-values ($p < 0.05$) are in bold.

	Parametric Terms	**Coeff**	**SE**	**t**	**p**	**R^2**	**DEV (%)**	**n**
log_{10} (total weight) ~ phenotype + sex + year + month	Intercept (BWR)	0.371	0.020	18.151	**<0.001**	0.434	44.2	820
	FWR	-0.096	0.014	-6.759	**<0.001**			
	MIG	0.011	0.013	0.820	0.412			
	Male	-0.040	0.006	-6.138	**<0.001**			
	Smooth Terms	**EDF**	**RDF**	**F**	**p**			
	Year	5.498	6.000	33.050	**<0.001**			
	Month	2.895	2.991	84.160	**<0.001**			

	Parametric Terms	**Coeff**	**SE**	**t**	**p**	**R^2**	**DEV (%)**	**n**
Fork length ~ phenotype + sex + year + month	Intercept (BWR)	68.287	1.165	58.618	**<0.001**	0.419	42.7	820
	FWR	-4.335	0.709	-6.112	**<0.001**			
	MIG	0.851	0.655	1.300	0.194			
	Male	-1.832	0.326	-5.624	**<0.001**			
	Smooth Terms	**EDF**	**RDF**	**F**	**p**			
	Year	5.651	6.000	41.370	**<0.001**			
	Month	2.695	2.931	64.830	**<0.001**			

Table 4-6: Results of the 'overall' generalized additive models (GAM) for Delta Smelt reproductive metrics.

Estimated coefficients (*Coeff*), standard error (SE), *t*-statistic (*t*), and *p*-values (*p*) are displayed for parametric terms, and estimated degrees of freedom (*EDF*), reference degrees of freedom (*RDF*), *F*-ratio (*F*), and *p*-values (*p*) are provided for the smooth terms. The overall R^2, deviance explained (*DEV*), and sample sizes (*n*) are provided for each model. Significant *p*-values ($p < 0.05$) are in bold.

	Parametric Terms	***Coeff***	***SE***	***t***	***p***	***R^2***	***DEV (%)***	***n***
$\log_{10}$(gonad weight) ~ phenotype + maturity substage + year + month	Intercept (BWR)	-1.713	0.114	-15.018	**<0.001**	0.849	85.5	376
	FWR	-0.118	0.035	-3.325	**<0.001**			
	MIG	0.003	0.032	0.097	0.923			
	Maturity substage (3.2)	-0.115	0.106	-1.092	0.276			
	Maturity substage (3.3)	0.197	0.099	1.994	**0.047**			
	Maturity substage (4.1)	0.429	0.100	4.274	**<0.001**			
	Maturity substage (4.2)	0.677	0.100	6.732	**<0.001**			
	Maturity substage (4.3)	1.008	0.101	9.957	**<0.001**			
	Smooth Terms	***EDF***	***RDF***	***F***	***p***			
	Year	5.532	6.000	12.860	**<0.001**			
	Month	2.329	2.707	18.200	**<0.001**			
	Parametric Terms	***Coeff***	***SE***	***t***	***p***	***R^2***	***DEV (%)***	***n***
Clutch size ~ phenotype + maturity substage + year + month	Intercept (BWR)	890.710	251.560	3.541	**<0.001**	0.395	41.9	339
	FWR	-349.320	82.210	-4.249	**<0.001**			
	MIG	-58.540	74.000	-0.791	0.429			
	Maturity substage (3.2)	54.040	240.500	0.225	0.822			
	Maturity substage (3.3)	12.170	222.170	0.055	0.956			
	Maturity substage (4.1)	83.560	224.410	0.372	0.710			
	Maturity substage (4.2)	184.130	224.860	0.819	0.413			
	Maturity substage (4.3)	447.100	226.820	1.971	**0.050**			
	Smooth Terms	***EDF***	***RDF***	***F***	***p***			
	Year	5.407	6.000	16.640	**<0.001**			
	Month	1.000	1.001	15.500	**<0.001**			
	Parametric Terms	***Coeff***	***SE***	***t***	***p***	***R^2***	***DEV (%)***	***n***
Oocyte area ~ phenotype + maturity substage + year + month	Intercept (BWR)	-2.739	0.217	-12.627	**<0.001**	0.842	86.5	337
	FWR	0.070	0.062	1.120	0.263			
	MIG	0.048	0.055	0.862	0.389			
	Maturity substage (3.2)	-0.714	0.219	-3.265	**0.001**			
	Maturity substage (3.3)	-0.066	0.208	-0.317	0.751			
	Maturity substage (4.1)	0.361	0.211	1.717	0.087			
	Maturity substage (4.2)	0.877	0.210	4.169	**<0.001**			
	Maturity substage (4.3)	1.444	0.211	6.836	**<0.001**			
	Smooth Terms	***EDF***	***RDF***	***F***	***p***			
	Year	2.434	3.000	4.251	**0.002**			
	Month	2.301	2.683	5.486	**0.002**			

Table 4-7: Results of the 'size-adjusted' generalized additive models (GAM) for Delta Smelt fitness and reproductive metrics.

Estimated coefficients (*Coeff*), standard error (SE), *t*-statistic (*t*), and *p*-values (*p*) are displayed for parametric terms, and estimated degrees of freedom (*EDF*), reference degrees of freedom (*RDF*), *F*-ratio (*F*), and *p*-values (*p*) are provided for the smooth terms. The overall R^2, deviance explained (*DEV*), and sample sizes (*n*) are provided for each model. Significant *p*-values ($p < 0.05$) are in bold.

	Parametric Terms	***Coeff***	***SE***	***t***	***p***	***R^2***	***DEV (%)***	***n***
log_{10} (total weight) ~ fork length*phenotype + sex + year + month	Intercept (Female)	0.350	0.012	30.072	**<0.001**	0.852	85.5	820
	Male	-0.009	0.003	-2.683	**0.007**			
	Smooth Terms	***EDF***	***RDF***	***F***	***p1***			
	Fork length*Phenotype	6.845	29.000	339.278	**<0.001**			
	Year	5.069	6.000	4.075	**<0.001**			
	Month	2.865	2.985	18.834	**<0.001**			
	Parametric Terms	***Coeff***	***SE***	***t***	***p***	***R^2***	***DEV (%)***	***n***
log_{10} (gonad weight) ~ total weight*phenotype + maturity substage + year + month	Intercept (Maturity substage 3.1)	-1.511	0.111	-13.568	**<0.001**	0.897	90.3	376
	Maturity substage (3.2)	-0.101	0.088	-1.151	0.251			
	Maturity substage (3.3)	0.134	0.082	1.631	0.104			
	Maturity substage (4.1)	0.318	0.084	3.777	**<0.001**			
	Maturity substage (4.2)	0.544	0.085	6.434	**<0.001**			
	Maturity substage (4.3)	0.853	0.085	10.016	**<0.001**			
	Smooth Terms	***EDF***	***RDF***	***F***	***p***			
	Total weight*Phenotype	8.804	29.000	33.704	**<0.001**			
	Year	5.416	6.000	7.155	**<0.001**			
	Month	2.535	2.850	7.750	**<0.001**			
	Parametric Terms	***Coeff***	***SE***	***t***	***p***	***R^2***	***DEV (%)***	***n***
Clutch size ~ total weight*phenotype + maturity substage + year + month	Intercept (Maturity substage 3.1)	1069.360	216.940	4.929	**<0.001**	0.59	61.3	339
	Maturity substage (3.2)	87.910	199.130	0.441	0.659			
	Maturity substage (3.3)	-102.610	186.020	-0.552	0.582			
	Maturity substage (4.1)	-123.020	189.370	-0.650	0.516			
	Maturity substage (4.2)	-64.360	190.800	-0.337	0.736			
	Maturity substage (4.3)	136.020	192.460	0.707	0.480			
	Smooth Terms	***EDF***	***RDF***	***F***	***p***			
	Total weight*Phenotype	8.804	29.000	33.704	**<0.001**			
	Year	5.416	6.000	7.155	**<0.001**			
	Month	2.535	2.850	7.750	**<0.001**			
	Parametric Terms	***Coeff***	***SE***	***t***	***p***	***R^2***	***DEV (%)***	***n***
Oocyte area ~ gonad weight*phenotype + maturity substage + year + month	Intercept (Maturity substage 3.1)	-2.188	0.289	-7.581	**<0.001**	0.902	89.9	336
	Maturity substage (3.2)	-0.510	0.193	-2.641	**0.009**			
	Maturity substage (3.3)	0.041	0.182	0.224	0.823			
	Maturity substage (4.1)	0.323	0.185	1.743	0.082			
	Maturity substage (4.2)	0.631	0.188	3.356	**<0.001**			
	Maturity substage (4.3)	0.903	0.195	4.627	**<0.001**			
	Smooth Terms	***EDF***	***RDF***	***F***	***p***			
	Gonad weight*Phenotype	10.022	29.000	3.774	**<0.001**			
	Year	0.880	3.000	0.376	0.273			
	Month	2.481	2.813	2.466	0.112			

FIGURES

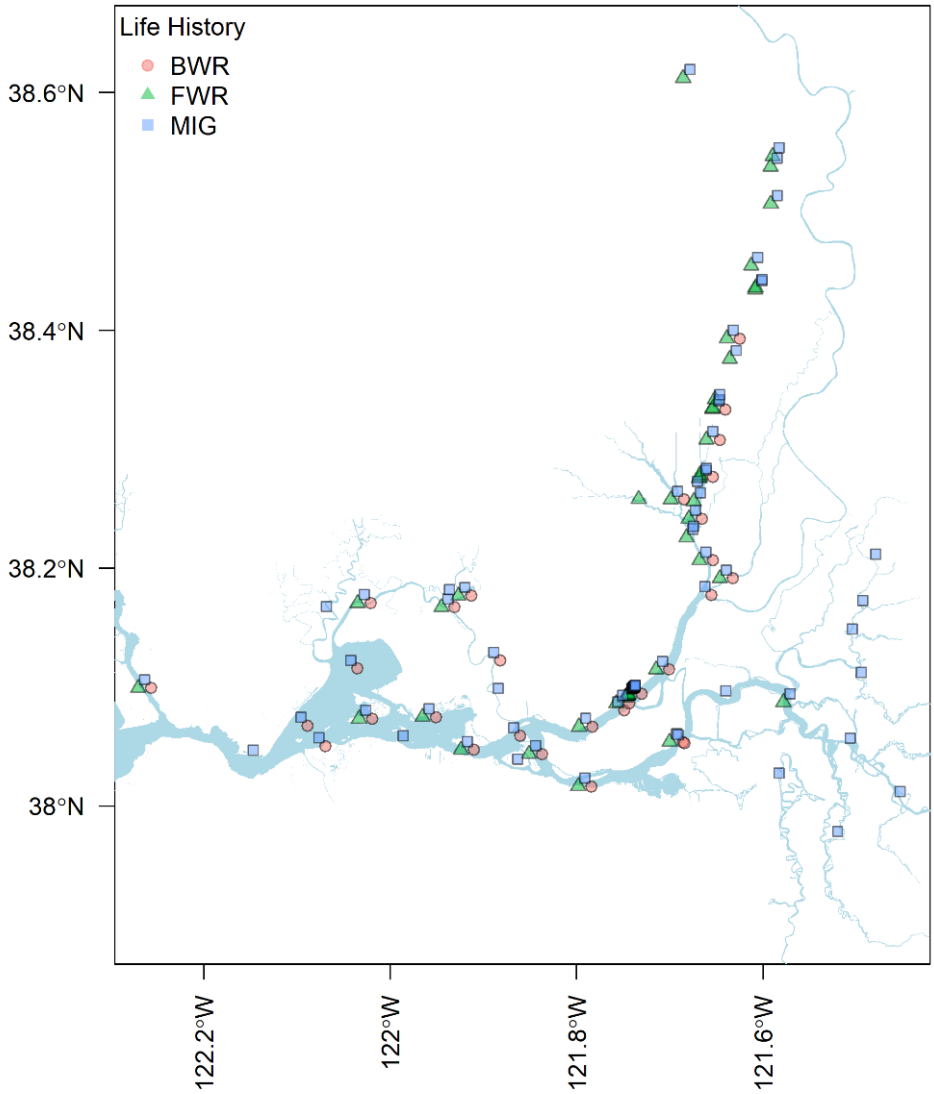

Figure 4-1: Spring Kodiak Trawl sampling stations where Delta Smelt (*Hypomesus transpacificus*) were collected for this study from the upper San Francisco Estuary, California, USA.

Each sampling station is represented with a separate marker for Freshwater residents (FWR, green triangle); Brackish-water residents (BWR, red circle); and Migrants (MIG, blue rectangle) if they were observed at the given station.

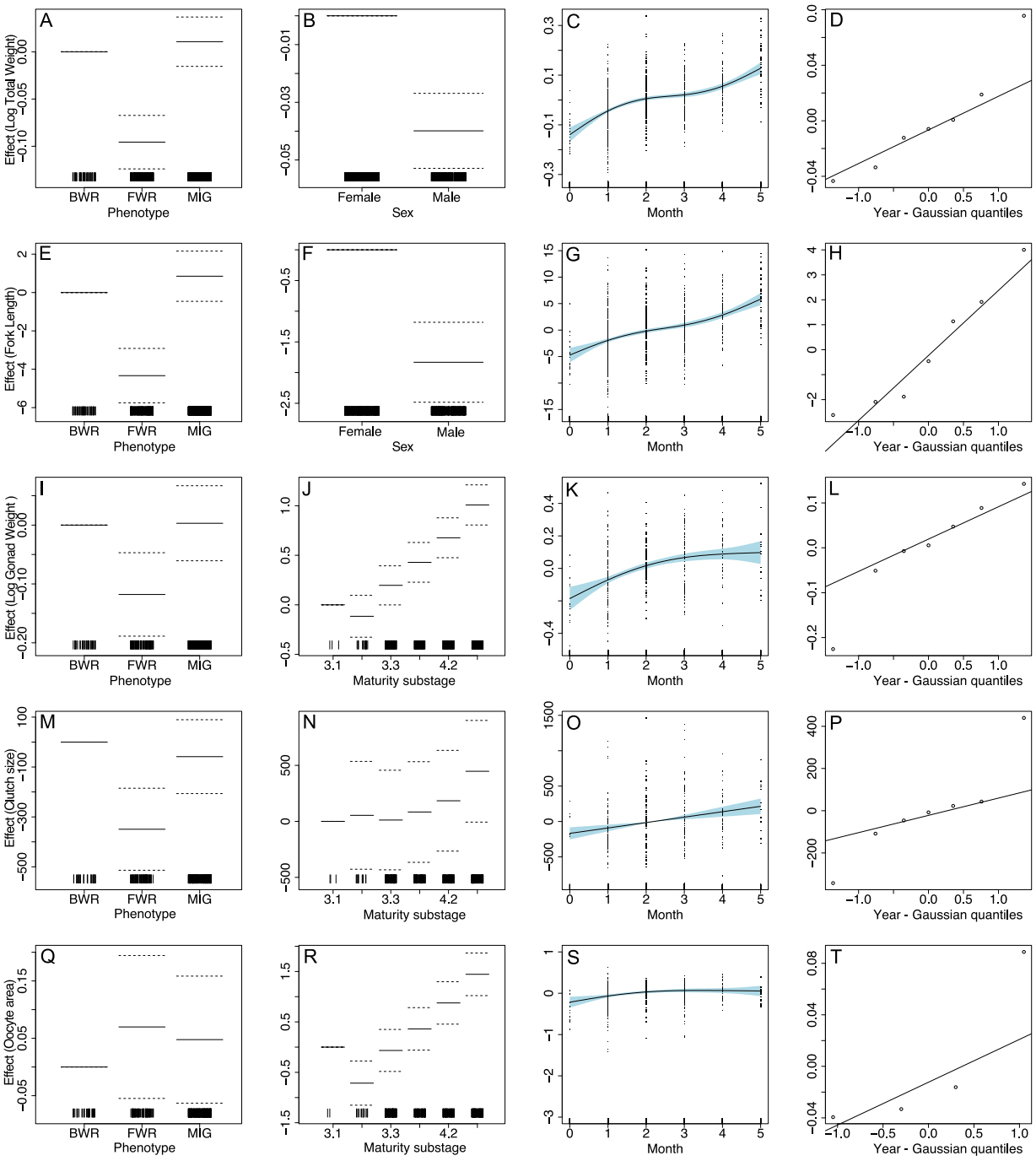

Figure 4-2: Overall GAM models for the body and reproductive metrics of wild Delta Smelt.

Partial residual smooth plots for the additive effects of phenotype type (BWR: brackish-water resident; FWR: freshwater resident; MIG: migrant), sex (females, males), maturity substage, month and year on the total weight (A-D), fork length (E-H), gonad weight (I-L), clutch size (M-P), and oocyte area (Q-T) of adult specimens collected in the upper San Francisco Estuary, California, USA. Phenotype, sex, and maturity substage were included as fixed parametric terms, month as a fixed nonparametric smooth term, and year as a random effect. Month 0 = December of the previous calendar year.

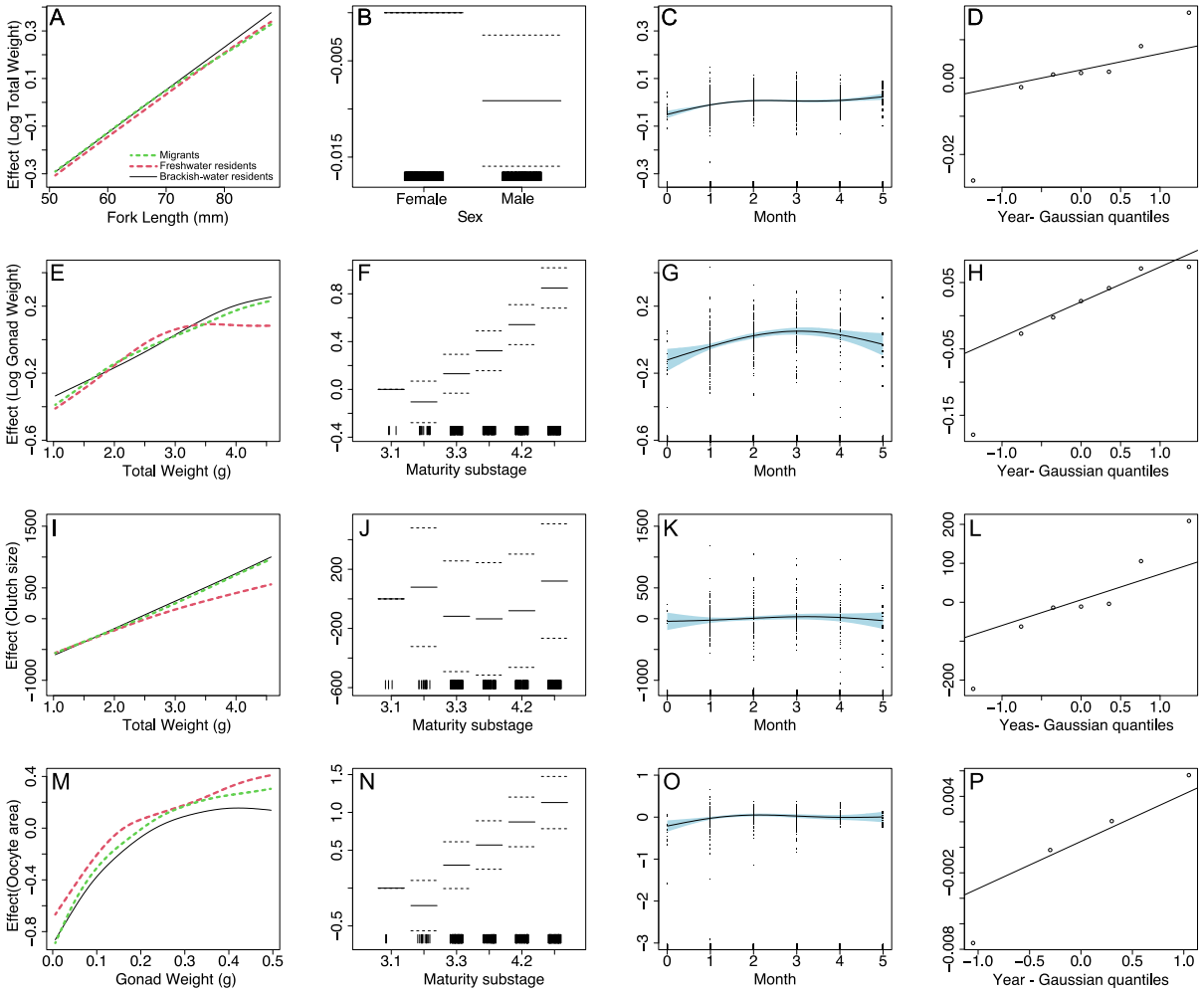

Figure 4-3: Size-adjusted GAM models for the body and reproductive metrics of wild Delta Smelt.

Partial residual smooth plots for the additive effects of phenotype type (brackish-water resident; freshwater resident; migrant), sex (females, males), maturity substage, month and year on the total weight (A-D), gonad weight (E-H), clutch size (I-L), and oocyte area (M-P) of adult specimens collected in the upper San Francisco Estuary, California, USA. Group-level smoothers with similar wiggliness (model GS) are denoted for each life-history phenotype. Sex and maturity substage were included as fixed parametric factors, month as a nonparametric smooth, and year as a random effect. Month 0 = December of the previous calendar year.

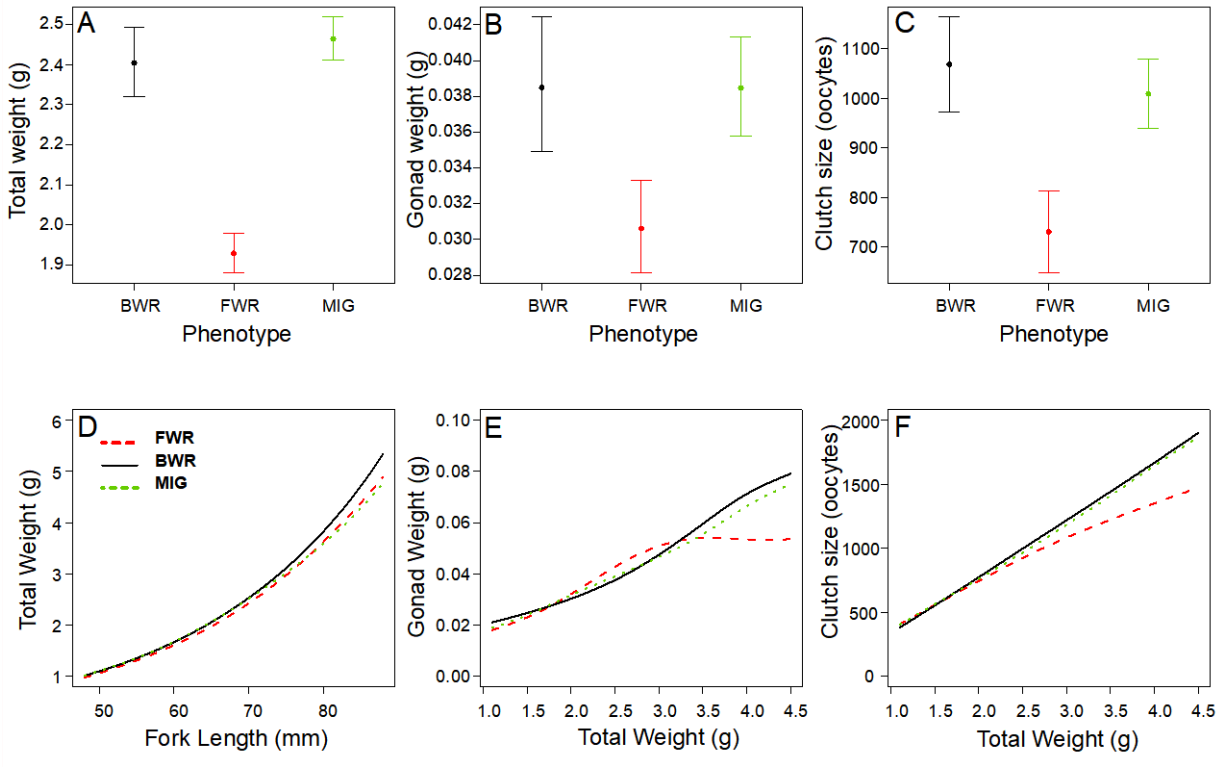

Figure 4-4: Predictions for the overall and size-adjusted GAM models.

Predicted (A) total weight, (B) gonad weight, and (C) clutch size among the main phenotypes (FWR: fresh-water residents; BWR: brackish-water residents; and MIG: migrants) of Delta Smelt using the overall model. Predicted (D) total weight, (E) gonad weight, (F) clutch size group-specific smoothers among the main phenotypes (FWR: fresh-water residents; BWR: brackish-water residents; and MIG: migrants) of Delta Smelt using the size-adjusted model.

SUPPLEMENTARY TABLES

Table S4-1: Candidate 'overall' generalized additive models (GAM) for Delta Smelt fitness and reproductive metrics.

TW: total weight; FL: Fork length; GW: gonad weight. Smoothed predictor variables are denoted by "s", and random effects by "re". The effective degree of freedom (EDF), deviance explained (%) and AIC for each model is displayed. Selected models are depicted in bold and followed a single common smoother plus phenotype group-level smoothers with same wiggliness (bs= "fs"), a random effect of year, four basis function (k=4) for the nonparametric smooth function for month, and either a fixed parametric term for sex (body metrics) or maturity substage (reproductive metrics).

Response variable	**Predictor variables**	**EDF**	**DE (%)**	**AIC**
log_{10}(TW)	Phenotype	3.00	5.79	-1172.37
	Phenotype + s(year, bs="re")	9.15	20.90	-1307.07
	Phenotype + s(year, bs="re") + s(month, k=4)	11.95	42.00	-1563.77
	Phenotype + s(year, bs="re") + s(month, k=4) + sex	12.39	44.20	-1608.08
FL	Phenotype	3.00	5.15	5386.63
	Phenotype + s(year, bs="re")	9.42	24.00	5212.58
	Phenotype + s(year, bs="re") + s(month, k=4)	12.02	40.80	5007.60
	Phenotype + s(year, bs="re") + s(month, k=4) + sex	12.34	42.70	4812.47
log_{10}(GW)	Phenotype	3.00	0.25	434.72
	Phenotype + maturity substage	8.00	78.90	-139.78
	Phenotype + maturity substage + s(year, bs="re")	13.60	83.60	-222.14
	Phenotype + maturity substage + s(year, bs="re") + s(month, k=4)	15.86	85.50	-265.29
Clutch size	Phenotype	3.00	2.23	5148.26
	Phenotype + maturity substage	8.00	19.00	5094.57
	Phenotype + maturity substage + s(year, bs="re")	13.45	39.30	5007.51
	Phenotype + maturity substage + s(year, bs="re") + s(month, k=4)	14.41	41.90	4994.39
Oocyte area	Phenotype	3.00	2.19	-666.04
	Phenotype + maturity substage	8.00	84.90	-1310.20
	Phenotype + maturity substage + s(year, bs="re")	10.57	85.90	-1327.77
	Phenotype + maturity substage + s(year, bs="re") + s(month, k=4)	12.73	86.50	-1339.42

Table S4-2: Candidate 'size-adjusted' generalized additive models (GAM) for Delta Smelt fitness and reproductive metrics.

TW: total weight; FL: Fork length; GW: gonad weight. Smoothed predictor variables are denoted by "s", and random effect by "re". The effective degree of freedom (EDF), deviance explained (%) and AIC for each model is displayed. Selected models are depicted in bold and followed a single common smoother plus phenotype group-level smoothers with same wiggliness (bs= "fs"), a random effect of year, four basis function (k=4) for the nonparametric smooth functions for month and respective covariates (FL, TW, GW), and either a fixed parametric term for sex (body metrics) or maturity substage (reproductive metrics).

Response variable	Predictor variables	EDF	DE(%)	AIC
$\log_{10}$(TW)	s(FL)	4.65	84.3	-2682.31
	s(FL) + Phenotype	6.71	84.5	-2687.32
	s(FL, Phenotype, bs="fs")	14.5	84.7	-2690.44
	s(FL, Phenotype, bs="fs") + s(year, bs="re")	17.45	85.2	-2709.21
	s(FL, Phenotype, bs="fs") + s(year, bs="re") + s(month, k=4)	16.78	86.2	-2762.49
	s(FL, Phenotype, bs="fs") + s(year, bs="re") + s(month, k=4) + sex	22.75	85.5	-2703.50
$\log_{10}$(GW)	s(TW)	4.65	45.4	211.18
	s(TW) + Phenotype	6.71	49.5	186.57
	s(TW, Phenotype, bs="fs")	10.62	49.8	191.78
	s(TW, Phenotype, bs="fs") + maturity substage	15.69	88.3	-345.21
	s(TW, Phenotype, bs="fs") + maturity substage + s(year, bs="re")	20.58	89.7	-383.96
	s(TW, Phenotype, bs="fs") + maturity substage + s(year, bs="re") + s(month, k=4)	22.75	90.3	-403.06
Clutch size	s(TW)	2	49.9	4919.74
	s(TW) + Phenotype	4	50.5	4919.50
	s(TW, Phenotype, bs="fs")	10.64	54.3	4905.50
	s(TW, Phenotype, bs="fs") + maturity substage	15.02	57.6	4888.90
	s(TW, Phenotype, bs="fs") + maturity substage + s(year, bs="re")	17.58	60.9	4867.08
	s(TW, Phenotype, bs="fs") + maturity substage + s(year, bs="re") + s(month, k=4)	19.49	61.3	4867.44
Oocyte area	s(GW)	4.93	38.6	4889.69
	s(GW) + Phenotype	6.88	41.2	4874.98
	s(GW, Phenotype, bs="fs")	9.08	41.6	4877.04
	s(GW, Phenotype, bs="fs") + maturity substage	19.28	57	4793.03
	s(GW, Phenotype, bs="fs") + maturity substage + s(year, bs="re")	23.39	62.5	4754.09
	s(GW, Phenotype, bs="fs") + maturity substage + s(year, bs="re") + s(month, k=4)	24.17	62.6	4754.61

SUPPLEMENTARY FIGURES

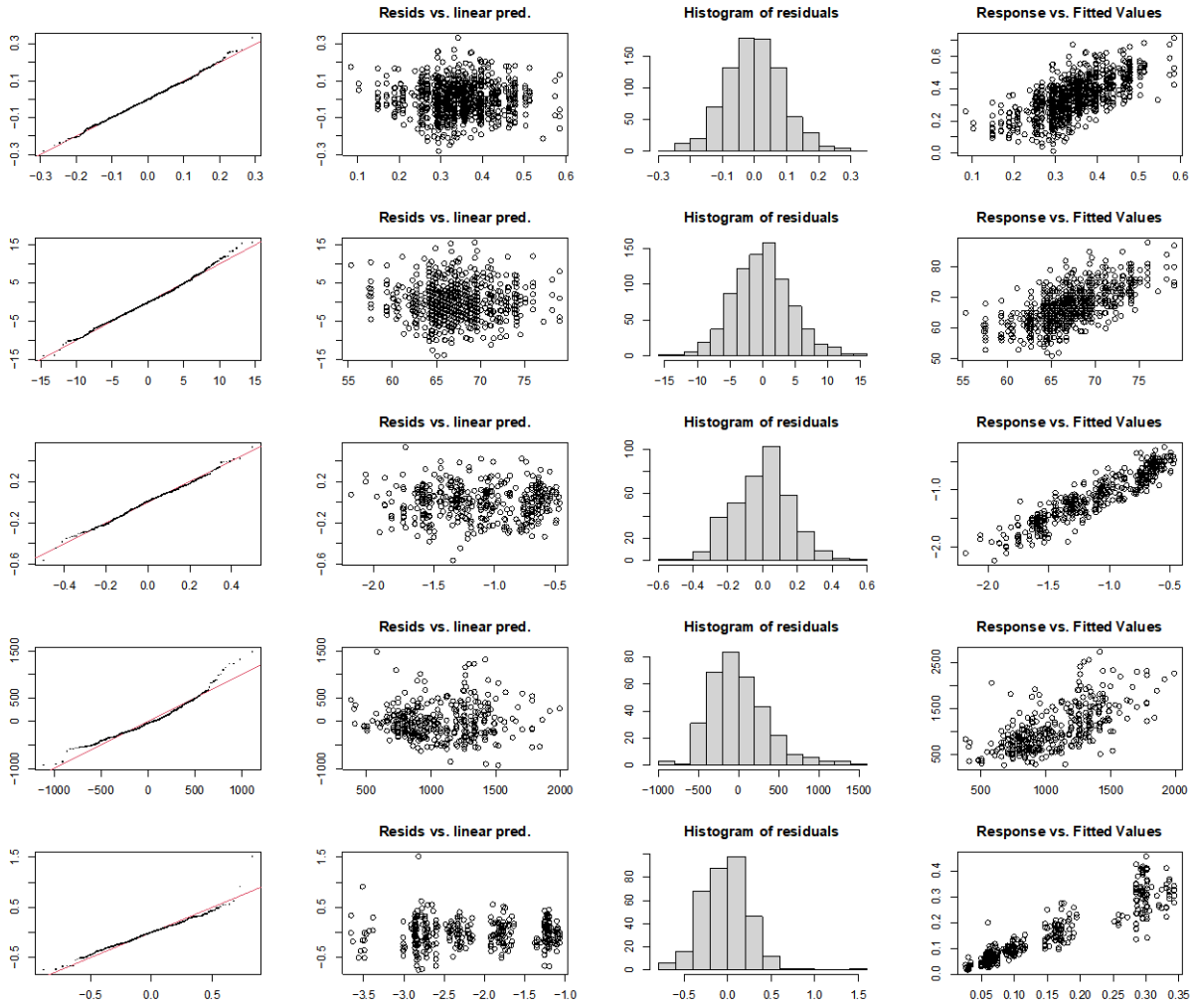

Figure S4-1: Diagnostic plot for 'overall' generalized additive models fitted to Delta Smelt total weight (first row), fork length (second row), gonad weight (third row), clutch size (forth row), and oocyte area (fifth row) response variables.

At each row, from left to right; QQ-plot of residuals (black dots); residuals vs. linear predicted values; histogram of residuals; and response vs. fitted values.

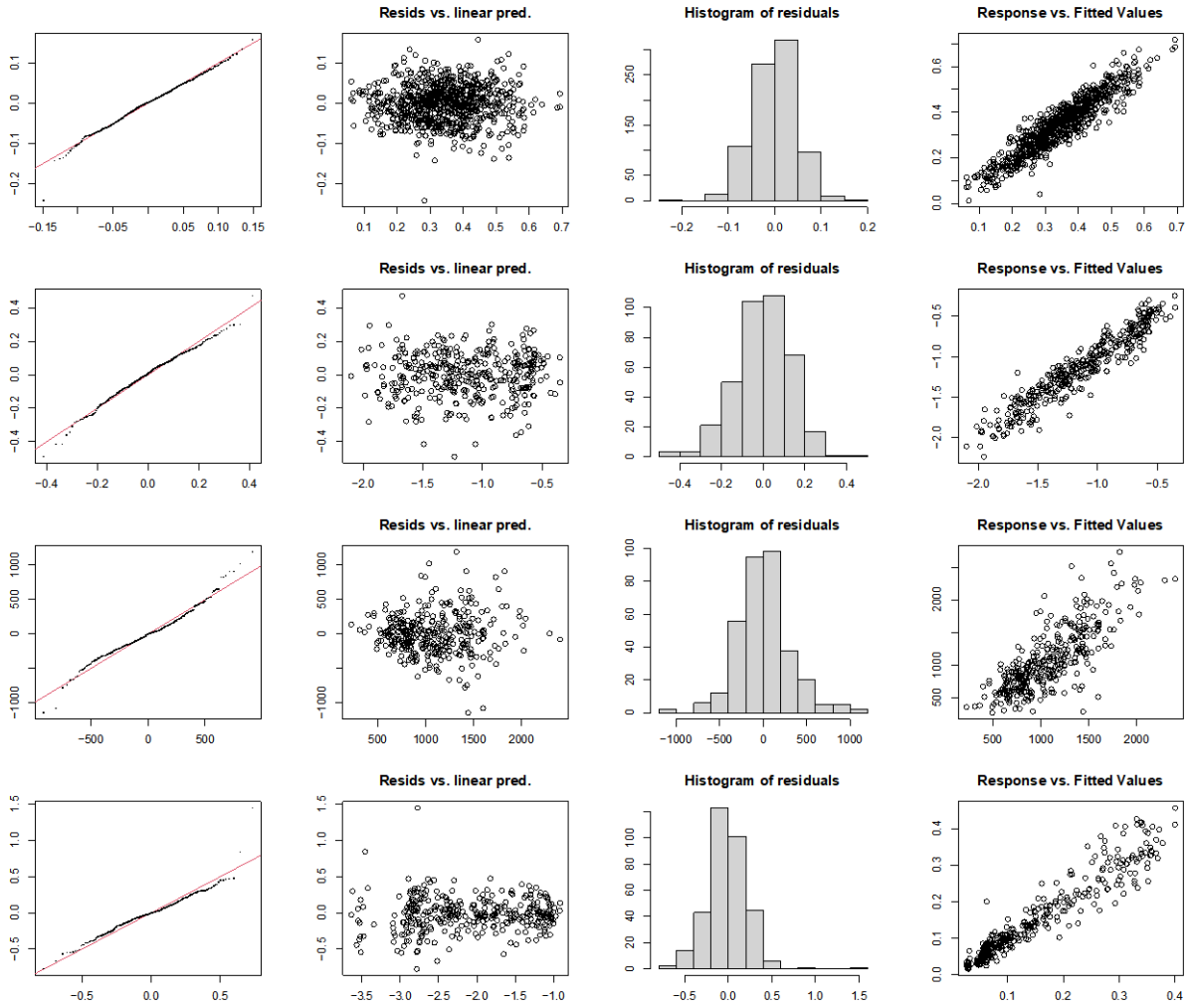

Figure S4-2: Diagnostic plot for 'size-adjusted' generalized additive models fitted to Delta Smelt total weight (first row), gonad weight (second row), clutch size (third row), and oocyte area (forth row) response variables.

At each row, from left to right; QQ-plot of residuals (black dots); residuals vs. linear predicted values; histogram of residuals; and response vs. fitted values.

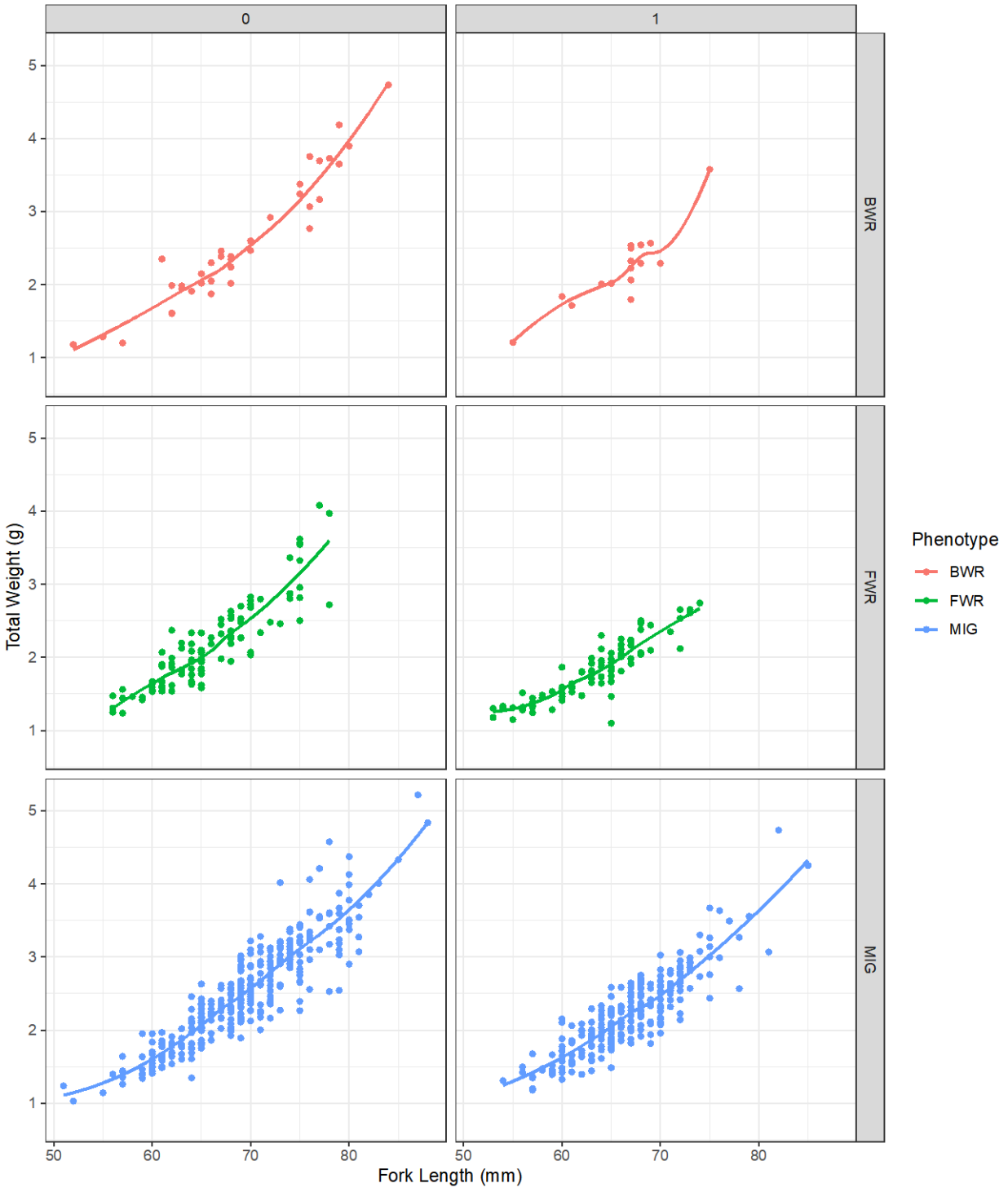

Figure S4-3: Delta Smelt length-weight relationship for females (0) and males (0) across three main phenotypes: brackish-water residents (BWR), freshwater resident (FWR), and semi-anadromous migrants (MIG).

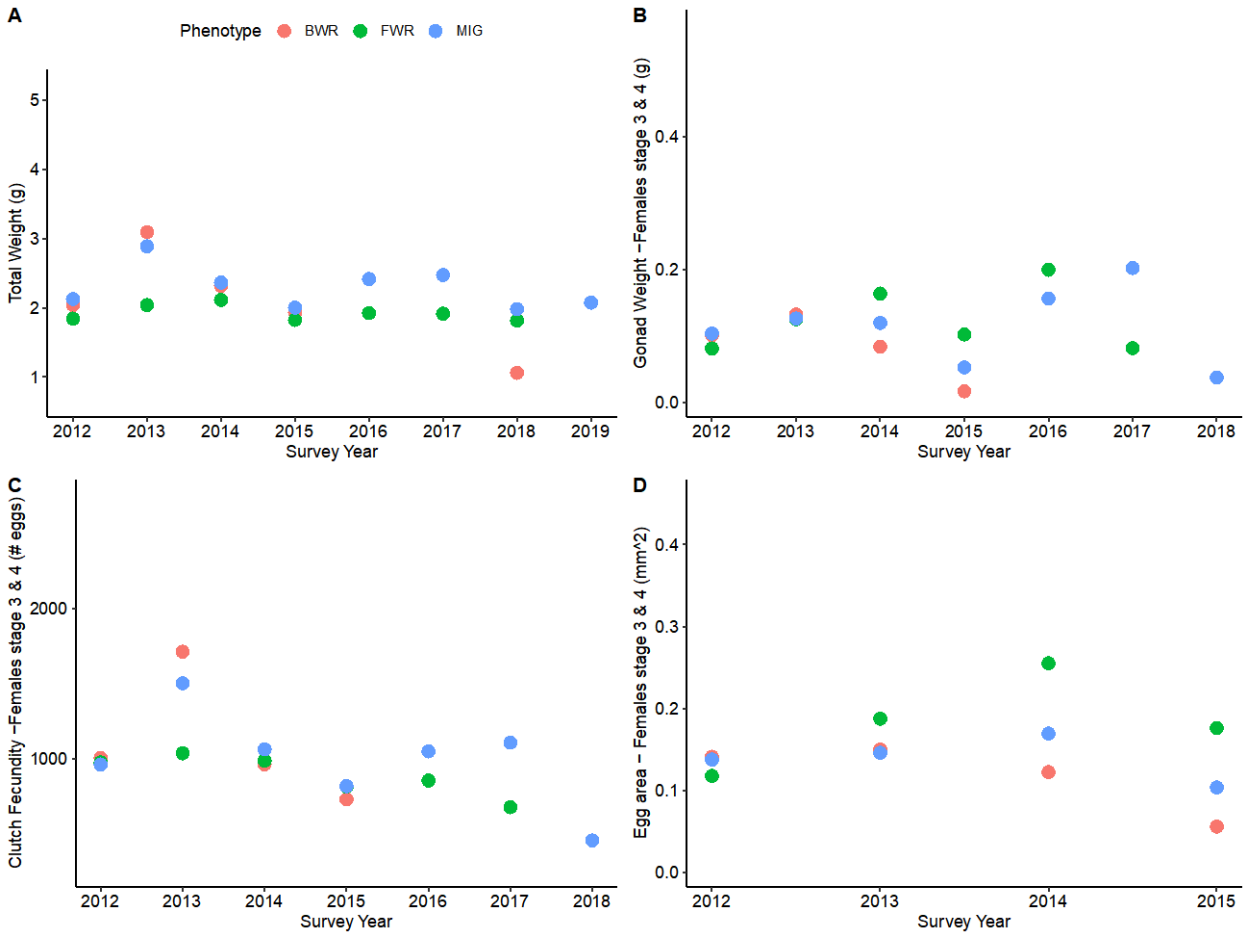

Figure S4-4: Delta Smelt (A) total weight, (B) gonad weight, (C) clutch fecundity, and (D) and egg area for each phenotype (red: brackish-water resident; green: freshwater resident; and blue: migrant) among survey years. Larger dots are the means for each phenotype in each year.

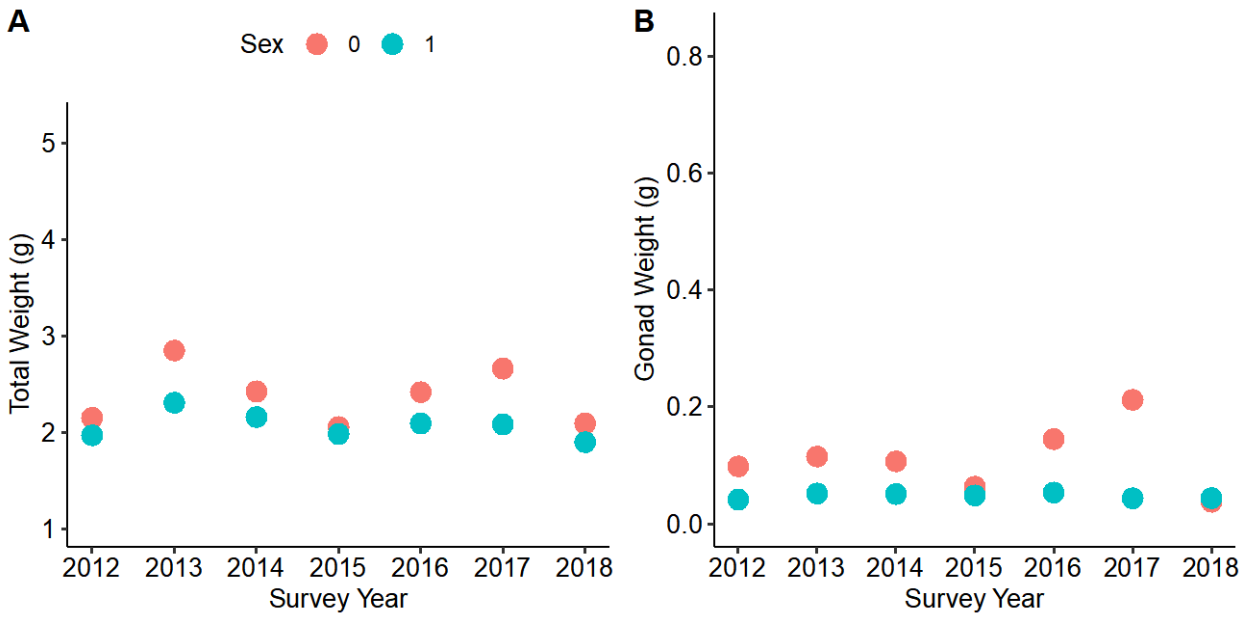

Figure S4-5: Delta Smelt (A) total weight, (B) gonad weight for each sex (red: female; blue: male) among survey years.

Larger dots are the means for each sex in each year.

This Page Intentionally Left Blank

Chapter 5: Effects of Four Preservatives on the Morphology, Histology, and Otolith Chemistry of a Critically Endangered Estuarine Fish

Authors:

Levi S. Lewis[1], Christian Denney[1], Leticia Cavole[1], Wilson Xieu[1], Feng Zhao[1], Jonathan Huang[1], James Hobbs[1], Malte Willmes[2], Tien-Chieh Hung[3], Andrew Schultz[4,5], Swee Teh[6], Bruce G. Hammock[6]

[1] Department of Wildlife, Fish and Conservation Biology, University of California-Davis, Davis, CA, United States

[2] Norwegian Institute for Nature Research, Trondheim, Norway

[3] Fish Conservation and Culture Lab, Department of Biological and Agricultural Engineering, University of California-Davis, Byron, CA, United States

[4] US Bureau of Reclamation, Bay-Delta Office, Science Division, Sacramento, CA, United States

[5] U.S. Geological Survey, Southwest Biological Science Center, Grand Canyon Monitoring and Research Center, Flagstaff, AZ, United States

[6] Department of Anatomy, Physiology, and Cell Biology, School of Veterinary Medicine, University of California-Davis, Davis, CA, United States

***Corresponding Author:**

Levi S. Lewis[1]
[1]One Shields Ave., Davis, CA, 95616, United States
lewis.sci@gmail.com

ABSTRACT

Robust methods for preserving field-collected specimens are needed for the effective study of wild populations. Ideal methods would preserve whole-body morphology and internal structures, including soft tissues and calcified structures. This is especially important for endangered species, like Delta Smelt *Hypomesus transpacificus*, where each specimen is incredibly rare and valuable to science and conservation. Here, we tested four preservation methods (buffered 10% formalin, 95% ethanol, liquid nitrogen, and 100% ExCell Plus) and examined how each preservative affected standard length, body weight, otolith structure, otolith chemistry, and the histology of soft tissues (e.g., gills, livers, and gonads) at 1, 4, 24, and 52 weeks. All preservatives resulted in 2-5% shrinkage in standard length, with effects increasing slightly over time. In contrast, changes in weight varied dramatically among preservatives, with liquid

nitrogen having the smallest (~5% loss) and most stable effect. In contrast, ethanol preservation resulted in up to a 40% loss in weight with diminishing effects over time, ExCell Plus up to an 18% loss in weight with no change over time, and formalin up to a 10% gain in weight with increasing effects over time. Histological examination of gill, liver, and gonad tissues indicated that formalin and liquid nitrogen preservation yielded the highest quality tissue preparations. Both formalin and ExCell Plus were corrosive to otoliths, whereas ethanol and liquid nitrogen appeared to preserve the integrity of otolith structures. Dissolution due to ExCell Plus resulted in unstable and unreliable otolith microchemistry, whereas formalin, ethanol, and liquid nitrogen exhibited limited overall effects on otolith chemistry. While each preservative has a unique suite of strengths and weaknesses, our results highlight the value of liquid nitrogen as a preservation method that maximizes the utility and value of archived fish specimens for the broadest use in scientific investigations.

INTRODUCTION

Legacy and importance of archived fish collections

Museums, agencies, and universities around the world are responsible for storing and preserving biological specimens to better catalog Earth's natural history and biodiversity patterns (Duckworth *et al.*, 1993; Graham *et al.*, 2004). Since major oceanographic expeditions such as the H.M.S. Challenger (1872-1876) and Albatross (1947-1948), storing and preserving specimens is an important first step to allow scientists to access many decades of work, utilize new techniques (e.g., isotopes, comparative genomics, and phylogenetics, population genetic, environmental DNA), and gain valuable insights regarding evolution, ecology, population dynamics, and environmental and anthropogenic influences on living organisms. Within vertebrates, fishes might be the group with the most historical samples available, offering the valuable potential to monitor anthropogenic changes, such as climate change, habitat fragmentation, and overexploitation, provided that preserved samples retain tissues and structures in useful condition (Nielsen & Hansen, 2008).

Preservation of whole fish specimens

All preservation methods have tradeoffs that require careful consideration of the analyses to be performed on archived specimens. For small pelagic fishes, preservation of the entire organism is often the most efficient method for storing specimens in the field. Key considerations for archiving fish in the field include the preservative type, concentration, and expected duration of preservation. For example, many studies have used ethanol concentrations of 70%, 80%, and 95%, buffered formalin at concentrations of 2.5%, 5%, and 10%, and freezing at -20°C or -80°C (Fowler & Smith, 1983; Jawad, 2003; Buchheister & Wilson, 2005; Nordeide, 2020). However, the effectiveness and consequences of various preservation methods differ for a variety of morphometrics and tissue types (e.g., calcified structures, soft tissues, and genetic material), thus complicating the identification of an optimal preservation method for a given fish specimen archive.

Formalin as a preservative

Formalin (a solution of water and formaldehyde, with 100% formalin containing 37% formaldehyde) is relatively low cost, yields excellent histological preparations of soft tissues, and effectively preserves planktonic organisms and fish stomach contents (Nyuji *et al.*, 2022). However, formalin preservation can make DNA extraction from tissues fairly difficult (Schander & Kenneth, 2003). Furthermore, formaldehyde is highly carcinogenic and mutagenic (Blackwell *et al.*, 1981). Formalin can also change the length and weight of fish specimens (Fowler & Smith, 1983; Cunningham *et al.*, 2000; Joh *et al.*, 2003). Last, in the absence of buffering agents, formalin decreases the pH of the preservative solution over time, thus compromising the integrity of calcified structures (Brothers, 1987) and altering their chemistry (Storm-Suke *et al.*, 2007).

Ethanol as preservative

Ethanol is relatively low cost, preserves morphological characteristics, facilitates molecular (i.e., DNA) studies, and preserves calcified structures such as otoliths (Hedges *et al.*, 2004; Baldwin & Johnson, 2014). Thus ethanol is commonly used as a preservative, however it is also flammable, may not provide adequate fixation for histology (S. Teh, personal communication, February 1, 2023), and may alter otolith chemistry (Storm-Suke *et al.*, 2007). Furthermore, ethanol also leads to significant shrinkage of samples, often with taxon-specific shrinkage factors (Cunningham *et al.*, 2000; Joh *et al.*, 2003; Melo *et al.*, 2010). At concentrations above 80-85%, ethanol can preserve otolith crystalline structures (Radtke & Waiwood, 1980; Butler, 1992), but may alter the abundances of elements that bind loosely to the otolith matrix (Proctor & Thresher, 1998).

Alternative preservative methods

Other preservation methods are less commonly used for preserving whole fish specimens but may prove valuable for certain studies and archival programs. ExCell Plus is commonly used for fixing soft tissues for histological, molecular, and fluorescence analysis, with the benefit of being less flammable than ethanol and less toxic than formalin. As a result, ExCell Plus has been proposed as an alternative to formalin for preserving small fishes (Gilbert & Pease, 2019; Hart *et al.*, 2022). Similarly, liquid nitrogen (flash-freezing) is increasingly being used to preserve specimens that are intended to inform state and federal monitoring, management, and conservation programs (Teh *et al.*, 2016). Both preservatives serve as less-toxic alternatives to formalin and non-flammable alternatives to ethanol; thereby increasing safety and reducing costs associated with storage and disposal. Although freezing is commonly used to store fishes, it results in cell lysis, tissue degradation, changes in body morphometrics, and can even affect otolith chemistry (Milton & Chenery, 1998; Proctor & Thresher, 1998). In contrast, flash-freezing in liquid nitrogen can mitigate some of these effects, especially for the preservation of tissues for histological analysis (Teh *et al.*, 2016). Nevertheless, experimental studies are needed to quantify variation in the short-term and long-term effects of liquid nitrogen and ExCell Plus (relative to formalin and ethanol) on body morphometrics, soft tissues, and calcified structures of small pelagic fishes such as Delta Smelt.

Preservative effects on otoliths

Given that otoliths ('ear stones') provide valuable information about the population dynamics, movements, and condition of fish populations (Campana & Thorrold, 2001; Reis-Santos *et al.*, 2022), effective preservation of these calcified structures is key to fisheries management and conservation. Although common practices (e.g., dry storage, ethanol, glycerin) have long been established, few comparative studies have contrasted the effects of various whole-fish preservation methods on the structure and chemical composition of otoliths. In particular, little is known regarding the effects of long-term (> 200 days) preservation (Hedges *et al.*, 2004; Kristoffersen & Salvanes, 1998; Proctor & Thresher, 1998). Furthermore, most studies that have examined preservation effects have focused largely on marine species (Proctor & Thresher, 1998; Rooker *et al.*, 2001) with only a few exceptions (Milton & Chenery, 1998; Greszkiewicz & Fey, 2018). Similarly, many such studies have focused on smaller larval and juvenile life stages rather than adult life stages (Fox, 1996; Fey, 1999; Cunningham *et al.*, 2000; Joh *et al.*, 2003; Hedges *et al.*, 2004).

The San Francisco Estuary

Many fish species are at risk of extinction throughout North America and across the globe (Arthington *et al.*, 2016; Warren & Burr, 1994). In California (USA) alone, seven fish species have gone extinct and another 33 species are at risk of extinction, including several that reside within the San Francisco Estuary (SFE) (Hobbs *et al.*, 2017; Moyle *et al.*, 2011). For example, threatened and endangered species such as Delta Smelt (*Hypomesus transpacificus*) and Longfin Smelt (*Spirinchus thaleichthys*) have declined rapidly in the SFE, likely due to several interacting anthropogenic changes in hydrology, geomorphology, food webs, invasive species, water quality, and the global climate (Hobbs *et al.*, 2017; Mac Nally *et al.*, 2010; Moyle *et al.*, 2018). The Delta Smelt, in particular, is critically endangered, with only a few wild-spawned individuals observed each year, despite extensive monitoring throughout the region (Stompe *et al.*, 2020; Tempel *et al.*, 2021).

The value of archived specimens

For rare and endangered species, like Delta Smelt, archives of specimens and tissues from numerous long-term monitoring programs (Stompe *et al.*, 2020) are highly valuable for facilitating studies of their biology and ecology. For example, the preservation and archival of whole fish in the field has been vital in supporting a variety of scientific studies of organismal health, condition, growth, migration, and reproduction (Hammock *et al.*, 2019; Hobbs *et al.*, 2019; Lewis *et al.*, 2021; Teh *et al.*, 2020), with results informing key ecosystem management and conservation policies. However, significant variation in preservation methods exists among surveys and research groups in the SFE, limiting the integration of archived specimens across surveys and research groups to address key questions in space and time. Furthermore, novel preservation methods (e.g., flash-freezing in liquid nitrogen, preservation in ExCell Plus) are becoming increasingly common, but have yet to be fully evaluated. Therefore, experiments that can inform the selection of optimal preservation methods that facilitate the broadest use and

value of archived specimens are key for supporting a variety of fisheries science and management needs long into the future.

Study objectives

Several aspects of each preservation method should be assessed prior to the adoption of a preferred method. These include the associated costs (acquisition, storage, and disposal), safety (e.g., toxicity and stability), and effects of each preservation method on gross morphology (length, weight, appearance), tissues (e.g., gills, liver, gonads, muscle, bone), and molecules of interest (e.g., DNA, RNA, proteins, and lipids). Although costs and safety can readily be evaluated, comparative experiments are needed to quantify the effects of different preservation methods on key metrics of interest for a given sample archival program. Here, we conducted a comparative experiment to examine the effects of four liquid preservatives (95% ethanol, 10% buffered formalin, 100% ExCell Plus, and liquid nitrogen) on the morphometrics, otolith structure, otolith chemistry, and tissue histology of adult Delta Smelt. Effects were evaluated at multiple time points (1, 4, 24, and 52 weeks) over the course of the one-year study. We expected that these preservatives would affect various metrics and tissues differently and that effects would vary with time. By quantifying and contrasting these patterns, we hope to inform and enhance the value and utility of specimen archives that will be used to inform the science and management needs of future generations.

MATERIAL AND METHODS

Experimental design

The objective of this study was to contrast the effects of different preservation methods on fish morphometrics, tissue histology, and otolith structures and geochemistry. Adult Delta Smelt were reared at the Fish Conservation and Culture Lab (FCCL), Department of Biological and Agricultural Engineering, University of California-Davis, Byron, CA, USA, following established protocols (Lindberg *et al.*, 2013; Tsai *et al.*, 2022). Specimens (n=420) were euthanized with buffered tricaine methanesulfonate (MS-222; dosage: 500 mg/L) and each measured in length to the nearest mm (standard length; SL), blotted-dry, weighed (total weight, TW), imaged, and assigned a unique ID tag. At the start of the experiment (control; week 0), 20 “fresh” (control) individuals were immediately dissected and processed. Of the remaining 400 fish, 300 were placed in individual perforated plastic bags (Whirl-Pak®) and each bag (with its specimen and identification tag) was randomly assigned and placed into one of three 4-L jugs containing either 95% ethanol, 10% buffered formalin, or 100% ExCell Plus. The final 100 fish were wrapped individually in aluminum foil with their identification tags and stored in liquid nitrogen following Teh et al. (2016).

Preserved fish were reanalyzed in the laboratory after being in their respective preservatives for 1, 4, 24, and 52 weeks. Morphometrics were quantified on a total of 320 preserved fish (20 individuals per preservative per time point), with 160 of these also examined for histology (10 individuals per preservative per time point), and 65 of these (5 individuals per preservative for

the 1-, 4-, and 24-wk time points, and 5 wk-0 control) selected for otolith analyses. Otoliths were not examined at week 52 due to the degradation of otoliths in the ExCell Plus treatment. Individual changes in morphometrics were calculated and group differences among time points, treatments, and initial controls, when relevant, were examined for each morphologic, histologic, and otolith-based metric.

Delta Smelt storage, body measurements, and dissections

All 420 specimens were measured for standard length (SL) and total weight (WT) at the start of the experiment. Specimens were rinsed in deionized water, blotted dry, and weight was measured on an analytical balance (to 0.001 g). Each fish and its unique identification label (ID) were then placed on a flat surface with a metric ruler, the body was horizontally aligned, the fins were spread out, and the standard length (to the nearest 1 mm) was recorded. Individual pictures were taken to obtain digital body measurements. To quantify the effects of each preservative and preservation duration on body morphometrics, a total of 20 individual fish from each preservative were measured (SL and WT) and imaged a second time at weeks 1, 4, 24, and 52 (n = 320). Of the 20 control fish and 320 re-measured and re-imaged experimental fish, a total of 170 individuals (10 per preservative per time point + 10 control) were dissected, with the otoliths, gills, liver, and gonads removed and prepared for further analysis.

Histology of soft tissues

Upon dissection, soft tissues (gills, livers, and gonads) were prepared for histological examination. Dissected tissues were prepared for histology by being placed into cassettes, dehydrated using a graded ethanol series, and then embedded in paraffin. Tissue blocks were sectioned at 3µm, stained with Hematoxylin & Eosin (H&E), and a cover slip was applied. Tissues from the liquid nitrogen treatment were prepared similarly to other treatments but were first fixed for 48 hours post-dissection in 10% phosphate-buffered formalin. Thus, at the seven-day timepoint, tissues in liquid nitrogen spent seven days in liquid nitrogen and 2 days in formalin prior to histological preparation. To evaluate variation in tissue quality and fixation-induced artifacts, the quality and integrity of each prepared tissue was qualitatively evaluated with respect to its (1) tissue integrity; (2) H&E fixation quality and color; (3) cellular structure characteristics; and (4) staining quality following (Teh *et al.*, 1997, 2016).

Otoliths

During dissections, the right and left otoliths were removed from the vestibular system in the inner ear of each of the 20 fish from each treatment at 1, 4, 24, and 52 weeks, and from 10 control fish at week 0 (initial). Otoliths were dissected following established procedures (Xieu *et al.*, 2021), then were rinsed in deionized water, and all adherent tissue was then removed. Otoliths were dried for at least 24 hours and stored in clean 0.5 or 1 ml polypropylene microcentrifuge tubes. Otoliths were imaged at 20X magnification using a stereomicroscope, and dorsal-ventral and rostral-postrostral dimensions were quantified from images using ImageJ (v. 1.53k, National Institute of Health). As for histological preparations, otolith images were examined qualitatively to assess variation in structural appearance and integrity.

Of the 170 fish that were dissected, a total of 65 fish were selected for further otolith analysis, including 5 fish per preservative per time point (weeks 1, 4, and 24) and 5 control fish. Otoliths were not prepared from fish at wk-52 due to severe degradation observed in the ExCell Plus treatment. Left otoliths were utilized first, with the right otolith selected only when the left otolith was lost or damaged. Delta Smelt exhibit limited variation between left and right otoliths (Xieu et al. 2021). Selected otoliths were mounted onto glass microscope slides, polished with sandpaper and alumina polish, and imaged at 200X magnification using an Olympus CH30 compound microscope. Polished otoliths were then sonicated for 5 minutes in Milli-Q ultra-pure water to remove impurities and were mounted onto glass petrographic slides for geochemical analysis. A separate, single, whole (unpolished) otolith from each preservative at weeks 1, 4, and 24 was submitted to the UC Berkeley Department of Earth and Planetary Science for imaging on a Zeiss EVO-10 Variable Vacuum Scanning Electron Microscope to examine fine-scale detail in the structural integrity of the otolith surface.

Otolith microchemical analysis

Microchemical analysis of otoliths was conducted in March 2021 at the UC Davis Interdisciplinary Center for Plasma Mass Spectrometry, California, Davis, USA using an Agilent 7700x Quadrupole Inductively Coupled Plasma Mass Spectrometer (LA-ICPMS) attached to a Photon Machines 193nm ArF Excimer laser with a HelEx dual-volume LA cell system. Select minor, trace, and major elements were examined including boron (^{11}B), barium (^{137}Ba), calcium (^{44}Ca and ^{43}Ca), copper (^{63}Cu), lithium (^{7}Li), magnesium (^{24}Mg), manganese (^{55}Mn), sodium (^{137}Ba) strontium (^{86}Sr), and zinc (^{66}Zn). Before collecting data, pre-ablations (10 Hz pulse rate, 100µm spot size, 80µm/s scan speed) were run to remove sample surface contamination. Analysis cycle time was set to 1 second so that all elements were measured every second and concentration was thus reported for each second of analysis. The surface of the otolith was then ablated (10 Hz pulse rate, 40 µm spot size, 5 µm/s scan speed, fluence of ~3 J/cm^2) from ~100µm before the core to the edge of the dorsal lobe, passing through the primordium, thus representing the full life history of each specimen. A 30-s washout occurred before and after each sample to remove residues from previous samples and collect background data. NIST 610 and 612 were monitored throughout the analytical session to facilitate data reduction and assess machine drift.

Data were reduced relative to NIST 612 using Iolite (Paton *et al.*, 2011) and ^{43}Ca as the internal standard using the X_Trace_Element_IS data reduction schema following standard best practices (Jochum *et al.*, 2011; Longerich *et al.*, 1996). Element-specific limits of detection were calculated for each element as 3 times the standard deviation of the element-specific background level, with values below detection being set to zero, indicating negligible abundance given the methodological precision. Assuming that otolith aragonite is 38.8 % Ca by weight (Hüssy *et al.*, 2016), counts of each element were converted to ppm (µg/g), and ppm values were converted into molar values (using each element's atomic mass). Molar values for each element (X_n), were then ratioed to Ca, thus providing element-to-calcium (X_n:Ca) profiles for each element with one value per element for each second of a scan across an otolith. Time (s) was converted to distance (µm) across the otolith using the known laser scan speed (5 µm/s). For statistical comparisons of

preservative effects on otolith chemistry, we averaged the X_n:Ca values for each element over the last 100 µm of each profile, leaving a 40 µm buffer from the edge (1 spot size) to avoid potential edge effects. Thus, each otolith was assigned a single mean edge X_n:Ca value for each element that was used to assess preservative effects on otolith chemistry.

Statistical Analyses

Variation in the preservation of whole fish bodies, histological preparations of gill, liver, and gonad tissues, and whole otoliths was qualitatively described based on digital images of each tissue in each preservative that were collected at each time point. Quantitative assessment of preservation effects on fish morphometrics (length and weight) and individual element-to-calcium ratios (X_n:Ca) were conducted using linear models with preservative, time point, and their interaction (P*T) included as fixed factors. Significance was set using alpha = 0.05, with significant results for preservative indicating variation among preservatives in their effects, for time indicating overall change through time, and the interaction indicating differing effects of each preservative over time. Due to the relatively extreme differences in X_n:Ca values for the ExCell Plus treatment at 24 weeks, otolith chemistry models were re-run while excluding the ExCell Plus treatment to compare variation among the other three preservatives through this time point. All statistical analyses were conducted in R v. 4.6.2 (R Core Team, 2022).

RESULTS

Preservative effects on body condition

Clear differences in the effects of each preservative on the appearance of whole Delta Smelt were apparent after 1 week of preservation, with differences persisting and remaining stable throughout the 52-wk study (Figure 5-1). In particular, ethanol-preserved specimens turned yellow, whereas ExCell Plus and formalin-preserved specimens turned a darker orange color, with a darkening of the eyes. In contrast, specimens fixed in liquid nitrogen showed no discoloration. Overall, characteristics such as eye quality, body shape, melanophores, and lateral line integrity all appeared to be reasonably well-preserved by all four preservatives.

Significant changes in length were observed, with effects varying among preservatives but with similar patterns through time (Table 5-1, Figure 5-2). All preservatives resulted in reduced lengths (shrinkage) of approximately 2-5%, with preservation effects increasing slightly by 1-2% over the duration of the 52-wk study. Specimens fixed in ExCell Plus and formalin exhibited similar shrinkage rates (mean ΔSL = 2-4%) throughout the experiment. Samples preserved in ethanol exhibited the smallest percent shrinkages in body length over the 52-week experiment (mean ΔSL = -1 to -3%). Specimens preserved in liquid nitrogen exhibited the greatest shrinkage rates (mean ΔSL = -4 to -5%) which were also highly variable, particularly at weeks 24 and 52.

Body weight also changed significantly due to preservation, with even greater differences among preservatives, and more variable changes in effects through time (Table 5-1, Figures 5-2 and 5-3). Liquid nitrogen resulted in the smallest effects on total weight (ΔWt. = -2%) with no

measurable change across the 52-wk experiment (Figure 5-2). In contrast, ethanol resulted in the largest loss of weight (ΔWt. = -37% at 1 wk), with effects decreasing with time (ΔWt. = -26% at 52 wk). Similar to ethanol, ExCell Plus also resulted in a substantial loss in weight (ΔWt. = -19%); however, with no variation across time points. Formalin was the only preservative to result in increased total weight, with mean weights increasing progressively from week 1 (ΔWt. = +3%) to week 52 wks (ΔWt. = +10%).

Preservative effects on otolith structure

High-resolution scanning electron microscopy (SEM) of the surface topography of otoliths indicated that otoliths preserved in liquid nitrogen and ethanol retained their structure throughout the study, with only a few surface cracks present at 1, 4, and 24 weeks (Figure 5-4). In contrast, otoliths preserved in formalin and ExCell Plus exhibited severely etched and eroded surface topography. At week 1, otoliths in formalin and ExCell Plus developed hundreds of small fractures across the entire surface of each otolith. At week 4, otoliths in formalin and ExCell Plus became highly brittle, cracking and disintegrating upon dissection and handling. After 24 weeks, otoliths fixed in ExCell Plus were reduced to soft, amorphic objects due to the erosion of the calcified structure. As a result, otolith structure and geochemical comparisons were limited to weeks 1, 4, and 24 (excluding week 52).

Preservative effects on otolith chemistry

Although a total of 65 fish were selected and prepared for otolith chemistry, one fish from the week 1 time point for liquid nitrogen and one fish from the week 0 control were excluded because the otolith broke during processing, resulting in a total of 63 geochemical profiles in the final dataset. Due to the demineralization of otoliths by ExCell Plus, element abundance estimates differed wildly in the week-24 ExCell Plus treatment from all other preservatives and time points (Table 5-2, Figure 5-5). These values were extreme outliers with unreasonable values, likely due to the violation of assumptions pertaining to the calcium content of the otoliths. With the ExCell Plus treatment excluded, results indicated limited differences in the effects of ethanol, formalin, or liquid nitrogen on otolith chemistry (Table 5-3, Figure 5-6). Only Na:Ca values appeared to differ among preservatives, with Na:Ca values in formalin-preserved otoliths being significantly lower than those from other treatments. Significant variation through time was observed for B, Mg, Mn, and Na, but not for Ba, Cu, Sr, or Zn (Table 5-3, Figure 5-6). The most commonly analyzed elements in otoliths (Sr and Ba) exhibited the least variation, with no significant differences in elemental ratios among preservatives or time points. In contrast, rarer elements (e.g., Mg, Mn, Li) exhibited higher degrees of temporal variation. For example, B:Ca increased with time for all treatments, Mg:Ca and Mn:Ca values increased at 24 weeks, and Li:Ca values declined at week 4 for all preservatives, but remained similar across all other time points, including the week-0 controls.

Histology of soft tissues

Preservation/fixation of Delta Smelt soft tissues in ethanol, ExCell Plus, formalin, or liquid nitrogen-formalin was adequate for the histological identification of each organ; however, the

quality of histological preparations for examining finer-scale cellular features varied greatly among treatments. Ethanol fixation was particularly inadequate for assessing the condition of gills and ovaries. For example, severe tissue separation between epithelial and pillar cells was observed in ethanol-preserved gills, which is indicative of edema (i.e., the accumulation of fluid due to cell damage) (Figure 5-7G1). Furthermore, ethanol resulted in inadequate fixation of the nucleus and cytoplasm contents of immature oocytes in Delta Smelt ovaries (Figure 5-7.O1). ExCell Plus fixation was also inadequate for gill tissue due to subsequent tissue separation (Figure 5-7G2). Importantly, tissues preserved/fixed in ExCell Plus were stained a more bluish color than the other three fixatives, indicating more cytoplasmic basophilia. This loss of cytoplasmic eosinophilia (pink coloration) may suggest the loss of cytoplasmic proteins and cellular matrix which usually stain more pinkish with eosin dye. This characteristic was especially evident in gill, liver, and ovary tissues (Figures 5-7G2, L2, and O2) as was reduced cytoplasmic detail, resulting in difficulty differentiating cell types when compared to the other preservatives. Freezing artifacts due to liquid nitrogen preservation were characteristic of this preservation method (Figure 5-7.T4); however, these artifacts were minor and did not limit the histological assessment of tissues. Preservation in liquid nitrogen followed by fixation in formalin yielded adequate histological tissue preparations that were similar to formalin preserved-fixed tissues. Despite minor freezing artifacts, liquid nitrogen appeared to facilitate histologic identification and exploration of structural status for multiple tissues, without impacting the analyst's interpretations.

DISCUSSION

Summary of main findings

Properly preserved archives of historical samples are central to providing new information regarding the biology and ecology of this species, with soft tissues providing important information regarding fish health and condition (Hammock *et al.*, 2019, 2020; Teh *et al.*, 2020); whereas preserved calcified structures (e.g., otoliths) provide key information regarding patterns in age structure, phenology, and growth (Lewis *et al.*, 2021; Xieu *et al.*, 2021), as well as patterns in habitat use and migratory life histories (Hobbs *et al.*, 2010, 2019). However, different preservation methods may be only suitable or preferred for specific scientific applications. For endangered species, like Delta Smelt, the optimal preservation method is that which facilitates the broadest use of specimens across a variety of scientific studies.

Here, we examined the long-term (up to 52 weeks) effects of 95% ethanol, 100% ExCell Plus, 10% buffered formalin, and liquid nitrogen on Delta Smelt morphometrics, soft tissues, and otoliths. All preservatives resulted in 2-5% shrinkage in standard length, with shrinking increasing slightly over time. In contrast, changes in weight varied dramatically among preservatives, with liquid nitrogen having the smallest (~5% loss) and most stable effect. In contrast, ethanol preservation resulted in up to a 40% loss in mass with diminishing effects over time, ExCell Plus up to an 18% loss in mass with no change over time, and formalin up to a 10% gain in mass with increasing effects over time. Histological examination of gill, liver, and gonad tissues indicated that formalin and liquid nitrogen-formalin preservation yielded the highest

quality tissue preparations. Both formalin and ExCell Plus were corrosive to otoliths, whereas ethanol and liquid nitrogen appeared to preserve the integrity of otolith structures. Dissolution due to ExCell Plus resulted in unstable and unreliable otolith microchemistry, whereas formalin, ethanol, and liquid nitrogen exhibited limited overall effects on otolith microchemistry. While each preservative has a unique suite of strengths and weaknesses, our results highlight the value of liquid nitrogen preservation for maximizing the value of archived fish specimens for the broadest use in scientific investigations.

Preservative effects on body length

Each of the preservatives resulted in reduced Delta Smelt lengths (shrinkage) by 2-5%, with shrinkage effects increasing slightly with duration over the 52-week study. Shrinkage in ExCell Plus and formalin were similar at approximately -3%, matching reductions observed in other formalin-preserved osmerid smelts, including 5% in larval Capelin *Mallotus villosus* (Kruse & Dalley, 1990) and ~ 5 to 7% in larval Ayu *Plecoglossus altivelis* (Takizawa *et al.*, 1994). Delta Smelt reductions in body length were also consistent with other small pelagic fishes (SPFs), such as 3.2% shrinkage rates in Inland Silverside *Menidia beryllina* (Cunningham *et al.*, 2000), and 2 to 7% in Pacific Herring *Clupea harengus pallasi* (Hay, 1982). Few studies examined shrinkage rates in later life stages for SPFs, observing shrinkage rates of ~ 3% in the adults of northern anchovy *Engraulis mordax* preserved in 10% formalin for one year (Blaxter & Hunter, 1982) and 7.1% in the juveniles of Round Sardinella, *Sardinella aurita,* preserved in 10% formalin for two days (Ajah & Nunoo, 2003). We found that ethanol preserved body lengths slightly better than formalin; however, several prior studies indicate higher shrinkage rates in ethanol-preserved specimens than in formalin-preserved specimens. Flash-frozen Delta Smelt showed the most variable shrinkage rates (up to ~ 9%) by weeks 24 and 52. These results are different from the Osmeriform Eulachon, *Thaleichthys pacificus*, in which the authors (Buchheister & Wilson, 2005) observed minor length loss of only ~ 1.4% in frozen-preserved specimens. These shrinkage rates are also considerably larger and more variable than those reported in Teh et al. (2016), in which fork length declined by 0.55% for Delta Smelt preserved in liquid nitrogen for 10 days. Of note, more variable effects of liquid nitrogen on body length measurements of frozen Delta Smelt might reflect measurement inaccuracies due to body deformation and incomplete thawing that can affect the accuracy of length measurements.

Preservative effects on body weight

Delta Smelt body weights were considerably reduced in ethanol (mean ΔWt. = -33%), with differences decreasing with the duration of preservation (ΔWt. ~ 26% at 52 weeks), suggesting a stabilization effect. Similarly, (Kristoffersen & Salvanes, 1998) observed mean ΔWt. changes of approximately -40% in both Mueller's pearlside, *Maurolicus muelleri,* and Glacier Lantern Fish, *Benthosema glaciale* that were preserved in ethanol. This loss in mass associated with ethanol preservation is likely due to tissue dehydration caused by ethanol, with weight loss associated with reductions in tissue water content. The decreasing effect of ethanol preservation on weight over time suggests that changes (e.g., the breakdown of lipid membranes) may occur that result in partial rehydration of body tissues.

ExCell Plus also reduced the total weight of Delta Smelt considerably (mean ΔWt. = -18%) but was stable over time. Although ExCell Plus and formalin are both aldehyde-based, they exerted very different effects on body mass. For example, in contrast to ethanol, formalin increased body weight, with effects increasing over time (mean ΔWt. = +10.03% at wk 52). Increased total weight in formalin-preserved specimens is commonly detected in freshwater and diadromous species, including increases of ~ 5 to12% in salmon *Oncorhynchus sp.* (Parker, 1963), 13.9% in Bluegill *Lepomis macrochirus* and 14.88% in White Crappie *Pomoxis annularis* (Yeh & Hodson, 1975), 5.3% in White Bass *Morone chrysops* (Sigler, 1949), and between 3.8 and 9.4% in yellow perch *Perca flavescens* (Stobo, 1972), thus bracketing the range of values observed here for Delta Smelt. The differences between ExCell Plus and formalin are likely due to the additional constituents in ExCell Plus (which also contains ethanol). In aggregate, these results emphasize the need for caution when contrasting estimates of body condition (e.g., Fulton's K) among fish from different preservatives, or even using the same preservatives but for different durations. Although some variation in length was observed, the greatest inter- and intra-preservative variation was observed in total weight, with significant preservative-specific and time-specific variation that could greatly alter the interpretation of condition metrics.

Unlike the other fixatives, liquid nitrogen had a small and stable effect on total weight of Delta Smelt throughout the duration of the experiment. This result was similar to the minor loss in total weight (mean ΔWt. = -1.1%) in Eulachon specimens that were frozen for up to 120 days (Buchheister & Wilson, 2005) and in Delta Smelt (mean ΔWt. = -0.21%) that were preserved in liquid nitrogen for ten days (Teh *et al.*, 2016). Freezing also had the least effect on percent weight changes of Central Stoneroller, *Campostoma anomalum,* compared to specimens preserved in isopropanol, ethanol, and 10% formalin (Distefano *et al.*, 1994). This differs from (Distefano *et al.*, 1994; Kristoffersen & Salvanes, 1998), who observed variable weight losses of 6 to 22%, and 9.65% in Glacier Lantern fish and the Central Stoneroller that were frozen for approximately 180-200 days, respectively. These differences suggest that frozen freshwater species might lose less weight than frozen marine ones, but future studies should be conducted to examine freezing effects by fish habitat.

Preservative effects on otolith structure

Preservatives can be corrosive to otoliths and other calcified structures, particularly when solutions are unbuffered and become acidic (Brothers, 1987; Butler, 1992; Kristoffersen & Salvanes, 1998). Here we observed severe degradation in the small otoliths (< 2mm in diameter) of adult Delta Smelt preserved in 10% buffered formalin or 100% ExCell Plus, but not in 95% ethanol. Formalin is known to dissolve a variety of naturally occurring groups of molecules, including glycogen, glucose, phospholipids, and inorganic salts (Steedman, 1976). For otoliths, formalin can cause etching, pitting, cracking, and dissolution of calcified structures. As a result, formalin is commonly buffered to reduce its corrosive properties; however, as observed in this study, buffering may not be sufficient to prevent all otolith degradation.

Ethanol is known to dissolve lipids but has limited effects on calcified structures (Glauert, 1974). In the present study, otoliths that were preserved in 95% ethanol or liquid nitrogen appeared

similar in structure and form to the control otoliths (stored dry), even after 6 months post-preservation. Although ethanol does not typically harm otolith structures directly, dilute (< 80%) ethanol mixtures (e.g., due to intentional dilution, large volumes of preserved organisms, or evaporation) can cause ethanol solutions to become acidic and degrade otolith structures. Smaller otoliths are more sensitive to such corrosion than larger otoliths, with larval otoliths (e.g., 0.1 mm in diameter) being the most sensitive due to their delicate structure and high surface area to volume ratios. Thus, higher concentrations (e.g., 95%) of ethanol, as used in this study, appear highly effective for otolith preservation.

To our knowledge, the effects of ExCell Plus on otoliths have not previously been tested. However, glyoxal, a dialdehyde, is a primary constituent (~25% by volume) that, like formaldehyde, can generate acidic aqueous solutions (O'Neil, 2001). The rapid degradation of otoliths from fish preserved in ExCell Plus confirms that ExCell Plus is highly corrosive to calcified structures. Studies are needed to examine whether buffered ExCell Plus solutions can preserve the benefits of ExCell Plus as a fish preservative while sufficiently reducing its corrosive properties.

Preservative effects on otolith chemistry

Preservatives are likely to exert different effects on the chemistry of otoliths, with effects varying among different element constituents. Within the otolith endolymph (growth medium), for example, 12 elements are present only in the proteinaceous fraction, 6 in the salt fraction, and 4 in both the proteinaceous and salt fractions (Thomas *et al.*, 2017). Thus, some elements (e.g., Ba, Sr) are more strongly bonded within the calcium carbonate matrix, whereas other elements (e.g., Mg, Zn) are weakly bonded and occur primarily within the protein-rich zones of otoliths (Sturrock *et al.*, 2012), where proteins comprise approximately ~ 3-10% of total otolith mass (Campana, 1999; Dauphin & Dufour, 2003). Therefore, preservation effects may vary among elements with respect to the ways in which they are incorporated and bonded within the otolith matrix.

Here, we observed limited effects of ethanol, buffered formalin, and liquid nitrogen preservation on the elemental chemistry of otoliths (except for Na:Ca values), indicating that otolith chemistry is broadly resistant to preservation effects for up to 6 months for these preservatives. After 4 weeks of preservation in ExCell Plus, however, otoliths started to exhibit markedly different elemental ratios from other preservatives, suggesting that even elements strongly bound to the salt fraction of otoliths (i.e., Li, Mn, and Mg) were affected by this fixative. At 24 weeks, ExCell Plus greatly increased the estimated elemental ratios for all elements far beyond normal values, except for Sr which was reduced (Figure 5-5). Although the mechanism behind these patterns was not tested experimentally, it is likely related to the corrosive properties identified by the SEM images of the otolith surface, with the dissolution of the $CaCO_3$ matrix resulting in unreliable abundance estimates for all element examined in the ExCell Plus treatment.

Exclusive of the corrosion observed due to ExCell Plus, limited preservative effects were observed on the otoliths of Delta Smelt (Figure 5-6), with only Na:Ca values varying (with lower values in the formalin treatment). These results suggest that preservation in formalin, ethanol,

and liquid nitrogen largely conserved the chemistry of otoliths for up to 6 months. Similar results have been observed in prior studies, particularly for Sr:Ca and Na:Ca values. For example, otoliths of juvenile Jackass Morwong, *Nemadactylus macropterus,* exhibited stable patterns for Sr:Ca and Ba:Ca values over time and among fish persevered in ethanol, formalin, or with freezing; whereas Na:Ca values differed among preservative treatments (Proctor & Thresher, 1998). Similarly, otolith Sr:Ca values in marine fishes appear to be unaffected by preservation method; whereas variable patterns in Na:Ca values were attributed to its loosely bound nature within the otolith matrix (Milton & Chenery, 1998; Proctor & Thresher, 1998). In freshwater Walleye, *Stizostedion vitreum*, Sr:Ca and Ba:Ca values in otoliths were also relatively stable and unaffected by preservation in ethanol (Hedges *et al.*, 2004).

Thus ethanol, formalin, and liquid nitrogen all appeared to satisfactorily preserve the elemental chemistry of Delta Smelt otoliths for up to 6 months, exclusive of Na which should likely be excluded from future microchemical analyses of otoliths. The limited effects of formalin were surprising given its effects on otolith structure; however, this is likely because it was buffered, thus reducing the rate of degradation and limiting the effects on otolith chemistry. Although variation among preservatives was rare, significant variation among time points was observed for 5 of the elements (B, Li, Mg, Mn, Na). For example, B:Ca values consistently increased with time for all fixatives. Similarly, Na:Ca values increased with time, except for the formalin treatment (the only significant preservative effect on chemistry in the study). For Li, values for all preservatives were lower at week 4 than all other time points. For Mn, values at week 24 were higher than for all other time points. Most of these elements exhibit weak bonds, are in the proteinaceous fraction of the otolith matrix, or were at very low concentrations; therefore, we believe this temporal variation was indicative of analytical sensitivity and variation that was independent of fixative effects. For example, temporal patterns were similar among preservatives, with no significant preservation x time (P*T) interactions, thus indicating that temporal patterns were not preservative-specific (except for Na:Ca values in formalin).

Fixative effects on tissue histology

As previously observed, formalin provided excellent fixation and preservation of cellular structures in soft tissues of Delta Smelt for histological examination, with prior freezing in liquid nitrogen, followed by formalin fixation, also providing comparable tissue preparations (Teh *et al.*, 2016). For shorter periods (~one month or less), formalin preservation performed best; however, for periods longer than one month, liquid nitrogen preservation yielded similar or superior histological results than formalin preservation. In contrast, ethanol led to cellular damage, degradation of oocytes, and edema which made it a poor preservative and fixative for histological studies. Although ExCell Plus is marketed as an effective alternative to formalin for soft tissue preservation and fixation, we found that ExCell Plus resulted in abnormal effects on cytoplasmic proteins and the cellular matrix of gills, liver, and gonads, resulting in poorer preparations for histological examination. Thus, for whole Delta Smelt, preservation in formalin and liquid nitrogen yielded the best results for histological examination of soft tissues.

Conclusions

Comparative experiments, like the present study, are excellent for addressing the tradeoffs among different preservation methods. For formalin, the corrosive effects on calcified structures and toxic nature of formaldehyde rendered it suboptimal for whole-fish preservation. Similarly, the flammable nature and negative effects of ethanol on histology resulted in it being deemed suboptimal for whole fish preservation. Although ExCell Plus can yield somewhat suitable tissue fixation with lower health risks, histological preps were inferior to liquid nitrogen and formalin, and the highly corrosive degradation that it caused to calcified structures (i.e., otoliths) rendered it unsuitable as a preservative for archiving whole Delta Smelt. In contrast, liquid nitrogen effectively preserved both soft tissues (for histological analysis) and calcified structures (for structural and geochemical analysis), while limiting the duration of formalin exposure and total volume required to only the 2-day fixation process for individual tissues, respectively. The primary limitation of liquid nitrogen preservation is the access and storage of liquid nitrogen (in dewars) itself, which can have high labor and supply costs, especially for larger-bodied fish. Ultimately, the most suitable preservation for a given program would consider each of these tradeoffs carefully. For endangered Delta Smelt in the San Francisco Estuary, our results indicate that liquid nitrogen preservation is feasible, effective, and maximizes the scientific value and utility of each specimen to better inform fisheries management and conservation.

ACKNOWLEDGEMENTS

We thank the many staff at the UC Davis Fish Conservation and Culture Laboratory for their expertise and efforts in culturing and rearing Delta Smelt. Furthermore, we acknowledge the many staff and student researchers at the UC Davis Department of Wildlife, Fish, and Conservation Biology, School of Veterinary Medicine, and Center for Aquatic Biology and Aquaculture for laboratory and logistical support in conducting the study and processing samples. Scanning electron microscopy was conducted by John Grimsich at the UC Berkeley Dept. of Earth and Planetary Sciences. This study was funded by the U.S. Bureau of Reclamation Directed Outflow Project (Grant Nos. R17AC00129 and R22AC00392) to Bruce G. Hammock, L. Lewis, J. Hobbs, and S. Teh. The views expressed herein are those of the authors and do not represent the official opinion of any employer, institution, or government agency.

REFERENCES

Ajah, P. O., & Nunoo, F. K. E. (2003). The effects of four preservation methods on length, weight and condition factor of the clupeid Sardinella aurita Val. 1847. *Journal of Applied Ichthyology*, *19*, 391–393.

Arthington, A. H., Dulvy, N. K., Gladstone, W., & Winfield, I. J. (2016). Fish conservation in freshwater and marine realms: status, threats and management. *Aquatic Conservation: Marine and Freshwater Ecosystems*, *26*, 838–857.

Baldwin, C. C., & Johnson, G. D. (2014). Connectivity across the Caribbean Sea: DNA barcoding and morphology unite an enigmatic fish larva from the Florida Straits with a new species of sea bass from deep reefs off Curaçao. *PloS one*, *9*, e97661.

Blackwell, M., Kang, H., Thomas, A., & Infante, P. (1981). Formaldehyde: evidence of carcinogenicity. *American Industrial Hygiene Association Journal*, *42*, A34.

Blaxter, J. H. S., & Hunter, J. R. (1982). The Biology of the Clupeoid Fishes. *Advances in Marine Biology* (pp. 1–223). Elsevier.

Brothers, E. B. (1987). Methodological approaches to the examination of otoliths in aging studies. *The age and growth of fish*, 319–330.

Buchheister, A., & Wilson, M. T. (2005). Shrinkage correction and length conversion equations for Theragra chalcogramma, Mallotus villosus and Thaleichthys pacificus. *Journal of Fish Biology*, *67*, 541–548.

Butler, J. L. (1992). Collection and preservation of material for otolith analysis. *Otolith microstructure examination and analysis. Can. Spec. Publ. Fish. Aquat. Sci*, *117*, 13–17.

Campana, S. (1999). Chemistry and composition of fish otoliths:pathways, mechanisms and applications. *Marine Ecology Progress Series*, *188*, 263–297.

Campana, S. E., & Thorrold, S. R. (2001). Otoliths, increments, and elements: keys to a comprehensive understanding of fish populations? *Canadian Journal of Fisheries and Aquatic Sciences*, *58*.

Cunningham, M. K., Granberry, W. F., & Pope, K. L. (2000). Shrinkage of Inland Silverside Larvae Preserved in Ethanol and Formalin. *North American Journal of Fisheries Management*, *20*, 816–818.

Dauphin, Y., & Dufour, E. (2003). Composition and properties of the soluble organic matrix of the otolith of a marine fish: Gadus morhua Linne, 1758 (Teleostei, Gadidae). *Comparative Biochemistry and Physiology Part A: Molecular & Integrative Physiology*, *134*, 551–561.

Distefano, R. J., Roell, M. J., Wagner, B. A., & Decoske, J. J. (1994). Relative Performances of Four Preservatives on Fish and Crayfish. *Transactions of the American Fisheries Society*, *123*, 817–823.

Duckworth, W. D., Genoways, H. H., & Rose, C. L. (1993). Preserving natural science collections: chronicle of our environmental heritage.

Fey, D. P. (1999). Effects of preservation technique on the length of larval fish: methods of correcting estimates and their implication for studying growth rates. *Archive of Fishery and Marine Research*, *47*, 17–29.

Fowler, G. M., & Smith, S. J. (1983). Length Changes in Silver Hake (Merluccius bilinearis) Larvae: Effects of Formalin, Ethanol, and Freezing. *Canadian Journal of Fisheries and Aquatic Sciences*, *40*, 866–870.

Fox, C. J. (1996). Length changes in herring (Clupea harengus) larvae: effects of capture and storage in formaldehyde and alcohol. *Journal of Plankton Research*, *18*, 483–493.

Gilbert, M. D., & Pease, A. A. (2019). Use of fragmented reservoir habitats by larval fish assemblages across years with contrasting hydrological conditions. *Environmental Biology of Fishes*, *102*, 857–871.

Glauert, A. M. (1974). Fixatives. *Practical methods in electron microscopy*, *3*, 5–48.

Graham, C., Ferrier, S., Huettman, F., Moritz, C., & Peterson, A. (2004). New developments in museum-based informatics and applications in biodiversity analysis. *Trends in Ecology & Evolution*, *19*, 497–503.

Greszkiewicz, M., & Fey, D. P. (2018). Effect of preservation in formalin and alcohol on the growth rate estimates of larval northern pike. *North American Journal of Fisheries Management*, *38*, 601–605.

Hammock, B. G., Hartman, R., Slater, S. B., Hennessy, A., & Teh, S. J. (2019). Tidal Wetlands Associated with Foraging Success of Delta Smelt. *Estuaries and Coasts*, *42*, 857–867.

Hammock, B. G., Ramírez-Duarte, W. F., Triana Garcia, P. A., Schultz, A. A., Avendano, L. I., Hung, T.-C., … Teh, S. J. (2020). The health and condition responses of Delta Smelt to fasting: A time series experiment. *PLOS ONE*, *15*, e0239358.

Hart, C., Goodman, A., Tobias, V., Gilbert, M., & Starks, H. (2022). ExCell Plus as a Substitute for Formalin: Decomposition Rates and DNA Extraction of Larval Stage Delta Smelt (Hypomesus transpacificus) https://www.usbr.gov/mp/TFFIP/docs/study-plan/tffip-fy22-proposal-package-final-508.pdf (accessed Feb 9, 2023).

Hay, D. E. (1982). Fixation Shrinkage of Herring Larvae: Effects of Salinity, Formalin Concentration, and Other Factors. *Canadian Journal of Fisheries and Aquatic Sciences*, *39*, 1138–1143.

Hedges, K. J., Ludsin, S. A., & Fryer, B. J. (2004). Effects of ethanol preservation on otolith microchemistry. *Journal of Fish Biology*, *64*, 923–937.

Hobbs, J. A., Lewis, L. S., Ikemiyagi, N., Sommer, T., & Baxter, R. D. (2010). The use of otolith strontium isotopes (87Sr/86Sr) to identify nursery habitat for a threatened estuarine fish. *Environmental Biology of Fishes*, *89*, 557–569.

Hobbs, J. A., Lewis, L. S., Willmes, M., Denney, C., & Bush, E. (2019). Complex life histories discovered in a critically endangered fish. *Scientific Reports*, *9*, 16772.

Hobbs, J. A., Moyle, P. B., Fangue, N., & Connon, R. E. (2017). Is Extinction Inevitable for Delta Smelt and Longfin Smelt? An Opinion and Recommendations for Recovery. *San Francisco Estuary and Watershed Science*, *15*, 1–19.

Hüssy, K., Gröger, J., Heidemann, F., Hinrichsen, H.-H., & Marohn, L. (2016). Slave to the rhythm: seasonal signals in otolith microchemistry reveal age of eastern Baltic cod (Gadus morhua). *ICES Journal of Marine Science: Journal du Conseil*, *73*, 1019–1032.

Jawad, L. A. (2003). The effect of formalin, alcohol and freezing on some body proportions of Alepes djeddaba (Pisces: Carangidae) collected from the Red Sea coast of Yemen. *Revista de Biología Marina y Oceanografía*, *38*, 5.

Jochum, K. P., Weis, U., Stoll, B., Kuzmin, D., Yang, Q., Raczek, I., … Enzweiler, J. (2011). Determination of reference values for NIST SRM 610-617 glasses following ISO guidelines. *Geostandards and Geoanalytical Research*, *35*, 397–429.

Joh, M., Takatsum, T., Nakaya, M., Imura, K., & Higashitani, T. (2003). Larvae Preserved in Formalin and in Ethanol Solutions. *Aquaculture Science*, *51*, 227–228.

Kristoffersen, J. B., & Salvanes, A. G. V. (1998). Effects of formaldehyde and ethanol preservation on body and otoliths of *Maurolicus muelleri* and *Benthosema glaciale*. *Sarsia*, *83*, 95–102.

Kruse, G. H., & Dalley, E. L. (1990). Length changes in capelin, Mallotus villosm (Muller), larvae due to preservation in formalin and anhydrous alcohol. *Journal of Fish Biology*, *36*, 619–621.

Lewis, L., Denney, C., Willmes, M., Xieu, W., Fichman, R., Zhao, F., … Hobbs, J. (2021). Otolith-based approaches indicate strong effects of environmental variation on growth of a Critically Endangered estuarine fish. *Marine Ecology Progress Series*, *676*, 37–56.

Lindberg, J. C., Tigan, G., Ellison, L., Rettinghouse, T., Nagel, M. M., & Fisch, K. M. (2013). Aquaculture Methods for a Genetically Managed Population of Endangered Delta Smelt. *North American Journal of Aquaculture*, *75*, 186–196.

Longerich, H. P., Jackson, S. E., & Günther, D. (1996). Laser ablation inductively coupled plasma mass spectrometric transient signal data acquisition and analyte concentration calculation. *Journal of Analytical Atomic Spectrometry*, *11*, 899–904.

Mac Nally, R., Thomson, J. R., Kimmerer, W. J., Feyrer, F., Newman, K. B., Sih, A., … Castillo, G. (2010). Analysis of pelagic species decline in the upper San Francisco Estuary using multivariate autoregressive modeling (MAR). *Ecological Applications*, *20*, 1417–1430.

Melo, M. T., Saturnino, C., Santos, J. N. S., Vasconcellos, R. M., Cruz-Filho, A. G., & Araújo, F. G. (2010). Correction of the weight and length for juveniles Atherinella brasiliensis (Actinopterygii: Atherinopsidae) after fixation in formalin and preservation in ethanol. *Zoologia (Curitiba)*, *27*, 892–896.

Milton, D. A., & Chenery, S. R. (1998). The effect of otolith storage methods on the concentrations of elements detected by laser-ablation ICPMS. *Journal of Fish Biology*, *53*, 785–794.

Moyle, P. B., Hobbs, J. A., & Durand, J. R. (2018). Delta Smelt and Water Politics in California. *Fisheries*, *43*, 42–50.

Moyle, P. B., Katz, J. V. E., & Quiñones, R. M. (2011). Rapid decline of California's native inland fishes: A status assessment. *Biological Conservation*, *144*, 2414–2423.

Nielsen, E. E., & Hansen, M. M. (2008). Waking the dead: the value of population genetic analyses of historical samples. *Fish and Fisheries*, *9*, 450–461.

Nordeide, J. T. (2020). Accuracy of body mass estimates of formalin-preserved fish – a review. *Journal of Fish Biology*, *96*, 288–296.

Nyuji, M., Yoneda, M., Nakamura, M., Watai, M., Yasuda, T., & Takasuka, A. (2022). Effects of formalin preservation on egg size of small pelagic fish as major target species in ichthyoplankton surveys. *Aquaculture, Fish and Fisheries*, *2*, 208–215.

O'Neil, M. J. (2001). *The Merck Index - An Encyclopedia of Chemicals, Drugs, and Biologicals*, 13th ed. Whitehouse Station, NJ803: Merck and Co., Inc.

Parker, R. R. (1963). Effects of formalin on length and weight of fishes. *Journal of the Fisheries Board of Canada*, *20*, 1441–1455.

Paton, C., Hellstrom, J., Paul, B., Woodhead, J., & Hergt, J. (2011). Iolite: Freeware for the visualisation and processing of mass spectrometric data. *Journal of Analytical Atomic Spectrometry*, *26*, 2508.

Proctor, C. H., & Thresher, R. E. (1998). Effects of specimen handling and otolith preparation on concentration of elements in fish otoliths. *Marine Biology*, *131*, 681–694.

R Core Team. (2022). R: A Language and Environment for Statistical Computing, 2022.

Radtke, R. L., & Waiwood, K. G. (1980). Otolith formation and body shrinkage due to fixation in larval cod (Gadus morhua). *Canadian Technical Report of Fisheries and Aquatic Sciences*, *929*, 15.

Reis-Santos, P., Gillanders, B. M., Sturrock, A. M., Izzo, C., Oxman, D. S., Lueders-Dumont, J. A., … Walther, B. D. (2022). Reading the biomineralized book of life: expanding otolith biogeochemical research and applications for fisheries and ecosystem-based management. *Reviews in Fish Biology and Fisheries*.

Rooker, J. R., Zdanowicz, V. S., & Secor, D. H. (2001). Chemistry of tuna otoliths: assessment of base composition and postmortem handling effects. *Marine Biology*, *139*, 35–43.

Schander, C., & Kenneth, H. M. (2003). DNA, PCR and formalinized animal tissue–a short review and protocols. *Organisms Diversity & Evolution*, *3*, 195–205.

Sigler, W. F. (1949). *Life history of the white bass, Lepibema chrysops (Rafinesque), of Spirit Lake, Iowa*. Agricultural Experiment Station, Iowa State College of Agriculture and …. Vol. 366.

Steedman, H. F. (1976). General and applied data on formaldehyde fixation and preservation of marine zooplankton. *Zooplankton fixation and priservation. Monographs on oceanographic methodology. The Unesco Press*, *4*, 103–154.

Stobo, W. T. (1972). Effects of formalin on the length and weight of yellow perch. *Transactions of the American Fisheries Society*, *101*, 362–364.

Stompe, D., Moyle, P., Kruger, A., & Durand, J. (2020). Comparing and Integrating Fish Surveys in the San Francisco Estuary: Why Diverse Long-Term Monitoring Programs are Important. *San Francisco Estuary and Watershed Science*, *18*.

Storm-Suke, A., Dempson, J. B., Caron, F., & Power, M. (2007). Effects of formalin and ethanol preservation on otolith δ18O stable isotope signatures. *Rapid Communications in Mass Spectrometry*, *21*, 503–508.

Sturrock, A. M., Trueman, C. N., Darnaude, A. M., & Hunter, E. (2012). Can otolith elemental chemistry retrospectively track migrations in fully marine fishes? *Journal of Fish Biology*, *81*, 766–795.

Takizawa, K., Fujita, Y., Ogushi, Y., & Matsuno, S. (1994). Relative change in body length and weight in several fish larvae due to formalin fixation and preservation. *Fisheries science*, *60*, 355–359.

Teh, S. J., Schultz, A. A., Duarte, W. R., Acuna, S., Barnard, D. M., Baxter, R. D., … Hammock, B. G. (2020). Histopathological assessment of seven year-classes of Delta Smelt. *SCIENCE OF THE TOTAL ENVIRONMENT*, *726*.

Teh, S. J., Adams, S. M., & Hinton, D. E. (1997). Histopathologic biomarkers in feral freshwater fish populations exposed to different types of contaminant stress. *Aquatic toxicology*, *37*, 51–70.

Teh, S. J., Baxa, D. V., Hammock, B. G., Gandhi, S. A., & Kurobe, T. (2016). A novel and versatile flash-freezing approach for evaluating the health of Delta Smelt. *Aquatic Toxicology*, *170*, 152–161.

Tempel, T. L., Malinich, T. D., Burns, J., Barros, A., Burdi, C. E., & Hobbs, J. A. (2021). The value of long-term monitoring of the San Francisco Estuary for Delta Smelt and Longfin Smelt. *California Fish and Wildlife Journal*, 148–171.

Thomas, O. R. B., Ganio, K., Roberts, B. R., & Swearer, S. E. (2017). Trace element–protein interactions in endolymph from the inner ear of fish: implications for environmental reconstructions using fish otolith chemistry. *Metallomics*, *9*, 239–249.

Tsai, Y.-J. J., Ellison, L., Stevenson, T., Mulvaney, W. J., Carson, E. W., & Hung, T.-C. (2022). Evaluating the Performance of a Small-Scale Culture System for Delta Smelt. *North American Journal of Aquaculture*, *84*, 370–380.

Warren, M. L., & Burr, B. M. (1994). Status of Freshwater Fishes of the United States: Overview of an Imperiled Fauna. *Fisheries*, *19*, 6–18.

Xieu, W., Lewis, L. S., Zhao, F., Fichman, R. A., Willmes, M., Hung, T.-C., … Hobbs, J. A. (2021). Experimental validation of otolith-based age and growth reconstructions across multiple life stages of a critically endangered estuarine fish. *PeerJ*, *9*, e12280.

Yeh, C. F., & Hodson, R. G. (1975). Effects of Formalin on Length and Weight of Bluegill and White Crappie from Lake Nasworthy, Texas. *The Southwestern Naturalist*, *20*, 315–321.

TABLES

Table 5-1: Results of linear models examining the effects of preservative, duration, and their interaction (P*T) on standard length (SL) and total body weight (TW).

Bold values indicate $p < 0.05$. DF = degrees of freedom, SS = sum of squared errors, MS = mean squared error, F = f-ratio, P_1 = term p-value, P_2 = model p-value, R^2 = model R^2.

Model	Factor	DF	SS	MS	F	P_1	P_2	R^2
SL	Preservative	3	65.077	21.6923	34.0707	**<0.001**		
	Time	3	30.655	10.2184	16.0494	**<0.001**	**<0.001**	0.32
	P*T	9	7.543	0.8381	1.3164	0.228		
TW	Preservative	3	15.3583	5.1194	375.694	**0.006**		
	Time	3	0.1711	0.057	4.1863	**<0.001**	**<0.001**	0.78
	P*T	9	0.2372	0.0264	1.9345	**0.047**		

Table 5-2: Results of individual linear models examining the effects of preservative type, time point, and their interaction (P*T) on the estimated abundance of each element in Delta Smelt otoliths, with the **ExCell Plus treatment included.**

Bold values indicate p < 0.05. Bold values indicate p < 0.05. DF = degrees of freedom, SS = sum of squared errors, MS = mean squared error, F = f-ratio, P_1 = term p-value, P_2 = model p-value, R^2 = model R^2.

Model	Factor	DF	SS	MS	F	P_1	P_2	R^2
	Preservative	3	1.98E-06	6.61E-07	5.7267	**0.002**		
Boron	Time	2	1.34E-06	6.70E-07	5.7983	**0.006**	**<0.001**	0.47
	P*T	6	3.92E-06	6.53E-07	5.6557	**<0.001**		
	Preservative	3	2.24E-06	7.48E-07	3.1333	**0.034**		
Barium	Time	2	1.50E-06	7.49E-07	3.1403	0.052	**0.003**	0.29
	P*T	6	4.41E-06	7.35E-07	3.0792	**0.012**		
	Preservative	3	0.004682	0.001561	4.4355	**0.008**		
Copper	Time	2	0.003168	0.001584	4.502	**0.016**	**<0.001**	0.40
	P*T	6	0.009388	0.001565	4.4469	**0.001**		
	Preservative	3	2.69E-10	8.97E-11	2.95	**0.042**		
Lithium	Time	2	1.84E-10	9.18E-11	3.0181	0.058	**0.005**	0.27
	P*T	6	5.38E-10	8.97E-11	2.9483	**0.016**		
	Preservative	3	0.002009	0.00067	13.673	**<0.001**		
Magnesium	Time	2	0.001361	0.000681	13.892	**<0.001**	**<0.001**	0.71
	P*T	6	0.004022	0.00067	13.684	**<0.001**		
	Preservative	3	1.19E-07	3.98E-08	3.0858	**0.036**		
Manganese	Time	2	8.53E-08	4.26E-08	3.3059	**0.045**	**0.003**	0.29
	P*T	6	2.36E-07	3.94E-08	3.0515	**0.013**		
	Preservative	3	0.013465	0.004488	23.833	**<0.001**		
Sodium	Time	2	0.009786	0.004893	25.982	**<0.001**	**<0.001**	0.82
	P*T	6	0.028494	0.004749	25.218	**<0.001**		
	Preservative	3	6.19E-06	2.06E-06	19.937	**<0.001**		
Strontium	Time	2	3.05E-06	1.53E-06	14.752	**<0.001**	**<0.001**	0.77
	P*T	6	1.17E-05	1.95E-06	18.844	**<0.001**		
	Preservative	3	2.22E-05	7.41E-06	11.229	**<0.001**		
Zinc	Time	2	1.46E-05	7.29E-06	11.042	**<0.001**	**<0.001**	0.65
	P*T	6	4.28E-05	7.14E-06	10.813	**<0.001**		

Table 5-3: Results of individual linear models examining the effects of preservative type, time point, and their interaction (P*T) on the estimated abundance of each element in Delta Smelt otoliths, with the **ExCell Plus treatment excluded.**

Bold values indicate $p < 0.05$. DF = degrees of freedom, SS = sum of squared errors, MS = mean squared error, F = f-ratio, P_1 = the term p-value, P_2 = the model p-value, R^2 = the model R^2.

Model	Factor	DF	SS	MS	F	P_1	P_2	R^2
	Preservative	2	9.90E-12	4.95E-12	2.2736	0.118		
Boron	Time	2	3.90E-11	1.95E-11	8.9431	**0.001**	**0.008**	0.29
	P*T	4	6.62E-12	1.65E-12	0.7596	0.559		
	Preservative	2	1.38E-10	6.88E-11	1.6482	0.207		
Barium	Time	2	6.12E-11	3.06E-11	0.7333	0.488	0.296	0.05
	P*T	4	2.22E-10	5.55E-11	1.328	0.279		
	Preservative	2	8.39E-14	4.19E-14	0.4017	0.672		
Copper	Time	2	1.17E-13	5.86E-14	0.5615	0.575	0.477	<0.01
	P*T	4	6.07E-13	1.52E-13	1.4539	0.237		
	Preservative	2	9.76E-16	4.88E-16	0.7668	0.472		
Lithium	Time	2	2.00E-14	9.98E-15	15.6893	**<0.001**	**0.001**	0.39
	P*T	4	1.53E-15	3.82E-16	0.5997	0.665		
	Preservative	2	5.62E-10	2.81E-10	2.6526	0.085		
Magnesium	Time	2	2.08E-09	1.04E-09	9.8102	**<0.001**	**0.001**	0.41
	P*T	4	1.31E-09	3.28E-10	3.0925	**0.028**		
	Preservative	2	1.12E-11	5.59E-12	1.2501	0.299		
Manganese	Time	2	7.15E-11	3.57E-11	7.9872	**0.001**	**0.023**	0.23
	P*T	4	1.10E-11	2.74E-12	0.6121	0.657		
	Preservative	2	3.47E-06	1.74E-06	14.3291	**<0.001**		
Sodium	Time	2	1.33E-06	6.66E-07	5.489	**0.008**	**<0.001**	0.44
	P*T	4	2.6E-07	6.49E-08	0.5354	0.711		
	Preservative	2	1.32E-07	6.61E-08	0.9303	0.404		
Strontium	Time	2	8.41E-08	4.20E-08	0.5914	0.559	0.746	<0.01
	P*T	4	1.42E-07	3.56E-08	0.5008	0.735		
	Preservative	2	3.38E-10	1.69E-10	1.1122	0.340		
Zinc	Time	2	3.33E-10	1.66E-10	1.0966	0.345	0.405	0.01
	P*T	4	6.31E-10	1.58E-10	1.0391	0.401		

FIGURES

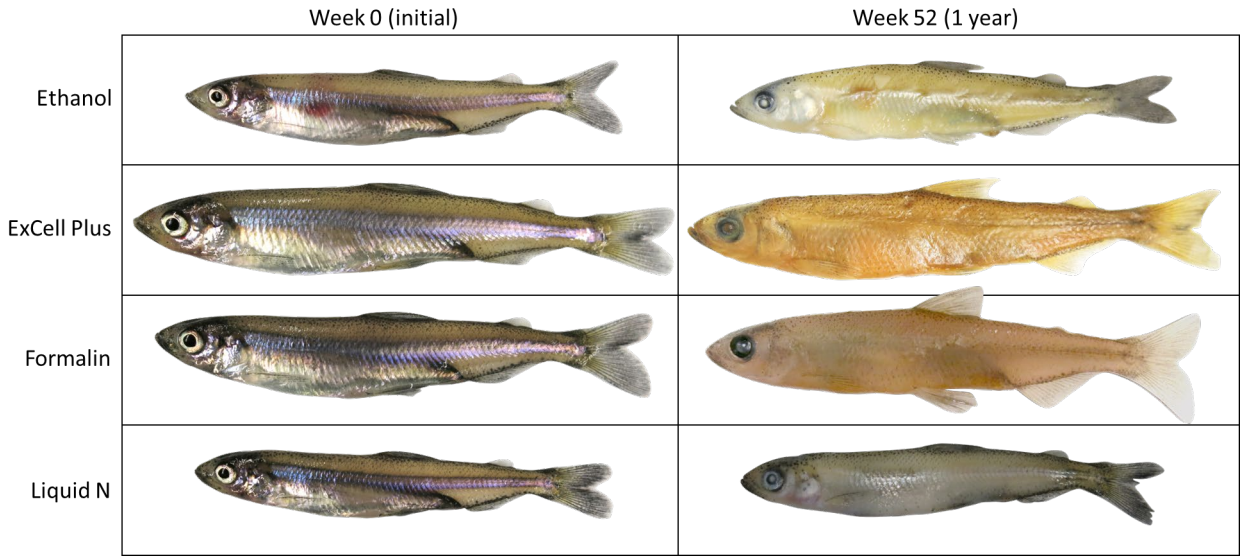

Figure 5-1: Examples of the effects of each preservative on the gross morphology, color, and overall appearance of Delta Smelt.

Here, initial appearances at week 0 (control, prior to preservation) are contrasted with appearances after 52 weeks (1 year) of storage in each preservative.

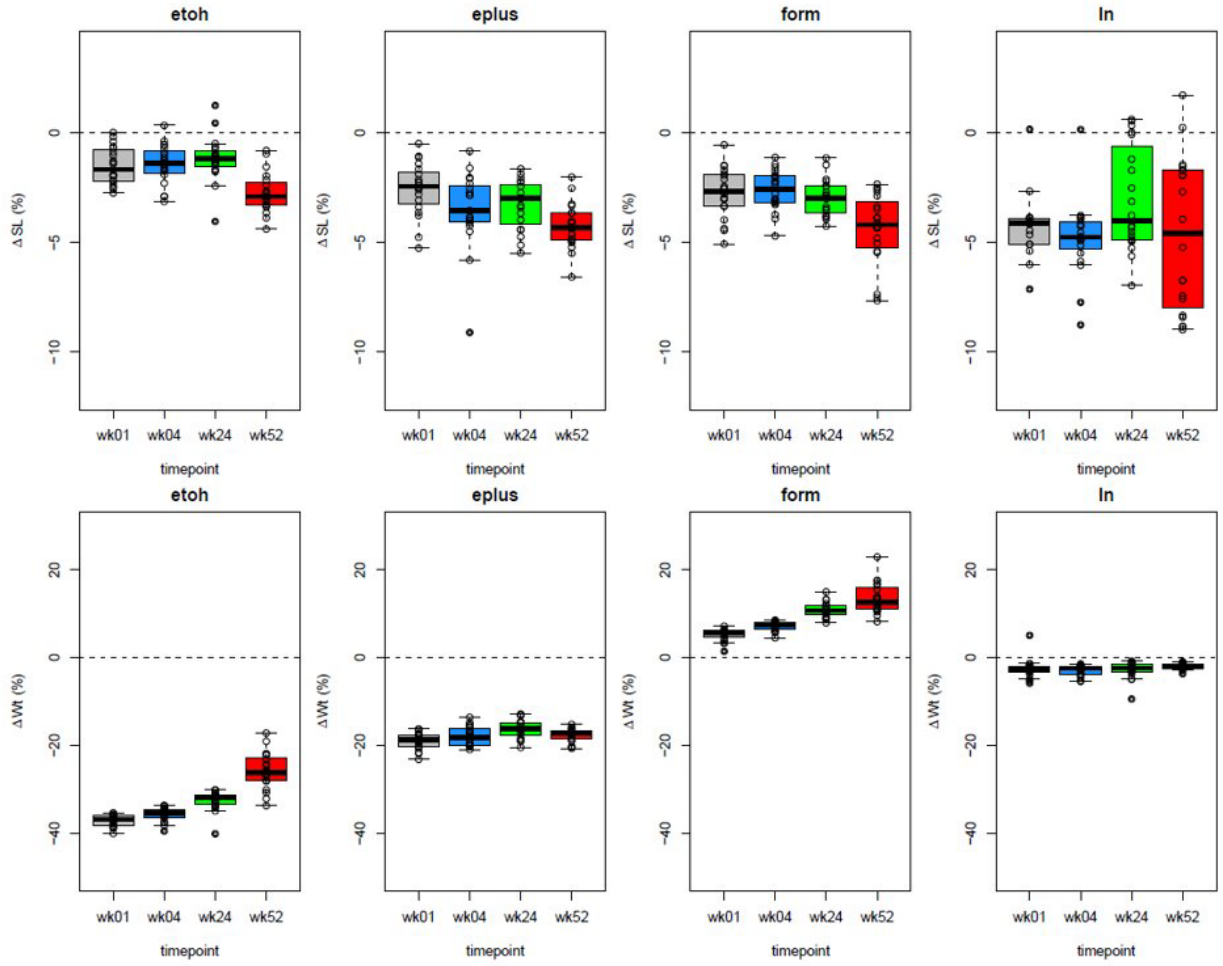

Figure 5-2: Percentage change (Δ) in standard length (ΔSL, top) and total weight (ΔWt., bottom) of Delta Smelt specimens fixed in ethanol (etoh), ExCell Plus (eplus), formalin (form) and liquid nitrogen (ln) at 1, 4, 24, and 52 weeks.

The percentage change values are relative to paired measurements for each individual fish at wk-0 and the corresponding time point.

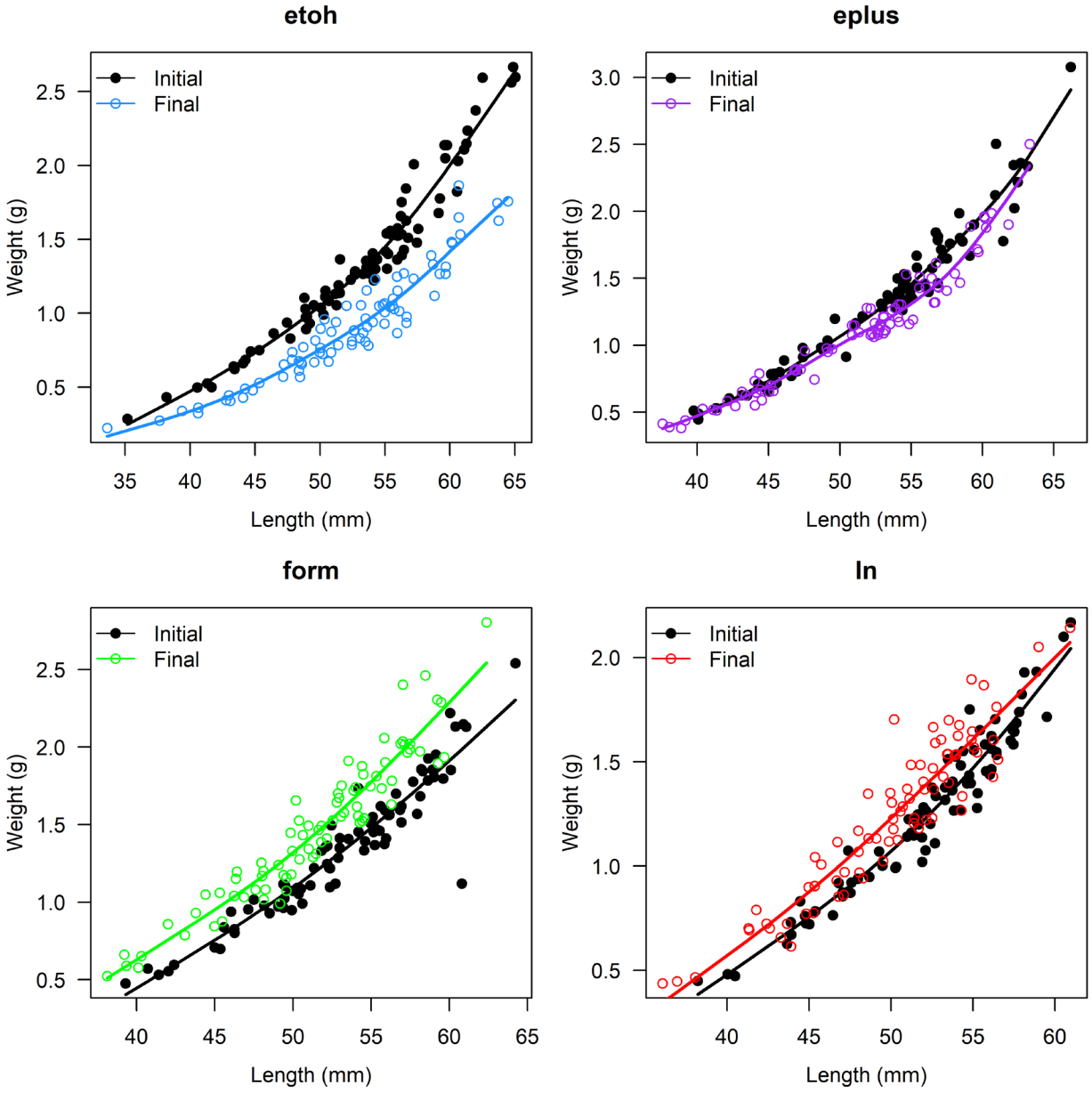

Figure 5-3: Length-weight relationships for Delta Smelt specimens stored in 95% ethanol (etoh), 100% ExCell Plus (eplus), 10% buffered formalin (form), and liquid nitrogen (ln).

Black filled dots and lines represent specimens measured at week 0 (control, prior to preservation). Open colored dots and lines represent specimens preserved and measured at 1, 4, 24 and 52 weeks post-preservation.

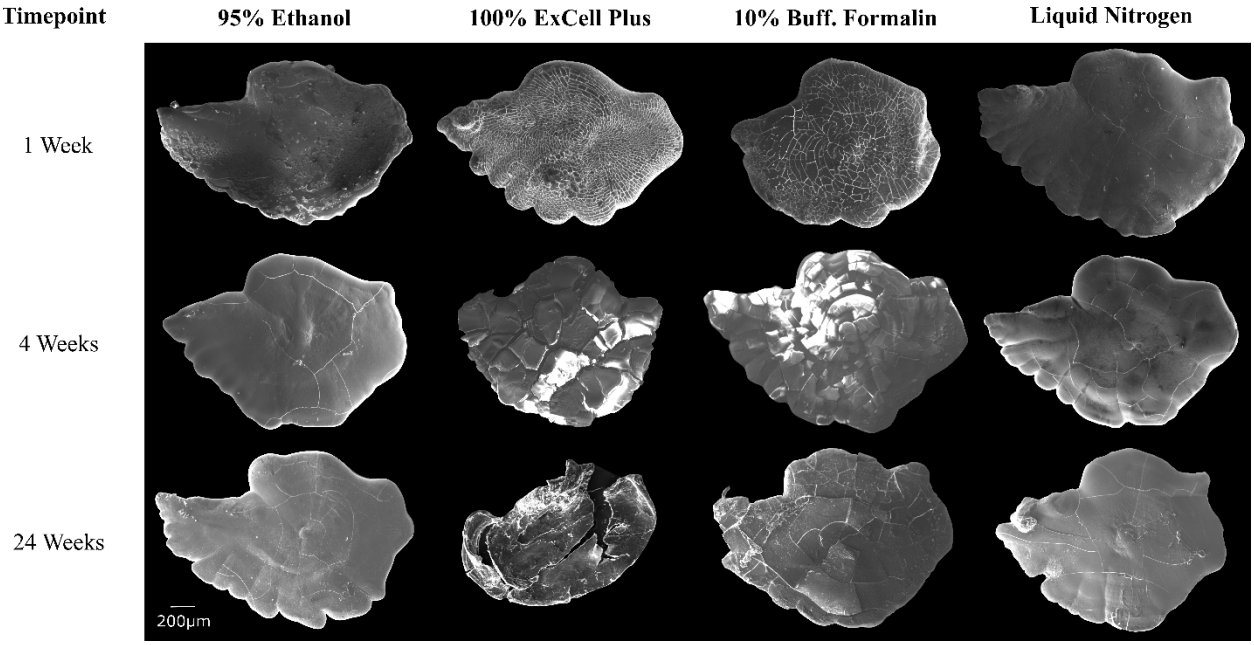

Figure 5-4: Scanning Electron Microscope (SEM) images of Delta Smelt otoliths preserved in each of the four preservatives for 1, 4, and 24 weeks.

Images show the high-resolution topography of the surface of each specimen.

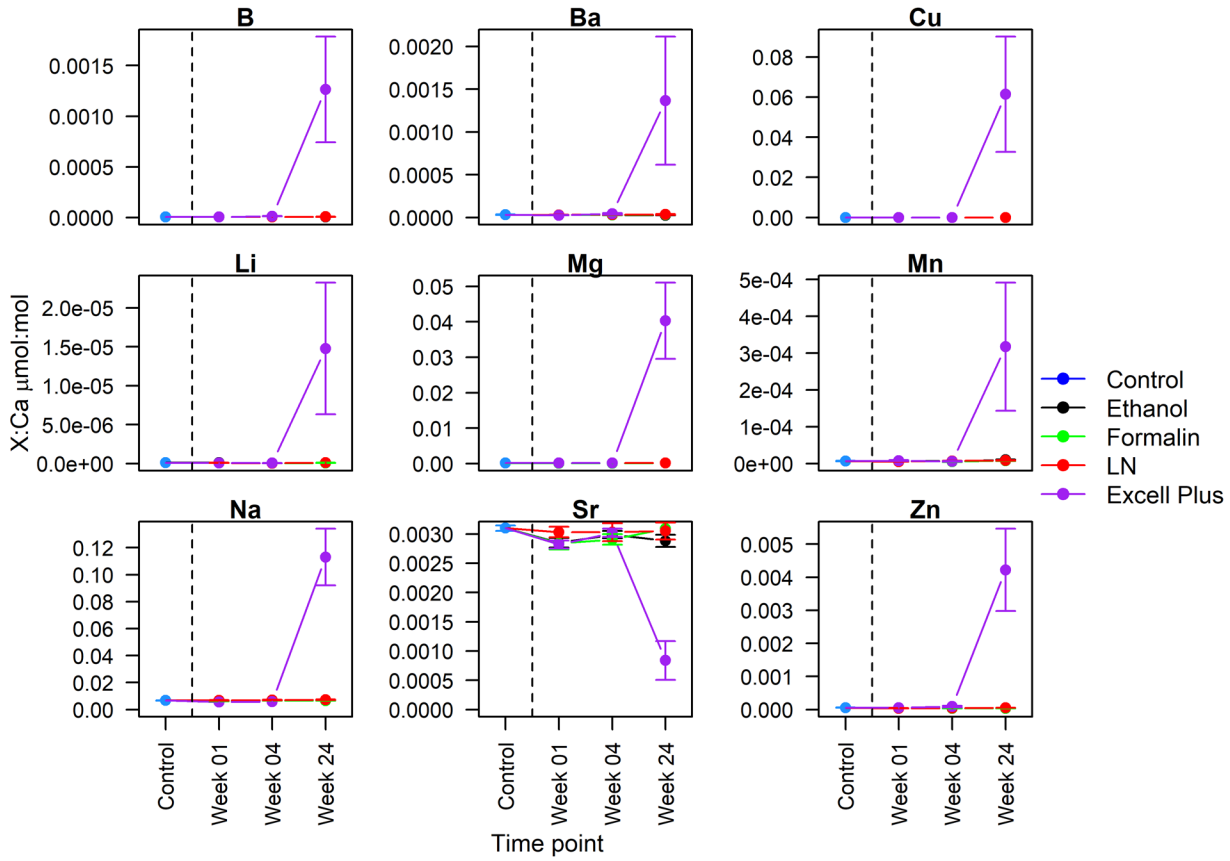

Figure 5-5: Preservative effects on the chemistry of Delta Smelt otoliths across time with the **ExCell Plus treatment included**.

Each color profile represents a different preservative method. Points are the average value +/- SE for each time point and preservative combination and are expressed in ratios of µmol of the given element to mols of Calcium.

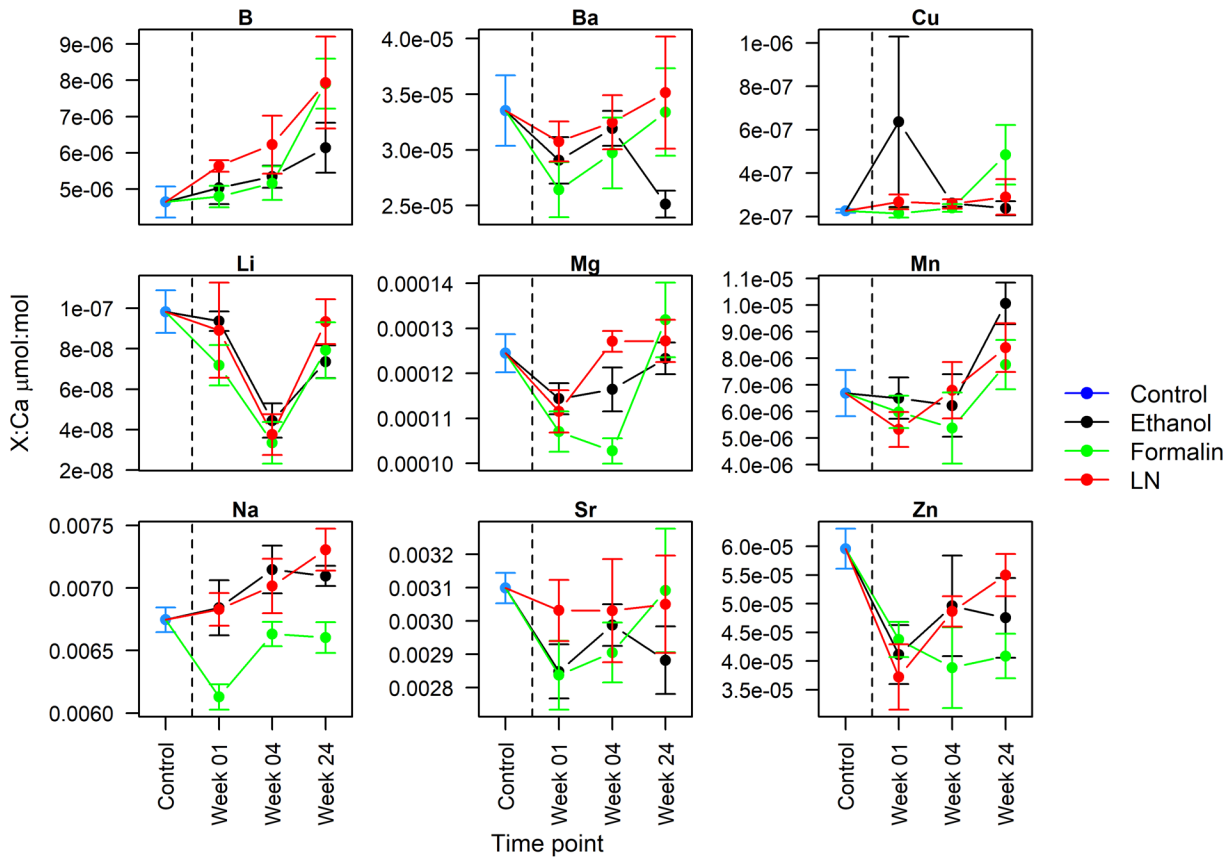

Figure 5-6: Preservative effects on the otolith chemistry of Delta Smelt across time points with the **ExCell Plus treatment excluded**.

Each color profile represents a different preservative method. Points are the average value +/- SE for each time point and preservative combination and are expressed in ratios of µmol of the given element to mols of Calcium.

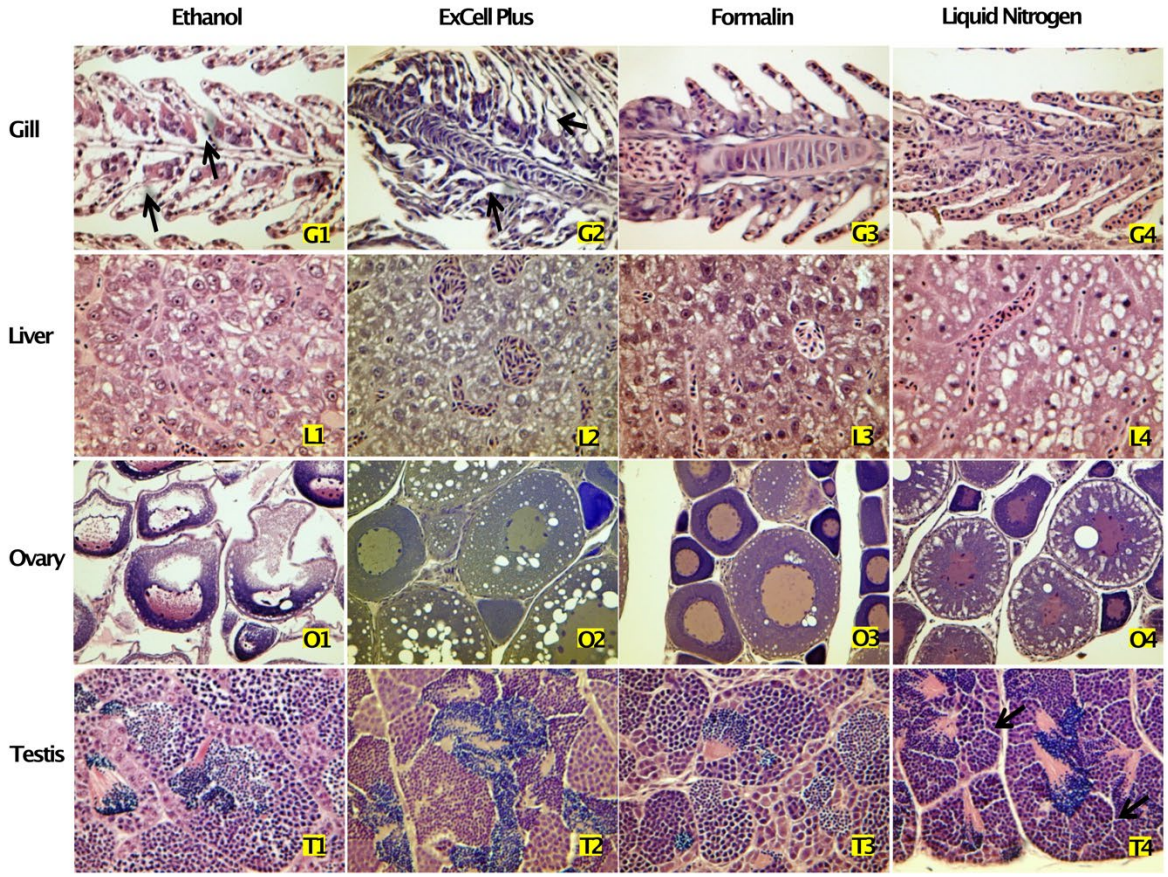

Figure 5-7: Histological sections of gill (G1-G4), liver (L1-L4), ovary (O1-O4) and testis (T1-T4) tissues preserved in ethanol, ExCell Plus, formalin and liquid nitrogen at 52 weeks post-preservation.

This Page Intentionally Left Blank

Chapter 6: Health and Reproduction of Endangered Delta Smelt, Endemic to a Highly Altered Estuary

Authors:

Calvin Y. Lee[1], Shawn Acuña[2], April G. Smith[1], Jason L. Hassrick[1], Bruce G. Hammock[4], Swee Teh[4]

[1]ICF, 980 9th Street, Suite 1200, Sacramento, CA 95814 USA.

[2]Metropolitan Water District of Southern California, 1121 L St, Sacramento, CA 95814

[4]Aquatic Health Program, UC Davis, 1 Shields Ave, Davis, CA 95616

Corresponding author:

Calvin.Lee@icf.com, (510) 381-0222

ABSTRACT

The health and nutrition of individuals in a population have important implications for reproductive success of imperiled species. We examined health and nutritional indices of delta smelt, *Hypomesus transpacificus,* in relation to their reproductive status under different hydrological conditions in the San Francisco Estuary and Sacramento-San Joaquin Delta. Adult delta smelt were collected by the Fall Midwater and Spring Kodiak Trawl monitoring surveys run by the California Department of Fish and Wildlife from 2011 to 2018, which corresponds with brood years 2011 to 2017. The hydrological conditions during this period ranged from high precipitation (2011 and 2017) to drought (2012-2016). Drought, amongst other related factors such as contaminants and food availability, is thought to influence reproduction of delta smelt. For each fish, we examined morphometric indicators (gill pathology and liver indices), nutritional indicators (RNA/DNA and liver glycogen depletion estimated histologically) and reproductive metrics (gonadosomatic indices [GSI], oocyte developmental stage, clutch size, oocyte size, oocyte weight, and estradiol [E2]). Fork length and condition factor had strong, positive correlations with reproductive metrics. Glycogen depletion was correlated with higher oocyte mass, oocyte area and GSI, while liver lipidosis (except 'severe' lipidosis) was associated with higher GSI. Gill and liver lesion severity, which are frequently caused by contaminant exposure, were negatively associated with oocyte area, estradiol levels, and GSI. Fish in Suisun Marsh and Cache Slough had the longest fork length and highest condition factor. Fish in Cache Slough had the highest reproductive metrics and proportion of post-spawned females and late-stage oocytes, indicating delta smelt use Cache Slough as a spawning area. There was no clear

pattern in reproduction indices by water-year type, suggesting factors other than outflow may influence reproductive success.

INTRODUCTION

Recovery of an endangered species depends on how successful reproduction is in the wild. However, reproductive success can be compromised by a myriad of human-induced stressors including, but not limited to, altered environmental conditions, reduced food availability, and exposure to contaminants (Burnett et al. 2013, Donelson et al. 2010). Environmental stressors may act independently on reproduction (Wiles et al. 2020, Petitjean et al. 2019) or interactively to significantly impact reproduction (Hani et al. 2019, Cardoso et al. 2017). Understanding how stressors affect reproduction is therefore critical to recovering endangered species populations.

Nutrition affects reproductive condition across a wide spectrum of taxa (Philips et al. 1996, Kreiter and Wise 2001, Allen and Ullrey 2004, Niehoff 2004, Volkoff and London 2018). Food limitation can impair maturation and reproductive success in fish (Yamamoto et al. 2011, Brooker et al. 2013, Volkoff and London 2018, Lopes et al. 2022) because maturation of gonadal tissue requires significant nutritional input. For instance, diets rich in highly saturated fatty acids are associated with increased reproductive success (Izquierdo et al. 2001, Rainuzzo et al. 1997). Nutritional requirements for energy investment into gametes is higher in females than males because eggs are nutritional storehouses (Hayward and Gillooly 2011). Thus, food limitation can reduce gonadal somatic indices (GSI), gonadal maturation, egg quality and spawning frequency (Volkoff and London 2018). Additionally, nutritional indices may reflect the high energetic costs of reproduction. For example, glycogen in the liver decreased in the Asian striped catfish during pre-spawning and spawning seasons (Sreevalli and Sudha 2022), at the beginning of gonadal recrudescence in domesticated rainbow trout (Soengas et al. 1993), and mid recrudescence in goldfish (Ladisa et al. 2022).

Contaminant exposure and stress can manifest at the cellular level in gills or the liver (Pereira et al. 2013, Carmago and Martinez 2007, Teh et al. 1997) and can damage reproductive organs thereby reducing reproductive success (as reviewed in Marlatt et al. 2022, Pandley et al. 2014 and Taslima et al. 2022). Sublethal contaminant stress can increase bioenergetic demands of individuals, resulting in less energy for reproduction (Brooks et al. 2012). Combined with stress from food limitation, contaminant stress can ultimately manifest in reduced reproductive success and declining health (Holmstrup et al 2010, Jørgensen et al 1999, Hopkins et al. 2002), although these effects are not always consistent across fish taxa (Hashemi et al. 2008).

In the upper San Francisco Estuary, including Suisun Bay, Suisun Marsh, and the Sacramento-San Joaquin Delta (hereafter collectively referred to as the “Bay-Delta”), fish must navigate a highly modified, dynamic environment where food resources change regionally and seasonally, and contaminant concentrations are influenced by precipitation and water management actions. Delta smelt (*Hypomesus transpacificus*) is an endemic Bay-Delta planktivorous fish with a predominantly annual life cycle (Lott 1998, Nobriga 2002, Feyrer et al. 2003, Hobbs et al. 2006, Slater and Baxter 2014, Hammock et al. 2019). While most individuals are semi-anadromous,

some complete their entire life cycle in brackish or fresh water (Hobbs et al. 2019). Adults spawn in winter to spring in freshwater to brackish water regions of the Bay-Delta. The eggs hatch during the spring and larval fish mature into juveniles during summer, with migratory individuals moving into brackish waters of the Bay-Delta to forage and grow into adults by winter (Moyle et al. 2016). Previous studies of delta smelt fecundity found that individuals could produce multiple clutches with the largest females reproducing early and having larger clutch sizes (Damon et al. 2016). Having multiple clutches can occur when temperatures are suitable across the spawning season and there is an adequate food supply (Damon et al. 2016).

Historically the Bay-Delta had a productive pelagic ecosystem; however, the food web has collapsed in recent decades, exhibiting severe phytoplankton, zooplankton, and pelagic fish abundance declines (Hammock et al. 2019, Winder and Jassby 2011, Baxter et al. 2008). Zooplankton size has declined over time, and native prey have been largely displaced by non-native species (Baxter et al. 2010, Winder and Jassby 2011). Like other pelagic fishes, the delta smelt is considered susceptible to food limitation from this collapse, reflected in poor condition, low abundance, and reduced growth and reproduction (Bennett and Moyle 1996, Sommer et al. 2007, Slater and Baxter 2014, Hammock et al. 2015). Nutritional condition is reflected across a suite of delta smelt health metrics including growth and survival (Moyle et al. 2016, Houde 1997, Post and Parkinson 2001). Impaired growth can also affect the reproductive status of adults, and underdeveloped gonads can result in delayed spawning and lower fecundity (Lindberg et al. 2013). Additionally, the Bay-Delta is a heterogenous environment, delta smelt caught in certain regions of the Bay-Delta (e.g. Suisun Marsh), were in better nutritional condition (Hammock et al. 2017) which may have implications for reproductive potential.

Delta smelt are also exposed to varying amounts of contaminants that differ regionally and fluctuate with changing outflow (Stillway et al. 2021, Weston et al. 2019, Weston et al. 2012, Hammock et al. 2015, De Parsia et al 2018, Jabusch et al 2018). Contaminants are another factor contributing to the decline of delta smelt across multiple generations (Fong et al. 2016). In lab studies, sub-lethal contaminant concentrations can negatively affect delta smelt behavior and protein synthesis (Segarra et al. 2021, Mundy et al. 2021, Jefferies et al. 2015, Connon 2009) and even extend to reproduction (Jin et al. 2018). While it may be difficult to demonstrate exposure and its corresponding biological response to contaminants in the wild, possible evidence of exposure can be inferred from histopathological examination of gill and liver tissue (Teh et al. 2020).

Here, we characterize the cohort (temporal) and regional (geographic) variation in condition, nutrition, and reproductive status of delta smelt collected from 2011 to 2018. This period encompasses a variety of hydrological conditions, from drought to above normal precipitation. This may have influenced the prey available to delta smelt and the type and concentrations of contaminants in the environment. Impaired reproduction due to contaminant exposure and food limitation may be contributing to the continued delta smelt population decline. Assessing the reproductive status of fish in relation to nutrition and health is critical for managing delta smelt in the wild. To this end, we address the following three hypotheses:

1. Larger female delta smelt and individuals with high nutritional indices (low glycogen depletion and high RNA/DNA) and with few histopathological lesions will exhibit higher reproductive status, as indicated by GSI, clutch size, estradiol levels, oocyte size, and mass.
2. Fish in the Suisun Marsh region will have high reproductive status because juveniles from there exhibited elevated stomach fullness and other nutritional indices and low incidence of histopathological lesions (Hammock et al. 2015).
3. Drought years (2012-2016) would have a negative impact on reproductive status because temperature, turbidity, and salinity during droughts are associated with poor reproductive success, as indicated by previous studies (Kurobe et al. 2022).

METHODS

2.1 Fish sampling

Delta smelt were collected from the Bay-Delta by long-term fish monitoring surveys conducted by the California Department of Fish and Wildlife (CDFW) from September to May from 2011 to 2017 by the Fall Midwater Trawl and Spring Kodiak Trawl (Figure 6-1). Environmental data, including specific conductivity (converted to salinity), water temperature (°C), and turbidity in Nephelometric Turbidity Units (NTU), was collected at each site. Outflow at Chipps Island was downloaded from CA Department of Water Resources Dayflow website and merged with the delta smelt data. Sampling occurred during daylight hours between sunrise and early afternoon (see Contreras et al. (2012) for a detailed description of the sampling effort and delta smelt catch). Following species identification, delta smelt were wrapped individually in labeled foil, frozen in liquid nitrogen, and transported to the Aquatic Health Program (AHP; University of California, Davis) for dissection per Teh et al (2016).

2.2. Dissection

A total of 1,258 delta smelt were dissected during this study by the AHP. Prior to dissection, fork lengths (FL) were measured to the nearest millimeter (mm) and body weights (W_B) were recorded to the nearest milligram (mg). During dissection, the viscera and gastrointestinal (GI) tract were removed from each fish, and gonads and liver were excised and weighed to the nearest mg to determine hepatosomatic (HSI) and gonadosomatic (GSI) indices, respectively. The liver was split into two portions, the first of which was stored in a -80°C freezer. The other part of the liver, the left gill, and a portion of the ovary were fixed in 10% buffered formalin for histopathology. The rest of the ovary was stored at –80°C to determine clutch size. White muscle along the dorsal section was dissected and frozen in liquid nitrogen. These muscle samples were homogenized and frozen at -80ºC for RNA/DNA determination.

2.3. Morphometry

Fulton's condition factor (K) was adjusted to remove the confounding weight (mg) of the gonad and used to determine the relative health measure of each delta smelt with the formula:

$$K = [(W_B - W_G) \times FL^{-3}] \times 100{,}000, \quad (1)$$

where, W_B is body wet weight, W_G is gonad weight (mg), and FL is fork length (mm) (Anderson and Neumann 1996). Hepatosomatic index (HSI) and GSI were used to determine relative differences in reproductive status of females, growth and health based on liver weight (Busacker et al. 1990), and the reproductive status of each fish based on gonad weight (Crim and Glebe 1990), respectively as:

$$HSI = (W_{L \text{ or } G} \times W_B^{-1}) \times 100, \quad (2)$$

where, W_L is liver weight.

2.4. Nutritional analysis

1-10 mg of ground muscle was used for RNA/DNA determination for each fish. Muscle nucleic acids were measured by an ethidium bromide fluorometric technique (Caldarone et al., 2001).

For Glycogen Depletion (GD), formalin-preserved liver samples were evaluated following Teh et al. (2020) and scored as detailed in section 2.5.

2.5. Histopathology

Histopathology was conducted on liver, gill, and gonadal tissue following Teh et al. (2020), to detect cellular damage (liver and gill), and following Kurobe et al. (2016) to stage the oocytes in the ovary. Briefly, gill, liver, and gonadal tissues were removed from 10% buffered formalin and dehydrated in a graded ethanol series. Tissues were embedded in paraffin where 2-3 micrometer (μm) serial sections were cut and stained with hematoxylin and eosin. Livers were scored for five lesions, including macrophage aggregate (MA), lipidosis (LIP), infiltration of inflammatory cells (INF), sinusoidal congestion (SC) and single cell necrosis (SCN). Livers were also scored for glycogen depletion (GD). Using a BH-2 Olympus microscope, lesions were scored on an ordinal ranking system with 0 = none/minimal, 1 = mild, 2 = moderate, and 3 = severe (see Teh et al. 2020 for lesion descriptions). Histopathology of gonadal tissue also determined oocyte size and oocyte stage. Oocyte size was determined following Kurobe et al. (2016) using a minimum of 10 of the most advanced staged oocytes with a visible nucleus. Clutch size was determined based on counts of dispersed oocytes from a weighed portion of the ovary following Kurobe et al. (2022).

Gill tissue was also screened for lesions. Gills were scored for epithelial cell necrosis (GCN), aneurysm (ANU), secondary lamellar fusion (Fusion), epithelial cell hyperplasia/hypertrophy (ECH), secondary lamellar edema (SLE), ionocytes hyperplasia/hypertrophy (CCH), mucus cell hyperplasia (MCH), and inflammation (GINF) according to Teh et al. (2021).

2.6. 17β-estradiol (E2) quantification by radioimmunoassay (RIA)

Hepatic estradiol concentration was measured by radioimmunoassay (RIA) as described in Kurobe et al. (2016). No replicates were obtained due to limited tissue mass. Estrogen was standardized for protein, which was measured using the Lowry assay performed in triplicate in a 96-well plate using a kit (DC Protein Assay, BioRad, Hercules, CA) with 1:2 serial dilutions of bovine serum albumin standards that ranged from 0.3125 to 40 mg/ml. The resulting estradiol concentration was expressed as picograms of estradiol per one milligram of liver protein.

2.7. Statistics

Our dataset contained information from over 900 individual delta smelt, which is unique given the critically endangered status of the species. However, there were numerous individuals with missing data points, including abiotic (e.g., salinity at time of collection) and biotic (e.g., liver lesion score) variables or both depending on the individual. Typical model building exercises cannot accommodate missing data; therefore, to retain all collected fish and associated covariates, we used the Multiple Imputation using Chained Equations (mice) package in R (Van Buuren and Groothuis-Oudshoorn 2011) to impute missing values from simulations of the missing data relative to the available data. The technique interprets patterns across 30 iterations and estimates the most likely value to replace the missing value based on the available data. We repeated this 100 times and then summarized the results to generate 100 imputed datasets (mice package version 3.14.0, collinear variables set to false, methods set to predictive mean matching for numerical data, polytomous regression for categorical variables and proportional odds model for ordered variables). This type of imputation reduces bias in standard error estimates, increasing efficiency (Van Buuren 2018, Meng 1994, Collins et al. 2001), decreasing risk of making missing-at-random assumptions for data that are not missing-at-random (Schafer 1997), and maximizes the number of variables that can be retained in the model. Backward model selection was used on the 100 imputed data sets to run model selection procedures in which a final model was selected based on calculated Akaike Information Criteria (AIC) (Bozdogan 1987).

Using imputed data as well as the original datasets of fish with complete data allows us to uniquely assess factors which influence reproductive status for a much larger number of individuals than a complete dataset alone would allow. Sample size increased from 124 individuals with no missing data, to 887 individuals with imputed data. Overall percentage of missing data ranged from 0 to 62% (Table 6-1). The variables collected on health status all contained the highest percentages of missing data while condition and environmental variables (fork length and condition factor, salinity, turbidity, and temperature) were missing at very minimal percentages (<1% but not 0). The reproductive end points ranged in missingness from 1 to 20%.

To address the first hypothesis, using fish from all regions and across the entire study period, a second backwards model selection was run on the reduced original data set only with fish with no missing data. Selected models from the imputed and the original datasets are presented for comparison. Sex was not included in the list of variables which can be imputed because it is a binary variable that can lead to misinterpretation of the entire study if it is imputed incorrectly. In addition, gender-specific variables may not be missing at-random if sex is missing. For example, if sex is missing, it is impossible to determine whether a missing data point for egg mass is because the fish is male. Therefore, all fish with sex missing were excluded from the analysis. Additionally, females with stage 5 oocyte development were removed from the analysis because they were actively spawning at capture, and uncounted oocytes can affect estimates of clutch size and GSI. All variables were inspected for normality and those that failed the Shapiro-Wilks test (p-<0.05) were log transformed before model selection.

To test our second and third hypotheses, we used the original dataset to compare the health and nutrition metrics across regions and cohort years. Categorical variables were transformed into prevalence by dividing the frequency of each score by the total number of fish scored in that cohort year or region. We used a Kruskal-Wallis test followed by Dunn's test with Bonferroni corrections for multiple comparisons of the continuous variables.

RESULTS

We determined that the original dataset models tended to be more inclusionary of the dependent variables than the imputation models during backwards model selection (Table 6-1). Convergent results where the original dataset and the imputed models agreed (e.g., positive correlation between condition factor and GSI in both models) suggest stronger support for the correlation. Models run on the imputed datasets found that fish length and condition factor were the most important explanatory variables, while environmental, nutritional status, and health variables were less likely to be included in final models. Similarly, length and condition factor were included in all of the final models for all dependent variables for the original dataset. Health, nutritional status and environmental variables were included more frequently in the original dataset compared to the imputed dataset.

Female Modeling Results

Condition factor and fork length had the strongest positive relationships with reproductive metrics for female fish (Figure 6-4). Temperature had the strongest negative relationship of any of the environmental variables; higher temperatures strongly predicted lower estradiol levels. There was a negative relationship between salinity and oocyte area, estradiol level, clutch size and GSI. Counter to our hypothesis, more severe glycogen depletion, a nutritional index, had a positive relationship with reproductive metrics. The other nutritional index, RNA/DNA, had a negative relationship with oocyte mass, estradiol level, clutch size and GSI. Measured health metrics such as liver and gill lesions score strongly predicted a decrease in oocyte area, estradiol levels, and GSI while lipidosis had a positive correlation with GSI.

Female Regional Differences

We found that the environmental, nutrition and health factors that influence female delta smelt reproductive metrics vary by region (Figure 6-5). Fish caught in Cache Slough and Suisun Marsh had the longest fork lengths. Fork lengths were similar between individuals from Sacramento Deep Water Ship Channel (SSC), the Confluence and Suisun Bay. Fish from Suisun Marsh had significantly higher condition factor measurements than those from SSC, the Confluence and Suisun Bay, but not Cache Slough.

Turbidity was significantly lower in Suisun Marsh than in the Confluence. Temperature was significantly different in Cache Slough, SSC, and Suisun Marsh, ranging from warmest to coolest respectively. Temperatures in the Confluence and Suisun Bay were not significantly different from the SSC and Suisun Marsh. Salinity was highest in Suisun Bay and Marsh and

lowest in Cache Slough with the SSC and the Confluence in between. Mean outflow was significantly higher when females were caught in Cache Slough compared to all other regions.

RNA/DNA of fish in Suisun Marsh and the Confluence was significantly higher than in Suisun Bay but similar to other regions (Figure 6-5). Cache Slough, SSC and Suisun Bay had the largest proportion of fish with the most severe glycogen depletion (Figure 6-7). The Confluence and Suisun Marsh had the largest proportion of fish with low glycogen depletion scores (< 2). Cache Slough, the SSC and Suisun Bay were the only regions where individuals were scored a 0 ranking.

There were high proportions of fish across most regions that had no to low (0-1) evidence of gill lesions, liver lesions and lipidosis. Fish caught in the Confluence and SSC had the highest proportion of the most extreme gill lesion, liver lesion and lipidosis scores. Some individuals from Suisun Marsh had high lipidosis scores, but no severe gill or liver lesion scores (>4) were observed. Cache Slough and Suisun Bay fish had only low-ranking gill (< 3) and liver lesion (< 2) scores. Moderate cases of lipidosis (a score of 2) were present at all regions.

Female Reproductive Metrics:

Fish caught in Cache Slough had the highest reproductive metrics while those of individuals from Suisun Bay and the Confluence were significantly lower (Figure 6-5). Mean oocyte mass was highest in Cache Slough and the SSC followed by Suisun Marsh, with the Confluence and Suisun Bay having the lowest mean. Mean clutch size was highest in Cache Slough and second highest in Suisun Marsh; however, mean clutch size in Suisun Marsh was not significantly different from SSC and Suisun Bay. Oocyte area and GSI had similar patterns; individuals in Cache Slough had the highest mean, those in SSC and Suisun Marsh the second highest mean, and individuals in the Confluence and Suisun Bay the lowest values. Estradiol levels were highest in Cache Slough and the SSC, whereas those in all other regions were alike. Higher proportions of late cortical alveolus stage, middle and late vitellogenic stage oocytes and post spawners (stages 4.1-6) were found in the freshwater regions of Cache Slough and SSC (Figure 6-7).

Female Temporal Differences

We found that drought conditions during the years 2012 through 2016 did not significantly predict health, nutrition, or environmental factors, nor was there a clear pattern across the years (Figure 6-6). Variability of the 2018 cohort was particularly high because so few female fish were caught (N = 8). Mean fork length was lowest in the 2011, 2014 and 2017 cohorts, while fish from the 2012 and 2015 cohorts had the highest mean fork lengths. 2016 and 2018 cohort mean fork length were not significantly different from other years. Condition factor remained consistent from 2011 to 2014 then dropped in 2015. Cohort years 2016 through 2018 were not significantly different than other years.

The hydrological conditions in which the fish were caught varied across wet and drought years. While mean annual turbidity remained consistent across the entire study period, temperature was lower for 2011 and 2012 cohorts, then increased for 2013 to 2015 cohorts. Temperatures in 2016

through 2018 were not significantly different from all other years. Salinity peaked for the 2013 cohort year class and was the lowest for the 2016 cohort with all other cohorts being similar. Mean outflow at time of catch was the highest for the 2016 cohort, while that for the 2013 cohort was the lowest.

The 2015 and 2016 cohorts had the lowest RNA/DNA. The highest mean RNA/DNA values were found in the 2017 cohort. Glycogen depletion was similar for all cohorts except for the 2017 cohort, which all individuals had at least mild glycogen depletion (Figure 6-8).

2011, 2012, 2014 and 2015 were the only cohorts where gill lesion scores greater than 6 were observed, while 2011, 2013, 2014 and 2017 had the largest proportion of low scores (<1). The most severe liver lesions were observed in cohorts 2012 and 2014, which also had higher proportions of liver lesion scores > 3. Cohorts 2015 through 2017 had the best liver lesion condition, for which all individuals had scores of 1 or less. The most severe lipidosis scores (3) were only observed in the 2012 to 2016 cohorts.

Mean oocyte mass was highest in the 2015 cohort and lowest in 2014 cohort (Figure 6-6). Mean clutch size was highest in the 2012 cohort while 2017 individuals were the least fecund. Egg area was highest in 2012 and 2013 and estradiol did not significantly change across the two years it was collected. Mean GSI was highest in the 2015 and 2016 cohorts, and lowest for the 2014 and 2017 cohorts. Oocyte stage prevalence was similar for cohorts 2011, 2012, 2013, and 2016 (Figure 6-8). There was no catch of post spawned fish (stage 6) in the 2014 and 2017 cohorts. The 2014 cohort had a higher proportion of stage 3.3 eggs, while the 2017 cohort had more early vitellogenin stage oocytes.

Male Modeling Results

Like female fish, male fork length and condition factor had strong positive effects on gonadosomatic index, while salinity had a smaller negative effect (Figure 6-4).

Male Regional Differences:

Males caught in Cache Slough had the longest mean fork length while fish in the SSC, Confluence and Suisun Bay had the shortest fork length (Figure 6-5). The mean condition factor was highest in Cache Slough, Suisun Bay, and Suisun Marsh.

Turbidity and temperature were similar in all regions except in the SSC, in which temperature was cooler. Salinity was highest in the seaward regions of Suisun Bay and Marsh. Mean outflow at time of catch was significantly lower in the Confluence than in Cache Slough and the SSC.

Mean RNA/DNA was highest in the Confluence and lowest in Cache Slough while values in the three other regions were in between (Figure 6-5). None of the individuals caught in Cache Slough were severely (3) glycogen depleted (Figure 6-7). Conversely, all fish caught in Suisun Bay had some degree of glycogen depletion. The SSC region had the highest proportion of fish with severe glycogen depletion.

Gill lesion scores were convoluted for males. While severity scores were the highest in the SSC, Confluence and Suisun Marsh, fish in these same regions also had a high proportion of no to low (0-1) gill lesions scores. Severe liver lesion scores were more prevalent in the SSC and Suisun Marsh relative to other regions but more than 75% of male fish caught in Suisun Marsh had scores of less than 2. Male fish caught in Cache Slough had the least severe liver lesion scores. Severe lipidosis was seen in all five regions, with the Cache Slough and Suisun Bay having the highest proportion, while the Confluence and Suisun Marsh had the lowest proportion.

Male GSI was highest in Suisun Marsh and lowest in Suisun Bay and the SSC (Figure 6-5); GSI values in all other regions were in between.

Male Temporal Differences:

The 2012 and 2013 cohorts had the longest fork lengths while the 2011, 2014, 2017 cohorts had the shortest fork lengths (Figure 6-6). Mean fish length from the 2015, 2016 and 2018 cohorts were not significantly different from other years. Condition factor was significantly higher in the 2011 cohort than in the 2012-2014 cohorts. Cohort years 2016 through 2018 were not different than other years.

Males had similar RNA/DNA in clusters. Cohort year classes 2011 and 2012, 2015 and 2016, and 2017 and 2018 were similar (Figure 6-6). Glycogen depletion was most severe in the 2011, 2012, 2014 and 2016 cohorts (Figure 6-8).

Turbidity and salinity showed no clear pattern, although 2011 was significantly more turbid than 2013 and 2017 and more saline than 2014 (Figure 6-6). The 2013 cohort individuals were caught in the highest mean salinity. Temperature was significantly cooler for the 2011 and 2012 cohorts than for the 2013, 2014 and 2016 cohorts. Outflow at time of catch was significantly higher in 2015 through 2017 than in 2011.

The highest gill lesion scores were found in the 2012 cohort (Figure 6-8). The 2016 cohort had a large proportion of fish with rank 2 gill lesions, otherwise the proportions of gill lesion severity across other years were similar. Liver lesions were most severe in the 2012 and 2014 cohorts, while only no to low (0-2) liver lesions scores were found in cohort years 2011 and 2015 to 2017. Severe lipidosis was only observed in 2012 and 2016, while scores in all other years were similar.

There were no significant differences in GSI for males across all years (Figure 6-6).

DISCUSSION

Results from seven years of sampling adult delta smelt show that the reproductive status of delta smelt varied across years and was largely related to size and influenced by their nutritional and health status as well environmental conditions. Our model results indicate that fork length and condition factor were more strongly correlated to all the reproductive metrics measured than other health, nutritional indices, and abiotic variables. The relationships between nutritional, health and reproductive indices were inconsistent with our hypotheses, suggesting either some

nutritional and health indices do not impact reproduction, or nutritional and health indices may be more indicative of reproductive status. For example, severe glycogen depletion may indicate energy reserves were being used for oocyte development rather than evidence of food limitation stress. At the regional scale, the Cache Slough region had the highest reproductive endpoints measured, further emphasizing the region's importance for delta smelt reproduction. We detected no clear patterns in nutrition, health or reproductive metrics by annual hydrologic conditions or environmental conditions. Some of the highest and lowest reproductive indices occurred during drought years, and indices in wet years were not significantly different from those in drought years. These results suggest that factors besides water year type influence delta smelt reproductive status.

Larger individuals were positively related to female delta smelt egg size, egg number, and estradiol as well as both male and female GSI. These results are supported by previous findings that larger females had higher fecundity (Damon et al. 2016, Kurobe et al. 2016). Maternal size effects can be particularly important for reproduction; for example, larger females have exponentially higher reproductive output than smaller individuals (Barneche et al. 2018) and positive length-reproduction relationships have been established for many fish species (Mion et al. 2018, Beyer et al. 2015, Olin et al. 2012, Óskarsson and Taggart 2006, Coates 1988). Fish size, such as fork length, is associated with long-term growth that integrates over an individual's entire life and the environmental conditions the fish experiences (such as temperature, salinity, turbidity, food limitation, contaminant exposure; Lewis et al. 2021, Hammock et al. 2022). Therefore, management actions focused on increasing recruitment success should also be focused on improving growth and condition of delta smelt during all life stages.

Other studies have argued that the length-fecundity relationship is often overinflated and other measurements, such as weight, are more important when examining relationships between reproduction and fish size (Koops et al. 2004). In our study, we included condition factor as an explanatory variable, which also showed a positive relationship (though not as strong as fork length) for the reproductive endpoints measured. Fork length during the subadult and adult life stages is relatively insensitive to recent conditions as growth in length is relatively lower; however, condition factor is more sensitive (Poletto et al. 2018, Jin et al. 2015). In delta smelt, condition factor has been shown to decline significantly in as soon as seven days due to fasting in sub-adults held at 16 °C (Hammock et al. 2020). Chronic food limitation would impact reproductive indices because female fish require significant energy investment for oocyte production (Volkoff et al. 2018, Kennedy et al. 2008) and has been cited as an important factor in explaining delta smelt declines (Hamilton and Murphy 2018, Baxter et al. 2015). Lower nutrient intake, increased metabolic demand, increased nutritional stress or any combination of these factors can decrease condition factor in a relatively short period of time. While our study may not be able to differentiate between potential causes of lower condition factor, the weaker relationship between condition factor and reproductive metrics may be due to the increased metabolization of lipids and other tissues for reproduction.

Nutritional indices of glycogen depletion and RNA/DNA had mixed relationships with reproductive indices. Our study suggests glycogen depletion in adult females is associated with

oocyte production because higher levels of glycogen depletion were positively associated with increased oocyte area, oocyte mass, fecundity and GSI. Glycogen depletion has been shown to be a sign of starvation or contaminant stress in some fish species (De Pedro et al. 2003, Mehner and Wieser 1994, Schwaiger et al. 1997, Rochman et al. 2013, Hugla et al. 1999, Palemero et al. 2008), including Delta Smelt (Hammock et al. 2020). However hepatic glycogen can be rapidly converted into glucose for energy needs such as the production of vitellogenin (Rinchard et al. 2003, Mommsen and Walsh 1988). Across regions and years, severity of glycogen depletion was higher for female fish than male fish. The higher reproductive metrics observed in females likely resulted from increased vitellogenin production by metabolizing energy reserves which is indicated by high glycogen depletion. Production of sperm is not as energetically intensive (Hayward and Gillooly 2011, Schärer and Robertson 1999) which is why proportion of severe glycogen depletion was lower in male fish. Rather than nutritionally robust (low glycogen depletion, see Figure 6-2) females producing large clutches as hypothesized, our results showed a strongly supported positive correlation between high glycogen depletion and egg mass. This supports other studies demonstrating that hepatic glycogen is used during vitellogensis (Rinchard and Kestemont 2003, Soengas et al. 1993, Ladisa et al. 2022).

Contrary to the glycogen depletion relationship, RNA/DNA, an indicator of nutritional status, had a weak negative relationship with egg mass, estradiol, clutch size and GSI, indicating that fecund fish were exhibiting some nutritional stress, which may include energetic costs for oocyte development. RNA/DNA values, also indicators of potential growth, are shown to be lower during stressful conditions such as overwintering or food limitation in a variety of fish (Calderone et al 2001, Mustafa et al 1991, Fonesca and Cabral 2007, Hussna et al. 2020), including delta smelt (Hammock et al. 2020). The relatively weak negative relationship suggests that reproductive maturation is either not too stressful or that the fish were of good nutritional status and were resilient. In sub-adult delta smelt, RNA/DNA is relatively insensitive to fasting, only showing significant decreases four weeks after fasting began (Hammock et al. 2020). In other fishes, RNA/DNA can change quite rapidly (Bulow 1970) and may be more relevant for larval and juvenile stages experiencing rapid growth when responses to fasting are more rapid (Tanaka et al. 2008, Hammock et al. 2020). The negative relationship seen in the analysis may suggest that muscle growth decreases as females provision oocytes. As gonadal development is likely more imperative than muscle development as a spawning adult, RNA/DNA extracted from gonadal tissue may be more useful as a reproductive metric compared to RNA/DNA in the muscle (Villamarín et al. 2016).

Indices of health based on liver and gill tissue histopathology were found to have mixed relationships with reproductive indices. We found somewhat limited support in the model for our hypothesis that increased gill and liver lesion severity and prevalence would lead to decreased reproductive indices. This suggests that factors that could lead to gill and/or liver damage may have a limited effect on the reproductive status of delta smelt, liver and/or gill damage may have indirect effects on reproductive status that we were not able to detect, or fish with significant liver/or gill damage did not survive long enough to reproduce. Interpreting lesion data can be difficult because lesions can develop relatively rapidly depending on a myriad of interactions and conditions such as the condition of the organism and its exposure to environmental stressors such

as contaminants (Teh et al 2020). For example, the gills are sometimes more responsive to contaminant exposure because of their direct contact with the water (Teh et al. 2020), while the liver can repair damage caused by contaminants depending on the severity (dos Santos Carvalho et al. 2012, Bagnasco et al. 1991, Teh et al. 2004). Delta smelt also accumulate liver lesions as they grow, possibly because larger individuals are more tolerant of liver and gill lesions (Teh et al. 2020). An individual that can grow large may be receiving enough nutrition and energy to also compensate for the energetic costs of contaminant exposure (Beyers et al. 1999). Individual lesions may be indicators of normal activity such as hyperproliferation of chloride cells of the gills during changes in salinity (Mallatt 1985). Liver cell hyperactivity like lipidosis can be related to contaminant exposure (Teh et al. 2020) or oocyte development (Sparks 2017). There was a weak positive effect of liver lipidosis, an indicator of hepatocyte cellular hyperactivity, with GSI suggesting that this lesion could be due to reproductive maturation instead of contaminant exposure. Other changes in liver activity have been associated with spawning events or oocyte development in other fish species (Rinchard et al. 2003, Nunes et al. 2011). While contaminants did not appear to have a strong direct effect on adult reproductive status measured as a part of this study, they may have a larger effect on survival, growth, and condition on previous life stages which may affect length, condition factor and ultimately reproductive status (Lebigre et al. 2022, Mohammed 2013, Evrard et al. 2010).

The environmental variables (salinity, temperature, and turbidity) had a relatively weak relationship with most of the reproductive metrics apart from the strong negative relationship between temperature and estradiol. In other fish species, elevated temperatures have a negative effect on estradiol concentrations (Miller et al. 2015, Dorts et al. 2012, Soria et al. 2008). However, we believe that the relationship between estradiol and temperature is related to oocyte maturity. In delta smelt, estradiol increased with oocyte maturity, peaking right before spawning during oocyte maturation and then dropping during spawning and afterwards (Table S3) like other fish species (Skjæraasen et al. 2017, Johnson et al. 1991). Warmer water temperatures appear to cause delta smelt to mature and spawn earlier (Damon et al. 2016, Kurobe et al. 2022), which may explain the negative relationship between estradiol and temperature, since estradiol drops rapidly during and after spawning.

The significant but weak relationships between other environmental variables (salinity and turbidity) and reproductive metrics likely reflect migratory movements of delta smelt to spawning habitat. Migration to freshwater regions is triggered by first winter rainfall events that increase turbidity due to land runoff (Sommer et al. 2011). Delta smelt also uses turbidity as a cue to facilitate upstream migrations utilizing tidal currents (Bennett and Burau 2015). Additionally, high salinities can negatively affect sperm motility and larval survival in other osmerids (Beirão et al. 2018, Purchase 2018) and estuarine species (Green et al. 2020), which may explain the importance of migrating to freshwater to spawn. The relatively weaker relationship between these environmental variables and reproductive metrics in delta smelt should not discount the effect of environmental conditions on the life history and reproduction in Delta Smelt, these variables are important in ways that may not be reflected in the metrics we examined.

The spatial analysis found that the adult delta smelt had elevated reproductive indices in the freshwater regions of Cache Slough and SSC relative to other regions. Additionally, these regions had the highest proportion of both fish with late-stage oocytes and post spawners suggesting these regions were destinations for migrating spawners. Given that eggs have not been found in the wild, the high proportion of late-stage oocytes and post spawned adults is a good line of evidence that spawning occurs in these areas. The fish caught in Cache Slough exhibited the lowest proportion of severe gill and liver lesions, suggesting fewer stressor impacts. This is in contrast with juvenile delta smelt in Cache Slough (Hammock et al. 2015), which may suggest that healthier adults from less contaminated regions are migrating into Cache Slough to spawn, or the contaminant impacts in Cache Slough are seasonal. Although fish caught in the SSC had similar elevated reproductive indices, they exhibited more severe gill and liver lesion scores indicating this region is more stressful and less ideal for spawning compared to Cache Slough and/or longer residency in the area. While contaminant stressors may be worse in some freshwater regions such as the SSC, spawning in the region may still confer benefits such as fewer top-down threats for eggs and larvae (Kedney et al. 2009), and high food availability earlier in the year (Hammock et al. 2017). Brackish regions are energetically rich later in the year, which would select for migratory phenotypes (Hammock et al. 2017). We note that some fish caught in Suisun Marsh, a more saline region, had significantly higher reproductive status than fish caught in the Confluence and Suisun Bay, as well as the third highest proportion of stage 4.3 oocytes. This suggests that Suisun Marsh may also be a location for spawning and supports the conclusion of Hobbs et al. (2019) that a subset of delta smelt are brackish water residents (i.e., do not migrate to freshwater to spawn). Fish caught in this region also had significantly longer fork lengths and higher condition factor, further suggesting that Suisun Marsh is important and relatively high-quality habitat for delta smelt (Hammock et al. 2019, Hammock et al. 2015).

As delta smelt have a predominantly annual life cycle, the nutritional, health, and reproductive indices were examined across different year classes from 2011 to 2018. Although the time frame included two high precipitation years in 2011 and 2017, a long dry period during 2012 to 2016, and a dry year in 2018, there was no clear pattern in indices among hydrologic conditions. Delta smelt from the high precipitation years did not exhibit significantly better reproductive status than fish reared during drought years, despite recent research suggesting wild delta smelt reproduction was negatively impacted by drought (Kurobe et al. 2022). This study expands on Kurobe et al. (2022) by including more years (2015-2018) with an additional wet year class, 2017. Year class 2013 had reproductive indices significantly greater than most of the other year classes while year class 2014 (also a dry year) had some of the lowest reproductive indices. It is difficult to be conclusive as sample size of the 2017 cohort was extremely low, but the results suggest that factors other than hydrology were more strongly related to the reproductive status of delta smelt.

CONCLUSION

The results of this study suggest that the reproductive status of delta smelt is dynamic across year class and region and is related to their health and nutritional status. Impaired reproductive status is likely to inhibit the recovery and resiliency of the species. The reproductive status did not seem to relate to water year type with drought years occasionally exhibiting better reproductive status than wet years. Regional differences quantified in this study support prior conceptual models as relatively better reproductive status correlated with theorized locations for spawning and rearing habitat in Cache Slough, SSC, and Suisun Marsh. Our study suggests that nutritional stress at earlier life stages (resulting in lower fork length and condition factor) is impairing the delta smelt population by limiting reproductive potential. Actions have been developed by the member agencies of the Interagency Ecological Program to address nutritional stress due to loss of productivity in the delta smelt habitat, primarily during the summer and autumn seasons. Our results suggest improving delta smelt growth and condition to result in larger spawning fish would have the greatest effect on increasing reproductive output. The reproductive status of delta smelt was also related to indices of health, including those indices that suggest contaminant exposure. The habitats for delta smelt have been shown to be contaminated, and this study suggests that contaminant exposure has reduced the reproductive status of the fish. Along with promoting greater productivity in delta smelt habitat throughout its lifespan to maturity, additional actions addressing contaminants in the Bay-Delta system would likely improve the reproductive output, and therefore resiliency of Delta smelt.

ACKNOWLEDGEMENTS

We are grateful to the CDFW, USFWS and UCD staff and scientists who conducted trawls, measured water quality, and provided our study with specimens. We also thank Ching Teh, Tomofumi Kurobe, and numerous UCD scientists and staff who assisted with compiling this dataset. We would also like to thank Randy Baxter for providing specimens for analysis early in this study.

Project funding was provided by US Bureau of Reclamation R17AC00129, R22AC00392, US Geological Survey G15AS00018, CDFW Ecosystem Restoration Program E1183004, Metropolitan Water District MSA#207468.

REFERENCES

Allen, M.E. and Ullrey, D.E., 2004. Relationships among nutrition and reproduction and relevance for wild animals. *Zoo Biology: Published in affiliation with the American Zoo and Aquarium Association*, *23*(6), pp.475-487.

Anderson, R.O., 1996. Length, weight, and associated structural indices. *Fisheries techniques*.

Bagnasco, M., Camoirano, A., De Flora, S., Melodia, F. and Arillo, A.N.D.A., 1991. Enhanced liver metabolism of mutagens and carcinogens in fish living in polluted seawater. *Mutation Research Letters*, *262*(2), pp.129-137.

Barneche, D.R., Robertson, D.R., White, C.R. and Marshall, D.J., 2018. Fish reproductive-energy output increases disproportionately with body size. *Science*, *360*(6389), pp.642-645.

Baxter, R., Breuer, R., Brown, L., Chotkowski, M., Feyrer, F., Gingras, M., Herbold, B., Mueller-Solger, A., Nobriga, M., Sommer, T. and Souza, K., 2008. Pelagic organism decline progress report: 2007 synthesis of results. *Interagency Ecological Program for the San Francisco Estuary. Retrieved on May*, *7*, p.2011.

Beirão, J., Lewis, J.A., Wringe, B.F. and Purchase, C.F., 2018. A novel sperm adaptation to evolutionary constraints on reproduction: Pre-ejaculatory sperm activation in the beach spawning capelin (Osmeridae). *Ecology and Evolution*, *8*(4), pp.2343-2349.

Bennett, W.A. and Burau, J.R., 2015. Riders on the storm: selective tidal movements facilitate the spawning migration of threatened Delta Smelt in the San Francisco Estuary. *Estuaries and Coasts*, *38*, pp.826-835.

Beyers, D.W., Rice, J.A., Clements, W.H. and Henry, C.J., 1999. Estimating physiological cost of chemical exposure: integrating energetics and stress to quantify toxic effects in fish. *Canadian Journal of Fisheries and Aquatic Sciences*, *56*(5), pp.814-822.

Beyer, S.G., Sogard, S.M., Harvey, C.J. and Field, J.C., 2015. Variability in rockfish (Sebastes spp.) fecundity: species contrasts, maternal size effects, and spatial differences. *Environmental biology of fishes*, *98*, pp.81-100.

Bozdogan, H., 1987. Model selection and Akaike's information criterion (AIC): The general theory and its analytical extensions. *Psychometrika*, *52*(3), pp.345-370.

Brooker, R. M., Jones, G. P., & Munday, P. L. (2013). Prey selectivity affects reproductive success of a corallivorous reef fish. *Oecologia*, *172*, 409-416.

Brooks, M.L., Fleishman, E., Brown, L.R., Lehman, P.W., Werner, I., Scholz, N., Mitchelmore, C., Lovvorn, J.R., Johnson, M.L., Schlenk, D. and van Drunick, S., 2012. Life histories, salinity zones, and sublethal contributions of contaminants to pelagic fish declines illustrated with a case study of San Francisco Estuary, California, USA. *Estuaries and Coasts*, *35*, pp.603-621.

Bulow, F.J., 1970. RNA–DNA ratios as indicators of recent growth rates of a fish. *Journal of the Fisheries Board of Canada*, *27*(12), pp.2343-2349.

Burnett, L.J., Sorenson, K.J., Brandt, J., Sandhaus, E.A., Ciani, D., Clark, M., David, C., Theule, J., Kasielke, S. and Risebrough, R.W., 2013. Eggshell thinning and depressed hatching success of California condors reintroduced to central California. *The Condor*, *115*(3), pp.477-491.

Busacker, G. P., I. R. Adelman, and E. M. Goolish. 1990. Growth, in C. B. Schreck, C.B and P. B. Moyle, P.B. (eds). *Methods for Fish Biology.* Bethesda, Maryland: American Fisheries Society, pp. 363-387

Caldarone, E., Wagner, M., St Onge-Burns, J. and Buckley, L.J., 2001. Protocol and guide for estimating nucleic acids in larval fish using a fluorescence microplate reader.

Camargo, M.M. and Martinez, C.B., 2007. Histopathology of gills, kidney and liver of a Neotropical fish caged in an urban stream. *Neotropical ichthyology*, *5*, pp.327-336.

Cardoso, P.G., Rodrigues, D., Madureira, T.V., Oliveira, N., Rocha, M.J. and Rocha, E., 2017. Warming modulates the effects of the endocrine disruptor progestin levonorgestrel on the zebrafish fitness, ovary maturation kinetics and reproduction success. *Environmental Pollution*, *229*, pp.300-311.

Coates, D., 1988. Length-dependent changes in egg size and fecundity in females, and brooded embryo size in males, of fork-tailed catfishes (Pisces: Ariidae) from the Sepik River, Papua New Guinea, with some implications for stock assessments. *Journal of Fish Biology*, *33*(3), pp.455-464.

Collins, L.M., Schafer, J.L. and Kam, C.M., 2001. A comparison of inclusive and restrictive strategies in modern missing data procedures. *Psychological methods*, *6*(4), p.330.

Connon, R.E., Geist, J., Pfeiff, J., Loguinov, A.V., D'Abronzo, L.S., Wintz, H., Vulpe, C.D. and Werner, I., 2009. Linking mechanistic and behavioral responses to sublethal esfenvalerate exposure in the endangered delta smelt; Hypomesus transpacificus (Fam. Osmeridae). *BMC genomics*, *10*, pp.1-18.

Contreras, D., K. Osborn, K. Hieb, R. Baxter, and S. Slater. 2012. 2011 Status and Trends Report for Pelagic Fishes of the Upper San Francisco Estuary. *Interagency Ecological Program for the San Francisco Estuary Newsletter 25(2)*, pp. 22-35.

Crain, C.M., Kroeker, K. and Halpern, B.S., 2008. Interactive and cumulative effects of multiple human stressors in marine systems. *Ecology letters*, *11*(12), pp.1304-1315.

Crim, L. W., and B. D. Glebe. 1990. Reproduction, in Schreck, C.B. and Moyle, P.B. (eds). *Methods for Fish Biology*. Bethesda, Maryland. American Fisheries Society, pp. 526-553

Damon, L.J., Slater, S.B., Baxter, R.D. and Fujimura, R.W., 2016. Fecundity and reproductive potential of wild female delta smelt in the upper San Francisco Estuary, California. *California Fish and Game*, *102*(4), pp.188-210.

De Parsia, M., Orlando, J.L., McWayne, M.M. and Hladik, M.L., 2018. *Pesticide inputs to the Sacramento–San Joaquin Delta, 2015–16: results from the delta regional monitoring program* (No. 1089). US Geological Survey.

De Pedro, N., Delgado, M.J., Gancedo, B. and Alonso-Bedate, M., 2003. Changes in glucose, glycogen, thyroid activity and hypothalamic catecholamines in tench by starvation and refeeding. *Journal of Comparative Physiology B*, *173*, pp.475-481.

Donelson, J.M., Munday, P.L., McCormick, M.I., Pankhurst, N.W. and Pankhurst, P.M., 2010. Effects of elevated water temperature and food availability on the reproductive performance of a coral reef fish. *Marine Ecology Progress Series*, *401*, pp.233-243.

Dorts, J., Grenouillet, G., Douxfils, J., Mandiki, S.N., Milla, S., Silvestre, F. and Kestemont, P., 2012. Evidence that elevated water temperature affects the reproductive physiology of the European bullhead Cottus gobio. *Fish Physiology and Biochemistry*, *38*, pp.389-399.

dos Santos Carvalho, C., Bernusso, V.A., de Araújo, H.S.S., Espíndola, E.L.G. and Fernandes, M.N., 2012. Biomarker responses as indication of contaminant effects in Oreochromis niloticus. *Chemosphere*, *89*(1), pp.60-69.

Evrard, E., Devaux, A., Bony, S., Burgeot, T., Riso, R., Budzinski, H., Du, M.L., Quiniou, L. and Laroche, J., 2010. Responses of the European flounder Platichthys flesus to the chemical stress in estuaries: load of contaminants, gene expression, cellular impact and growth rate. *Biomarkers*, *15*(2), pp.111-127.

FLOAT-MAST (Flow Alteration - Management, Analysis, and Synthesis Team). 2021. *Synthesis of data and studies relating to Delta Smelt biology in the San Francisco Estuary, emphasizing water year 2017* (No. 95). Interagency Ecological

Fong, S., Louie, S., Werner, I., Davis, J. and Connon, R.E., 2016. Contaminant effects on California Bay–Delta species and human health. *San Francisco Estuary and Watershed Science*, *14*(4).

Green, L., Niemax, J., Herrmann, J.P., Temming, A., Behrens, J.W., Havenhand, J.N., Leder, E. and Kvarnemo, C., 2021. Sperm performance limits the reproduction of an invasive fish in novel salinities. *Diversity and Distributions*, *27*(6), pp.1091-1105.

Hammock, B.G., Hartman, R., Dahlgren, R.A., Johnston, C., Kurobe, T., Lehman, P.W., Lewis, L.S., Van Nieuwenhuyse, E., Ramírez-Duarte, W.F., Schultz, A.A. and Teh, S.J., 2022. Patterns and predictors of condition indices in a critically endangered fish. *Hydrobiologia*, pp.1-21.

Hammock, B.G., Hartman, R., Slater, S.B., Hennessy, A. and Teh, S.J., 2019. Tidal wetlands associated with foraging success of Delta Smelt. *Estuaries and Coasts*, *42*, pp.857-867.

Hammock, B.G., Hobbs, J.A., Slater, S.B., Acuña, S. and Teh, S.J., 2015. Contaminant and food limitation stress in an endangered estuarine fish. *Science of the Total Environment*, *532*, pp.316-326.

Hammock, B.G., Moose, S.P., Solis, S.S., Goharian, E. and Teh, S.J., 2019. Hydrodynamic modeling coupled with long-term field data provide evidence for suppression of phytoplankton by invasive clams and freshwater exports in the San Francisco Estuary. *Environmental Management*, *63*, pp.703-717.

Hammock, B.G., Ramirez-Duarte, W.F., Triana Garcia, P.A., Schultz, A.A., Avendano, L.I., Hung, T.C., White, J.R., Bong, Y.T. and Teh, S.J., 2020. The health and condition responses of Delta Smelt to fasting: A time series experiment. *PloS one*, *15*(9), p.e0239358.

Hammock, B.G., Slater, S.B., Baxter, R.D., Fangue, N.A., Cocherell, D., Hennessy, A., Kurobe, T., Tai, C.Y. and Teh, S.J., 2017. Foraging and metabolic consequences of semi-anadromy for an endangered estuarine fish. *PloS one*, *12*(3), p.e0173497.

Hani, Y.M.I., Turies, C., Palluel, O., Delahaut, L., Bado-Nilles, A., Geffard, A., Dedourge-Geffard, O. and Porcher, J.M., 2019. Effects of a chronic exposure to different water temperatures and/or to an environmental cadmium concentration on the reproduction of the threespine stickleback (Gasterosteus aculeatus). *Ecotoxicology and environmental safety*, *174*, pp.48-57.

Hashemi, S., Blust, R. and De Boeck, G., 2008. The effect of starving and feeding on copper toxicity and uptake in Cu acclimated and non-acclimated carp. *Aquatic toxicology*, *86*(2), pp.142-147.

Hayward, A. and Gillooly, J.F., 2011. The cost of sex: quantifying energetic investment in gamete production by males and females. *PLoS One*, 6(1), p.e16557.

Hobbs, J.A., Lewis, L.S., Willmes, M., Denney, C. and Bush, E., 2019. Complex life histories discovered in a critically endangered fish. *Scientific Reports*, *9*(1), p.16772.

Holmstrup, M., Bindesbøl, A.M., Oostingh, G.J., Duschl, A., Scheil, V., Köhler, H.R., Loureiro, S., Soares, A.M., Ferreira, A.L., Kienle, C. and Gerhardt, A., 2010. Interactions between effects of environmental chemicals and natural stressors: a review. *Science of the Total Environment*, *408*(18), pp.3746-3762.

Hopkins, W.A., Snodgrass, J.W., Roe, J.H., Staub, B.P., Jackson, B.P. and Congdon, J.D., 2002. Effects of food ration on survival and sublethal responses of lake chubsuckers (Erimyzon sucetta) exposed to coal combustion wastes. *Aquatic Toxicology*, *57*(3), pp.191-202.

Houde, E.D., 1997. Patterns and trends in larval-stage growth and mortality of teleost fish. *Journal of Fish Biology*, *51*, pp.52-83.

Hugla, J.L. and Thomé, J.P., 1999. Effects of polychlorinated biphenyls on liver ultrastructure, hepatic monooxygenases, and reproductive success in the barbel. *Ecotoxicology and Environmental Safety*, *42*(3), pp.265-273.

Hussna, I.A., Asmi, O., Shah, F., Bhat, B., Hussain, T., Hafeez, M., Rashid, S., Razak, N. and Hussain, R.A., 2020. RNA: DNA ratio as an indicator of growth, nutritional status and condition of fish: A review. *Journal of Entomology and Zoology Studies*, *8*, pp.654-8.

Izquierdo, M.S., Fernandez-Palacios, H. and Tacon, A.G.J., 2001. Effect of broodstock nutrition on reproductive performance of fish. *Aquaculture*, *197*(1-4), pp.25-42.

Jabusch, T., Trowbridge, P., Heberger, M., Orlando, J., De Parsia, M. and Stillway, M., 2018. Delta Regional Monitoring Program Annual Monitoring Report for Fiscal Year 2015–16: Pesticides and Toxicity. *Richmond, CA: Aquatic Science Center. http://www. sfei. org/documents/delta-pesticides-2016*.

Jeffries, K.M., Komoroske, L.M., Truong, J., Werner, I., Hasenbein, M., Hasenbein, S., Fangue, N.A. and Connon, R.E., 2015. The transcriptome-wide effects of exposure to a pyrethroid pesticide on the Critically Endangered delta smelt Hypomesus transpacificus. *Endangered Species Research*, *28*(1), pp.43-60.

Jin, J., Kurobe, T., Ramírez-Duarte, W.F., Bolotaolo, M.B., Lam, C.H., Pandey, P.K., Hung, T.C., Stillway, M.E., Zweig, L., Caudill, J. and Lin, L., 2018. Sub-lethal effects of herbicides penoxsulam, imazamox, fluridone and glyphosate on Delta Smelt (Hypomesus transpacificus). *Aquatic Toxicology*, *197*, pp.79-88.

Jin, S., Yan, X., Zhang, H. and Fan, W., 2015. Weight–length relationships and Fulton's condition factors of skipjack tuna (Katsuwonus pelamis) in the western and central Pacific Ocean. *PeerJ*, *3*, p.e758.

Johnson, L.L., Casillas, E., Myers, M.S., Rhodes, L.D. and Olson, O.P., 1991. Patterns of oocyte development and related changes in plasma 17-β estradiol, vitellogenin, and plasma chemistry in English sole Parophrys vetulus Girard. *Journal of Experimental Marine Biology and Ecology*, 152(2), pp.161-185.

Jørgensen, E.H., Bye, B.E. and Jobling, M., 1999. Influence of nutritional status on biomarker responses to PCB in the Arctic charr (Salvelinus alpinus). *Aquatic Toxicology*, *44*(4), pp.233-244.

Kedney, G.I., Boule, V. and Fitzgerald, G.J., 1987. The reproductive ecology of threespine sticklebacks breeding in fresh and brackish water. In *American Fisheries Society Symposium* (Vol. 1, pp. 151-161).

Kennedy, J., Witthames, P.R., Nash, R.D.M. and Fox, C.J., 2008. Is fecundity in plaice (Pleuronectes platessa L.) down-regulated in response to reduced food intake during autumn?. *Journal of Fish Biology*, *72*(1), pp.78-92.

Kreiter, N.A. and Wise, D.H., 2001. Prey availability limits fecundity and influences the movement pattern of female fishing spiders. *Oecologia*, pp.417-424.

Koops, M.A., Hutchings, J.A. and McIntyre, T.M., 2004. Testing hypotheses about fecundity, body size and maternal condition in fishes. *Fish and fisheries*, *5*(2), pp.120-130.

Kurobe, T., Hammock, B.G., Damon, L.J., Hung, T.C., Acuña, S., Schultz, A.A. and Teh, S.J., 2022. Reproductive strategy of Delta Smelt Hypomesus transpacificus and impacts of drought on reproductive performance. *PloS one*, *17*(3), p.e0264731.

Kurobe, T., Park, M.O., Javidmehr, A., Teh, F.C., Acuña, S.C., Corbin, C.J., Conley, A.J., Bennett, W.A. and Teh, S.J., 2016. Assessing oocyte development and maturation in the threatened Delta Smelt, Hypomesus transpacificus. *Environmental biology of fishes*, *99*, pp.423-432.

Ladisa, C., Ma, Y. and Habibi, H.R., 2022. Metabolic Changes During Growth and Reproductive Phases in the Liver of Female Goldfish (Carassius auratus). *Frontiers in Cell and Developmental Biology*, 10.

Lange, K., Bruder, A., Matthaei, C.D., Brodersen, J. and Paterson, R.A., 2018. Multiple-stressor effects on freshwater fish: Importance of taxonomy and life stage. *Fish and Fisheries*, *19*(6), pp.974-983.

Lebigre, C., Aminot, Y., Munschy, C., Drogou, M., Le Goff, R., Briant, N. and Chouvelon, T., 2022. Trace metal elements and organic contaminants are differently related to the growth and body condition of wild European sea bass juveniles. *Aquatic Toxicology*, *248*, p.106207.

Lewis, L.S., Denney, C., Willmes, M., Xieu, W., Fichman, R.A., Zhao, F., Hammock, B.G., Schultz, A., Fangue, N. and Hobbs, J.A., 2021. Otolith-based approaches indicate strong effects of environmental variation on growth of a critically endangered estuarine fish. *Marine Ecology Progress Series*, *676*, pp.37-56.

Lindberg, J.C., Tigan, G., Ellison, L., Rettinghouse, T., Nagel, M.M. and Fisch, K.M., 2013. Aquaculture methods for a genetically managed population of endangered Delta Smelt. *North American Journal of Aquaculture*, *75*(2), pp.186-196.

Lopes, A.F., Murdoch, R., Martins-Cardoso, S., Madeira, C., Costa, P.M., Félix, A.S., Oliveira, R.F., Bandarra, N.M., Vinagre, C., Lopes, A.R. and Gonçalves, E.J., 2022. Differential Effects of Food Restriction and Warming in the Two-Spotted Goby: Impaired Reproductive Performance and Stressed Offspring. *Fishes*, *7*(4), p.194.

Lott, J. 1998. Feeding habits of juvenile and adult delta smelt from the Sacramento-San Joaquin River Estuary. *Interagency Ecological Program Newsletter, 11(1)*, pp.14-19.

Mallatt, J., 1985. Fish gill structural changes induced by toxicants and other irritants: a statistical review. *Canadian Journal of Fisheries and Aquatic Sciences*, *42*(4), pp.630-648.

McCool, J.I., 2012. *Using the Weibull distribution: reliability, modeling, and inference* (Vol. 950). John Wiley & Sons.

Mehner, T. and Wieser, W., 1994. Energetics and metabolic correlates of starvation in juvenile perch (Perca fluviatilis). *Journal of fish biology*, *45*(2), pp.325-333.

Meng, X.L., 1994. Multiple imputation with uncongenial sources of input (with discussion). *Statistical Science*, *9*(4), pp.538-573.

Miller, G.M., Kroon, F.J., Metcalfe, S. and Munday, P.L., 2015. Temperature is the evil twin: effects of increased temperature and ocean acidification on reproduction in a reef fish. *Ecological Applications*, *25*(3), pp.603-620.

Mion, M., Thorsen, A., Vitale, F., Dierking, J., Herrmann, J.P., Huwer, B., von Dewitz, B. and Casini, M., 2018. Effect of fish length and nutritional condition on the fecundity of distressed Atlantic cod Gadus morhua from the Baltic Sea. *Journal of fish biology*, *92*(4), pp.1016-1034.

Miranda, L.A., Chalde, T., Elisio, M. and Strüssmann, C.A., 2013. Effects of global warming on fish reproductive endocrine axis, with special emphasis in pejerrey Odontesthes bonariensis. *General and Comparative Endocrinology*, *192*, pp.45-54.

Mohammed, A., 2013. Why are early life stages of aquatic organisms more sensitive to toxicants than adults. *New insights into toxicity and drug testing*, pp.49-62.

Mommsen, T.P. and Walsh, P.J., 1988. Vitellogenesis and oocyte assembly. In *Fish physiology* (Vol. 11, pp. 347-406). Academic Press.

Moyle, P.B., Brown, L.R., Durand, J.R. and Hobbs, J.A., 2016. Delta smelt: life history and decline of a once-abundant species in the San Francisco Estuary. *San Francisco Estuary and Watershed Science*, *14*(2).

Mundy, P.C., Hartz, K.E.H., Fulton, C.A., Lydy, M.J., Brander, S.M., Hung, T.C., Fangue, N.A. and Connon, R.E., 2021. Exposure to permethrin or chlorpyrifos causes differential dose-and time-dependent behavioral effects at early larval stages of an endangered teleost species. *Endangered species research*, *44*, pp.89-103.

Niehoff, B., 2004. The effect of food limitation on gonad development and egg production of the planktonic copepod Calanus finmarchicus. *Journal of experimental marine biology and ecology*, *307*(2), pp.237-259.

Nunes, C., Silva, A., Soares, E. and Ganias, K., 2011. The use of hepatic and somatic indices and histological information to characterize the reproductive dynamics of Atlantic sardine Sardina pilchardus from the Portuguese coast. *Marine and Coastal Fisheries*, *3*(1), pp.127-144.

Olin, M., Jutila, J., Lehtonen, H., Vinni, M., Ruuhijärvi, J., Estlander, S., Rask, M., Kuparinen, A. and Lappalainen, J., 2012. Importance of maternal size on the reproductive success of perch, Perca fluviatilis, in small forest lakes: implications for fisheries management. *Fisheries Management and Ecology*, *19*(5), pp.363-374.

Óskarsson, G.J. and Taggart, C.T., 2006. Fecundity variation in Icelandic summer-spawning herring and implications for reproductive potential. *ICES Journal of Marine Science*, *63*(3), pp.493-503.

Palermo, F.A., Mosconi, G., Angeletti, M. and Polzonetti-Magni, A.M., 2008. Assessment of water pollution in the Tronto River (Italy) by applying useful biomarkers in the fish model Carassius auratus. *Archives of environmental contamination and toxicology*, *55*, pp.295-304.

Pandey, G. and Madhuri, S., 2014. Heavy metals causing toxicity in animals and fishes. *Research Journal of Animal, Veterinary and Fishery Sciences*, *2*(2), pp.17-23.

Pereira, S., Pinto, A.L., Cortes, R., Fontaínhas-Fernandes, A., Coimbra, A.M. and Monteiro, S.M., 2013. Gill histopathological and oxidative stress evaluation in native fish captured in Portuguese northwestern rivers. *Ecotoxicology and Environmental Safety*, *90*, pp.157-166.

Petitjean, Q., Jean, S., Gandar, A., Côte, J., Laffaille, P. and Jacquin, L., 2019. Stress responses in fish: From molecular to evolutionary processes. *Science of the Total Environment*, *684*, pp.371-380.

Phillips, R.A., Caldow, R.W.G. and Furness, R.W., 1996. The influence of food availability on the breeding effort and reproductive success of Arctic Skuas Stercorarius parasiticus. *Ibis*, *138*(3), pp.410-419.

Poletto, J.B., Martin, B., Danner, E., Baird, S.E., Cocherell, D.E., Hamda, N., Cech, Jr, J.J. and Fangue, N.A., 2018. Assessment of multiple stressors on the growth of larval green sturgeon Acipenser medirostris: implications for recruitment of early life-history stages. *Journal of fish biology*, *93*(5), pp.952-960.

Post, J.R. and Parkinson, E.A., 2001. Energy allocation strategy in young fish: allometry and survival. *Ecology*, *82*(4), pp.1040-1051.

Purchase, C.F., 2018. Low tolerance of salt water in a marine fish: new and historical evidence for surprising local adaption in the well-studied commercially exploited capelin. *Canadian Journal of Fisheries and Aquatic Sciences*, *75*(5), pp.673-681.

Rainuzzo, J.R., Reitan, K.I. and Olsen, Y., 1997. The significance of lipids at early stages of marine fish: a review. *Aquaculture*, *155*(1-4), pp.103-115.

Rinchard, J. and Kestemont, P., 2003. Liver changes related to oocyte growth in roach, a single spawner fish, and in bleak and white bream, two multiple spawner fish. *International Review of Hydrobiology: A Journal Covering all Aspects of Limnology and Marine Biology*, *88*(1), pp.68-76.

Rochman, C.M., Hoh, E., Kurobe, T. and Teh, S.J., 2013. Ingested plastic transfers hazardous chemicals to fish and induces hepatic stress. *Scientific reports*, *3*(1), pp.1-7.

Schafer, J.L., 1997. *Analysis of incomplete multivariate data*. CRC press.

Schärer, L. and Robertson, D.R., 1999. Sperm and milt characteristics and male v. female gametic investment in the Caribbean reef fish, Thalassoma bifasciatum. *Journal of Fish Biology*, 55(2), pp.329-343.

Schwaiger, J., Wanke, R., Adam, S., Pawert, M., Honnen, W. and Triebskorn, R., 1997. The use of histopathological indicators to evaluate contaminant-related stress in fish. *Journal of Aquatic Ecosystem Stress and Recovery*, *6*, pp.75-86.

Segarra, A., Mauduit, F., Amer, N.R., Biefel, F., Hladik, M.L., Connon, R.E. and Brander, S.M., 2021. Salinity changes the dynamics of pyrethroid toxicity in terms of behavioral effects on newly hatched delta smelt larvae. *Toxics*, *9*(2), p.40.

Skjæraasen, J.E., Devine, J.A., Godiksen, J.A., Fonn, M., OtterÅ, H., Kjesbu, O.S., Norberg, B., Langangen, Ø. and Karlsen, Ø., 2017. Timecourse of oocyte development in saithe Pollachius virens. *Journal of fish biology*, 90(1), pp.109-128.

Soengas, J.L., Sanmartín, B., Barciela, P., Aldegunde, M. and Rozas, G., 1993. Changes in carbohydrate metabolism in domesticated rainbow trout (Oncorhynchus mykiss) related to spermatogenesis. *Comparative Biochemistry and Physiology Part B: Comparative Biochemistry*, 105(3-4), pp.665-671.

Soria, F.N., Strüssmann, C.A. and Miranda, L.A., 2008. High water temperatures impair the reproductive ability of the pejerrey fish Odontesthes bonariensis: effects on the hypophyseal-gonadal axis. *Physiological and Biochemical Zoology*, *81*(6), pp.898-905.

Sommer, T., Mejia, F.H., Nobriga, M.L., Feyrer, F. and Grimaldo, L., 2011. The spawning migration of delta smelt in the upper San Francisco estuary. *San Francisco Estuary and Watershed Science*, 9, p.2.

Sparks, D.W., 2017. *Fish, Polychlorinated Biphenyls (PCBs) and Natural Resource Injury*. West Virginia University.

Sreevalli, N. and Sudha, H.R., 2022. Total protein, glycogen and cholesterol content in the ovary and liver during prespawning and spawning season in Mystus vittatus (Bloch). *Thanuj International Publishers, Tamil Nadu, India*, p.136.

Stillway M.E., Acuña S., Hung T.C., Schultz A.A., Teh, S.J. 2021. Assessment of acute toxicity and histopathology of environmental contaminants in Delta Smelt (Hypomesus transpacificus) in relation to delta outflow. In: Schultz AA, editor. Directed Outflow Project: Technical Report 2. U.S. Bureau of Reclamation. Mid-Pacific Region, Sacramento, CA: U.S Bureau of Reclamation, Bay-Delta Office,. p 61-150.

Tanaka, Y., Satoh, K., Yamada, H., Takebe, T., Nikaido, H. and Shiozawa, S., 2008. Assessment of the nutritional status of field-caught larval Pacific bluefin tuna by RNA/DNA ratio based on a starvation experiment of hatchery-reared fish. *Journal of Experimental Marine Biology and Ecology*, *354*(1), pp.56-64.

Taslima, Khanam, Md Al-Emran, Mohammad Shadiqur Rahman, Jabed Hasan, Zannatul Ferdous, Md Fazle Rohani, and Md Shahjahan. "Impacts of heavy metals on early development, growth and reproduction of fish–A review." *Toxicology Reports* (2022).

Teh, S.J., Adams, S.M. and Hinton, D.E., 1997. Histopathologic biomarkers in feral freshwater fish populations exposed to different types of contaminant stress. *Aquatic toxicology*, *37*(1), pp.51-70.

Teh, S.J., Deng, X., Deng, D.F., Teh, F.C., Hung, S.S., Fan, T.W.M., Liu, J. and Higashi, R.M., 2004. Chronic effects of dietary selenium on juvenile Sacramento splittail (Pogonichthys macrolepidotus). *Environmental science & technology*, *38*(22), pp.6085-6093.

Teh, S. J., D. V. Baxa, B. G. Hammock, S. A. Gandhi, and T. Kurobe. 2016. A novel and versatile flash-freezing approach for evaluating the health of Delta Smelt. *Aquatic Toxicology, 170*, pp.152-161.

Teh, S.J., Schultz, A.A., Duarte, W.R., Acuña, S., Barnard, D.M., Baxter, R.D., Garcia, P.A.T. and Hammock, B.G., 2020. Histopathological assessment of seven year-classes of Delta Smelt. *Science of The Total Environment*, *726*, p.138333.

Van Buuren, S., 2018. *Flexible imputation of missing data*. CRC press.

Van Buuren, S. and Groothuis-Oudshoorn, K., 2011. mice: Multivariate imputation by chained equations in R. *Journal of statistical software*, *45*, pp.1-67.

Villamarín, F., Magnusson, W.E., Jardine, T.D., Valdez, D., Woods, R. and Bunn, S.E., 2016. Temporal uncoupling between energy acquisition and allocation to reproduction in a herbivorous-detritivorous fish. *PLoS One, 11(3)*, e0150082.

Volkoff, H. and London, S., 2018. Nutrition and reproduction in fish. *Encyclopedia of reproduction*, *2*, pp.1-6.

Weston, D.P., Asbell, A.M., Lesmeister, S.A., Teh, S.J. and Lydy, M.J., 2014. Urban and agricultural pesticide inputs to a critical habitat for the threatened delta smelt (Hypomesus transpacificus). *Environmental toxicology and chemistry*, *33*(4), pp.920-929.

Weston, D., Moschet, C., Young, T., Johanif, N., Poynton, H., Major, K., Connon, R. and Hasenbein, S., 2019. Chemical and toxicological impacts to Cache Slough following storm-driven contaminant inputs. *San Francisco Estuary and Watershed Science*, *17*(3).

Wiles, S.C., Bertram, M.G., Martin, J.M., Tan, H., Lehtonen, T.K. and Wong, B.B., 2020. Long-term pharmaceutical contamination and temperature stress disrupt fish behavior. *Environmental Science & Technology*, *54*(13), pp.8072-8082.

Winder, M. and Jassby, A.D., 2011. Shifts in zooplankton community structure: implications for food web processes in the upper San Francisco Estuary. *Estuaries and Coasts*, *34*, pp.675-690.

Yamamoto, Y., Luckenbach, J.A., Goetz, F.W., Young, G. and Swanson, P., 2011. Disruption of the salmon reproductive endocrine axis through prolonged nutritional stress: Changes in circulating hormone levels and transcripts for ovarian genes involved in steroidogenesis and apoptosis. *General and Comparative Endocrinology*, 172(3), pp.331-343.

TABLES

Table 6-1: Frequency table showing number of times each variable was retained across backwards model selection done on 100 imputed datasets.

Numbers in bold indicate which variables were used for the pooled final model using imputed data. Asterisk (*) indicates variables included in the final model after backwards model selection using the original data set. Numbers in parentheses under each dependent variable is percent missing data. Percent missing in years $2011-2015 and ^ 2011-2013. Percent missing for GSI for females is 1.13% and males is 1.0%.

			Dependent Variables (Reproductive status)					
		Independent Variables	GSI (1%)	Clutch Size (20%)	Mass Per Egg (20%)	Egg Area (3%)	Estradiol Level (61%)	Percent Missing
Females	Condition	log(Condition Factor)	100*	100*	100*	100*	82*	<1
		log(Fork Length)	100	100*	100	100*	53*	<1
	Health Status	Glycogen Depletion	100*	39*	92*	74*	28*	62
		log(RNA/DNA)	91*	72*	37*	53	82*	57
		Liver Lesions	58*	4	45	28	10*	62
		Gill Lesions	46*	6	14	11*	6	62
		Lipidosis	3*	2	6	3	8	62
	Environment	log(Salinity)	14*	29*	76	93*	50	<1
		log(Temperature)	9	1	38	0	8*	<1
		log(Turbidity)	0	99*	98	2	1	<1
	Random Effects	Cohort Year	100*	95	100*	100	4	0
		Month	100*	69	100*	100	89	0
		Region	99	30	99	100	100	0
		Year Type	0	100*	100*	0	0	0
		None	0	0	0	0	0	
Males	Condition	log(Condition Factor)	93					0
		log(Fork Length)	100*					0
	Health Status	Glycogen Depletion	5					68
		log(RNA/DNA)	0					60
		Liver Lesions	3					68
		Gill Lesions	3					68
		Lipidosis	9					68
	Enviro-nment	log(Salinity)	1*					0
		log(Temperature)	0					0
		log(Turbidity)	0					0
	Random Effects	Cohort Year	0*					0
		Month	100					0
		Region	0					0
		Year Type	0					0
		None	0					

FIGURES

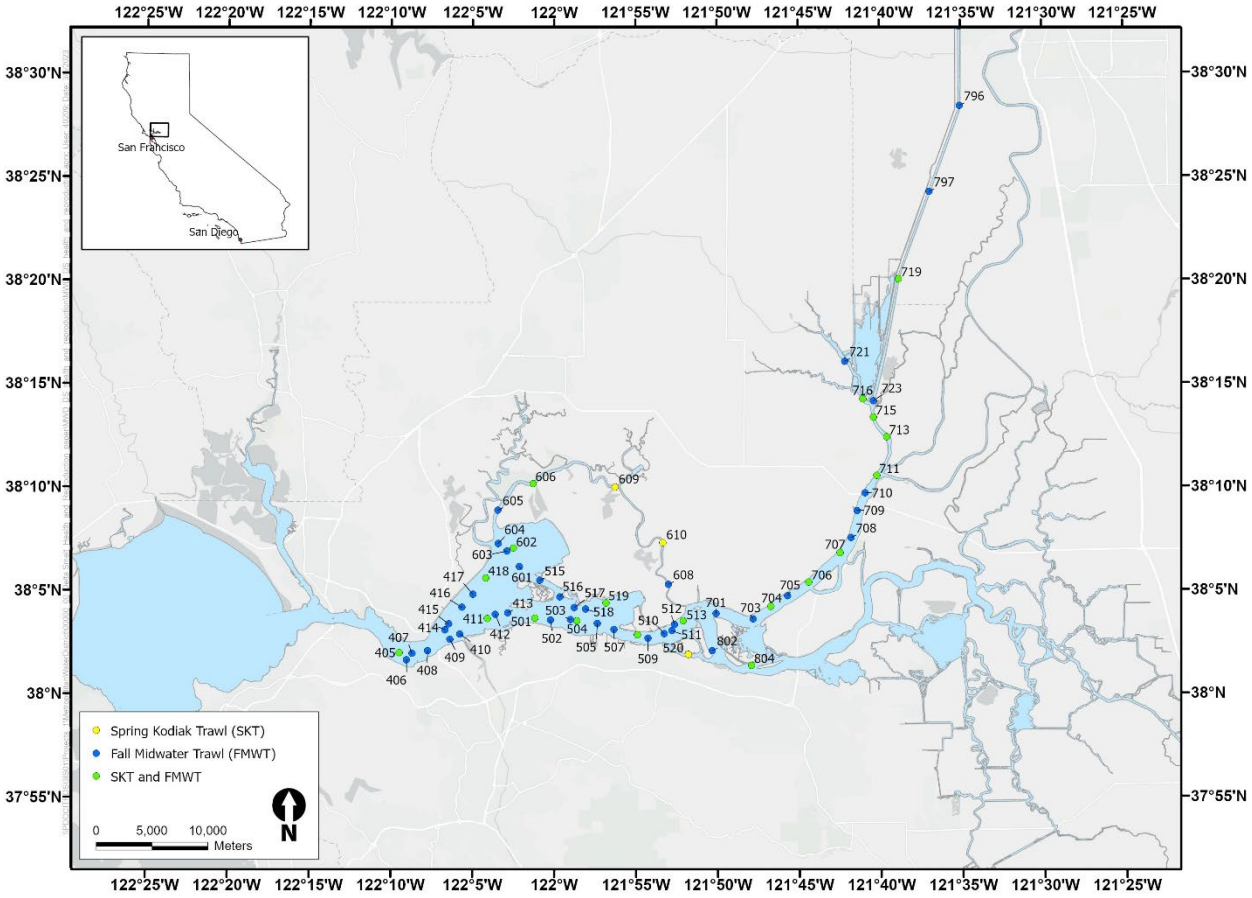

Figure 6-1: Map of the upper San Francisco Estuary and California Department of Fish and Wildlife sampling locations for Spring Kodiak Trawl survey.

The regions consisted of stations 719, 795, 796, and 797 for the Sacramento River Deep Water Ship Channel (SSC), 713, 715, 716, 721, and 723 for Cache Slough, 508, 509, 510, 511, 512, 513, 520, 701, 703, 704, 705, 706, 707, 711, 712, 713, 801, 802, 804, 806 and 807 for the Confluence of Sacramento and San Joaquin River (Confluence), 405, 407, 411, 412, 413, 416, 417, 418, 501, 502, 503, 504, 505, 507, 515, 516, 517, 518, 519, 601, 602 and 603 for Suisun Bay, and 605, 606, 609, and 610 for Suisun Marsh.

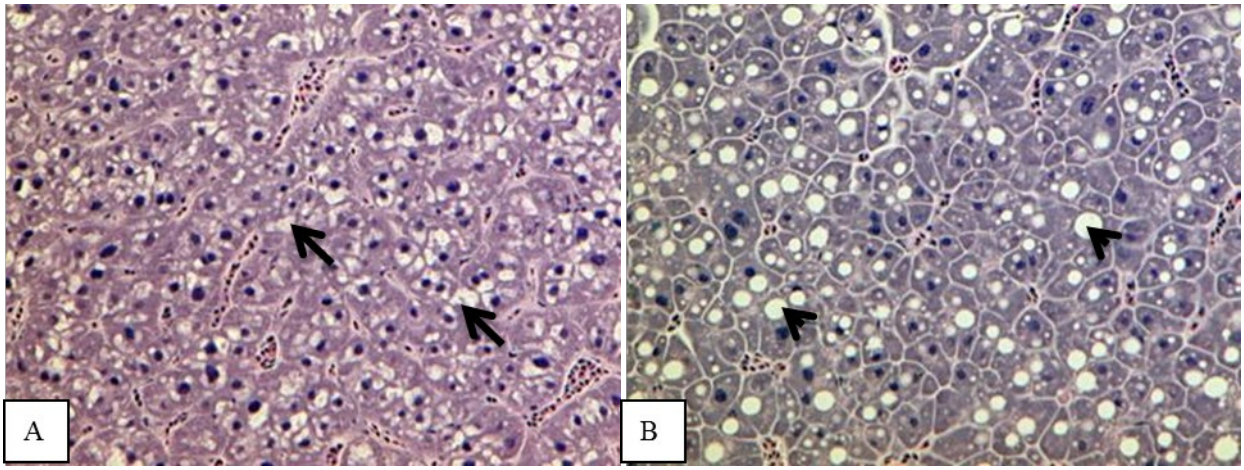

Figure 6-2: Histopathology of Delta smelt liver tissue showing A) glycogen (arrows) rich liver and B) Liver with severe Lipidosis (arrowheads) and exhibiting little to no glycogen.

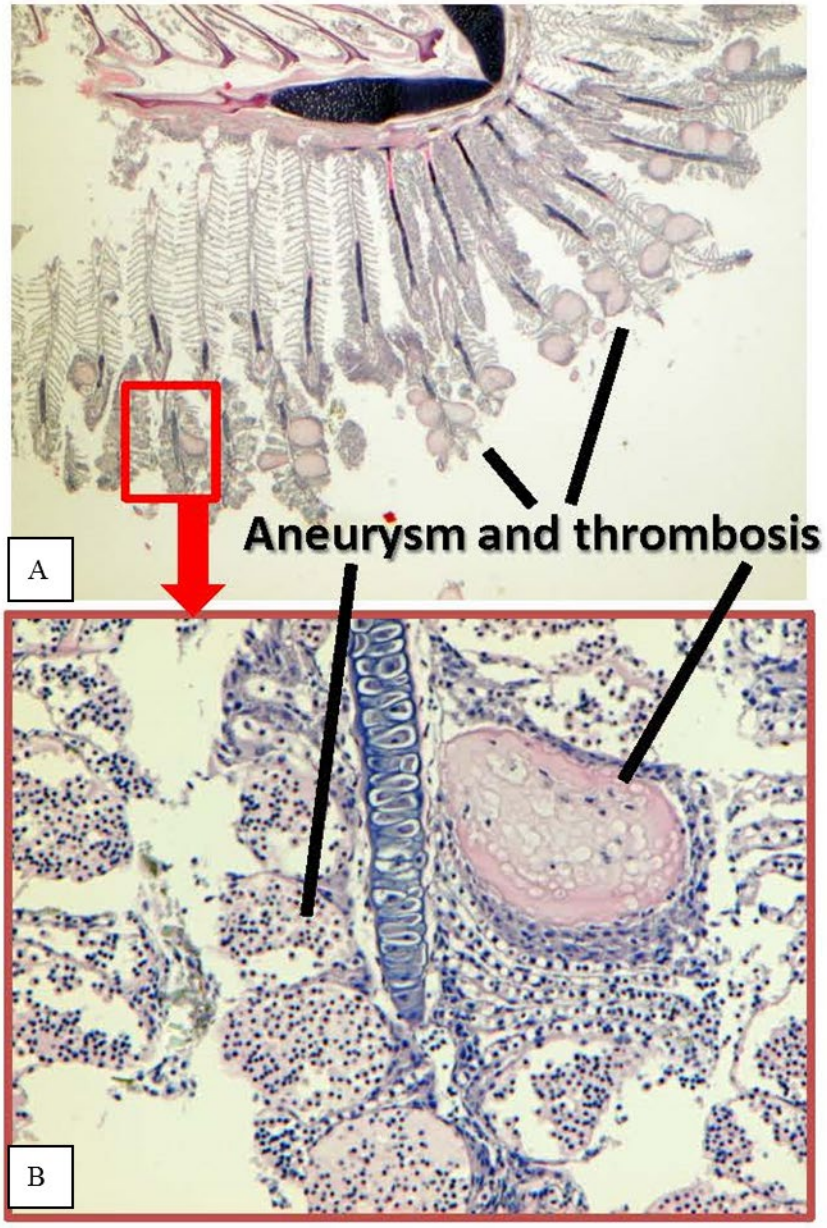

Figure 6-3: Histopathology of gill tissue for Delta smelt at A) 100x and B) 400x magnification.

The black lines designate Aneurysm and Thrombosis.

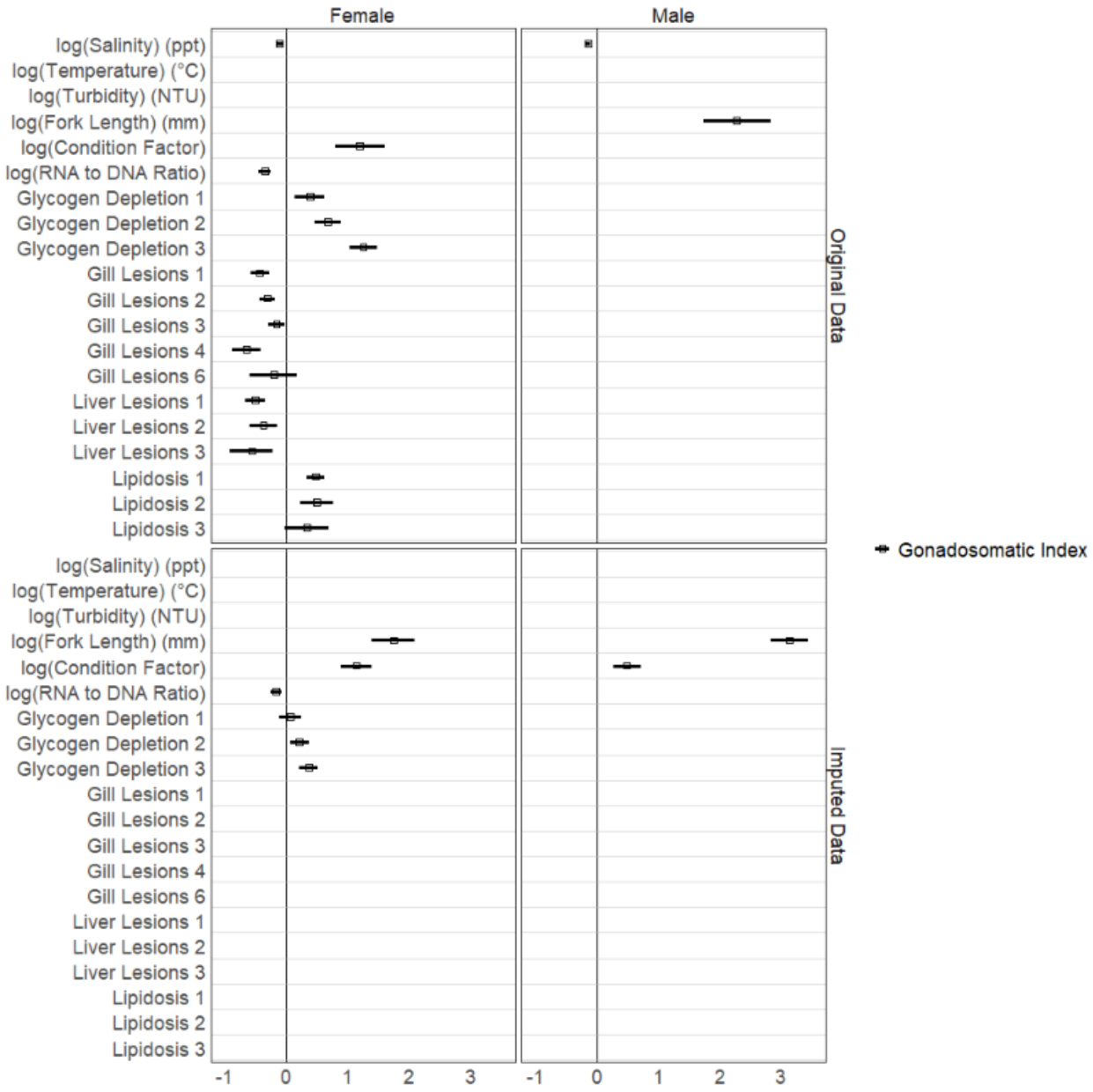

Figure 6-4: Model estimates and standard error for imputed and original data sets showing effects on reproductive outcomes for delta smelt collected in San Francisco Bay, CA, USA from 2011 to 2019.

Gonadosomatic index for males and females shown above. Other reproductive outcomes for females shown below. Standard error lines that cross zero show insignificant (p-value <0.05) model results. Reproductive outcomes without model estimates did not make final model.

Figure 6-4 continued.

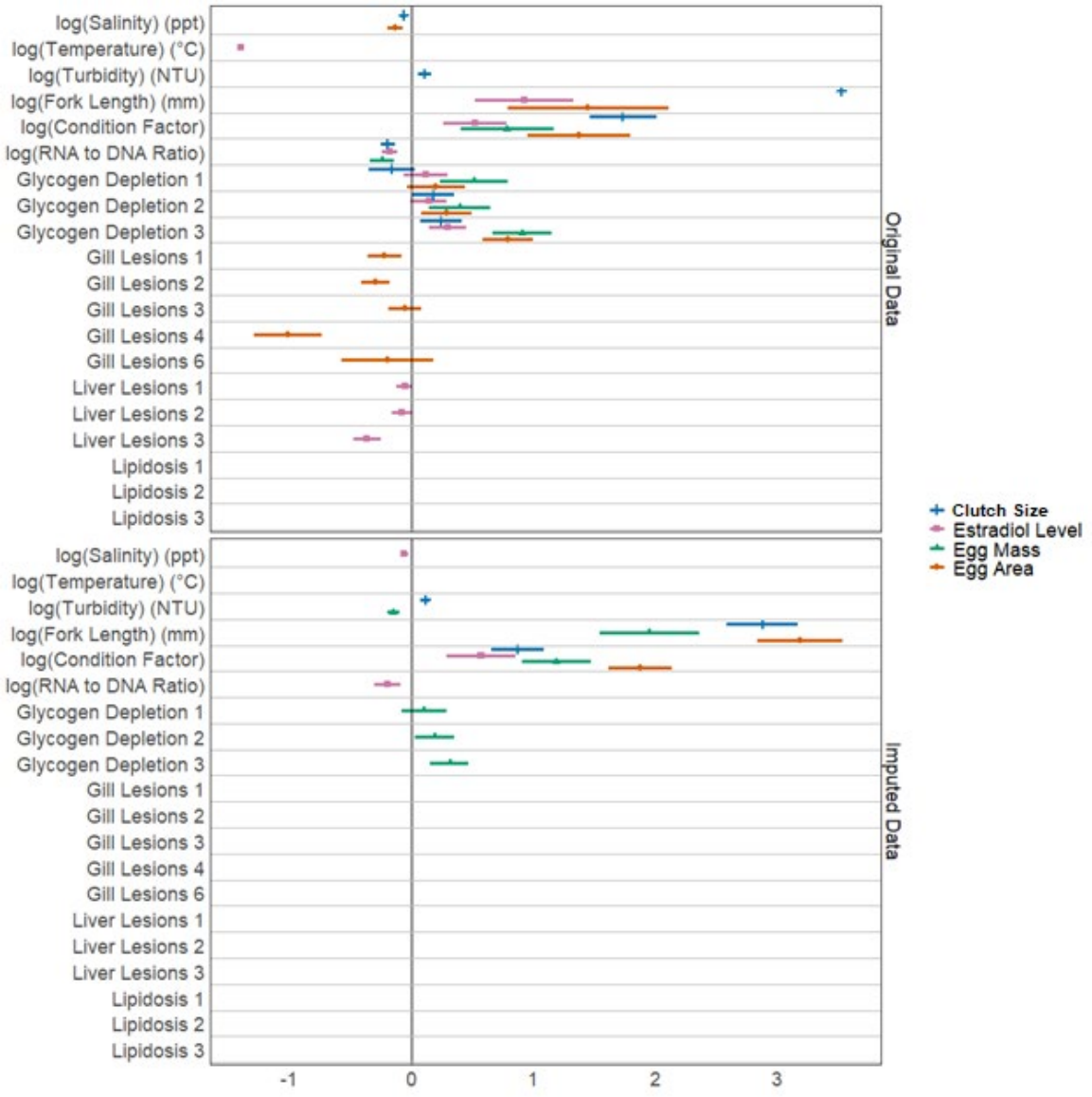

Female

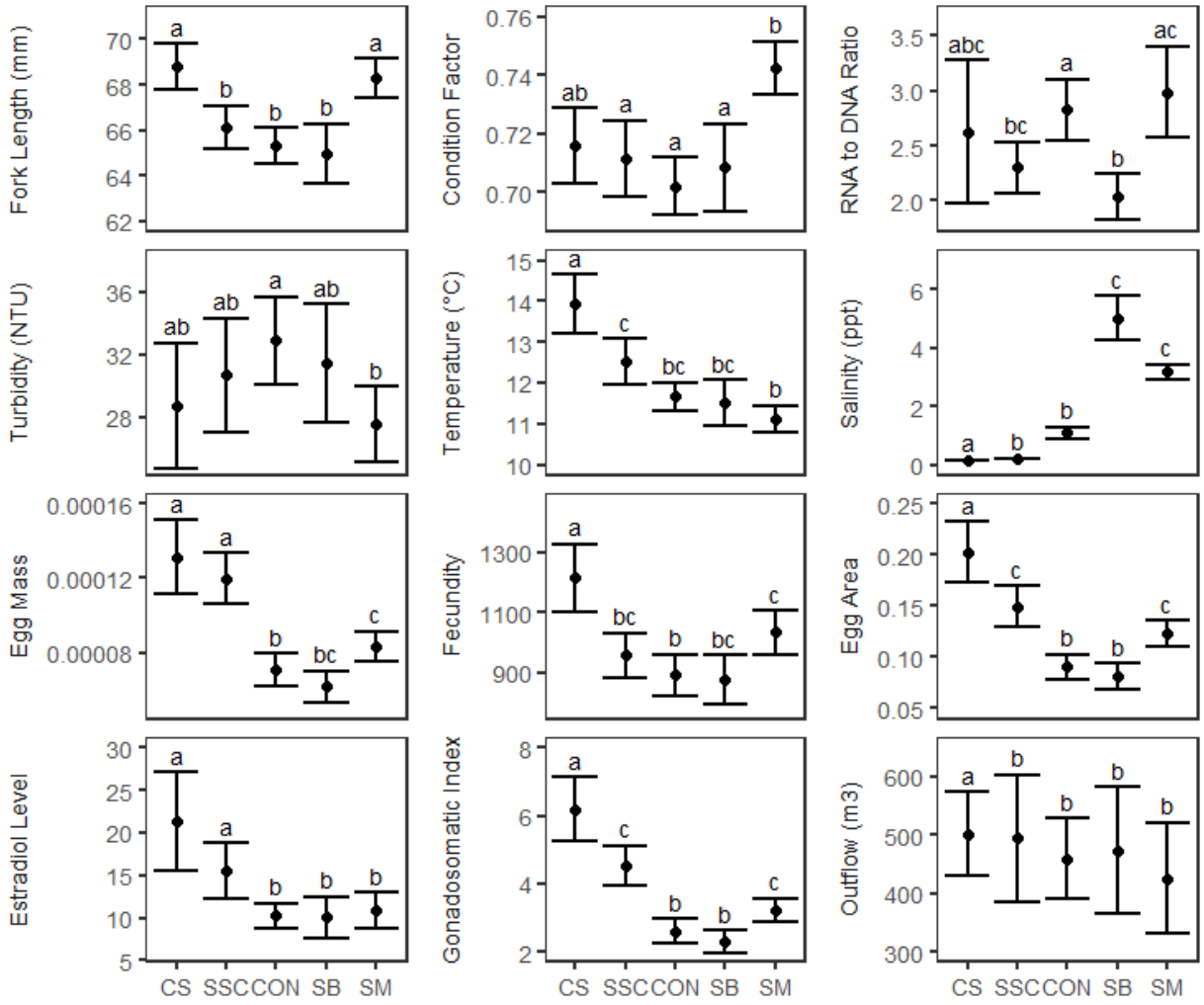

Figure 6-5: Mean and confidence interval plots for differences in water quality, health, and reproductive status within 5 regions of the San Francisco Estuary on days female (top) and male (bottom) fish were collected.

Lowercase letters indicate no significant differences were observed in the mean (95% confidence intervals) between the regions. Abbreviations: CS- Cache Slough, SSC - Sacramento Deep Water Ship Channel, CON - Confluence, SB - Suisun Bay, SM - Suisun Marsh.

Figure 6-5 continued.

Male

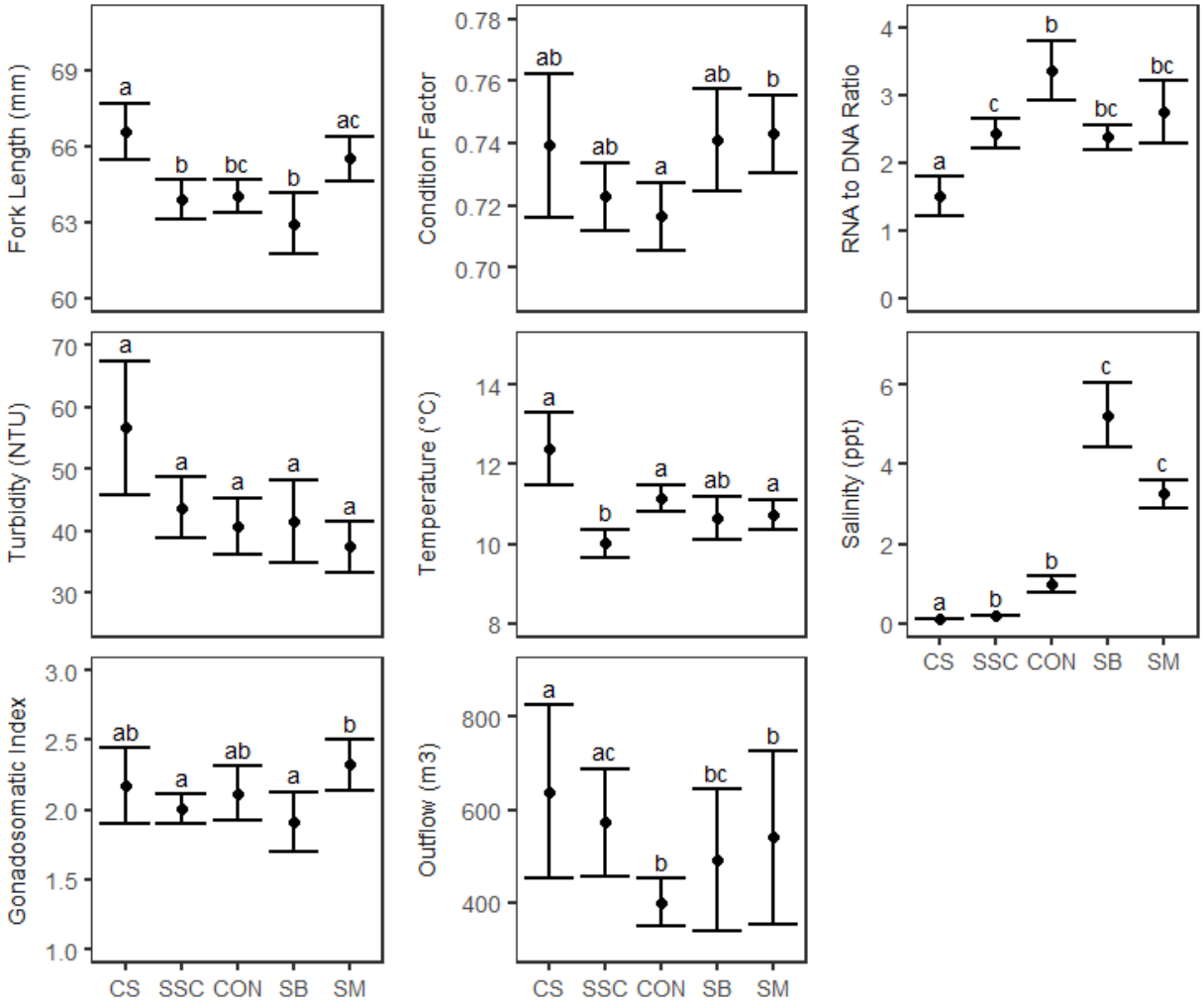

Female

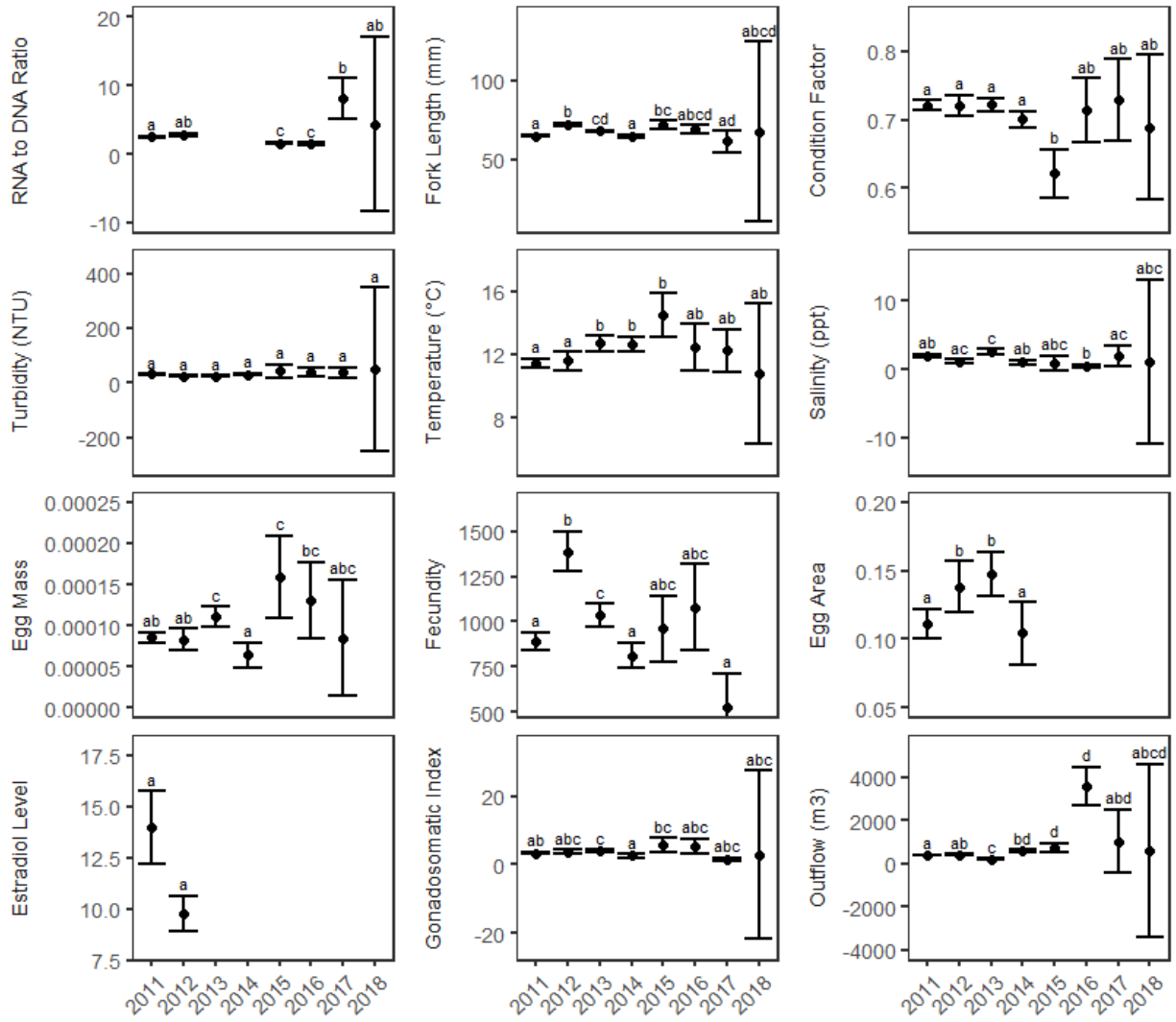

Figure 6-6: Mean and confidence interval plots indicating differences in water quality, health, and reproductive status across 8 years with variable water flow within the San Francisco Estuary on days female (top) and male (bottom) fish were collected.

Matching lowercase letters indicate no significant differences were observed between the regions.

Figure 6-6 continued.

Male

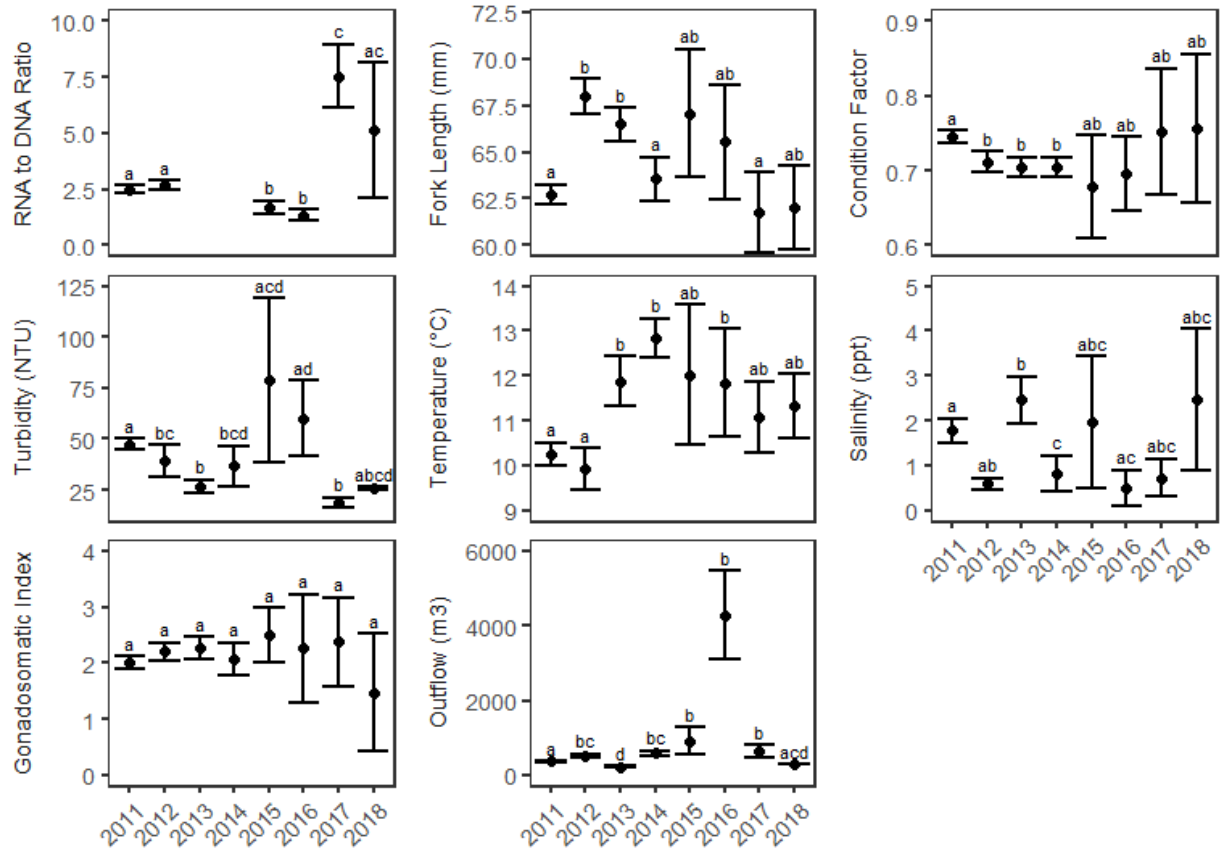

Abbreviations consistent with Figure 6-5.

Female

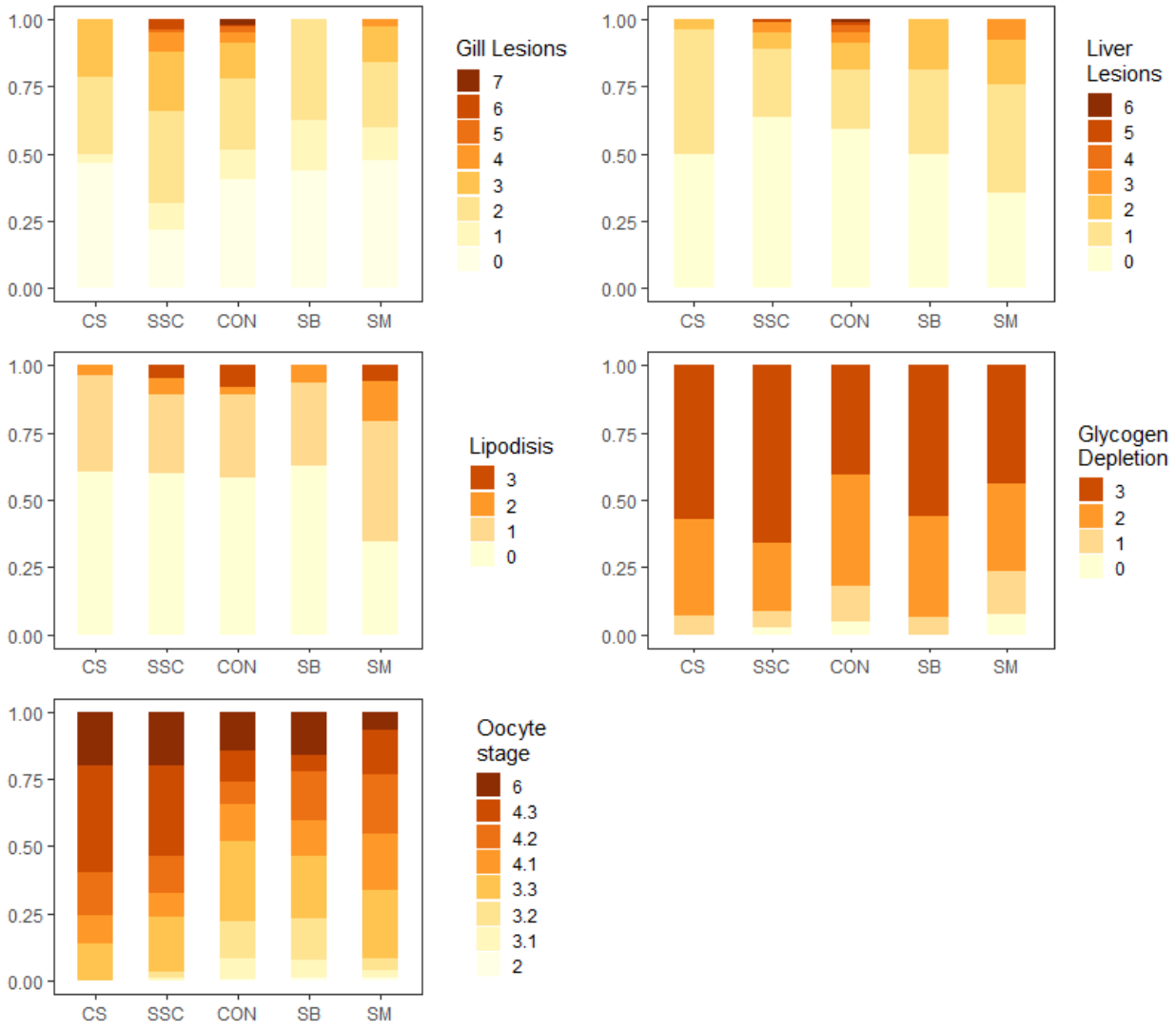

Figure 6-7: Prevalence of delta smelt lesion scores within 5 regions of the San Francisco Estuary for female (top) and male (bottom) fish.

Figure 6-7 continued.

Male

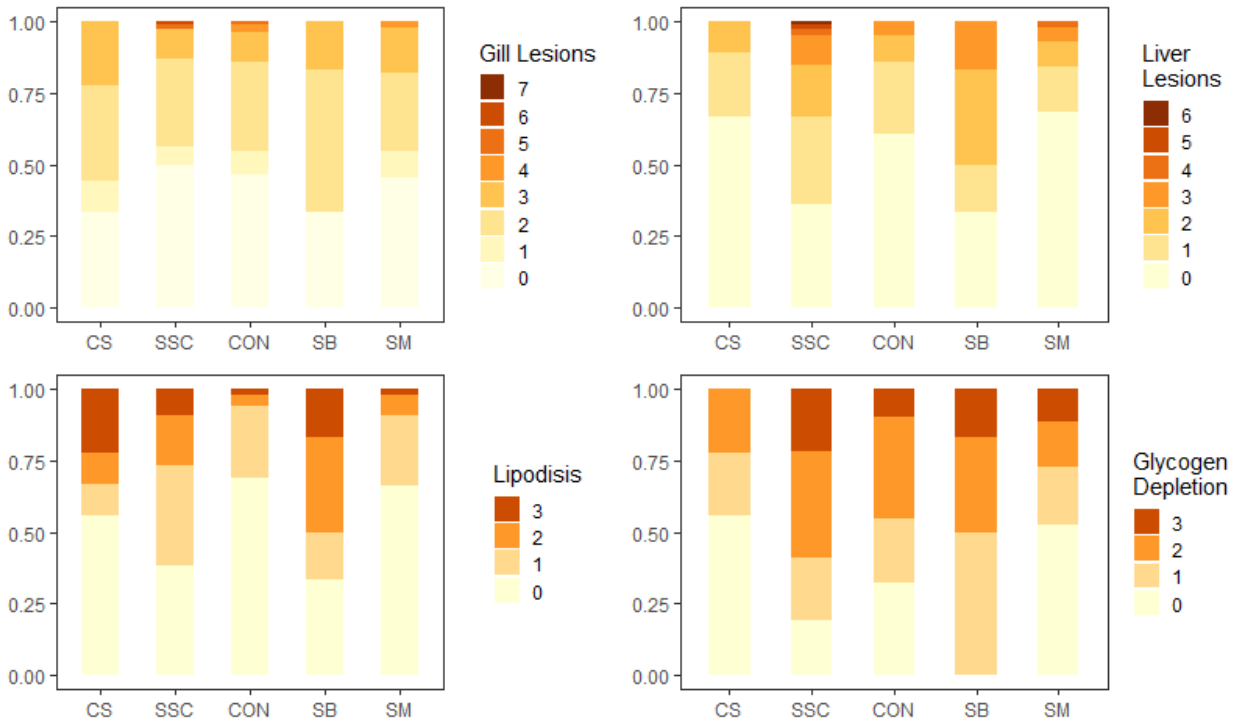

Female

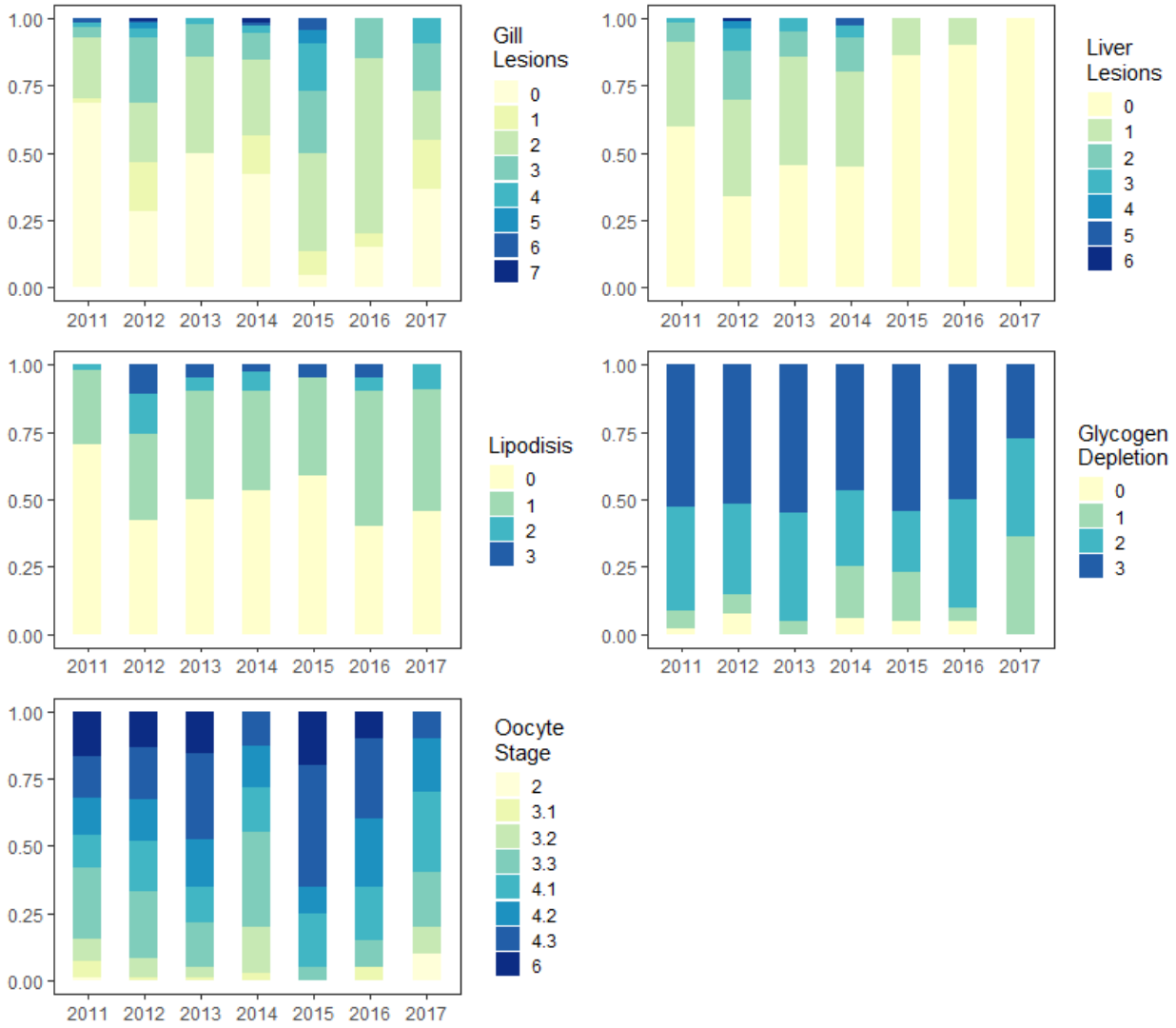

Figure 6-8: Prevalence of delta smelt Lesion scores within 8 years with variable water flow within the San Francisco Estuary for female (top) and male (bottom) fish.

*Males were collected but not processed in 2013.

Figure 6-8 continued.

Male

SUPPLEMENTAL TABLES

Table S6-1: Model Sample sizes, test of difference between full and reduced models for original data (Anova) and imputed data (Wald's Test), Akaike's information criteria total the total R^2 value explaining the proportion of the variance explained by the model.

Dependent Variable		Model	N	Anova or Wald Tests p-value	AIC	Total R2
GSI – Female	Original Data	Full Model	199	0.59	459	0.81
		Reduced Model	199		450	0.77
	Imputed Data	Full Model	887	0.47	3459	0.48
		Reduced Model	887		3410	0.45
Fecundity	Original Data	Full Model	168	0.73	268	0.65
		Reduced Model	168		216	0.63
	Imputed Data	Full Model	887	1.00	1443	0.43
		Reduced Model	887		1361	0.41
Mass Per Egg	Original Data	Full Model	168	0.29	385	0.73
		Reduced Model	168		346	0.77
	Imputed Data	Full Model	887	0.76	2008	0.54
		Reduced Model	887		1961	0.55
Egg Area	Original Data	Full Model	146	0.16	308	0.89
		Reduced Model	146		287	0.90
	Imputed Data	Full Model	887	0.61	1837	0.55
		Reduced Model	887		1776	0.56
Estradiol Level	Original Data	Full Model	124	0.33	157	0.97
		Reduced Model	124		118	0.96
	Imputed Data	Full Model	887	0.49	1210	0.20
		Reduced Model	887		1144	0.15
GSI – Male	Original Data	Full Model	160	0.81	360	0.36
		Reduced Model	160		303	0.27

Dependent Variable		Model	N	Anova or Wald Tests p-value	AIC	Total R2
	Imputed Data	Full Model	690	1.00	2179	0.30
		Reduced Model	690		2087	0.26

Table S6-2: Independent variables and random effects included in either original, imputed or both datasets used in analysis for either the full or reduced model.

				Independent Variables									Random Effects			
Dependent Variable	**Data Set**	**Model**	**Condition Factor**	**RNA/ DNA**	**Fork Length**	**Liver Lesions**	**Lipidosis**	**Glycogen Depletion**	**Gill Lesions**	**Temperature**	**Salinity**	**Turbidity**	**Month**	**Region**	**Cohort Year**	**Year Type**
All Dependent Variables	Original and Imputed	Full	X	X	X	X	X	X	X	X	X	X	X	X	X	X
Egg Area	Imputed	Reduced	X		X								X	X	X	
Egg Area	Original	Reduced	X		X			X	X		X		X	X	X	X
Estradiol Level	Imputed	Reduced	X	X							X		X	X		
Estradiol Level	Original	Reduced	X	X	X	X		X		X			X	X	X	
Fecundity	Imputed	Reduced	X		X							X	X		X	X
Fecundity	Original	Reduced	X	X	X			X			X	X				X
GSI - Female	Imputed	Reduced	X	X	X			X					X	X	X	
GSI - Female	Original	Reduced	X	X		X	X	X	X		X		X		X	
GSI - Male	Imputed	Reduced	X		X								X			
GSI - Male	Original	Reduced			X						X				X	
Mass Per Egg	Imputed	Reduced	X		X			X				X	X	X	X	X
Mass Per Egg	Original	Reduced	X	X				X					X		X	X

Table S6-3: Mean estradiol levels for each oocyte stage for female delta smelt.

Oocyte Stage	Mean estradiol Level
2.0	6.392
3.1	6.793
3.2	8.116
3.3	6.740
4.1	9.790
4.2	18.197
4.3	25.960
5.0	7.897
6.0	7.391

Chapter 7: Interactive Effects of Temperature and Food Availability on Survival, Growth, Otolith Accretion, and Otolith Geochemistry in adult Delta Smelt (*Hypomesus transpacificus*)

Authors:

Rachel A. Fichman[1]*, Leticia Cavole[1], Malte Willmes[2], Wilson Xieu[1], Feng Zhao[1], Tien-Chieh Hung[3], Luke Ellison[3], Troy Stevenson[3], Andrew Schultz[4,5], Bruce G. Hammock[6], Swee Teh[6], Nann Fangue[1], Robert Lusardi[1], Levi S. Lewis[1]

[1] Department of Wildlife, Fish and Conservation Biology, University of California Davis, Davis, CA

[2] Norwegian Institute for Nature Research, Trondheim, Norway

[3] Fish Conservation and Culture Laboratory, University of California Davis, Byron, CA

[4] United States Bureau of Reclamation, Bay-Delta Office, Science Division, Sacramento, CA, United States

[5] U.S. Geological Survey, Southwest Biological Science Center, Grand Canyon Monitoring and Research Center, Flagstaff, AZ, United States[6] Department of Anatomy, Physiology, and Cell Biology, University of CA, Davis, CA

[*]**Corresponding author:**

rafichman@ucdavis.edu

ABSTRACT

The analysis of fish otoliths ("ear stones") to reconstruct the age, growth, and migration of fishes provides a valuable tool for exploring population dynamics and life-history diversity to inform fisheries science and management. This is particularly valuable for studying and informing conservation of rare and endangered species, such as Delta Smelt (*Hypomesus transpacificus*), a critically endangered migratory fish that is endemic to the upper San Francisco Estuary (SFE). Several otolith-based approaches have recently been applied to Delta Smelt to better describe their biology and help enhance conservation efforts. However, the effects of ontogeny and environmental variation on the interpretation of otolith-based indicators for Delta Smelt have not been experimentally examined. Here, we conducted a 70-day experiment examining the additive and interactive effects of temperature (14°C and 18°C) and food availability (no feed and *ad libitum* feed) on survival, somatic growth, otolith accretion, and otolith geochemistry of Delta

Smelt. Specifically, we used individually tagged cultured Delta Smelt of known age (294 days-post-hatch) to assess the effects of environmental variation on otolith-somatic proportionality and otolith geochemistry.

Results indicated strong interactive effects of food limitation and temperature on survival, with high-temperature no-feed treatments resulting in 366% greater mortality relative to both fed treatments, where ample food supply eliminated any effect of temperature on survival. Although otolith size linearly tracked fish size, intercepts differed by treatment. Furthermore, otolith accretion rates during the experiment were largely decoupled from changes in mass, length, or condition; indicating that otolith increments in adult (e.g., ~ 300 dph) Delta Smelt do not reflect changes in growth or condition. We also found that otolith chemistry can be altered by variation in environmental conditions, with the magnitude of effects varying among different element constituents. Given that otolith-derived metrics are commonly used to estimate population parameters that can help guide policy decisions and the conservation of imperiled fishes, like Delta Smelt, these results highlight the importance of experimentally testing and carefully considering the effects of ontogenetic and environmental factors in the design and interpretation of otolith-derived metrics for wild fish populations.

INTRODUCTION

Aquatic organisms are experiencing rapidly changing environments due to climate change, and these changes are impacting their distributions, life histories, and population dynamics globally (Pershing et al., 2015; Morley et al., 2018; Avaria-Llautureo et al., 2021). Estuarine fishes have evolved to survive in variable, stochastic conditions, but even highly resilient species are being challenged by combined effects of climate change and anthropogenic degradation of habitats (Moyle et al., 2010; Potter et al., 2013; Swain et al., 2018). In the San Francisco Estuary (SFE), USA, anthropogenic impacts like channelization, elevated salinities and increased water diversions and exports (Nichols et al., 1986; Cloern et al., 2011; Swain et al., 2018) have combined with global trends of warming waters and extreme droughts and floods (Gasith & Resh, 1999), to drive several fish species towards extinction (Moyle, Katz & Quiñones, 2011; Brown et al., 2016; Hobbs et al., 2017; Moyle & Lusardi, 2017).

One such species, the Delta Smelt (*Hypomesus transpacificus*), is an annual forage fish in the family Osmeridae and is endemic to the fresh and low-salinity waters of the SFE (Moyle et al., 1992). This species has rapidly declined to less than 1% of its historical abundance (Mac Nally et al., 2010; Thomson et al., 2010; Moyle et al., 2016; Hobbs et al., 2017), likely due to the combined effects of non-native species (Nobriga, Loboschefsky & Feyrer, 2013), pollution (Fong et al., 2016), habitat loss (Feyrer, Nobriga & Sommer, 2007; Nobriga et al., 2008), and climate change (Knowles & Cayan, 2002; Cloern et al., 2011; Brown et al., 2016; Lewis et al., 2021). There is also evidence that the abundance of their prey (e.g., calanoid copepods like *Erytemora affinis* and *Pseudodiaptomus forbesi*) have been suppressed by top-down controls of invasive clams (Kimmerer, Gartside & Orsi, 1994; Slater & Baxter, 2014; Hammock et al., 2017, 2019), resulting in food limitation that can impact Delta Smelt survival and recruitment. Consequently, Delta Smelt have been listed as threatened (U.S. Fish and Wildlife Service, 1993),

endangered (CDFG, 2010), and critically endangered (IUCN, 2012), placing this fish in the crossfire between wildlife management and agricultural advocates due to demands for freshwater flows (Moyle, Hobbs & Durand, 2018; Scoville, 2019; Reis, Howard & Rosenfield, 2019).

Opportunities for Delta Smelt recovery and management in the face of warming conditions and exacerbated food web disruption can be strengthened by assessments of intraspecific life history diversity, or the variation in survival and reproductive strategies within a species (Cole, 1954; Moyle et al., 2016; Hobbs et al., 2019). Managers can more accurately mitigate these detrimental impacts by understanding the mechanisms behind observed individual and population-level responses in the species. This is increasingly urgent considering the implementation of recovery methods like the release of captive-cultured Delta Smelt into the SFE to supplement wild populations (Hobbs et al., 2017; Finger et al., 2018; Lessard et al., 2018). One method to describe life history diversity and how environmental stressors, such as temperature and food availability, affect Delta Smelt survival, and potentially the survival of planted fish, is the use of analytical tools like otolith microstructure and chemistry.

Otoliths, or fish "ear stones," are small, paired calcium carbonate ($CaCO_3$) structures that are present in the inner ear of most bony fishes (Pannella, 1971; Campana & Neilson, 1985). These sensory structures are used by fishes for orientation, hearing, acceleration, and vibration sensing (Schulz-Mirbach et al., 2019). Otoliths generally accrete periodic layers of $CaCO_3$ and protein matrix on daily, seasonal, and annual scales (Miller & Storck, 1982; Campana, 1990), using elements sourced from surrounding water and consumed prey. Since otoliths are metabolically inert and not resorbed over time, they function as a permanent record of the growth and environmental history of the individual (Campana, 1990; Starrs, Ebner & Fulton, 2016). More specifically, the structure and chemistry of otoliths are powerful resources for reconstructing life history phenotypes, age, growth, phenology, and experienced environmental, physiological and metabolic conditions of fishes (Stevenson & Campana, 1993; Campana, 1999; Hobbs et al., 2005; Sturrock et al., 2014, 2015; Martino et al., 2020).

Since Delta Smelt otoliths accrete layers on a daily scale (Hobbs et al., 2007a), we can ascertain hatch dates and total ages from their structure (Miller & Storck, 1982; Campana, 1990, 2001). With an otolith-somatic growth relationship, where daily otolith accretion is proportional to body growth, we can also infer information about ontogenetic growth patterns and their correlation with environmental conditions throughout time (Hobbs et al., 2007a). For Delta Smelt, this otolith-somatic growth relationship has been validated through the use of captive-reared smelt at various life stages (Hobbs et al., 2007a; Xieu et al., 2021) in typical, artificially controlled conditions (Lindberg et al., 2013). However, the assessment of how extrinsic factors (e.g., temperature and food) may alter this relationship is unknown.

Temperature and food availability are important determinants of fish growth and condition, it is prudent to experimentally examine their relationships to otolith-based metrics used to back-calculate fish age and size, and life history characteristics. Somatic growth, and the use of otoliths to infer it, is a useful metric for understanding fish population dynamics due to its effect on age and size at first reproduction (Heino, Dieckmann & Godø, 2002), reproductive output (Barneche et al., 2018), recruitment (Sponaugle, Grorud-Colvert & Pinkard, 2006; Johnson et al.,

2014), and interspecific or intraspecific interactions (Audzijonyte et al., 2013) for individuals of a species. For many species, including Delta Smelt, otolith size is positively correlated with body size, though metabolic rates may be more influential in controlling otolith accretion rates (Wright, 1991; Hüssy, 2008). By experimentally assessing the stability of these relationships, and how extrinsic and intrinsic factors impact them, we can improve confidence in their interpretation related to movement patterns (Starrs, Ebner & Fulton, 2016), population dynamics (Campana & Thorrold, 2001) and somatic growth (Campana, 1990; Barber & Jenkins, 2001; Baumann et al., 2005).

Climate change and its impact on temperature and food availability for a fish species can also alter the incorporation of elements into otolith crystalline and protein structures, further influencing inferences made using otolith-based techniques. Otolith accretion is a complex, bioenergetically regulated process (Sturrock et al., 2015; Hüssy et al., 2020), with incorporation rates of elements from surrounding water into otoliths (i.e., otolith partition coefficients). It varies among species, elements, isotopes, environmental factors, metabolic rates, and/or growth rates (Campana, 1999; Sturrock et al., 2015). For example, strontium isotopic ratios (^{87}Sr:^{86}Sr), and strontium to calcium ratios (Sr:Ca) are key to tracking fish migrations through differing salinities (Kraus & Secor, 2004; Hicks, Closs & Swearer, 2010) and tracing natal rearing and migration locations through landscape geology (Barnett-Johnson et al., 2005, 2008; Hobbs et al., 2007b; Willmes et al., 2016), while barium to calcium ratios (Ba:Ca) largely reflects differences in diet (Buckel, Sharack & Zdanowicz, 2004) and ambient water concentrations (Walther et al., 2010; Doubleday et al., 2013). Lithium (Li) may be incorporated variably as a function of temperature (Tanner et al., 2013) or salinity (Hicks, Closs & Swearer, 2010), while zinc (Zn) has been connected with variation in diet (Ranaldi & Gagnon, 2008), though less is known about these elements compared to commonly researched elements like Ba, Sr, and magnesium (Mg) (Izzo, Reis-Santos & Gillanders, 2018). Overall, experimental assessments of how otolith accretion and geochemistry vary among multiple factors are required to accurately apply and interpret otolith-based tools to fisheries conservation concerns (Campana, 1999; Sturrock et al., 2015). The species-specific incorporation of various elements into otoliths and their relationship with ambient water elemental concentrations have not yet been assessed in Delta Smelt. Quantifying the impact of temperature and food limitation on commonly used proxies for Delta Smelt growth, condition, and experienced environmental conditions in otoliths helps us understand the mechanisms controlling these metrics, and how best to interpret the information accurately.

Here we experimentally examined the additive and interactive effects of temperature and food availability on survival, somatic growth, otolith accretion rates, and elemental incorporation rates into otoliths. Specifically, we examined how variation in the thermal and trophic environment affects (1) survival, body condition, and otolith accretion, (2) the stability of otolith-somatic proportionality, (3) elemental partition coefficients in Delta Smelt otolith-to-water relationships, and (4) how these relationships impact our interpretation of otoliths in conservation research applications. We expected Delta Smelt somatic growth to be highest where food was abundant and temperatures were warm, whereas growth was expected to be lowest where temperatures were lower and food was least available. However, if the high temperature treatment causes

thermal stress, we would expect decreased growth due to energetic costs of stress responses (Kooijman, 2000; Jeffries et al., 2016). We also expected fish survival to be lower in unfed treatments than fed treatments due to the depletion of energetic resources (Hammock et al., 2020). If Delta Smelt otoliths exhibit constant proportionality, we expected no effects of temperature, feed, or their interaction on the slope between otolith accretion rate and somatic growth rate. Finally, we expected the effects of temperature and food availability on element incorporation coefficients to vary among elements (Hüssy et al., 2020). Results of this study are key for understanding the responses of Delta Smelt to multiple stressors and documenting the stability of otolith-based tools that are used to inform population models and key management decisions for this endangered species.

METHODS

Experimental Design

Delta Smelt culture and experimentation was conducted at the UC Davis Fish Conservation and Culture Laboratory (FCCL), in Byron, CA. Fish were reared in bead-filtered, UV-treated, and temperature-controlled water pumped from the Sacramento-San Joaquin Delta following standard protocols (Lindberg et al., 2013). For the experiment, tanks were arranged in two separate recirculating systems with four tanks per system. Each tank was black, plastic, cylindrical, and had a working volume of 290L (60cm depth, 47cm wetted depth, and 100cm diameter). Systems were randomly assigned to one of two temperatures (14°C or 18°C), and tanks within each system were assigned one of two food treatments (no feed or *ad libitum* feed) (Figure 7-1A). Temperatures were selected to represent values commonly experienced by subadult Delta Smelt during summer and fall in the SFE, below thresholds that cause acute or chronic thermal stress (Komoroske et al., 2014; Davis et al., 2019a; Hammock et al., 2022). Additionally, chosen temperatures were only ±2°C from optimal rearing temperatures at FCCL (~16°C) to reduce potential stress (Lindberg et al., 2013). Feed rations of a commercial fish meal diet (BioVita Mash #1, Bio-Oregon; www.bio-oregon.com) followed established protocols developed and used by prior experiments on Delta Smelt (Lindberg et al., 2013; Tigan et al., 2020; Hammock et al., 2020; Hung et al., 2022a). *Ad libitum* feedings occurred five times per day, while tank bottoms were siphoned three days per week to clear away excess food. Tanks had 5μm filters installed prior to the spray bars to ensure no food particles moved among tanks during water recirculation. Water samples were collected approximately weekly from each temperature-controlled system. Water quality (temperature and dissolved oxygen) was measured using a Yellow Springs 3300 Sonde to confirm that temperature treatments were consistently maintained in the cool (14.11°C ± 0.131) and warm (18.02°C ± 0.476) systems throughout the study period. Experimental setup, food rations, and husbandry protocols were modelled after those used in Hammock et al, 2020, enabling this experiment to build upon recent research on Delta Smelt responses to food scarcity. Treatments and procedures were conducted under approved UC Davis Institutional Animal Care and Use Committee Protocols #18071 and #19841.

Experimental fish hatched on January 18, 2019 and were reared in freshwater (salinity of 0.1 parts-per-thousand) at 16°C until they reached ~50-60mm in total length, where they were then acclimated to a lower temperature (12°C) to reduce stress during tagging procedures. Subadult (201 or 207 days-post-hatch or dph) Delta Smelt were tagged and imaged on August 7 or August 13 and haphazardly allocated to the eight experimental tanks (n=99 per tank, 88 experimental fish and 11 non-experimental fish) on August 21, 2019 (215 dph). All 88 experimental fish were implanted with Visible Implant Alphanumeric (VI Alpha) tags to track experimental effects on individual fish (Sandford, Castillo & Hung, 2020). Fish acclimated from an initial holding temperature (12°C) to treatment temperatures (14°C or 18°C) over the course of 10 or 6 days, respectively, and from initial feeding to treatment rations 9 days later, on August 30, 2019, marking the beginning of the experimental period.

Over the course of 70 days, fish experienced the four treatment conditions, defined as 14F (14°C, fed *ad libitum*), 14NF (14°C, no feed), 18F (18°C, fed *ad libitum*) and 18NF (18°C, no feed) (Figure 7-1A). Henceforth, the length of the experimental period can be described as days-post-imaging (dpi, 87 or 93 days) for image analyses, or days-post-experiment initiation (dpe, 70 days) for the time period over which all four treatment combinations were experienced. Mortalities during the experiment were excluded from all analyses and removed from tanks daily. Surviving fish (n=629) were euthanized in accordance with the UC Davis IACUC protocol using a 500 mg/L buffered solution of tricaine methanesulfonate (MS-222) on November 8, 2019 (294 dph). After euthanasia, fish were preserved by freezing at -20 °C. This experimental design, including fish size, tank densities, feed regimens, and study length, were chosen to complement Hammock et al. (2020), where the effects of food- limitation alone were assessed for Delta Smelt that were not individually tagged.

Fish Morphometric Measurements

To facilitate individual growth estimates, all fish (n=824) were imaged prior to beginning the experiment using a mounted Canon Powershot digital camera (Canon Solutions America Inc., Melville, New York, USA). Images included millimeter markers affixed to the stage to facilitate image calibration and measurements. Initial manual (hand) measurements and weights were not collected to minimize mortalities due to handling stress. At the end of the experiment, all surviving fish (n=629) were frozen for later processing, with a subset (n = 120) of surviving fish also processed fresh, immediately following euthanasia, to quantify and account for preservation (freezing) effects. All frozen fish were later thawed until pliable and then measured and imaged. For fish collected at the end of the experiment, manual measurements for standard length (*SL*), fork length (*FL*), and total length (*TL*) to the nearest 1 millimeter, and body mass (*WT*) to the nearest 0.001 g were recorded prior to imaging; this included all frozen fish (n = 629) and the subset that were also processed fresh (n = 120). For all digital images of each fish (including initial fresh, final frozen, and the subset of final fresh images), all lengths (*SL, FL, TL*) and body depth (*BD*) were measured digitally using ImageJ (version 1.53f) (Figure 7-1B) (Abramoff, Magelhaes & Ram, 2004).

Standardization of Fish Measurements

Digital and manual measurements of fresh standard length (SL_f) yielded nearly identical measurements (mean difference = 0.57 mm or 1.08%), and thus could be used interchangeably as needed. To standardize comparisons of fish measurements between fresh and frozen specimens, we calculated "corrected" standard lengths (SL_c) using empirical relationships, similar to previous studies (Fowler & Smith, 1983; Fey, 1999). Frozen measurements were corrected to fresh values using empirical linear models developed for specimens that were measured both fresh and frozen (at -20 ºC) (Xieu et al., 2021). Models were developed for standard length (mm) (SL_c, slope = 1.027, intercept = 1.036, R^2 = 0.982, n=40), mass (g) (WT_c, slope = 0.908, intercept = -0.123, R^2 = 0.994, n=40), and body depth (mm) (BD_c, slope = 0.986, intercept = 0.061, R^2 = 0.95, n=40) (Supplement 1A-C). Linear conversion models were calculated using the "lm" function in the R software environment version 4.2.0 (R Core Team, 2022).

Since fish specimens were not weighed at the initial timepoint (to reduce stress-induced mortality), we created a mass index value (mm^2) ($MASS_i$) by multiplying BD_c with SL_c, to represent a 2-dimensional proxy for mass. We then ran a generalized additive model (GAM) using corrected weight (WT_c) and mass index ($MASS_i$) from the final fish dataset (including the control group fish) to predict and create estimated masses using the "gam" function in the "mgcv" package (edf=5.384, Ref.df=6.549, F=5577, $p<0.001$, $R^2_{adj.}$ = 0.982, n=656) (Supplement 1D) (Wood, 2022). We then used this predictive GAM to create estimated masses for the initial fish images (n=535) based on their mass index values using the "predict" function. These GAM-predicted estimated masses (g) ($MASS_e$) were used to track individual growth and to calculate condition factor for pre-experiment to post-experiment timepoint morphometrics. Fish morphometrics encompass the 87 or 93 days since initial imaging (dpi), containing the 70 days of the treatment experiment (dpe). Condition factor was calculated as ($K = 100 \times (MASS_e / SL_c^3)$). Of the 629 surviving fish, 89 did not have tags (recall that 11 fish per tank, or 88 total, were originally untagged), and initial photographs were unavailable for 5 tagged fish, leading to a total of 535 fish used for individual growth analyses. Fish missing final SL_c (n=1) and $MASS_e$ (n=3) measurements, for example due to damage post-freezing, were excluded from analyses as needed.

Otolith Preparation and Imaging

Sagittal otoliths were removed from a subset of the Delta Smelt (n=108, 15 fish per tank) after the completion of the experimental period using size 10 scalpel blades and fine tipped forceps. Otoliths were imaged, with a ruler for calibration, at 20x or 30x using an Amscope MU1000 10MP camera (Amscope, Irvine, CA, USA) attached to a Leica S6E dissecting microscope (Leica Camera AG, Wetzlar, Germany) with manual zoom. Once air-dried, otoliths were mounted on glass slides using Crystalbond™ (Ted Pella, Redding, CA, USA) thermoplastic glue so they could be sanded for microstructure and chemical analyses. Otoliths were wet sanded with 800 or 1200 grit Buehler MicroCut silicon carbide paper and polished with 0.3-µm Buehler MicroPolish alumina on a Buehler MicroCloth (Buehler, Lake Bluff, Illinois, USA) on both sides to reveal the core and daily growth increments. Left otoliths were initially sanded following historical protocols, however, if the left otolith was broken, lost, or of poor quality, the right

otolith was prepared in its place (Campana, 1990; Hobbs et al., 2007a). Polished otoliths were then imaged at 400x on an Amscope MU1000 10MP camera attached to an Olympus CH30 compound microscope (Olympus Corporation, Tokyo, Japan), then stitched together using the photo merge function in Adobe Photoshop 2020 (v. 21.1.1). Additional images were taken of the core and edge increments for improved readability for age and growth measurements (Xieu et al., 2021). Slides with sanded otoliths were sonicated in Milli-Q ultrapure water, then airdried before being broken and attached to petrographic slides using double-sided tape.

Otolith Age and Growth Analyses

Pre-polished whole otolith images (Figure 7-2A) were measured in both dorsal-ventral and rostrum-post-rostrum orientations for all dissected otoliths (n=216, two otoliths per fish) using ImageJ (version 1.53f). This provided gross otolith size metrics for comparisons of otolith left-right symmetry and otolith-somatic sizes for each fish. Images were calibrated from pixels to microns (μm) using a scale bar with 1 mm increments in each photo.

Polished otolith (n=108) images were rated for quality (0 = not usable; 1= not particularly good; 2= good; and 3 = excellent), and only samples rated as sufficient for aging (quality = 2 or 3) were used in age and growth analyses. Increments were annotated and quantified using ImageJ (version 1.53f) following established practices (Hobbs et al., 2007a; Xieu et al., 2021). If the otolith morphology or preparation did not allow for dorsal measurements, a dorsally oriented lobe along the anti-rostrum was used. Increment widths were converted from pixels to microns using an AmScope 0.01-mm stage micrometer. The last 100 increments were then measured from the dorsal edge of the otolith towards the core, thus encompassing the entire experimental period, followed by a measurement from increment 100 to the hatch check (Figure 7-2C).

Left (L) and right (R) sagittal otoliths from each fish were compared for symmetry in two dimensions, dorsal-ventral (DV) and rostral-postrostral (RP), to test if left and right otoliths were relatively symmetrical and could be used interchangeably. Our otolith increments were taken on the dorsal side of the otolith, so DV is the most important dimension to test for symmetry. Linear models comparing left and right otoliths indicated that Delta Smelt otoliths were largely symmetrical overall in both dimensions, with R^2 of 0.951 for dorsal-ventral, and 0.926 for rostral-postrostral, including the occasional broken otoliths seen as outliers (Supplement 4). Therefore, for this study, left and right otoliths were used interchangeably.

Otolith and Water Trace Element Microchemistry Analyses

Elemental concentrations in otoliths were measured using laser ablation inductively coupled plasma mass spectrometry (LA-ICPMS) in the Department of Earth and Planetary Sciences, University of California Davis. Otolith material was ablated from the surface of each sample using a Photon Machines 193nm ArF Excimer laser with a HelEx dual-volume LA (laser ablation) cell. Three spots along three transects were established on each otolith, with a series of spots ablated from the dorsal edge toward the core with a size of 40 μm and a spacing of 200 μm (Figure 7-2B). Prior to data collection, a cleaning run (pre-ablation) was performed across the same spots with a larger (100 μm) spot size to remove potential surface contaminants. The

"edge" spot was ablated near the dorsal edge of the otolith, thus lying fully within the experimental period. The "middle" spot was just prior to the beginning of the experimental period, and the "pre-experiment" spot represented conditions before the experiment. Given that 100% of the otolith material within edge spots (but not the middle or pre-experiment spots) was accreted during the experimental period, only edge spot measurements were used to contrast element incorporation rates (D_x) among treatments, with the three replicate edge spots per otolith averaged to provide a single abundance estimate for each element in each otolith.

Otolith material was ablated by a pulsed Excimer laser and transported by a helium gas stream to the inductively coupled plasma where it was then ionized into elements and transported via argon gas to the mass spectrometer, i.e. "LA-ICPMS". This was accomplished using either an Agilent 7700x Quadrupole ICPMS (Interdisciplinary Center for Plasma Mass Spectrometry, or UCD ICPMS) or a Themo Element XR HR-ICPMS (Yin Lab) in Davis, California. The second ICPMS was used due to a mechanical failure of the first instrument. For each spot, the repetition rate of the laser was set at 10 Hz, fluence was ~3 J/cm^2, with dwell and pause times of 10 and 5 seconds on the first machine, and 13 and 10 seconds on the second machine. We measured a large suite of potentially informative elements including lithium, boron, sodium, magnesium, calcium, manganese, copper, zinc, strontium, and barium (^{7}Li, ^{11}B, ^{23}Na, ^{24}Mg, ^{43}Ca, ^{44}Ca, ^{55}Mn, ^{63}Cu, ^{66}Zn, ^{88}Sr, and ^{137}Ba, respectively). Due to potential contamination impacting Mg concentrations on the HR-ICPMS, Mg was excluded from analyses, and one otolith was excluded from analyses due issues with helium levels before changing tanks (n=107).

Otolith data were reduced relative to NIST 610 and ^{43}Ca as the internal standard using the Trace Element data reduction schema following established best practices using Iolite (Longerich, Jackson & Günther, 1996; Jochum et al., 2011; Paton et al., 2011; Howell et al., 2013). Otoliths were assumed to contain 38.8 wt.% Ca (µg/g) (Yoshinaga et al., 2000). NIST 610 and 612 glasses were measured prior to and between samples throughout processing as external reference materials to correct for instrument drift.

Water samples from each system were analyzed for trace element concentrations using triple quadrupole inductively coupled plasma mass spectrometry (QQQ-ICP-MS) at UCD ICPMS. We analyzed the same elements as listed above, ^{7}Li, ^{11}B, ^{23}Na, ^{24}Mg, ^{43}Ca, ^{44}Ca, ^{55}Mn, ^{63}Cu ^{66}Zn, ^{88}Sr, and ^{137}Ba, allowing us to directly compare the ambient water chemistry from the two recirculating systems (14°C and 18°C) with the chemistry of the otoliths from each treatment. By comparing the chemistry of the water sources of each system, we could confirm whether element concentrations in the water were similar among treatments such that differences in otolith geochemistry among treatments could be attributed to treatment effects and not differences in ambient concentrations among systems.

Element concentrations were reported in parts-per-million (ppm) for otolith samples and parts-per-billion (ppb) for water samples. Element concentrations that were below the limits of detection were set to 0.000001, a value well below actual concentrations. This allowed for "zero" values to be log-transformed for analyses. Element concentrations in otoliths and water were converted into µmol using the respective molar mass, and each element ratioed to ^{44}Ca (*X:Ca*; µmol/mol), thus allowing for comparisons among studies (Elsdon & Gillanders, 2003) and

species (Bath et al., 2000; Miller & Hurst, 2020). The relative incorporation rate from the water into the otolith for each element (x) was calculated as the element-specific partition coefficient, (D_X) following Equation 1; where D_x equals the ratio of the element-specific molar *X:Ca* values in otoliths, $[X:Ca]_{otolith}$ to that of water $[X:Ca]_{water}$. Values of $[X:Ca]_{water}$ were averaged within each water system (i.e., either the 14°C or 18°C system), with mean values used in the calculation of partition coefficients for each fish from its respective system (Table 7-1).

$$\text{Equation 1: } D_x = \frac{[X:Ca]_{otolith}}{[X:Ca]_{water}}$$

Statistical Analyses

A linear model was used to examine differences in survival rates among tanks as a function of the fixed effects of temperature, feed, and their interaction. Linear mixed-effects (LME) models were used to examine variation in each growth response (Y) variable, including otolith growth rate (M_{oto}), somatic growth rate (M_{som}), and otolith partition coefficients (D_x), as functions of the fixed effects of temperature (T = 14, 18°C), food availability (F = fed *ad libitum*, unfed), and their two-way interaction, with tank included as a random effect, and each model fitted by maximizing the log-likelihood (method = "ML") (Equation 2).

$$\text{Equation 2: } lme(Y \sim F + T + F * T,\ random = \sim 1|tank,\ data,\ method = "ML")$$

To assess the effect of treatments on otolith-somatic proportionality, we used additive LME models examining somatic growth (M_{som}) as a function of the fixed categorical effects of each treatment combination (tr = 14F, 14NF, 18F and 18NF), otolith growth (M_{oto}) as a linear covariate, and tank as a random effect (Equation 3).

$$\text{Equation 3: } lme(M_{som} \sim M_{oto} + tr, random = \sim 1|tank,\ data,\ method = "ML")$$

All models were run using the "lme" function from the "nlme" package (Pinheiro, Bates & R Core Team, 2022) in the R software environment (v. 4.2.0) (R Core Team, 2022) with maximum likelihood (method = "ML") and a Gaussian family distribution. Model assumptions were visually examined using Q-Q and residual plots, while the F-test in the "ANOVA" function was used to compare each model to its null model (intercept only, with random tank effect). Marginal and conditional pseudo-R^2 values were assessed using the "r.squaredGLMM" function in the "MuMIn" (Bartoń, 2022) package. Data were tested for normality using the Shapiro-Wilke normality test. Chemistry data were $\log_{10}$-transformed to meet assumptions of normality for the LME.

RESULTS

Survival

Significant variation in survival was observed among treatments, with feed, temperature, and their interaction each having significant effects ($p<0.01$, Table 7-2). Feed had the strongest effects, with fish from the 14F and 18F treatments exhibiting the highest survival rates (90.9% ±

5.71%, and 89.9% ± 0%, respectively) (Figure 7-3). In contrast, survival was lowest in warm, unfed treatments (18NF, 57.6% ± 1.43%), with cool, unfed treatments exhibiting intermediate values (14NF, 79.3% ± 2.14%). Thus, fed treatments were unaffected by variation in temperature, whereas food limitation in warmer conditions resulted in 366% higher mortality, and food limitation in cooler conditions resulted in 128% higher mortality, and relative to fed treatments (Figure 7-3).

Somatic Growth & Otolith Accretion

Although standard length (SL_c) increased for all treatment combinations, both mass and condition decreased in unfed treatments (Figure 7-4). Mean changes in SL_c (mean ± s.d., n = 534) were 12.338 ± 0.094 mm (14F), 11.441 ± 0.365 mm (18F), 1.726 ± 0.066 mm (14NF), and 2.215 ± 0.099 mm (18NF) (Figure 7-4A). Mean changes in $MASS_e$ (mean ± s.d., n = 532) were 1.121 ± 0.039 g (14F), 0.907 ± 0.021g (18F), -0.220 ± 0.015 g (14NF), -0.295 ± 0.008 g (18NF) (Figure 7-4B). Mean changes in K (mean ± s.d., n = 532) were 1.708e-04 ± 3.223e-05 (14F), 1.021e-04 ± 1.161e-05 (18F), -2.327e-04 ± 8.049e-06 (14NF), -2.683e-04 ± 2.310e-06 (18NF) (Figure 7-4C).

As expected, feed had a significant positive effect on all somatic growth metrics, including ΔSL_c ($F_{1,4}$ = 390.185, p-value<0.001), $\Delta MASS_e$ ($F_{1,4}$ = 431.261, p-value<0.001) and ΔK ($F_{1,4}$ = 786.4, p-value <0.001), with fixed effects accounting for 65.6-75.8% of the variance, and random tank effects accounting for <1 % of the variance (SL_c: marginal R^2 = 0.651, conditional R^2 = 0.659, $MASS_e$: marginal R^2 = 0.6548, conditional R^2 = 0.662, K: marginal R^2 = 0.7545, conditional R^2 = 0.7580) (Table 7-3). Only K was affected by temperature ($F_{1,4}$ = 786.4, p-value=0.02), with changes in K being slightly higher at 14°C than 18°C at each food ration (Table 7-3, Figure 7-4).

In contrast to somatic metrics, the change in otolith accretion exhibited a statistically significant, but relatively weak, positive response to food availability ($F_{1,4}$ = 15.906, p-value=0.02, R^2 = 0.1910, n=104) (Table 7-3, Figure 7-4). However, otolith accretion rates varied throughout the experiment (Figure 7-5), with the 18NF treatment exhibiting the lowest rates, the18F treatment exhibiting the fastest rates, and the two cooler treatments (14F and 14NF) exhibiting similar, intermediate accretion rates toward the end of the experiment (Figure 7-5).

Otolith-Somatic Relationships

Overall, fish size (SL_c) increased linearly with total otolith size (slope = 0.067, intercept = 5.827), with otolith radius alone explaining 57% of the variance in standard length. In the additive LME model, the effects of treatment ($F_{3,4}$ = 11.003, p-value = 0.02) and otolith radius ($F_{1,95}$ = 175.676, p-value<0.001) were both significant and explained 68% of the variance in SL_c (Table 7-4, Figure 7-6). The additive LME was selected given that no significant radius*treatment interaction was observed (df = 10, L.Ratio=4.82, p=0.19). Pairwise comparisons of estimated marginal means of the intercepts for each treatment indicated that the otolith-somatic relationship for 14F fish was significantly higher than both unfed treatments (p<0.05), but not from the warmer fed treatment (18F, p=0.09); while the two unfed treatments were the least different from each other (p=0.95) (Table 7-5, Figure 7-6).

For the experimental period, linear relationships between somatic growth and otolith accretion differed by food regime, with no-feed conditions exhibiting a near-zero slope, thus indicating a decoupling of otolith-somatic growth during the experiment (Table 7-6, Figure 7-7). Fed and unfed groups, in particular, exhibited distinct otolith-somatic relationships, with inclusion of variable slopes resulting in improved model fit. For SL_c growth and total otolith accretion (Figure 7-7A), there were differences between 14F and 14NF ($p<0.001$) and 14F and 18NF ($p<0.001$) for the interactive terms, with the overall model accounting for 79.6% of variance ($R^2 = 0.796$). For body mass ($MASS_e$) (Figure 7-7B), the interactive terms for all treatments compared against 14F were significant (14NF $p=0.002$, 18F $p=0.04$, and 18NF $p=0.002$, $R^2 = 0.749$). Similar trends held true for condition factor (Figure 7-7C), with significant differences among treatments (14NF $p<0.001$, 18F $p=0.02$, and 18NF $p<0.001$, $R^2 = 0.855$). Between food-limited groups, slopes differed for *K* only.

Elemental Ratios and Partition Coefficients

Significant differences among water systems were observed for all elemental ratios (X:Ca, p-value <0.05) except for Na:Ca (t = -0.308, df = 9, p-value = 0.77, mean difference = -11310.83μmol/mol) and Sr:Ca (t = 0.904, df = 9, p-value = 0.39, mean difference = 19.747μmol/mol) (Table 7-1, Figure 7-8).

The effects of temperature and feed treatments on log10-transformed partition coefficients (D_x) varied by the element assessed (Figure 7-8, Table 7-7), with no significant interactive terms. There was a significant effect of feed on D_{Ba} ($F_{1,4} = 24.59$, $p<0.01$), D_{Mn} ($F_{1,4} = 134.249$, $p<0.001$), and D_{Na} ($F_{1,4} = 23.2$, $p<0.01$), while temperature was significant for D_{Cu} ($F_{1,4} = 11.503$, <0.05) and D_{Zn} ($F_{1,4} = 10.076$, $p<0.05$). Corresponding explanations of variance using marginal and conditional R^2 values also varied by element (Table 7-7), explaining 23.1%-58.3% of the variance, with some evidence of tank effects for D_{Cu} (marginal $R^2 = 0.345$, conditional $R^2 = 0.452$), D_{Na} (marginal $R^2 = 0.483$, conditional $R^2 = 0.602$), D_{Zn} (marginal $R^2 = 0.265$, conditional $R^2 = 0.394$) and D_B (marginal $R^2 = 0.038$, conditional $R^2 = 0.045$), though the model for D_B did not show any significant treatment effects nor effectively explain the variance among treatments (Table 7-7).

The relationships between D_x and temperature or feed also varied by element (Figure 7-9); starvation conditions led to lower D_{Na} and D_{Mn}, but higher D_{Ba}, than the fed treatment groups, while higher temperatures led to lower D_{Cu} and D_{Zn} than lower temperature treatments (Figure 7-9). D_{Li} was not explained by treatment effects due to most data points (97.5%) being below our limits of detection. The only treatment with more than one valid otolith partition coefficient for Li was 18F (Figure 7-9). In contrast, D_{Sr} was also not affected by treatment, but appeared to have slightly lower values for 18F than the other treatments. Water chemistry was similar among temperature treatments; thus results of LMEs contrasting D_x among treatments were similar to those contrasting *X:Ca* ratios among treatments (Supplement 4).

DISCUSSION

This study assessed the direct relationship between water temperature and food limitation on somatic growth, otolith accretion, otolith-somatic relationship, and elemental incorporation for an estuarine, semi-anadromous species using linear mixed-effect models. We found positive, synergistic effects of temperature and food availability on survival, positive food effects on somatic growth and body condition, and weaker feed effects on otolith accretion rates. The mismatch in differential effects between the relative somatic and otolith growth metrics highlights the conservative nature of otolith-based inferences in their reflection of growth and condition, particularly during periods of starvation. Additionally, elemental incorporation coefficients were influenced by physiological processes and environmental conditions to differing degrees, and certain elements warrant further investigation into their use as proxies for food limitation or temperature in the wild. The discovery of otolith trace element proxies for fish condition can provide additional tools for the conservation and management of target species. In summary, since many otolith-based metrics are used in the management and conservation of the species, it is imperative that we understand which metrics best estimate certain conditions, and where otoliths lack adequate specificity, allowing managers to make sound management decisions.

Interactive effects of high temperature and low food on fish survival

Although food limitation resulted in higher mortality in both temperature treatments, the highest mortality rates occurred in warmer conditions when food was also limited. Specifically, the mortality rates for the 18°C-unfed (18NF) was 128% higher than 14°C-unfed treatments and 366% higher than both fed treatments, independent of temperature (Figure 7-3). These differences in survival are striking, especially considering how temperatures only differed by ±2°C from ideal rearing temperatures (~16°C) (Lindberg et al., 2013), and thermal differences between replicate tanks were also very low (0-8%). This suggests that warming conditions are likely to exacerbate the effects of food limitation on wild Delta Smelt. Laboratory experiments have shown that Delta Smelt stress responses, survival, metabolic rate, and activity levels are highly sensitive to rising temperature (Komoroske et al., 2014, 2015; Davis et al., 2019b; Hung et al., 2022b), and that food limitation quickly limits growth and condition while increasing mortality (Hammock et al., 2020). Previous research has shown how Delta Smelt juveniles increase their swimming velocity, decrease turning angles, and increased inter-individual distances in a warm temperature treatment (21°C), compared to a lower temperature treatment (17°C) (Davis et al., 2019b), suggesting behavioral responses that impact energy stores are thermally-driven. Similarly, wild Delta Smelt collected from warmer habitats exhibited lower growth rates and poorer body condition than those collected from cooler habitats (Hammock 2017, Lewis et al. 2021), all of which potentially increase mortality.

Interestingly, temperature alone had no effect on survival when food was plentiful during the experiment, suggesting that Delta Smelt could metabolically compensate for thermal stress when sufficient prey was available. This is supported by the increased mesozooplankton abundance in the stomachs of freshwater populations of Delta Smelt during the summer when thermal refugia

are unavailable (Hammock et al., 2017). Similar trends have been found in juvenile Coho Salmon (*Oncorhynchus kisutch*), where absolute growth rates peaked at high temperatures and remained high in maximum temperatures where survival was reduced (Lusardi et al., 2020). Overall, these findings suggests that productive ecosystems and cool temperature refugia are both important management tools for conserving the Delta Smelt in the food limited Delta region of San Francisco Estuary (Moyle et al., 2016).

Food limitation, not temperature, determines somatic growth

Despite the negative impact of combining high temperatures and food limitation on survival, only food availability was positively correlated with increased growth and condition among treatments (Figure 7-4A-C). Adult Delta Smelt have exhibited declining growth rates at water temperatures above 20°C and high growth rates between 13°C and 20°C in otolith-based reconstructions (Lewis et al., 2021), while their critical thermal maximum is around 27°C (Komoroske et al., 2014; Hung et al., 2022b). In contrast, condition factor (*K*) has been positively correlated with indicators of primary productivity and zooplankton abundance in the wild, peaking at lower temperatures (10-13°C) (Hammock et al., 2022). Further, the deleterious effects of starvation on growth and condition metrics are known to begin after only a few days in experimental conditions (Hung et al., 2019; Hammock et al., 2020). Similarly, Rainbow Smelt (*Osmerus mordax*) were observed to have increased mortality rates after experiencing low-quality feeding conditions, while survival was linked to increased adulthood growth rates (Sirois & Dodson, 2000). These factors, in combination with temperatures so close to ideal rearing conditions (Lindberg et al., 2013), suggest that the degree of difference between food rations in our experiment (e.g., fed *ad libitum* versus starvation) represented a greater difference in significant physiological impacts than those of a 4°C ambient water difference. This could, in part, explain the lack of significant differences between temperature treatments.

However, a more substantial factor in the lack of additive effects of food and temperature pressures on the 18NF group may be associated with a disparity in survivorship among unfed treatments. With stronger selective pressure (i.e., lower survival rates) associated with 18NF fish, there may have been signs of size-selective mortality. Size-selective mortality suggests that faster-growing, larger individuals exhibit a survival advantage due to increased resistance to starvation, lower susceptibility to thermal stress, and often decreased risk of predation (Sogard, 1997). If the survivors experiencing higher temperatures and no food were faster-growing and less susceptible to thermal stress, that could have ultimately produced mean morphometrics similar to those of 14NF fish (Figure 7-4A-C), even if 18NF fish experienced greater negative treatment effects on growth and condition. Size-dependent mortality has been associated with models explaining Delta Smelt population trends (Bennett, Hobbs & Teh, 2008), particularly with respect to differences between “good” and “bad” years for the species (Rose et al., 2013). This further supports the importance of meeting the energetic demands of Delta Smelt (O’Brien, 1979; Moyle et al., 1992) via our conservation efforts, yet suggests there may be minimal thermal consequences for the smaller percentage of survivors experiencing higher temperatures and food limitation during adulthood.

Food limitation effects in otolith accretion rates

Like the strong positive correlation between feed and somatic growth metrics (Figure 7-4A-C), otolith accretion was also positively correlated with increased feed, but less sensitively than somatic metrics (Figure 7-4D). This difference suggests that otolith accretion is a conservative proxy for somatic growth and condition. Otolith-based reconstructions have been known to underestimate somatic growth for many decades (Campana, 1990), requiring researchers to closely assess the accuracy of back-calculation models like Fraser-Lee and the biological-intercept model (Titus, Volkoff & Snider, 2004; Hobbs et al., 2007a) before applying them for conservation applications. Concerningly, despite the significant effect of feed on otolith accretion, the variance within the linear model was mostly explained by individual variation, not treatment effects. This mismatch is highlighted in the linear relationships between the total change in somatic growth and otolith accretion (Figure 7-7), where the amount of otolith growth was positive and varied among individuals, while somatic growth stagnated or even decreased. Similar disruptions of otolith-somatic constant proportionality have been observed in short-term experiments assessing growth rates in juvenile Sprat (*Sprattus sprattus*), where changes in food ration temporarily decoupled otolith and somatic growth, even after re-establishing *ad libitum* food rations; otoliths also only tracked changes in length, not condition, during periods of food deprivation (Peck et al., 2015). The decoupling of this relationship in unfed fish means that their otoliths may have a limited ability to track somatic growth rates in poor foraging conditions. We suggest using caution in analyzing otoliths as proxies for growth during periods when condition or mass, not length, are the strongest indicators of physiological stress, like when assessing older fish or fish that are preparing to spawn.

Similar to survival trends, temperature did not significantly affect linear relationships between otolith accretion and somatic growth, except potentially in the difference among treatments when observing grouped otolith-somatic linear models. For instance, at the cooler temperatures (14°C), fed fish (14F) exhibited a distinct relationship from other treatments (Figure 7-6), where fish were predicted to be larger at a specific otolith size than other treatments, perhaps in opposition to trends in survival where the warmer and poorly fed fish exhibited poorer condition. Though this can support an inverse relationship to that seen in fish survival, it could also relate to discrepancies in daily otolith accretion rates seen at the beginning of the experiment (Figure 7-5). Shortly after the fish were tagged and placed in their respective tanks, the 14F fish exhibited a steeper decline in daily growth than other groups, with accretion rates then increasing throughout the experimental period. Though it is unclear why this dip in otolith growth occurred, it is possible that it could reflect differences among groups prior to the beginning of the experiment.

An additional caveat related to the conservative nature of our otolith treatment effects relates to the potential limits of the daily age methods used for older subadult Delta Smelt. Previously, Delta Smelt otoliths were validated for daily periodicity, confirming that otolith microstructure was accreted on a daily scale, up to 270 dph (Xieu et al., 2021), an increase from previous limits due to improved imaging technologies (Hobbs et al., 2007a). Our experimental fish were over 3 weeks older than the oldest validated fish (294 dph), and did not experience the regular, near-optimal rearing conditions utilized in the validation study (Lindberg et al., 2013). Considering

the long-term nature of this study (e.g., 70-days) and the advanced age of the fish upon experimental completion, we could have been nearing the furthest extent of our abilities to age Delta Smelt otoliths on a daily scale. As Delta Smelt matured, their somatic growth rates and otolith accretion rates decline, potentially to such a slow rate that daily increments are no longer discernable, or differences among growth rates are negligible. This is additionally impacted by the long-term food limitation, decreasing accretion and somatic growth rates further. Therefore, part of the minimization of treatment effects represented in otoliths could be related to this ontogenetic slowing of otolith growth as Delta Smelt age (Walther et al., 2010; Xieu et al., 2021). This suggests utility in running similar temperature and feed experiments on younger fish where the periodicity of daily accretion is more certain.

Element-to-calcium ratios and partition coefficients in Delta Smelt otoliths

Otolith chemistry has been used to address ecological questions around natal origins (Hobbs et al., 2005; Barnett-Johnson et al., 2008), environmental reconstructions (Tanner et al., 2013; Izzo et al., 2016), and life history movements (Elsdon & Gillanders, 2003; Gillanders, 2005; Hobbs et al., 2019; Lewis et al., 2021) in Delta Smelt and other teleost fishes throughout the world. Such research is conducted under the general assumption that otolith microchemistry reflects external conditions. However, it is well known that intrinsic and extrinsic factors impact this process in (sometimes) predictable ways. Elements like Mn Sr, and Ba are commonly examined in euryhaline fishes via otoliths (Miller & Hurst, 2020), but additional elements like Li, Na, Cu, Zn, and B are less understood. Elemental incorporation is modulated by various barriers between external conditions and the otolith; thus, rates of incorporation can vary drastically depending on the element, where that element incorporates into the matrix of the otolith, and what external conditions are being experienced.

For Delta Smelt, little is known about the species-specific fractionation of elements from ambient water into otoliths. Further, there is a gap in knowledge around how and when this process is influenced by external factors like temperature or food availability. By assessing species-specific trace element signatures in Delta Smelt we can uncover proxies for key ecological conditions, thus enhancing the utility of otolith chemistry in the management and conservation of the species. In this experiment, we found that average *X:Ca* values (μmol/mol), varied by element and treatment (Table 8), as did average partition coefficients (D_X), a value describing the fraction of ambient water elemental concentrations represented in the otolith (Table 9). These values enable us to assess Delta Smelt otoliths among experimental treatments and assess how these values compare to those of other estuarine and freshwater species (Table 7-10) and identify potential chemical proxies for environmental conditions of conservation and management concern.

Food Availability: Manganese, Barium, and Sodium

The partition coefficients for three elements, Mn, Ba, and Na, were correlated with food availability, suggesting their potential use as proxies for food limitation in Delta Smelt (Table 7-7). However, these responses can be quite variable among studies or species (Table 7-10). For example, increased food rations exhibited a positive effect on D_{Mn} in juvenile Pacific Cod

(*Gadus macrocephalus*) in laboratory studies (Miller & Hurst, 2020). The authors hypothesized that Mn concentrations decreased with declining food availability due to the association of Mn with the proteinaceous part of the otolith (Izzo et al., 2016), which, in turn, affected the amount of protein accreted in the otolith. Otoliths from unfed fish in our experiment did, anecdotally, appear more transparent on the edges than fed fish, and they had smaller partition coefficients (Table 9), supporting the idea that less protein, or less opacity, are correlated with lower concentrations of Mn. However, Mn is also known to substitute in the calcium carbonate structure of the otolith, explaining the mixed correlation results throughout the literature with fish growth (often positive), temperature (positive only if very warm ambient water), or other environmental conditions (mixed overall) (Hüssy et al., 2020). Our study provides additional support, finding that higher Mn:Ca ratios and D_{Mn} are related to higher food availability and fish growth (Stanley et al., 2015), suggesting its use as a proxy for growth or food consumption.

Both Ba:Ca in otoliths and D_{Ba} were negatively correlated with increased food availability (Table 7-7), similar to findings in a Tropical Damselfish (*Acanthochromis polyacanthus*) (Walther et al., 2010), Black Bream (*Acanthopagrus butcheri*) (Elsdon & Gillanders, 2003, 2005), and European Plaice (*Pleuronectes platessa L.*) (Sturrock et al., 2015) where up to 20% of the Ba:Ca in otoliths was not directly connected to ambient water concentrations alone. Interestingly, Ba:Ca and Sr:Ca were previously considered highly correlated with ambient water element concentrations (Campana, 1999), not with metabolic processes, though Miller and Hurst et al. (2020) highlighted research observing correlations with both (Miller & Hurst, 2020). While some studies have observed correlations between D_{Ba} and ambient temperature (Collingsworth et al., 2010), we did not find such a relationship. Overall, Ba:Ca could indicate signs of feeding conditions in Delta Smelt otoliths, though more research is necessary to solidify this concept.

The partition coefficients and concentration ratios of Na showed significant, positive effects of feed. The lack of temperature effects further supports our understanding of how Na:Ca in otoliths is not directly correlated with ambient temperature (Hoff & Fuiman, 1995) due to the strong physiological barriers between ambient water Na:Ca and otolith Na:Ca (Campana, 1999; Hüssy et al., 2020). Furthermore, studies have observed within-individual changes in otolith Na:Ca seasonally (Fuiman & Hoff, 1995), and with age (Grammer et al., 2017), likely due to changes in reproduction or physiological stressors. This could be, in part, why the elemental composition of diet sources have also not been correlated directly with otolith Na:Ca (Hoff & Fuiman, 1995; Buckel, Sharack & Zdanowicz, 2004) in species like Bluefish (*Pomatomus saltatrix*). These findings suggest that the feed treatment effects in our study are connected solely with the physiological differences between well-fed fish and fish experiencing starvation conditions (Hammock et al., 2020). As such, we propose the use of relative Na:Ca as a potential proxy for physiological stress in Delta Smelt.

Temperature: Zinc and Copper

Zinc to calcium ratios (Zn:Ca) show a negative effect of temperature (Table 7-11), suggesting it might be an effective proxy for fish condition and stress in estuarine fishes. For D_{Zn} and Zn:Ca, the highest mean value was associated with 14F (cool and well-fed), with 14NF and 18F showing intermediate values, and the lowest partition coefficient for 18NF (warm, not fed). This

is likely explained by the strong association of Zn with protein in otoliths (Miller et al., 2006), and the modulation of protein concentrations around the otolith by abiotic factors (Hüssy et al., 2020). Experimental studies of Pink Snapper (*Pagrus auratus*) found no connection between high waterborne Zn concentrations and Zn concentrations in otoliths, but did see a significant increase when juvenile snapper were fed with a Zn-enriched diet (Ranaldi & Gagnon, 2008). This suggests that Zn concentrations in otoliths are derived from diet more so than ambient conditions. Despite no significant food ration effects, there does appear to be a non-significant interactive effect regarding average Zn:Ca and D_{Zn} values in our experiment (Figure 7-9), where higher feed correlates with higher Zn concentrations. Since our higher temperature treatment caused stress, as seen by heightened mortality rates (Figure 7-3, Table 7-2), this interactive effect could be more closely related to metabolic stress on the fish, where proteins in otoliths are mobilized due to endogenous processes (Sturrock et al., 2015). Further investigation is needed to understand exactly what D_{Zn} indicates in Delta Smelt otoliths.

Interestingly, Cu is also linked almost solely to the protein matrix of the otolith, with 70-100% of Cu atoms binding to otolith protein, so one would expect fish under starvation conditions to exhibit lower Cu:Ca ratios (Miller et al., 2006) with minimal influence of ambient water conditions (Campana, 1999). Despite this, there were no significant effects of feed on D_{Cu} or Cu:Ca in our experiment, thought there were significant effects of temperature. There are marked differences in average Cu concentration in the ambient water samples taken throughout the experiment (Table 7-1, Figure 7-8A) which likely drives the differences seen in otolith partition coefficients.

Non-significant effects on otolith chemistry

For Sr, a mix of relationships between D_{Sr} and both temperature and feed have been reported in the literature, like the positive relationship between D_{Sr} and food rations in Pacific Cod (Miller & Hurst, 2020) or the negative relationship with growth rate in Japanese Eel (*Anguilla japonica*) (Lin et al., 2007). Overall, consensus in the scientific literature states that Sr:Ca in otoliths very closely tracks ambient water concentrations (Campana, 1999; Bath et al., 2000; Doubleday et al., 2013). Similarly, Sr:Ca ratios did not differ significantly among treatments in this experiment, suggesting that Sr:Ca is likely a fairly robust indicator of the chemical environment (e.g., salinity) experienced by each fish.

D_{Li} and D_B are far less understood in the literature and were not significantly impacted by treatment conditions in our experiment. A negative association between ambient water temperature and Li:Ca in European Plaice (Sturrock et al., 2015), and D_{Li} in Common Sole (*Solea solea*) (Tanner et al., 2013) has been observed, suggesting the potential use of Li as a thermal proxy, but we were unable to detect temperature effects in Delta Smelt due to low concentrations of Li in most otoliths. This is unsurprising, as Li:Ca for both otolith and water tracks ambient salinity, which was very low in our freshwater experiment (Hicks, Closs & Swearer, 2010; Martino et al., 2021). The B:Ca, in contrast, has only recently been observed in direct relationship with ambient pH in a single-celled marine eukaryote (Allen et al., 2011), suggesting potential uses of B:Ca in $CaCO_3$ structures like otoliths to be a proxy for pH, and therefore temperature due to the weak negative correlation between the two (Hemming &

Hanson, 1992; Martino et al., 2017). However, this potential proxy is not supported by either our experiment, or that of Martino et al. (2017). Average Li:Ca and B:Ca in ambient water were similar among temperature treatments. Thus, the results were inconclusive as to the significance of ambient temperatures during the experiment or the physiological processes moderating random incorporation into otoliths. Further research is necessary to see if B or Li could be useful in otolith chemical analyses in Delta Smelt.

Conservation Implications

Otolith-based reconstructions of growth rates and chemical histories can directly link aspects of ontogeny, location, environmental conditions, and seasonal variation. However, as with any proxy, there are limits, constraints, and discrepancies that impact their interpretation (Campana, 1990, 2001; Stevenson & Campana, 1993). Delta Smelt otolith accretion rates have been validated as representative proxies for age and size (Hobbs et al., 2007a; Xieu et al., 2021) for most of their annual lifespan (e.g. 270 dph). Additionally, natal habitat discrimination has been successful at broad scales using trace element concentrations (Hobbs et al., 2007b), while diverse life history strategies have been differentiated using Sr isotope ratios (Hodge et al., 2016; Hobbs et al., 2019), both providing information crucial to the conservation of the species. Recently, otolith-based reconstructions of growth rates were utilized to assess the quality of different habitats throughout the San Francisco Estuary, comparing recent otolith accretion (last 14 days) with environmental parameters where adult fish were caught *in situ* (Lewis et al., 2021). As the use of and reliance on otoliths-based techniques expands, and the geographic or time scales assessed are refined, it is important to understand the discrete, direct relationships between otoliths and the conditions they represent.

In this experiment, we found that otolith-based growth estimates generally exhibited similar trends across treatments as somatic growth metrics, but greatly underestimated the magnitudes of these differences. For example, we observed a high degree of overlap across treatments in otolith accretion (Figure 7-4D), but not in somatic growth (Figure 7-4A-C). Additionally, otoliths were unable to reflect negative change in $MASS_e$ and K, due to the continuous accretion of otolith material (Campana, 1990). Therefore, otoliths could not discriminate between a slow growth rates in mass or *any* degree of mass reduction, whether minor or severe. This was also true, to a lesser degree, for SL_c, because fish that did not grow at all (0 mm change) still accumulated at least 80 μm of otolith material. Therefore, otoliths overestimated somatic growth when it was low or negative and thus provided a conservative estimate of growth differences due to variation in food availability. This decoupling is common in subadult and adult fish (here, 224 - 294 dph), when fish are beginning to experience annulus formation. Whether similar patterns occur in younger life stages has yet to be explored. Overall, these findings suggest that the negative impacts of warming waters and food web disruption on Delta Smelt may be even more detrimental than previously estimated using otolith-based tools (Lewis et al., 2021).

CONCLUSIONS

Using a controlled experiment, we demonstrated how temperature and food availability affect the survival, otolith-somatic proportionality, and otolith microchemistry of adult Delta Smelt. Results indicated strong interactive effects of food limitation and temperature on survival, with high-temperature no-feed treatments resulting in 366% greater mortality relative to both fed treatments, where ample food supply eliminated any effect of temperature on survival. Although otolith size linearly tracked fish size, intercepts differed by treatment. Furthermore, otolith accretion rates during the experiment were largely decoupled from changes in mass, length, or condition; indicating that otolith increments in adult (e.g., ~ 300 dph) Delta Smelt do not reflect changes in growth or condition. We also found that otolith chemistry can be altered by variation in environmental conditions, with the magnitude of effects varying among different element constituents. Given that otolith-derived metrics are commonly used to provide valuable information to inform management and policy decisions for the recovery of endangered and threatened fish species, like Delta Smelt; these results highlight the importance of considering the effects of ontogenetic and environmental factors in the design and interpretation of otolith-derived metrics for wild fish populations.

ACKNOWLEDGEMENTS

We thank the many staff at the UC Davis Fish Conservation and Culture Laboratory for their expertise and efforts in culturing and rearing Delta Smelt. Furthermore, we acknowledge the many staff and student researchers at the UC Davis Department of Wildlife, Fish, and Conservation Biology; School of Veterinary Medicine; and Center for Aquatic Biology and Aquaculture for laboratory and logistical support in conducting the study and processing samples. Funding for this study was provided by the US Bureau of Reclamation (USBR) contracts R13AP20022, R17AC00129, and R22AC00392 to B.G. Hammock, L.S. Lewis, J. Hobbs, and S. Teh, and contract R15AC00030 to T.C. Hung. The content and views expressed herein are those of the authors and do not represent the official opinion of any employer, institution, or government agency.

REFERENCES

Abramoff MD, Magelhaes PJ, Ram SJ. 2004. Image Processing with ImageJ. *Biophotonics International* 11:36–42.

Allen KA, Hönisch B, Eggins SM, Yu J, Spero HJ, Elderfield H. 2011. Controls on boron incorporation in cultured tests of the planktic foraminifer Orbulina universa. *Earth and Planetary Science Letters* 309:291–301. DOI: 10.1016/j.epsl.2011.07.010.

Audzijonyte A, Kuparinen A, Gorton R, Fulton EA. 2013. Ecological consequences of body size decline in harvested fish species: positive feedback loops in trophic interactions amplify human impact. *Biology Letters* 9:20121103. DOI: 10.1098/rsbl.2012.1103.

Avaria-Llautureo J, Venditti C, Rivadeneira MM, Inostroza-Michael O, Rivera RJ, Hernández CE, Canales-Aguirre CB. 2021. Historical warming consistently decreased size, dispersal and speciation rate of fish. *Nature Climate Change* 11:787–793. DOI: 10.1038/s41558-021-01123-5.

Barber MC, Jenkins GP. 2001. Differential effects of food and temperature lead to decoupling of short-term otolith and somatic growth rates in juvenile King George whiting. *Journal of Fish Biology* 58:1320–1330. DOI: 10.1111/j.1095-8649.2001.tb02289.x.

Barneche DR, Robertson DR, White CR, Marshall DJ. 2018. Fish reproductive-energy output increases disproportionately with body size. *Science* 360:642–645. DOI: 10.1126/science.aao6868.

Barnett-Johnson R, Pearson TE, Ramos FC, Grimes CB, MacFarlane RB. 2008. Tracking natal origins of salmon using isotopes, otoliths, and landscape geology. *Limnology and Oceanography* 53:1633–1642. DOI: 10.4319/lo.2008.53.4.1633.

Barnett-Johnson R, Ramos FC, Grimes CB, MacFarlane RB. 2005. Validation of Sr isotopes in otoliths by laser ablation multicollector inductively coupled plasma mass spectrometry (LA-MC-ICPMS): opening avenues in fisheries science applications. *Canadian Journal of Fisheries and Aquatic Sciences*. DOI: 10.1139/f05-194.

Bartoń K. 2022. MuMIn: Multi-Model Inference.

Bath GE, Thorrold SR, Jones CM, Campana SE, McLaren JW, Lam JWH. 2000. Strontium and barium uptake in aragonitic otoliths of marine fish. *Geochimica et Cosmochimica Acta* 64:1705–1714. DOI: 10.1016/S0016-7037(99)00419-6.

Baumann H, Peck MA, Herrmann J-P, Baumann H, Peck MA, Herrmann J-P. 2005. Short-term decoupling of otolith and somatic growth induced by food level changes in postlarval Baltic sprat, Sprattus sprattus. *Marine and Freshwater Research* 56:539–547. DOI: 10.1071/MF04140.

Bennett WA, Hobbs JA, Teh SJ. 2008. *Interplay of environmental forcing and growth-selective mortality in the poor year-class success of delta smelt in 2005. Final report to the POD*

Management Team of the Interagency Ecological Program for the San Francisco Estuary, Sacramento, CA, USA.

Brown LR, Komoroske LM, Wagner RW, Morgan-King T, May JT, Connon RE, Fangue NA. 2016. Coupled Downscaled Climate Models and Ecophysiological Metrics Forecast Habitat Compression for an Endangered Estuarine Fish. *PLOS ONE* 11:e0146724. DOI: 10.1371/journal.pone.0146724.

Buckel JA, Sharack BL, Zdanowicz VS. 2004. Effect of diet on otolith composition in Pomatomus saltatrix, an estuarine piscivore. *Journal of Fish Biology* 64:1469–1484. DOI: 10.1111/j.0022-1112.2004.00393.x.

Campana SE. 1990. How reliable are growth back-calculations based on otoliths? *Canadian Journal of Fisheries and Aquatic Sciences* 47. DOI: 10.1139/f90-246.

Campana SE. 1999. Chemistry and composition of fish otoliths: pathways, mechanisms and applications. *Marine Ecological Progress Series* 188:263–297.

Campana SE. 2001. Accuracy, precision and quality control in age determination, including a review of the use and abuse of age validation methods. *Journal of Fish Biology* 59:197–242. DOI: 10.1111/j.1095-8649.2001.tb00127.x.

Campana SE, Neilson JD. 1985. Microstructure of Fish Otoliths. *Canadian Journal of Fisheries and Aquatic Sciences* 42:1014–1032. DOI: 10.1139/f85-127.

Campana SE, Thorrold SR. 2001. Otoliths, increments, and elements: keys to a comprehensive understanding of fish populations? *Canadian Journal of Fisheries and Aquatic Sciences* 58:30–38. DOI: 10.1139/f00-177.

CDFG. 2010. State & federally listed endangered & threatened animals of California. California Department of Fish & Game,State of California, The Natural Resources Agency, California. *The Natural Rsources Agency, California*.

Cloern JE, Knowles N, Brown LR, Cayan D, Dettinger MD, Morgan TL, Schoellhamer DH, Stacey MT, van der Wegen M, Wagner RW, Jassby AD. 2011. Projected Evolution of California's San Francisco Bay-Delta-River System in a Century of Climate Change. *PLoS ONE* 6:e24465. DOI: 10.1371/journal.pone.0024465.

Cole LC. 1954. The population consequences of life history phenomena. *The Quarterly review of biology* 29:103–137. DOI: 10.1086/400074.

Collingsworth PD, Van Tassell JJ, Olesik JW, Marschall EA. 2010. Effects of temperature and elemental concentration on the chemical composition of juvenile yellow perch (Perca flavescens) otoliths. *Canadian Journal of Fisheries and Aquatic Sciences* 67:1187–1196. DOI: 10.1139/F10-050.

Davis BE, Cocherell DE, Sommer T, Baxter RD, Hung TC, Todgham AE, Fangue NA. 2019a. Sensitivities of an endemic, endangered California smelt and two non-native fishes to serial

increases in temperature and salinity: Implications for shifting community structure with climate change. *Conservation Physiology* 7. DOI: 10.1093/conphys/coy076.

Davis BE, Hansen MJ, Cocherell DE, Nguyen TX, Sommer T, Baxter RD, Fangue NA, Todgham AE. 2019b. Consequences of temperature and temperature variability on swimming activity, group structure, and predation of endangered delta smelt. *Freshwater Biology* 64:2156–2175. DOI: 10.1111/fwb.13403.

Doubleday Z, Izzo C, Woodcock S, Gillanders B. 2013. Relative contribution of water and diet to otolith chemistry in freshwater fish. *Aquatic Biology* 18:271–280. DOI: 10.3354/ab00511.

Elsdon T, Gillanders B. 2003. Relationship between water and otolith elemental concentrations in juvenile black bream Acanthopagrus butcheri. *Marine Ecology Progress Series* 260:263–272. DOI: 10.3354/meps260263.

Elsdon TS, Gillanders BM. 2005. Alternative life-history patterns of estuarine fish: barium in otoliths elucidates freshwater residency. *Canadian Journal of Fisheries and Aquatic Sciences* 62:1143–1152. DOI: 10.1139/f05-029.

Fey D. 1999. Effects of preservation technique on the length of larval fish: Methods of correcting estimates and their implication for studying growth rates. *Archive of Fishery and Marine Research* 47:17–29.

Feyrer F, Nobriga ML, Sommer TR. 2007. Multidecadal trends for three declining fish species: habitat patterns and mechanisms in the San Francisco Estuary, California, USA. *Canadian Journal of Fisheries and Aquatic Sciences* 64:723–734. DOI: 10.1139/f07-048.

Finger AJ, Mahardja B, Fisch KM, Benjamin A, Lindberg J, Ellison L, Ghebremariam T, Hung TC, May B. 2018. A conservation hatchery population of delta smelt shows evidence of genetic adaptation to captivity after 9 generations. *Journal of Heredity* 109. DOI: 10.1093/jhered/esy035.

Fong S, Louie S, Werner I, Connon RE. 2016. Contaminant Effects on California Bay–Delta Species and Human Health. *San Francisco Estuary and Watershed Science* 14. DOI: 10.15447/sfews.2016v14iss4art5.

Fowler GM, Smith SJ. 1983. Length Changes in Silver Hake (Merluccius bilinearis) Larvae: Effects of Formalin, Ethanol, and Freezing. *Canadian Journal of Fisheries and Aquatic Sciences* 40. DOI: 10.1139/f83-113.

Fuiman LA, Hoff GR. 1995. Natural variation in elemental composition of sagittae from red drum. *Journal of Fish Biology* 47:940–955. DOI: 10.1111/j.1095-8649.1995.tb06020.x.

Gasith A, Resh VH. 1999. Streams in Mediterranean Climate Regions: Abiotic Influences and Biotic Responses to Predictable Seasonal Events. *Annual Review of Ecology and Systematics* 30:51–81. DOI: 10.1146/annurev.ecolsys.30.1.51.

Gillanders BM. 2005. Otolith chemistry to determine movements of diadromous and freshwater fish. *Aquatic Living Resources* 18:291–300. DOI: 10.1051/alr:2005033.

Grammer GL, Morrongiello JR, Izzo C, Hawthorne PJ, Middleton JF, Gillanders BM. 2017. Coupling biogeochemical tracers with fish growth reveals physiological and environmental controls on otolith chemistry. *Ecological Monographs* 87:487–507. DOI: 10.1002/ecm.1264.

Hammock BG, Hartman R, Dahlgren RA, Johnston C, Kurobe T, Lehman PW, Lewis LS, Van Nieuwenhuyse E, Ramírez-Duarte WF, Schultz AA, Teh SJ. 2022. Patterns and predictors of condition indices in a critically endangered fish. *Hydrobiologia* 849:675–695. DOI: 10.1007/s10750-021-04738-z.

Hammock BG, Moose SP, Solis SS, Goharian E, Teh SJ. 2019. Hydrodynamic Modeling Coupled with Long-term Field Data Provide Evidence for Suppression of Phytoplankton by Invasive Clams and Freshwater Exports in the San Francisco Estuary. *Environmental Management* 63:703–717. DOI: 10.1007/s00267-019-01159-6.

Hammock BG, Ramírez-Duarte WF, Triana Garcia PA, Schultz AA, Avendano LI, Hung T-C, White JR, Bong Y-T, Teh SJ. 2020. The health and condition responses of Delta Smelt to fasting: A time series experiment. *PLOS ONE* 15:e0239358. DOI: 10.1371/journal.pone.0239358.

Hammock BG, Slater SB, Baxter RD, Fangue NA, Cocherell D, Hennessy A, Kurobe T, Tai CY, Teh SJ. 2017. Foraging and metabolic consequences of semi-anadromy for an endangered estuarine fish. *PLoS ONE* 12. DOI: 10.1371/journal.pone.0173497.

Heino M, Dieckmann U, Godø OR. 2002. Measuring Probabilistic Reaction Norms for Age and Size at Maturation. *Evolution* 56:669–678. DOI: 10.1111/j.0014-3820.2002.tb01378.x.

Hemming NG, Hanson GN. 1992. Boron isotopic composition and concentration in modern marine carbonates. *Geochimica et Cosmochimica Acta* 56:537–543. DOI: 10.1016/0016-7037(92)90151-8.

Hicks AS, Closs GP, Swearer SE. 2010. Otolith microchemistry of two amphidromous galaxiids across an experimental salinity gradient: A multi-element approach for tracking diadromous migrations. *Journal of Experimental Marine Biology and Ecology* 394:86–97. DOI: 10.1016/j.jembe.2010.07.018.

Hobbs JA, Bennett WA, Burton JE, Baskerville-Bridges B. 2007a. Modification of the biological intercept model to account for ontogenetic effects in laboratory-reared delta smelt (Hypomesus transpacificus). *Fishery Bulletin* 105.

Hobbs JA, Bennett WA, Burton J, Gras M. 2007b. Classification of Larval and Adult Delta Smelt to Nursery Areas by Use of Trace Elemental Fingerprinting. *Transactions of the American Fisheries Society* 136:518–527. DOI: 10.1577/T06-087.1.

Hobbs JA, Lewis LS, Willmes M, Denney C, Bush E. 2019. Complex life histories discovered in a critically endangered fish. *Scientific Reports* 9:16772. DOI: 10.1038/s41598-019-52273-8.

Hobbs J, Moyle P, Fangue N, Connon RE. 2017. Is extinction inevitable for Delta Smelt and Longfin Smelt? An opinion and recommendations for recovery. *San Francisco Estuary and Watershed Science* 15. DOI: 10.15447/sfews.2017v15iss2art2.

Hobbs JA, Yin QZ, Burton J, Bennett WA. 2005. Retrospective determination of natal habitats for an estuarine fish with otolith strontium isotope ratios. In: *Marine and Freshwater Research*. DOI: 10.1071/MF04136.

Hodge BW, Wilzbach MA, Duffy WG, Quiñones RM, Hobbs JA. 2016. Life History Diversity in Klamath River Steelhead. *Transactions of the American Fisheries Society* 145:227–238. DOI: 10.1080/00028487.2015.1111257.

Hoff GR, Fuiman LA. 1995. Environmentally Induced Variation in Elemental Composition of Red Drum (Sciaenops Ocellatus) Otoliths. *Bulletin of Marine Science* 56:578–591.

Howell D, Griffin WL, Pearson NJ, Powell W, Wieland P, O'Reilly SY. 2013. Trace element partitioning in mixed-habit diamonds. *Chemical Geology* 355:134–143. DOI: 10.1016/j.chemgeo.2013.07.013.

Hung T-C, Ellison L, Stevenson T, Sandford M, Schultz AA, Eads AR. 2022a. Early Weaning in Endangered Delta Smelt: Effect of Weaning Time on Growth and Survival. *North American Journal of Aquaculture* 84:249–260. DOI: 10.1002/naaq.10230.

Hung T-C, Hammock BG, Sandford M, Stillway M, Park M, Lindberg JC, Teh SJ. 2022b. Temperature and salinity preferences of endangered Delta Smelt (Hypomesus transpacificus, Actinopterygii, Osmeridae). *Scientific Reports* 12:16558. DOI: 10.1038/s41598-022-20934-w.

Hung T-C, Rosales M, Kurobe T, Stevenson T, Ellison L, Tigan G, Sandford M, Lam C, Schultz A, Teh S. 2019. A pilot study of the performance of captive-reared delta smelt Hypomesus transpacificus in a semi-natural environment. *Journal of Fish Biology* 95:1517–1522. DOI: 10.1111/jfb.14162.

Hüssy K. 2008. Otolith accretion rates: Does size really matter? *Journal of Experimental Marine Biology and Ecology* 362:131–136. DOI: 10.1016/j.jembe.2008.06.016.

Hüssy K, Limburg KE, de Pontual H, Thomas ORB, Cook PK, Heimbrand Y, Blass M, Sturrock AM. 2020. Trace Element Patterns in Otoliths: The Role of Biomineralization. *Reviews in Fisheries Science and Aquaculture*. DOI: 10.1080/23308249.2020.1760204.

IUCN. 2012. Hypomesus transpacificus: NatureServe: The IUCN Red List of Threatened Species 2014: e.T10722A174778740. DOI: 10.2305/IUCN.UK.2014-3.RLTS.T10722A174778740.en.

Izzo CA, Doubleday ZA, Grammer GL, Gilmore KL, Alleway HK, Barnes TC, Disspain MCF, Giraldo AJ, Mazloumi N, Gillanders BM. 2016. Fish as proxies of ecological and environmental change. *Reviews in Fish Biology and Fisheries* 26. DOI: 10.1007/s11160-016-9424-3.

Izzo C, Reis-Santos P, Gillanders BM. 2018. Otolith chemistry does not just reflect environmental conditions: A meta-analytic evaluation. *Fish and Fisheries* 19:441–454. DOI: 10.1111/faf.12264.

Jeffries KM, Connon RE, Davis BE, Komoroske LM, Britton MT, Sommer T, Todgham AE, Fangue NA. 2016. Effects of high temperatures on threatened estuarine fishes during periods of extreme drought. *Journal of Experimental Biology* 219:1705–1716. DOI: 10.1242/jeb.134528.

Jochum KP, Weis U, Stoll B, Kuzmin D, Yang Q, Raczek I, Jacob DE, Stracke A, Birbaum K, Frick DA, Günther D, Enzweiler J. 2011. Determination of Reference Values for NIST SRM 610-617 Glasses Following ISO Guidelines. *Geostandards and Geoanalytical Research* 35:397–429. DOI: 10.1111/j.1751-908X.2011.00120.x.

Johnson DW, Grorud-Colvert K, Sponaugle S, Semmens BX. 2014. Phenotypic variation and selective mortality as major drivers of recruitment variability in fishes. *Ecology Letters* 17:743–755. DOI: 10.1111/ele.12273.

Kimmerer W, Gartside E, Orsi J. 1994. Predation by an introduced clam as the likely cause of substantial declines in zooplankton of San Francisco Bay. *Marine Ecology Progress Series* 113:81–93. DOI: 10.3354/meps113081.

Knowles N, Cayan DR. 2002. Potential effects of global warming on the Sacramento/San Joaquin watershed and the San Francisco estuary. *Geophysical Research Letters* 29:38-1-38–4. DOI: 10.1029/2001GL014339.

Komoroske LM, Connon RE, Jeffries KM, Fangue NA. 2015. Linking transcriptional responses to organismal tolerance reveals mechanisms of thermal sensitivity in a mesothermal endangered fish. *Molecular Ecology* 24:4960–4981. DOI: 10.1111/mec.13373.

Komoroske LM, Connon RE, Lindberg J, Cheng BS, Castillo G, Hasenbein M, Fangue NA. 2014. Ontogeny influences sensitivity to climate change stressors in an endangered fish. *Conservation Physiology* 2:cou008–cou008. DOI: 10.1093/conphys/cou008.

Kooijman SALM. 2000. *Dynamic Energy and Mass Budgets in Biological Systems*. Cambridge University Press.

Kraus RT, Secor DH. 2004. Incorporation of strontium into otoliths of an estuarine fish. *Journal of Experimental Marine Biology and Ecology* 302:85–106. DOI: 10.1016/j.jembe.2003.10.004.

Lessard JA, Cavallo B, Anders P, Sommer T, Schreier B, Gille D, Schreier A, Finger A, Hung TC, Hobbs J, May B, Schultz A, Burgess O, Clarke R. 2018. Considerations for the use of captive-reared delta smelt for species recovery and research. *San Francisco Estuary and Watershed Science* 16. DOI: 10.15447/sfews.2018v16iss3art3.

Lewis L, Denney C, Willmes M, Xieu W, Fichman R, Zhao F, Hammock B, Schultz A, Fangue N, Hobbs J. 2021. Otolith-based approaches indicate strong effects of environmental variation

on growth of a Critically Endangered estuarine fish. *Marine Ecology Progress Series* 676:37–56. DOI: 10.3354/meps13848.

Lin S-H, Chang C-W, Iizuka Y, Tzeng W-N. 2007. Salinities, not diets, affect strontium/calcium ratios in otoliths of Anguilla japonica. *Journal of Experimental Marine Biology and Ecology* 341:254–263. DOI: 10.1016/j.jembe.2006.10.025.

Lindberg JC, Tigan G, Ellison L, Rettinghouse T, Nagel MM, Fisch KM. 2013. Aquaculture methods for a genetically managed population of endangered Delta Dmelt. *North American Journal of Aquaculture* 75. DOI: 10.1080/15222055.2012.751942.

Longerich HP, Jackson SE, Günther D. 1996. Inter-laboratory note. Laser ablation inductively coupled plasma mass spectrometric transient signal data acquisition and analyte concentration calculation. *Journal of Analytical Atomic Spectrometry* 11:899–904. DOI: 10.1039/JA9961100899.

Lusardi RA, Hammock BG, Jeffres CA, Dahlgren RA, Kiernan JD. 2020. Oversummer growth and survival of juvenile coho salmon (Oncorhynchus kisutch) across a natural gradient of stream water temperature and prey availability: an in situ enclosure experiment. *Canadian Journal of Fisheries and Aquatic Sciences* 77:413–424. DOI: 10.1139/cjfas-2018-0484.

Mac Nally R, Thomson JR, Kimmerer WJ, Feyrer F, Newman KB, Sih A, Bennett WA, Brown L, Fleishman E, Culberson SD, Castillo G. 2010. Analysis of pelagic species decline in the upper San Francisco Estuary using multivariate autoregressive modeling (MAR). *Ecological Applications* 20:1417–1430. DOI: 10.1890/09-1724.1.

Martino JC, Doubleday ZA, Chung M-T, Gillanders BM. 2020. Experimental support towards a metabolic proxy in fish using otolith carbon isotopes. *Journal of Experimental Biology* 223:jeb217091. DOI: 10.1242/jeb.217091.

Martino JC, Doubleday ZA, Fowler AJ, Gillanders BM. 2021. Identifying physiological and environmental influences on otolith chemistry in a coastal fishery species. *Marine and Freshwater Research* 72:904. DOI: 10.1071/MF20196.

Martino J, Doubleday ZA, Woodcock SH, Gillanders BM. 2017. Elevated carbon dioxide and temperature affects otolith development, but not chemistry, in a diadromous fish. *Journal of Experimental Marine Biology and Ecology* 495:57–64. DOI: 10.1016/j.jembe.2017.06.003.

Miller MB, Clough AM, Batson JN, Vachet RW. 2006. Transition metal binding to cod otolith proteins. *Journal of Experimental Marine Biology and Ecology* 329:135–143. DOI: 10.1016/j.jembe.2005.08.016.

Miller JA, Hurst TP. 2020. Growth Rate, Ration, and Temperature Effects on Otolith Elemental Incorporation. *Frontiers in Marine Science* 7.

Miller SJ, Storck T. 1982. Daily Growth Rings in Otoliths of Young-of-the-Year Largemouth Bass. *Transactions of the American Fisheries Society* 111:527–530. DOI: 10.1577/1548-8659(1982)111<527.

Morley JW, Selden RL, Latour RJ, Frölicher TL, Seagraves RJ, Pinsky ML. 2018. Projecting shifts in thermal habitat for 686 species on the North American continental shelf. *PLOS ONE* 13:e0196127. DOI: 10.1371/journal.pone.0196127.

Moyle PB, Bennett WA, Fleenor WE, Lund JR. 2010. Habitat Variability and Complexity in the Upper San Francisco Estuary. *San Francisco Estuary and Watershed Science* 8. DOI: 10.15447/sfews.2010v8iss3art1.

Moyle PB, Brown LR, Durand JR, Hobbs JA. 2016. Delta smelt: Life history and decline of a once-abundant species in the San Francisco estuary. *San Francisco Estuary and Watershed Science* 14. DOI: 10.15447/sfews.2016v14iss2art6.

Moyle PB, Herbold B, Stevens DE, Miller LW. 1992. Life History and Status of Delta Smelt in the Sacramento-San Joaquin Estuary, California. *Transactions of the American Fisheries Society* 121:67–77. DOI: 10.1577/1548-8659(1992)121<0067:LHASOD>2.3.CO;2.

Moyle PB, Hobbs JA, Durand JR. 2018. Delta Smelt and Water Politics in California. *Fisheries* 43. DOI: 10.1002/fsh.10014.

Moyle PB, Katz JVE, Quiñones RM. 2011. Rapid decline of California's native inland fishes: A status assessment. *Biological Conservation* 144:2414–2423. DOI: 10.1016/j.biocon.2011.06.002.

Moyle PB, Lusardi RA. 2017. State of the Salmonids: Status of California's Emblematic Fishes 2017. DOI: 10.13140/RG.2.2.24893.97761.

Nichols FH, Cloern JE, Luoma SN, Peterson DH. 1986. The Modification of an Estuary. *Science* 231:567–573. DOI: 10.1126/science.231.4738.567.

Nobriga ML, Loboschefsky E, Feyrer F. 2013. Common Predator, Rare Prey: Exploring Juvenile Striped Bass Predation on Delta Smelt in California's San Francisco Estuary. *Transactions of the American Fisheries Society* 142:1563–1575. DOI: 10.1080/00028487.2013.820217.

Nobriga ML, Sommer TR, Feyrer F, Fleming K. 2008. Long-Term Trends in Summertime Habitat Suitability for Delta Smelt, Hypomesus transpacificus. *San Francisco Estuary and Watershed Science* 6. DOI: 10.15447/sfews.2008v6iss1art1.

Pannella G. 1971. Fish Otoliths: Daily Growth Layers and Periodical Patterns. *Science* 173:1124. DOI: 10.1126/science.173.4002.1124.

Paton C, Hellstrom J, Paul B, Woodhead J, Hergt J. 2011. Iolite: Freeware for the visualisation and processing of mass spectrometric data. *Journal of Analytical Atomic Spectrometry* 26:2508–2518. DOI: 10.1039/C1JA10172B.

Peck MA, Baumann H, Clemmesen C, Herrmann J-P, Moyano M, Temming A. 2015. Calibrating and comparing somatic-, nucleic acid-, and otolith-based indicators of growth and condition in young juvenile European sprat (Sprattus sprattus). *Journal of Experimental Marine Biology and Ecology* 471:217–225. DOI: 10.1016/j.jembe.2015.06.011.

Pershing AJ, Alexander MA, Hernandez CM, Kerr LA, Le Bris A, Mills KE, Nye JA, Record NR, Scannell HA, Scott JD, Sherwood GD, Thomas AC. 2015. Slow adaptation in the face of rapid warming leads to collapse of the Gulf of Maine cod fishery. *Science* 350:809–812. DOI: 10.1126/science.aac9819.

Pinheiro J, Bates D, R Core Team. 2022. nlme: Linear and Nonlinear Mixed Effects Models.

Potter IC, Tweedley JR, Elliott M, Whitfield AK. 2013. The ways in which fish use estuaries: A refinement and expansion of the guild approach. *Fish and Fisheries* 16:230–239. DOI: 10.1111/faf.12050.

R Core Team. 2022. R: A language and environment for statistical computing.

Ranaldi MM, Gagnon MM. 2008. Zinc incorporation in the otoliths of juvenile pink snapper (Pagrus auratus Forster): The influence of dietary versus waterborne sources. *Journal of Experimental Marine Biology and Ecology* 360:56–62. DOI: 10.1016/j.jembe.2008.03.013.

Reis G, Howard J, Rosenfield J. 2019. Clarifying Effects of Environmental Protections on Freshwater Flows to—and Water Exports from—the San Francisco Bay Estuary. *San Francisco Estuary and Watershed Science* 17. DOI: 10.15447/sfews.2019v17iss1art1.

Rose KA, Kimmerer WJ, Edwards KP, Bennett WA. 2013. Individual-Based Modeling of Delta Smelt Population Dynamics in the Upper San Francisco Estuary: II. Alternative Baselines and Good versus Bad Years. *Transactions of the American Fisheries Society* 142:1260–1272. DOI: 10.1080/00028487.2013.799519.

Sandford M, Castillo G, Hung T-C. 2020. A review of fish identification methods applied on small fish. *Reviews in Aquaculture* 12:542–554. DOI: 10.1111/raq.12339.

Schulz-Mirbach T, Ladich F, Plath M, Heß M. 2019. Enigmatic ear stones: what we know about the functional role and evolution of fish otoliths: The role of fish otoliths in inner ear function. *Biological Reviews* 94:457–482. DOI: 10.1111/brv.12463.

Scoville C. 2019. Hydraulic society and a “stupid little fish”: toward a historical ontology of endangerment. *Theory and Society* 48:1–37. DOI: 10.1007/s11186-019-09339-3.

Slater S, Baxter R. 2014. Diet, Prey Selection, and Body Condition of Age-0 Delta Smelt, Hypomesus transpacificus, in the Upper San Francisco Estuary. *San Francisco Estuary and Watershed Science* 12. DOI: 10.15447/sfews.2014v12iss3art1.

Sogard SM. 1997. Size-Selective Mortality in the Juvenile Stage of Teleost Fishes: A Review. *Bulletin of Marine Science* 60:1129–1157.

Sponaugle S, Grorud-Colvert K, Pinkard D. 2006. Temperature-mediated variation in early life history traits and recruitment success of the coral reef fish Thalassoma bifasciatum in the Florida Keys. *Marine Ecology Progress Series* 308:1–15. DOI: 10.3354/meps308001.

Stanley RRE, Bradbury IR, DiBacco C, Snelgrove PVR, Thorrold SR, Killen SS. 2015. Environmentally mediated trends in otolith composition of juvenile Atlantic cod (Gadus morhua). *ICES Journal of Marine Science* 72:2350–2363. DOI: 10.1093/icesjms/fsv070.

Starrs D, Ebner BC, Fulton CJ. 2016. All in the ears: Unlocking the early life history biology and spatial ecology of fishes. *Biological Reviews* 91. DOI: 10.1111/brv.12162.

Stevenson DK, Campana SE. 1993. Otolith microstructure examination and analysis. *ICES Journal of Marine Science* 50. DOI: 10.1006/jmsc.1993.1053.

Sturrock AM, Hunter E, Milton JA, Johnson RC, Waring CP, Trueman CN, EIMF. 2015. Quantifying physiological influences on otolith microchemistry. *Methods in Ecology and Evolution*. DOI: 10.1111/2041-210X.12381.

Sturrock AM, Trueman CN, Milton JA, Waring CP, Cooper MJ, Hunter E. 2014. Physiological influences can outweigh environmental signals in otolith microchemistry research. *Marine Ecology Progress Series* 500. DOI: 10.3354/meps10699.

Swain DL, Langenbrunner B, Neelin JD, Hall A. 2018. Increasing precipitation volatility in twenty-first-century California. *Nature Climate Change* 8:427–433. DOI: 10.1038/s41558-018-0140-y.

Tanner SE, Reis-Santos P, Vasconcelos RP, Fonseca VF, França S, Cabral HN, Thorrold SR. 2013. Does otolith geochemistry record ambient environmental conditions in a temperate tidal estuary? *Journal of Experimental Marine Biology and Ecology* 441:7–15. DOI: 10.1016/j.jembe.2013.01.009.

Thomson JR, Kimmerer WJ, Brown LR, Newman KB, Mac Nally R, Bennett WA, Feyrer F, Fleishman E. 2010. Bayesian change point analysis of abundance trends for pelagic fishes in the upper San Francisco Estuary. *Ecological Applications* 20:1431–1448. DOI: 10.1890/09-0998.1.

Tigan G, Mulvaney W, Ellison L, Schultz A, Hung T-C. 2020. Effects of light and turbidity on feeding, growth, and survival of larval Delta Smelt (Hypomesus transpacificus, Actinopterygii, Osmeridae). *Hydrobiologia* 847:2883–2894. DOI: 10.1007/s10750-020-04280-4.

Titus RG, Volkoff MC, Snider WM. 2004. Use of Otolith Microstructure to Estimate Growth Rates of Juvenile Chinook Salmon from a Central Valley, California Stock. *American Fisheries Society Symposium* 39:181–202.

U.S. Fish and Wildlife Service. 1993. Determination of Threatened Status for the Delta Smelt. *Federal Register*:12854-12864.

Walther BD, Kingsford MJ, O'Callaghan MD, McCulloch MT. 2010. Interactive effects of ontogeny, food ration and temperature on elemental incorporation in otoliths of a coral reef fish. *Environmental Biology of Fishes* 89:441–451. DOI: 10.1007/s10641-010-9661-6.

Willmes M, Glessner JJG, Carleton SA, Gerrity PC, Hobbs JA. 2016. 87 Sr/ 86 Sr isotope ratio analysis by laser ablation MC-ICP-MS in scales, spines, and fin rays as a nonlethal alternative to otoliths for reconstructing fish life history. *Canadian Journal of Fisheries and Aquatic Sciences* 73:1852–1860. DOI: 10.1139/cjfas-2016-0103.

Wood S. 2022. mgcv: Mixed GAM Computation Vehicle with Automatic Smoothness Estimation.

Wright PJ. 1991. The influence of metabolic rate on otolith increment width in Atlantic salmon parr, Salmo salar L. *Journal of Fish Biology* 38:929–933. DOI: 10.1111/j.1095-8649.1991.tb03632.x.

Xieu W, Lewis LS, Zhao F, Fichman RA, Willmes M, Hung T-C, Ellison L, Stevenson T, Tigan G, Schultz AA, Hobbs JA. 2021. Experimental validation of otolith-based age and growth reconstructions across multiple life stages of a critically endangered estuarine fish. *PeerJ* 9:e12280. DOI: 10.7717/peerj.12280.

Yoshinaga J, Nakama A, Morita M, Edmonds JS. 2000. Fish otolith reference material for quality assurance of chemical analyses. *Marine Chemistry* 69:91–97. DOI: 10.1016/S0304-4203(99)00098-5.

TABLES

Table 7-1: Mean ± s.d. concentrations (in ppb) of each element (X), and the respective molar ratios of each element to calcium (X:Ca, in µmol/mol) in water samples from the 14 °C and 18 °C systems.

Concentration (ppb)			**Molar Ratio (X:Ca, µmol/mol)**		
X	**14 °C**	**18 °C**	**X:Ca**	**14 °C**	**18 °C**
B	60.41 ± 13.69	61.69 ± 14.22	B:Ca	18452.18 ± 2524.45	18302.5 ± 2506.43
Ba	16.81 ± 2.14	17.04 ± 1.96	Ba:Ca	409.07 ± 48.62	403.34 ± 44.64
Ca	12028.78 ± 1050.46	12383.03 ± 1181.05	Ca:Ca	1 ± 0	1 ± 0
Cu	4.06 ± 0.41	2.93 ± 0.69	Cu:Ca	213.28 ± 17.43	152.54 ± 47.2
Li	1.71 ± 0.2	1.86 ± 0.19	Li:Ca	821.88 ± 43.93	866.35 ± 43.95
Mn	0.62 ± 0.08	0.51 ± 0.16	Mn:Ca	38.02 ± 6.83	30.05 ± 9.84
Na	21493.8 ± 2320.8	22141.3 ± 2108.3	Na:Ca	3116238.9 ± 198064.6	3127549.7 ± 263785.9
Sr	112.85 ± 11.41	115.55 ± 11.55	Sr:Ca	4289.79 ± 141.82	4270.04 ± 151.8
Zn	11.29 ± 0.91	9.87 ± 0.83	Zn:Ca	579.58 ± 71.55	492.51 ± 59.34

Table 7-2: Statistical results of the linear model examining the additive and interactive effects of temperature (14°C vs 18°C) and feed (fed vs unfed) on survival of Delta Smelt.

Significant p-values are in **bold**. DF—degrees of freedom, SS—sum of squared errors, MS—mean squared error, F—f-value, P—p-value.

Factor	**DF**	**SS**	**MS**	**F**	**P**
temp	1	253.12	253.12	26.299	**0.007**
feed	1	946.12	946.12	98.299	**<0.001**
temp:feed	1	210.13	210.13	21.831	**0.01**
Residuals	4	38.5	9.62		

Table 7-3: Statistical results of the LME model assessing the fixed effects of feed, temperature, and their interaction on changes in standard length (SL_c), mass ($MASS_e$), condition factor (K), and Otolith Accretion, while accounting for random tank effects. DF_{num}—numerator degrees of freedom, DF_{den}—denominator degrees of freedom, F—f-value, P—p-value.

Significant p-values ($p < 0.05$) are in **bold**.

Model		**DF_{num}**	**DF_{den}**	**F**	**P**	**$R^2_{marg.}$**	**$R^2_{cond.}$**
ΔSL_c n = 534	(Intercept)	1	526	826.9191	**<0.001**	0.651	0.569
	feed	1	4	390.1852	**<0.001**		
	temp	1	4	0.2496	0.64		
	feed:temp	1	4	1.9476	0.24		
$\Delta MASS_e$ n=532	(Intercept)	1	524	189.8594	**<0.001**	0.655	0.662
	feed	1	4	431.2607	**<0.001**		
	temp	1	4	6.0563	**0.07**		
	feed:temp	1	4	1.3436	0.31		
ΔK n = 532	(Intercept)	1	524	37.5868	**<0.001**	0.755	0.758
	feed	1	4	786.3995	**<0.001**		
	temp	1	4	15.2656	**0.017**		
	feed:temp	1	4	1.5257	0.284		
ΔOtolith Accretion, n = 104	(Intercept)	1	96	2224.5056	**<0.001**	0.191	0.191
	feed	1	4	15.9061	**0.02**		
	temp	1	4	0.9204	0.39		
	feed:temp	1	4	6.5625	0.06		

Table 7-4: Statistical results of the LME model examining fish length as a function of the additive fixed effects of treatment (18F, 18NF, 14F, 14NF) and otolith size (radius), excluding the non-significant treatment*radius interaction. R^2 = 0.680. DF_{num}—numerator degrees of freedom, DF_{den}—denominator degrees of freedom, F—f-value, P—p-value.

Significant p-values ($p < 0.05$) are in **bold**.

Factor	DF_{num}	DF_{den}	F	P
(Intercept)	1	95	20764.769	**<0.001**
radius	1	95	175.676	**<0.001**
treat	3	4	11.003	**0.02**

Table 7-5: Pairwise contrasts of estimated marginal means of the intercepts for each treatment group in the LME model examining fish length as a function of the additive fixed effects of treatment (18F, 18NF, 14F, 14NF) and otolith size (radius).

The intercept (or initial size at age) for 14F is significantly larger than unfed treatments (14NF, 18NF) with no significant differences among the other treatments (18F, 18NF, 14NF). The difference between fed group intercepts (14F, 18F) nears significance. Contrast—treatment pairs being compared, Estimate—estimated difference between treatments, SE—standard error, DF—degrees of freedom, T—t-ratio, P—p-value. Significant p-values ($p < 0.05$) are in bold.

Contrast	Estimate	SE	DF	T	P
14F – 14NF	5.96	1.15	4	5.176	**0.02**
14F – 18F	3.888	1.15	4	3.371	**0.09**
14F – 18NF	5.359	1.13	4	4.755	**0.03**
14NF – 18F	-2.072	1.25	4	-1.657	0.45
14NF – 18NF	-0.601	1.11	4	-0.539	0.94
18F – 18NF	1.471	1.19	4	1.233	0.64

Table 7-6: Results of LME models examining relationships between changes in otolith accretion and fish body morphometrics (ΔSL_c, $\Delta MASS_e$, ΔK).

Significant p-values are in bold. SE—standard error, DF—degrees of freedom, T—t-ratio, P—p-value. R^2_{cond}—conditional R^2 value. Significant p-values ($p < 0.05$) are in bold.

Model	Coefficient	Value	SE	DF	T	P	R^2_{cond}
ΔSL_C n = 104	(Intercept)	-9.143	3.88648	92	-2.3525	**0.02**	0.796
	oto acc.	0.11472	0.01996	92	5.74656	**<0.001**	
	14NF	6.89869	4.6592	4	1.48066	0.21	
	18F	6.74144	5.6379	4	1.19574	0.3	
	18NF	7.7927	4.80072	4	1.62324	0.18	
	oto acc.:14NF	-0.0989	0.02361	92	-4.188	**<0.001**	
	oto acc.:18F	-0.0531	0.02704	92	-1.9653	**0.05**	
	oto acc.:18NF	-0.0996	0.02466	92	-4.0403	**<0.001**	
$\Delta MASS_e$ n = 104	(Intercept)	-1.0174	0.50472	91	-2.0157	**0.05**	0.749
	oto acc.	0.01086	0.00259	91	4.18827	**<0.001**	
	14NF	0.62002	0.60507	4	1.0247	0.36	
	18F	1.24792	0.73443	4	1.69917	0.17	
	18NF	0.58339	0.62345	4	0.93575	0.4	
	oto acc.:14NF	-0.01	0.00307	91	-3.2681	**0.002**	
	oto acc.:18F	-0.0075	0.00353	91	-2.1403	**0.04**	
	oto acc.:18NF	-0.0101	0.0032	91	-3.15	**0.002**	
ΔK n = 104	(Intercept)	-0.0004	0.00011	91	-3.8749	**<0.001**	0.855
	oto acc.	3E-06	1E-06	91	5.51948	**<0.001**	
	14NF	0.00016	0.00013	4	1.1763	0.31	
	18F	0.00029	0.00016	4	1.80812	0.15	
	18NF	0.00018	0.00014	4	1.35497	0.25	
	oto acc.:14NF	-3E-06	1E-06	91	-4.2544	**<0.001**	
	oto acc.:18F	-2E-06	1E-06	91	-2.3865	**0.02**	
	oto acc.:18NF	-3E-06	1E-06	91	-4.5035	**<0.001**	

Table 7-7: Results of LME models examining the additive and interactive effects of temperature and feed on element-specific Partition Coefficients (D_x).

DF_{num}—numerator degrees of freedom, DF_{den}—denominator degrees of freedom, $R^2_{cond.}$—conditional R^2, $R^2_{marg.}$—marginal R^2, F—f-value, P—p-value. Significant p-values ($p < 0.05$) are in bold.

D_x	Term	DF_{num}	DF_{den}	F	P	$R^2_{marg.}$	$R^2_{cond.}$
D_B	(Intercept)	1	99	37081.3	**<0.001**	0.038	0.045
	temp	1	4	0.1	0.77		
	feed	1	4	3.08	0.15		
	temp:feed	1	4	0.55	0.5		
D_{Ba}	(Intercept)	1	99	33093.7	**<0.001**	0.231	0.231
	temp	1	4	2.02	0.23		
	feed	1	4	24.59	**0.008**		
	temp:feed	1	4	4.04	0.12		
D_{Cu}	(Intercept)	1	99	198.992	**<0.001**	0.345	0.452
	temp	1	4	11.503	0.03		
	feed	1	4	3.452	**0.14**		
	temp:feed	1	4	3.336	0.14		
D_{Li}	(Intercept)	1	99	3827.34	**<0.001**	0.128	0.128
	temp	1	4	5.182	0.09		
	feed	1	4	6.383	**0.07**		
	temp:feed	1	4	3.353	0.14		
D_{Mn}	(Intercept)	1	99	340.197	**<0.001**	0.583	0.583
	temp	1	4	4.836	0.09		
	feed	1	4	134.249	**<0.01**		
	temp:feed	1	4	3.821	0.12		
D_{Na}	(Intercept)	1	99	334285	**<0.001**	0.483	0.602
	temp	1	4	1.5	0.29		
	feed	1	4	23.2	**0.009**		
	temp:feed	1	4	0.1	0.83		
D_{Sr}	(Intercept)	1	99	26767.4	**<0.001**	0.128	0.128
	temp	1	4	3.771	0.12		
	feed	1	4	5.741	**0.08**		
	temp:feed	1	4	5.521	0.08		
D_{Zn}	(Intercept)	1	99	64.584	**<0.0001**	0.265	0.394
	temp	1	4	10.076	0.03		
	feed	1	4	0.844	**0.41**		
	temp:feed	1	4	0.464	0.53		

Table 7-8: Variation in mean (+/- standard deviation) *X:Ca* (μmol/mol) ratios in otoliths among treatments.

	Fed		Non-Fed	
X:Ca	**14 °C**	**18 °C**	**14 °C**	**18 °C**
B:Ca	17.012 ± 3.48	17.518 ± 3.65	26.574 ± 37.33	18.967 ± 5
Ba:Ca	5.633 ± 1.86	4.735 ± 1.55	6.297 ± 0.99	6.408 ± 1.33
Cu:Ca	0.398 ± 0.42	0.102 ± 0.15	0.598 ± 1.18	0.157 ± 0.13
Li:Ca	0.007 ± 0.04	0.446 ± 0.85	0 ± 0	0.036 ± 0.19
Mn:Ca	3.977 ± 2.45	4.268 ± 2.55	0.312 ± 0.48	0.146 ± 0.42
Na:Ca	13256.204 ± 902.83	13607.72 ± 616.63	12074.469 ± 517.86	12351.213 ± 478.65
Sr:Ca	1274.581 ± 101.29	1187.701 ± 104.45	1276.447 ± 113.17	1273.584 ± 75.22
Zn:Ca	24.404 ± 12.93	9.185 ± 7	12.669 ± 6.28	1.476 ± 4.02

Table 7-9: Variation in mean (+/- standard deviation) element-specific partition coefficients (D_X) among treatments.

	Fed		**Non-Fed**	
DX ± s.d.	**14 °C**	**18 °C**	**14 °C**	**18 °C**
DB	0.00092 ± 0.00019	0.00144 ± 0.00202	0.00096 ± 0.0002	0.00104 ± 0.00027
DBa	0.01377 ± 0.00455	0.01539 ± 0.00241	0.01174 ± 0.00383	0.01589 ± 0.00329
DCu	0.00187 ± 0.00195	0.0028 ± 0.00555	0.00067 ± 0.00099	0.00103 ± 0.00084
DLi	0.00001 ± 0.00004	0 ± 0	0.00051 ± 0.00098	0.00004 ± 0.00022
DMn	0.10462 ± 0.06432	0.00821 ± 0.01268	0.14203 ± 0.08486	0.00487 ± 0.01408
DNa	0.00425 ± 0.00029	0.00387 ± 0.00017	0.00435 ± 0.0002	0.00395 ± 0.00015
DSr	0.29712 ± 0.02361	0.29755 ± 0.02638	0.27815 ± 0.02446	0.29826 ± 0.01762
DZn	0.04211 ± 0.0223	0.02186 ± 0.01083	0.01865 ± 0.01421	0.003 ± 0.00815

Table 7-10: Studies that examined *X:Ca* (μmol/mol) and partition coefficients for fresh and brackish water fish species.

Temp (C) includes if temperature treatments were experimentally assessed. Study focus: F = feed, T = temperature, P = population identification, PC = partition coefficients, S = salinity. Species habitat: F = freshwater, M = marine, E = estuarine)

Focus	Study	Species	Habitat	Temp (C)	X:Ca (μmol:mol)	Value	Partition Coefficient	Value
F/T/P	Clarke et al. 2011	*Menidia menidia*	E/M	15, 21, 27	Mn:Ca	3.75 - 5.0	D_{Mn}	1.0 - 5.0
					Sr:Ca	2100 - 2500	D_{Sr}	0.21 - 0.3
					Ba:Ca	2.0 - 2.6	D_{Ba}	0.1 - 0.5
PC/T	Collingsworth et al. 2010	*Perca flavescens*	F	10, 15, 20	Mn:Ca	2.5 - 17.0	D_{Sr}	0.3
					Sr:Ca	900 - 1200	D_{Ba}	0.001 - 0.0003
					Ba:Ca	1.5 - 4.5		
F/T	Fichman 2022, this study	*Hypomesis transpacificus*	E/F	14, 18	Li:Ca	0 - 0.446	D_{Li}	0 - 0.001
					B:Ca	17.0 - 26.6	D_{B}	0.001 - 0.002
					Na:Ca	12075 - 13608	D_{Na}	0.004
					Mn:Ca	0.15 - 4.26	D_{Mn}	0.005 - 0.142
					Cu:Ca	0.102 - 0.598	D_{Cu}	0.001 - 0.003
					Zn:Ca	1.48 - 24.4	D_{Zn}	0.003 - 0.042
					Sr:Ca	1188 - 1276	D_{Sr}	0.278 - 0.298
					Ba:Ca	4.7 - 6.4	D_{Ba}	0.012 - 0.016
S	Hicks et al. 2010	*Galaxias maculatus, Galaxias argenteus*	M	14	Li:Ca	1	D_{Li}	0.002
					B:Ca	20.0 - 120.0	D_{Sr}	0.15
					Mn:Ca	0.5 - 2.9	D_{Ba}	0.005
					Cu:Ca	1.0 - 3.0		
					Zn:Ca	20		
					Sr:Ca	200		
					Ba:Ca	1.8 - 3.0		

Focus	Study	Species	Habitat	Temp (C)	X:Ca (µmol:mol)	Value	Partition Coefficient	Value
N	Hobbs et al. 2011	*Hypomesis transpacificus*	E/F		Sr:Ca	500 - 3000		
					Ba:Ca	0.01 - 0.06		
PC	Melacon et al. 2009	*Lota lota*	F				D_{Mn}	0.021
							D_{Sr}	0.35
							D_{Ba}	0.034
		Salvelinus namaycush					D_{Mn}	0.054
							D_{Sr}	0.28
							D_{Ba}	0.0037
P	Pangle et al. 2010	*Perca flavescens*	F		Li:Ca	0.69 - 1.50		
					Sr:Ca	168.33 - 810.53		
					Ba:Ca	3.15 - 10.80		
P	Wells et al. 2003	*Oncorhynchus clarki lewisi*	F		Sr:Ca	1500	D_{Sr}	0.4
					Ba:Ca	100 - 200	D_{Ba}	0.04

Table 7-11: Significant relationships between treatment factors and partition coefficients

DX	Temperature	Food Availability
DB	----------	----------
DBa	----------	negative
DCu	negative	----------
DLi	----------	----------
DNa	----------	positive
DMn	----------	positive
DSr	----------	----------
DZn	negative	----------

FIGURES

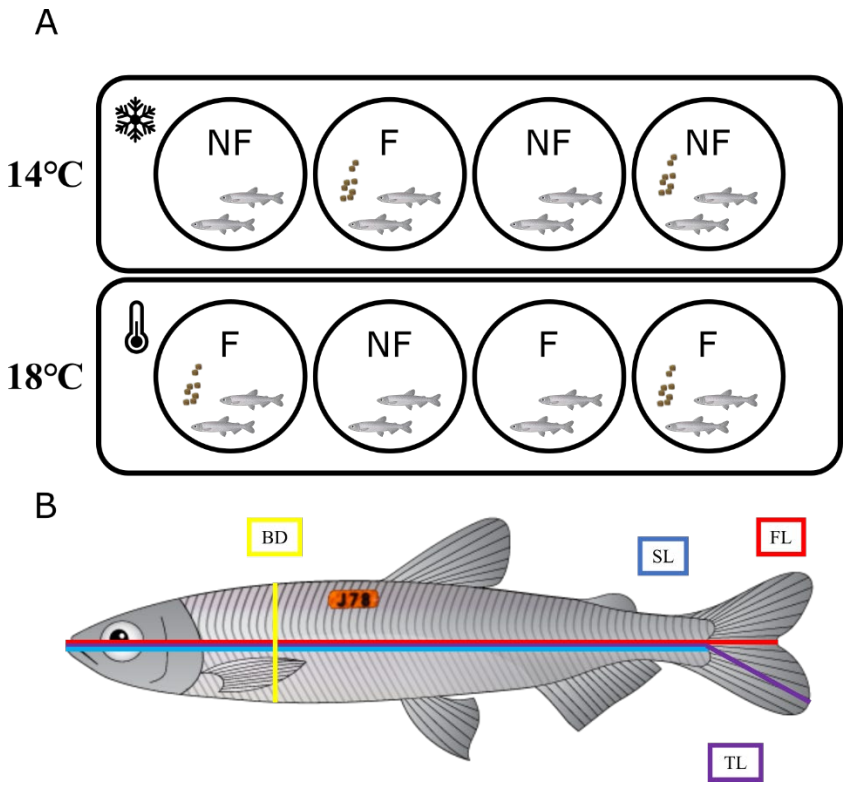

Figure 7-1: (A) Experimental array of temperatures (14°C and 18°C) and feed (Fed and Not Fed) treatments.* (B) Model of Delta Smelt with a VI Alpha tag (J78) and various somatic growth measurements: standard length (SL, blue), fork length (FL, red), total length (TL, purple), body depth (BD, yellow).**

*Each combination had two replicates to account for tank effects.

**The mass index of each fish was calculated as BD*SL and used to estimate the total mass of each fish at the initial time point. Fish artwork by Adi Khen.

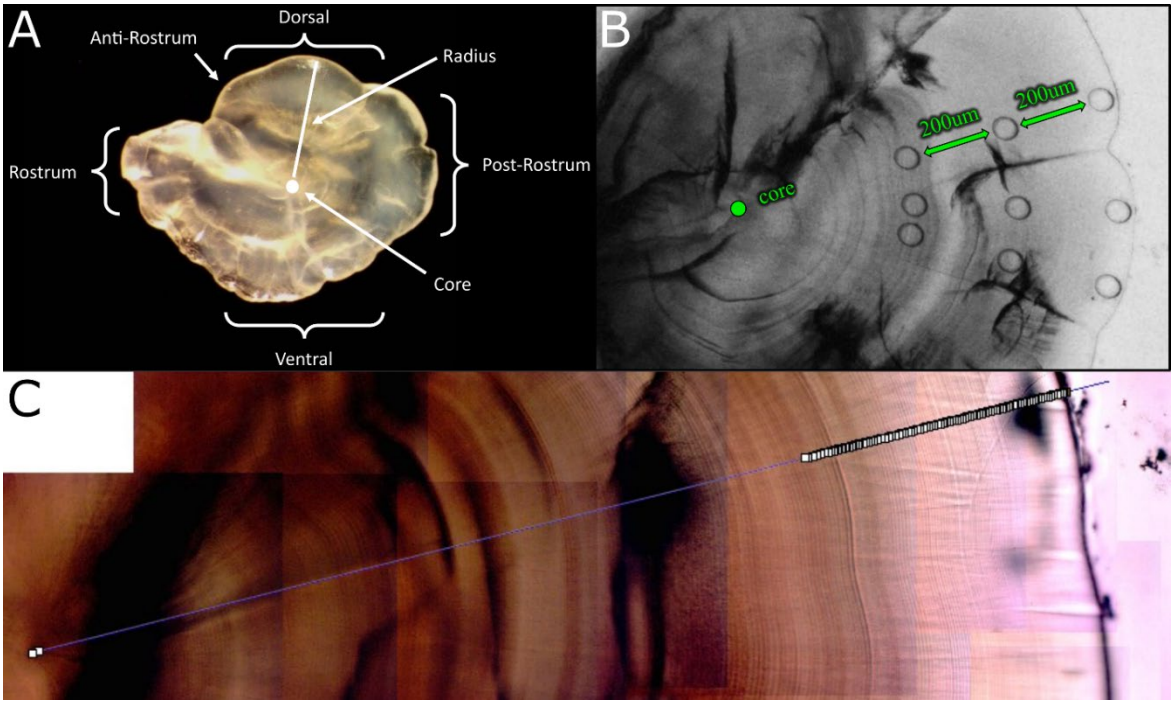

Figure 7-2: Images of otoliths with annotations to identify morphological structures, chemical spots, and daily increments.

(A) Otolith morphology and terminology. The dorsoventral (dv) measurement is the maximum distance from ventral edge to the dorsal edge (i.e., otolith diameter) while the otolith radius measurement is the distance between the core (0 dph) and the dorsal edge (294 dph). (B) Sagittal section of a Delta Smelt otolith showing three spot transects (dorsal edge to core), with each containing three 40μm ablation spots, where each spot is 200 μm from the next. The 3 spots along the outer edge of the otolith were used to assess the effects of experimental treatments on changes in otolith chemistry. (C) Image of an otolith aging trajectory, with digital marks from the edge (right) towards the core (left) for the last 100 daily increments (i.e., rings).

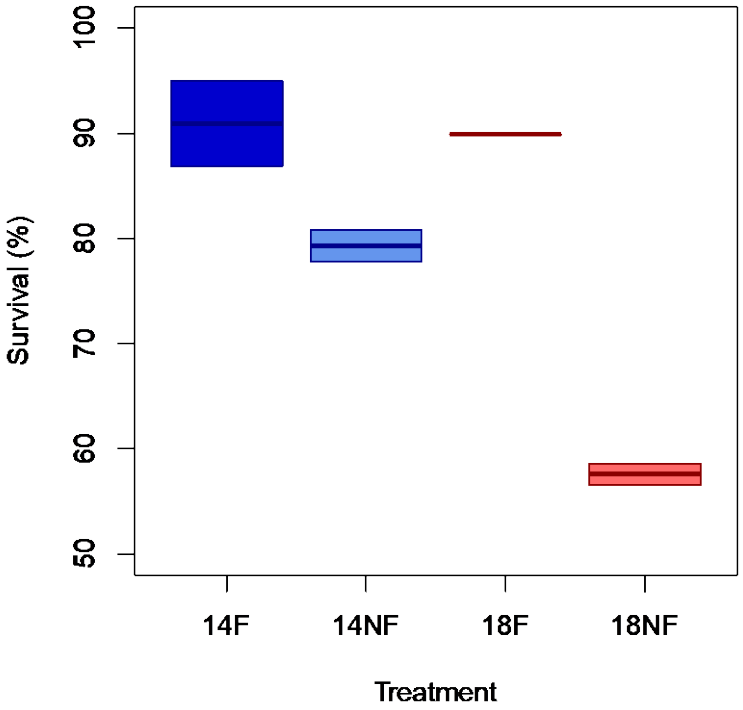

Figure 7-3: Survival rates (over 70 days) of Delta Smelt among temperature*feed treatments.

Colors represent high (red-18) and low (blue-14) temperature treatments; dark and light shading indicate the presence (F) or absence (NF) of feed. Each box encompasses the upper and lower bounds of the 2 tanks for each treatment, with the mean shown as a horizontal line.

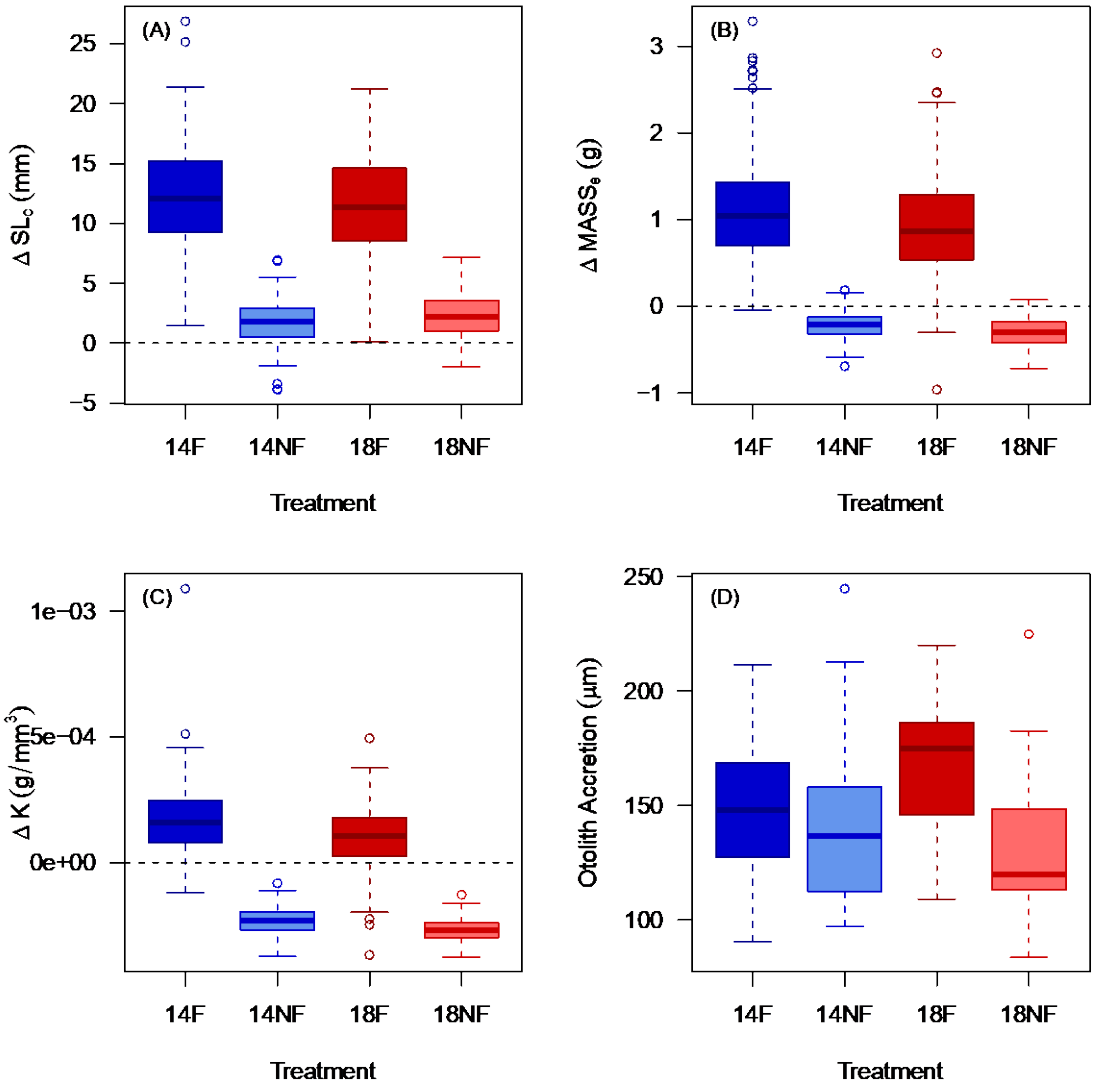

Figure 7-4: Effects of experimental treatments on changes in (A) standard length, SL_c, (B), mass, $MASS_e$, (C) condition factor, K, and (D), otolith accretion.

Dotted horizontal line in A-C represents no growth between pre- and post-experiment measurements (n=532, for 87 or 93 days). Otolith accretion (D) is shown for the experimental period (70 days) for the subset of fish for which otolith increment widths were quantified (n=104).

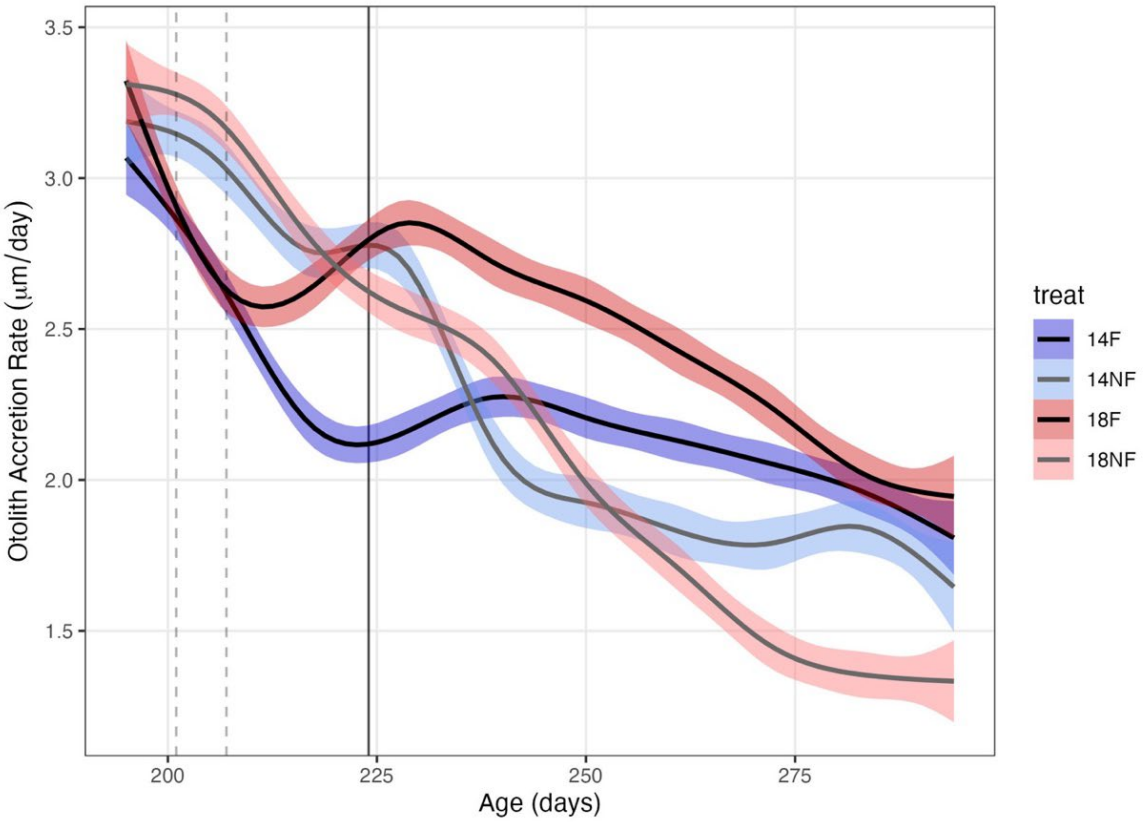

Figure 7-5: Delta Smelt daily accretion rates (μm) for the last 100 days prior to collection.

The beginning of the experimental period (solid vertical line at 224 dph) and tagging/imaging dates (dashed vertical lines at 201 dph and 207 dph) are shown. Tagging and initial imaging was completed before the beginning of the experiment to allow recovery time for the fish.

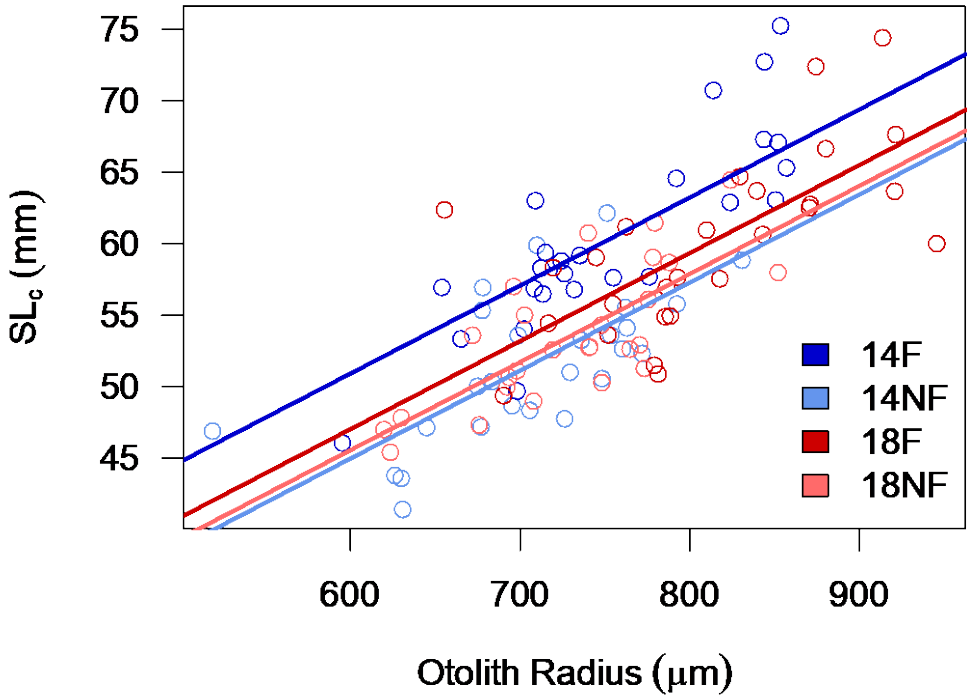

Figure 7-6: Otolith size (radius) versus fish size (SL_c) relationships for fish within each of the four treatment combinations, assuming equal slopes.

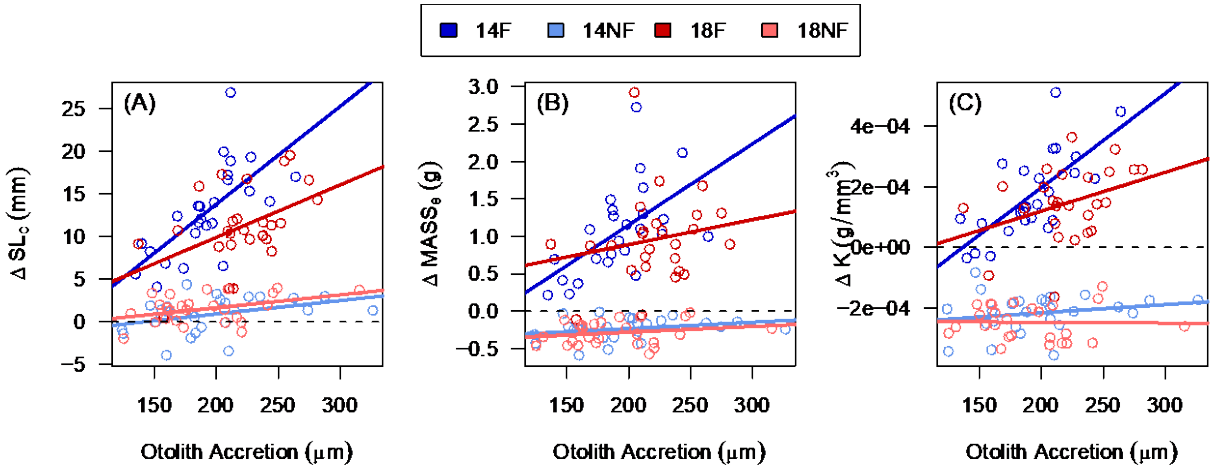

Figure 7-7: Results of linear models examining relationships between changes in (A) standard length, (B) mass, and (C) condition factor in relation to changes in otolith size (accretion) during the experimental period.

Horizontal, dashed line represents no change (0 growth or change in condition).

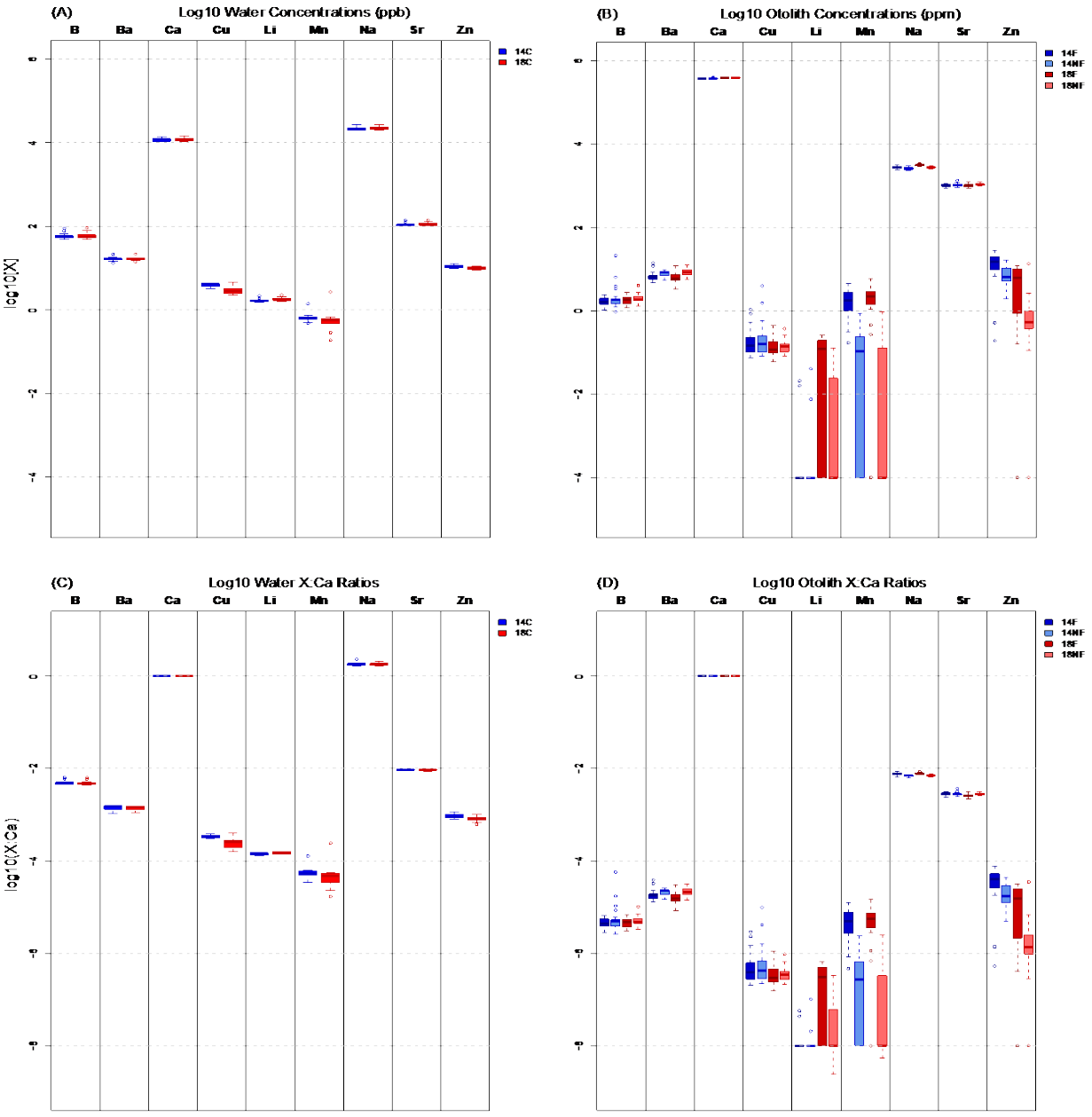

Figure 7-8: Elemental concentrations (log_{10}-transformed) in water (ppb) and otoliths (ppm) (A-B), and X:Ca ratios for all elements for water and otolith samples (µmol/mol) (C-D).

Water data were grouped by temperature (14°C or 18°C) and otolith data by treatment (14F, 14NF, 18F, and 18NF). Values below detection were set to 10^{-4} in (B) and (10^{-8}) in D.

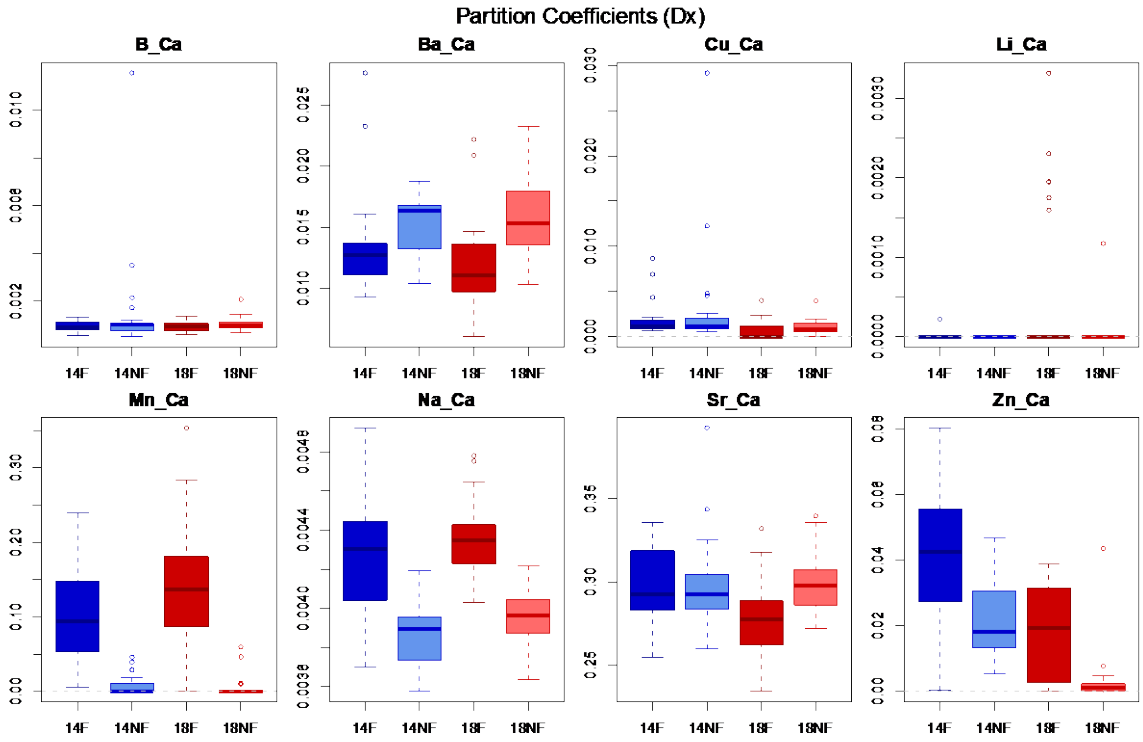

Figure 7-9: Box plots of the element-specific partition coefficients (D_X) by treatment for each element measured in Delta Smelt otoliths.

SUPPLEMENTARY INFORMATION

Supplement 1

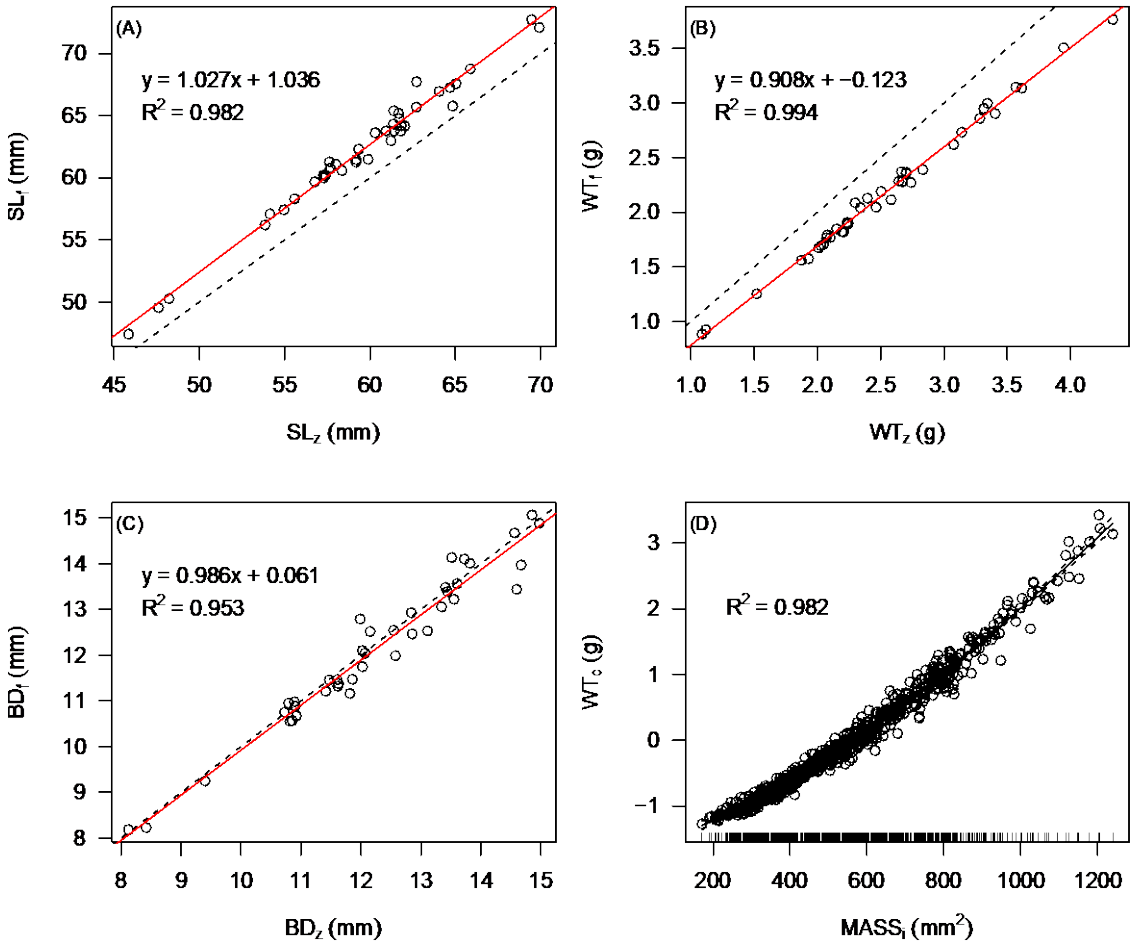

Figure S7-1: Length conversion equations for converting standard length (SL), weight, and body depth (BD) from frozen to corrected-fresh values (A-C) for adult Delta Smelt.

Dashed lines represent 1:1; red lines represent the respective linear models. Generalized additive model used to estimate mass (*MASSe*) based on weight (*WTc*) and mass index (*MASSi*) relationships (D).

Suppl. 1(D) EQ: $MASS_e = gam(WT_c \sim s(MASS_i), data)$

Supplement 2

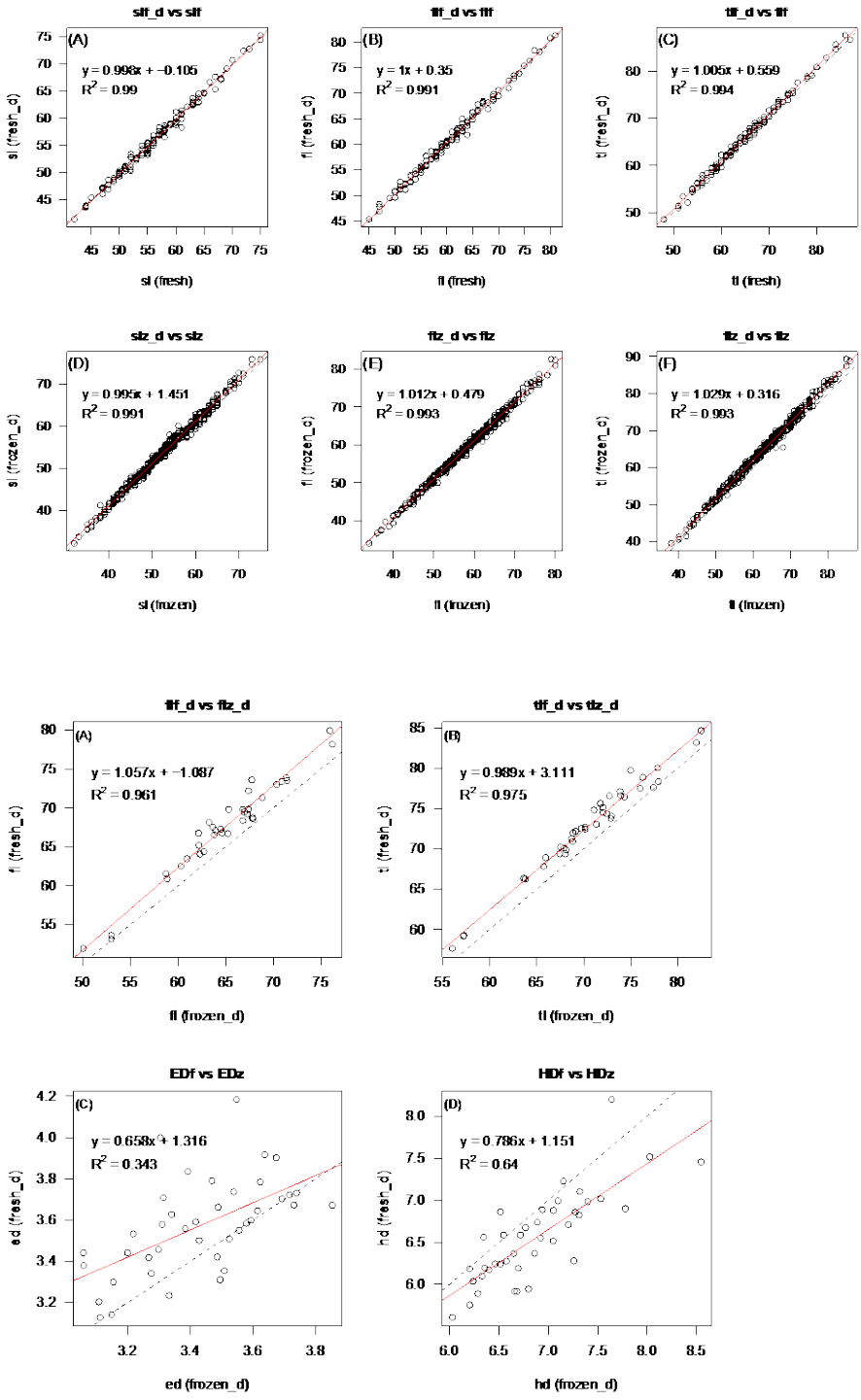

Figure S7-2: Linear conversion equations for all other metrics.

These relationships were checked but not used for calculations or analyses.

Supplement 3

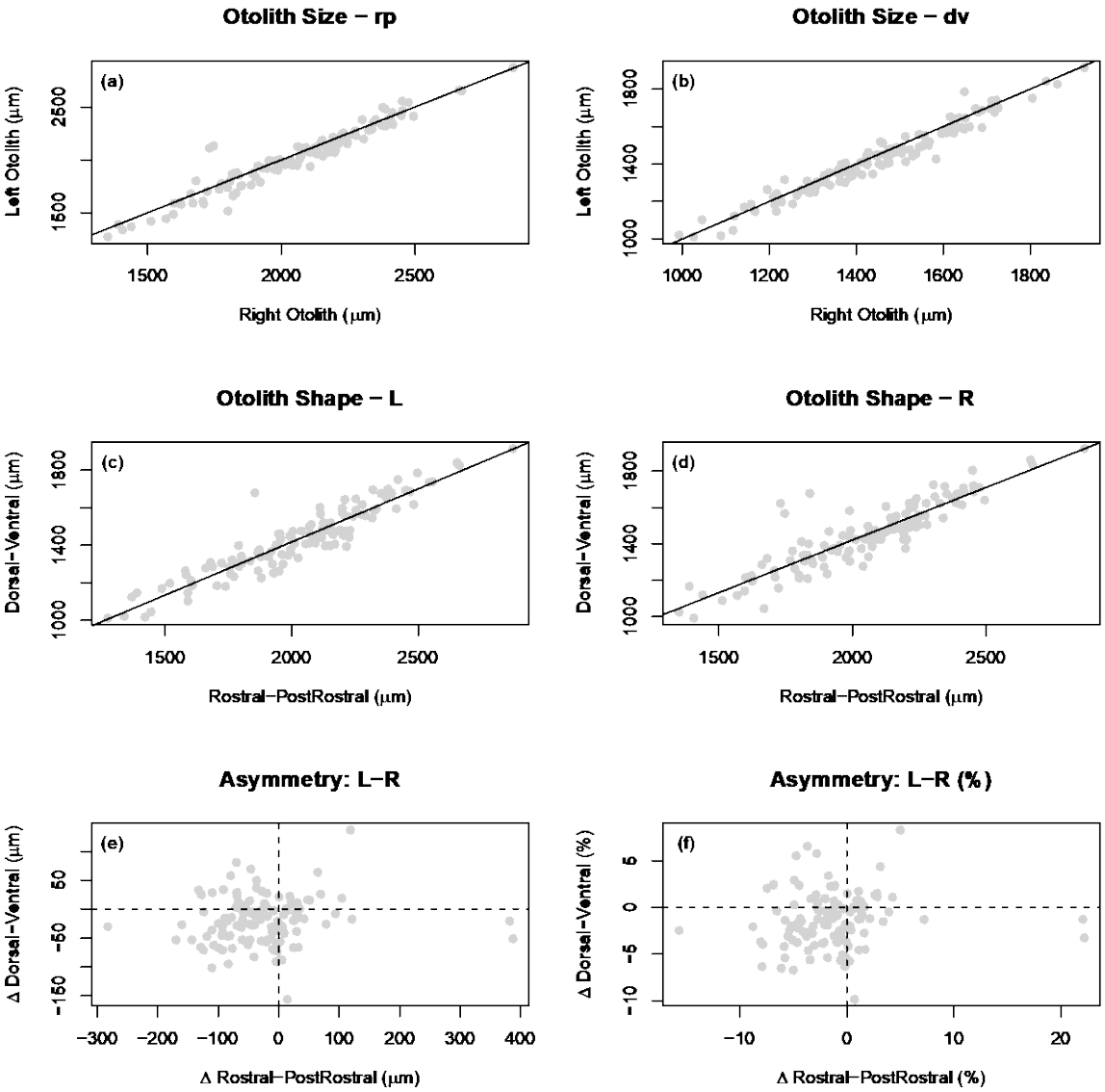

Figure S7-3A-F: Linear models comparing Left and Right otoliths per fish (a-b), DV and RP planes by otolith for left and right (c-d) and percent difference between left and right otoliths using both planes.

No significant differences between otoliths per fish.

Supplement 4

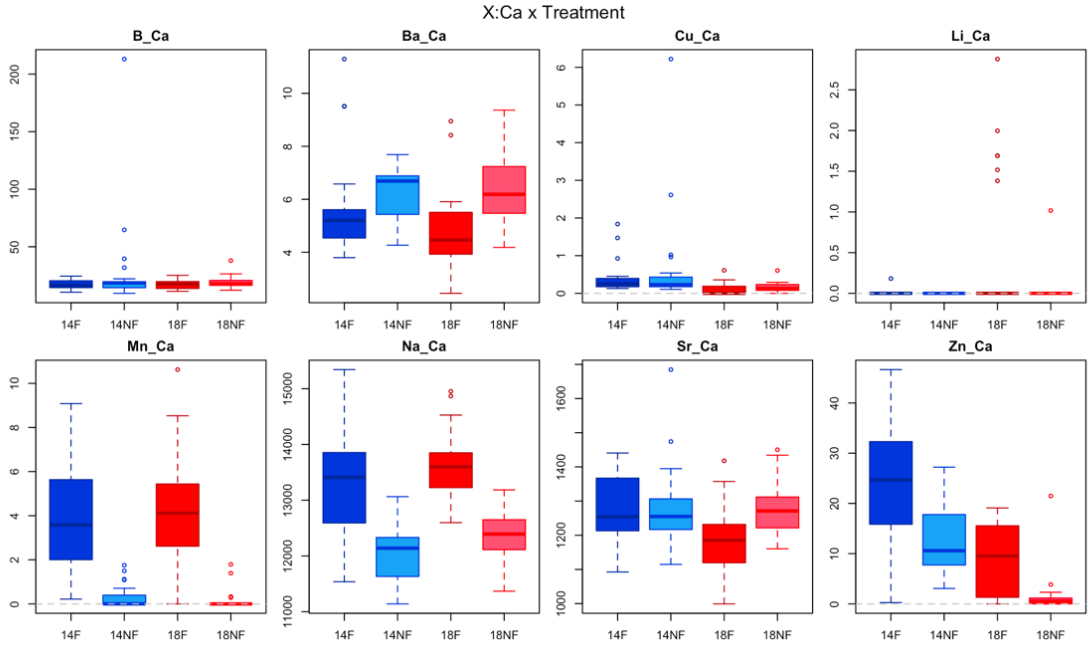

Figure S7-4: Otolith X:Ca values for each element by treatment.

Table S7-4: ANOVA results for X:Ca in otoliths

Element	Term	DF_{num}	DF	F	P	R^2m	R^2c
B:Ca	(Intercept)	1	99	6488.23	**<0.0001**	0.039	0.046
	temp	1	4	0.182	0.692		
	feed	1	4	3.08	0.154		
	temp*feed	1	4	0.552	0.499		
Ba:Ca	(Intercept)	1	99	5348.45	**<0.0001**	0.236	0.236
	temp	1	4	2.963	0.160		
	feed	1	4	24.59	**0.008**		
	temp*feed	1	4	4.041	0.115		
Cu:Ca	(Intercept)	1	99	31.186	**<0.0001**	0.368	0.471
	temp	1	4	13.444	0.022		
	feed	1	4	3.452	0.137		
	temp*feed	1	4	3.336	0.142		
Li:Ca	(Intercept)	1	99	1393.58	**<0.0001**	0.131	0.131
	temp	1	4	5.628	0.077		
	feed	1	4	6.383	0.065		
	temp*feed	1	4	3.353	0.141		
Mn:Ca	(Intercept)	1	99	104.459	**<0.0001**	0.586	0.586
	temp	1	4	6.12	0.069		
	feed	1	4	134.249	**<0.001**		
	temp*feed	1	4	3.821	0.122		
Na:Ca	(Intercept)	1	99	987836	**<0.0001**	0.488	0.606
	temp	1	4	2	0.230		
	feed	1	4	23.2	**0.009**		
	temp*feed	1	4	0.1	0.834		
Sr:Ca	(Intercept)	1	99	898866	**<0.0001**	0.138	0.138
	temp	1	4	5.1	0.088		
	feed	1	4	5.7	0.075		
	temp*feed	1	4	5.5	0.079		
Zn:Ca	(Intercept)	1	99	0.004	0.949	0.276	0.404
	temp	1	4	10.754	**0.031**		
	feed	1	4	0.844	0.410		
	temp*feed	1	4	0.464	0.533		